Bulletin
of
The Geological Society of America

VOLUME 69 April 1958 NUMBER 4

CONTENTS

	Pages
Petrology of underclays. By Leonard G. Schultz	363–402
Uranium deposits under conglomeratic sandstone of the Morrison Formation, Colorado and Utah. By David A. Phoenix	403–418
Geology and petrology of the Masinloc chromite deposit, Zambales, Luzon, Philippine Islands. By W. C. Stoll	419–448
Textural and spectrochemical studies of the White Tank quartz monzonite, California. By John J. W. Rogers	449–464
Experimental deformation and faulting in Wombeyan Marble. By M. S. Paterson	465–476
Short Notes	
Flowtill in southeastern Massachusetts. By Joseph H. Hartshorn	477–482
Differentiation of the mantle. By Francis Birch	483–486

Subscription $15.00 per year.
Printing Office: Mt. Royal & Guilford Aves., Baltimore 2, Md.
Communications for publications should be addressed to The Geological Society of America, Dr. H. R. Aldrich, Secretary, 419 West 117 Street, New York, N. Y.
Please give notice of change of address 4 weeks in advance. Claims for nonreceipt of the Bulletin of a given month must be sent to the Secretary of the Society before the end of the second succeeding month.

Entered as second-class matter at the Post Office at Baltimore, Md.
under the Act of Congress of July 16, 1894.
Accepted for mailing at special rate of postage provided for in Section 1103
Act of October 3, 1917, authorized on July 8, 1918.

PAPERS IN PRESS FOR FORTHCOMING ISSUES

Infolded Metasedimentary Rocks Near the Axial Zone of the Catoctin Mountain-Blue Ridge Anticlinorium in Virginia. By Edwin O. Gooch

Chemical Data on Desert Varnish. By Celeste G. Engel and Robert P. Sharp

Glacial Chronology of the New Zealand Pleistocene. By Maxwell Gage and R. P. Suggate

Drainage Evolution in Northeastern Montana and Northwestern North Dakota. By Arthur David Howard

Stratigraphy and Structure of the St. Albans Area, Northwestern Vermont. By A. B. Shaw

Malaspina Glacier, Alaska. By Robert P. Sharp

BULLETIN OF THE GEOLOGICAL SOCIETY OF AMERICA
VOL. 69, PP. 363-402, 14 FIGS. APRIL 1958

PETROLOGY OF UNDERCLAYS

BY LEONARD G. SCHULTZ

ABSTRACT

The mineralogy of Pennsylvanian underclays and associated rocks collected from the Appalachian, Illinois, and Mid-Continent basins was determined to see how it varied regionally, stratigraphically, and within underclay profiles.

Underclays are composed principally of kaolinite of a poorly crystallized type, illite, mixed-layer illite-montmorillonite, quartz, and in many places a 14 Å component ranging from vermiculite to chlorite. Mixed-layer material is the only clay mineral common to all underclays. Although the mineralogy of shales from above coals in most cases does not differ greatly from that of underclays, most of the shales contain less kaolinite and mixed-layer clay minerals and more and better-crystallized 14 Å clay material than do the underclays. Shales, slates, sandstones, and calcareous rocks from below coals are mineralogically even more like associated underclays than are the shales from above coals.

Underclays from the central parts of the geosynclinal basins differ from those of the shelf in the same way shales in general differ from their associated underclays. They contain less kaolinite and more 14 Å clay, both of which are usually slightly better crystallized, and also contain less mixed-layer clay. Most underclays from parts of the column in which marine beds are common contain abundant mixed-layer montmorillonite. Stratigraphically, lower Pennsylvanian underclays are more kaolinitic than those of the upper Pennsylvanian; the change came earliest in the Mid-Continent Basin and occurs at progressively higher horizons toward the east where the decrease in kaolinite content is less marked.

Field observations show that underclays were formed before deposition of coal-forming material began and therefore cannot be the residual soils on which the coal-forming flora grew. The mineral distribution within underclay profiles also indicates that underclays are not residual soils. Yet, the mineralogy of underclays in general does resemble that of modern soils in several ways. The excess kaolinite and mixed-layer clay is thought to result from soil formation in the source area, and regional and stratigraphic variations in the mineralogy of underclays result from different lengths of time and types of weathering in the various source areas. Slickensides and lack of bedding in underclays are attributed to flocculation of the clay combined with slipping when the hydrous mass was compacted.

CONTENTS

TEXT

	Page
Introduction	364
General	364
Problems involved	364
Stratigraphic and geographic extent	365
Stratigraphic correlations	365
Acknowledgments	366
Analytical procedure	366
Varieties and amounts of clay minerals	367
Interpretation of X-ray data	367
Construction of pie diagrams	368
Arrangement of pie diagrams in figures	368
Relationships between mineralogical determinations and field observations	371
Underclay profiles	371
Relationships between underclays and other rock types	374
General	374
Shales	377
Sandstones	377
Calcareous rocks	380
Red beds	380
Mississippian soils	380
Field evidence of coal-underclay time relationships	380
Slickensides and flint clays	382
Regional and stratigraphic variations of underclays	384
Shelf-geosynclinal relationships	384
Stratigraphic variations	388
Source areas	389
Interbasin correlations	390
Summary	390
References cited	392
Appendix. Sample localities	394

ILLUSTRATIONS

Figure		Page
1.	Calculation of mineral percentages from spectrometer traces	369
2.	Clay-mineral analyses: Mississippian soils	370
3.	Clay-mineral analyses: zone 1	372
4.	Clay-mineral analyses: zone 2	373
5.	Clay-mineral analyses: zone 3	375
6.	Clay-mineral analyses: zone 4	376
7.	Clay-mineral analyses: zone 5	378
8.	Clay-mineral analyses: zone 6	379
9.	Clay-mineral analyses: zone 7	381
10.	Clay-mineral analyses: zone 8	383
11.	Clay-mineral analyses: zone 9	385
12.	Clay-mineral analyses: zone 10	386
13.	Coal-underclay field relationships	387
14.	Sediment transportation directions in Pennsylvanian basins	388

TABLES

Table		Page
1.	Coal correlation chart	365
2.	Mineral composition variations in underclay profiles	371
3.	Mineralogical relationships between underclays and associated rocks	377
4.	Organic content and slickensiding in underclays	382
5.	Average kaolinite content of underclays	384

Introduction

General

Underclays are the nonlaminated argillaceous beds averaging a few feet thick that occur below coal beds. They are particularly common in Pennsylvanian rocks, but in most places below coals of other ages they are rare or poorly developed. In many places they exhibit excellent plant impressions and polished, randomly oriented cleavage surfaces called slickensides. The highly kaolinitic underclays are well known because of their economic importance in the ceramic and refractory industries.

The reason for the common association of coal and underclays has been a source of speculation for the last century. Although one may occur without the other, the relationship of underclay to coal is too consistent to be fortuitous; if an unaccompanied coal or clay is traced laterally, the missing member will in most cases be seen in its proper place. Worthen (1866, p. 46) was the first in this country to speculate on the origin of underclays. Observing the traces of tree roots penetrating downward from a coal into its underclay, he reasoned that the underclay "was the original subsoil on which the vegetation that formed the coal grew, and . . . the trunks and branches have contributed to form the coal." Later Stout (1923, p. 542) proposed a less direct relationship between the coal and underclay. He believed that the period of abundant plant growth was divided into two phases. In the first, all the plant material was oxidized and formed organic acids. These acids leached the soluble components not only from the underlying shales but also from terriginous materials which were deposited contemporaneously in the swamp forest. The altered materials and the plant-ash residuum of the decayed plants formed the underclays. During the second phase of abundant vegetation some of the plant material was not oxidized but accumulated and eventually formed the coal. Thus, there was no abrupt change in plant growth, but only a change from decay to at least partial preservation. Recently, Grim and Allen (1938) observed that underclays show none of the weathering effects common in modern soil profiles; the clay minerals and feldspar appear fresh, or if altered, there is no vertical variation suggestive of soil formation. They favor the view that underclays were deposited in essentially their present condition with subsequent weathering sufficient only to leach calcite.

Much has been published on the ceramic and refractory properties of underclays in areas where they are of considerable economic importance. Most of the detailed mineralogical work on clays of Pennsylvanian age has centered on relatively small, isolated flint-clay deposits, particularly those of Pennsylvania and Missouri. However, except in Illinois (Grim and Allen, 1938; Grim, 1935; W. A. White, in preparation), the plastic underclays have not been studied on a broad regional and stratigraphic basis.

Problems Involved

The over-all study is composed of several general problems. One problem is to determine how the mineralogy of underclays varies throughout the Pennsylvanian column. In Illinois Grim (1935) found that kaolinite was dominant in underclays below the No. 2 coal, whereas illite was dominant in those above. The present study is intended to see whether similar generalizations could be made for the

Mid-Continent and the Appalachian basins and to compare the underclays in shelf areas of thin sediments and those in geosynclinal areas of thick sediments within the same basin.

Another problem is to determine whether any differences in the mineralogy of the upper

TABLE 1.—COAL CORRELATION CHART

Zone	series	group	Mid-Continent Basin: S. Okla. & Arkansas	Mid-Continent Basin: Kansas & N. Okla	Mid-Continent Basin: Missouri & Iowa	Illinois Basin: Illinois	Illinois Basin: Indiana	Illinois Basin: Western Kentucky	Appalachian Basin: Ohio & Penn.	Appalachian Basin: W. Va.	Appalachian Basin: Kentucky & Tenn.	Anthracite Basins	series
10	Virgil		Ada redbed	Nodaway		Woodbury Gila		Geiger Lake	Pittsburgh				Cone-Monongahela
9	Missouri			Thayer Coffeyville	Ovid	No. 8	VIII a		Mahoning				
8	Des Moines	Marathon		Lexington	Mystic	No. 6	VI	No. 11	Middle Kittanning				Allegheny
7				Mulky	Mulky	No. 4	IV a	No. 8b	(no equivalent)				
6		Cherokee	Senora redbed	*Croweburg Henryetta Broken Arrow	Tebo	No. 2	III a	No. 8	Lower Kittanning	No. 5 block	High Splint Hindman	Buck Mt. Red Ash	
5			Boggy redbed	Pilot (Tebo) Weir-Pittsburg					Brookville	Winifrede	Hazard		
4	Lampasas		Philpot Secor	Bluejacket		Rock Island	Minshall	Mannington	Middle Mercer	Chilton	*Dean Fire Creek Wind Rock		Pottsville
3									Van Dusen		Amburgy Grassy-Elkhorn Lily		Kanawha
2	Morrow		McAlester Hartshorne	Rowe Riverton	Dederick	Babylon			Quakertown	War Eagle	Ravenscroft		
1			Baldwin			Battery Rock	Ia	Main Nolin	Sharon	Sewell	Sewanee	Lykens No. 2	Lee
							Hindostan			Fire Creek Pocahontas	Nelson		

*{different names for same coal

and lower parts of underclays indicate soil development. If underclays are residual soils as hypothesized by Worthen and Stout, one would expect mineralogical variations between the more leached upper and less leached lower parts of the underclay. Numerous samples were taken to determine whether such profile variations were present. Samples were also taken of shales, sandstones, and other rocks associated with the underclays to determine how much they differ from underclays.

Stratigraphic and Geographic Extent

During the summer of 1953 the writer collected 400 samples from 10 underclay zones, ranging in age from lowermost Pottsville to Monongahela, and a few samples from the weathered zone below the Mississippian-Pennsylvanian contact; analytical data from them were obtained during the following year. The underclay zones were numbered from 1 to 10 in ascending order. Geographically, sampling was fairly well distributed throughout the three major coal-bearing Pennsylvanian basins of the eastern United States except in two areas: the southernmost part of the Appalachian Basin in Alabama and part of the Illinois Basin. In order to avoid repetition of work of the Illinois State Geological Survey only a few samples were taken from that part of the basin in Illinois. Generalizations involving the underclays of the State of Illinois used in this paper for comparative purposes are derived for the most part from the works of Grim (1935), Grim and Allen (1938), and work now in progress by W. Arthur White.

Stratigraphic Correlations

The correlations used in this study are shown in Table 1 and for the most part are taken from Moore *et al.* (1944). A few changes were made in the light of more recent work.

In the Mid-Continent Basin correlations were modified in one major respect. The Seville Limestone which overlies the Rock Island Coal of western Illinois has recently been identified in southwestern Missouri just above the Bluejacket sandstone and coal (H. R. Wanless, oral communication). On this basis, the Bluejacket and Rock Island coals are equivalent, and rocks below the Bluejacket, which Moore *et al.* show as equivalents of the Seville Limestone, must actually be correlative with rocks below the Seville Limestone in Illinois.

One major change was also necessary in the

correlations in the Appalachian Basin. Here the Upper Mercer Limestone was considered the equivalent of the Winifrede and Magoffin limestones of West Virginia and Kentucky. More recent work (H. R. Wanless, oral communication) has shown the Lower Mercer Limestone to be equivalent to the Winifrede and Magoffin beds; this makes the Middle Mercer Coal correlative to the Chilton and Fire Clay coals of the deep part of the basin.

Moore *et al.* (1944) point out that correlations are doubtful in many cases. Correlation of a single coal from a shelf to a geosynclinal area is perhaps unrealistic, since in the shelf area a series of rocks with only a few coals may be equivalent to a much thicker geosynclinal section containing 10 times as many coal beds, one or several of which may have been contemporaneous with a single shelf coal. In spite of their possible limitations, the correlations are believed to be adequate for this study. The mineralogical characteristics did not vary randomly from one zone to the next, so that only correlations of zone 6 proved to be critical.

Acknowledgments

This paper incorporates the major part of the writer's Ph.D. thesis submitted at the University of Illinois in 1954. Special thanks are extended to Dr. R. E. Grim who was the principal thesis advisor, to Dr. H. R. Wanless who advised on stratigraphic problems and helped prepare the sampling itinerary, and to Dr. W. F. Bradley and Dr. W. D. Johns who offered helpful suggestions on interpretation of the X-ray diffraction data. Dr. R. E. Grim and Dr. H. R. Wanless of the University of Illinois, and Mrs. E. F. Overstreet and Dr. J. S. Williams of the U. S. Geological Survey read the manuscript and offered many helpful suggestions. The following people kindly helped the writer locate outcrops: Dr. Harold Arndt, Dr. A. T. Cross, Mr. R. S. Holmes, Mr. M. E. Hopkins, Dr. C. B. Moke, Dr. Hayden Murray, Dr. Norman Plummer, Mr. David Reinertson, Dr. Myron Sturgeon, Dr. A. G. Unklesbay, Dr. W. Arthur White, and Mr. Gordon Wood.

The writer is grateful to the Illinois Clay Products Company and the University of Illinois for financial assistance during the study.

Analytical Procedure

Sample preparation consisted of separation of a fine fraction of each sample for study of the clay components and a coarse fraction for study of the nonclay minerals. The less-than-2-micron clay portion was separated by differential settling in distilled water, after which the water was evaporated. As evaporation progressed, the clay slips settled on glass slides in the bottom of the evaporating dish and formed oriented clay aggregates. The coarse, non-clay part was separated by washing the sample through a 64-micron (325-mesh) sieve. Highly calcareous samples were first leached with one-third normal hydrochloric acid, then washed, and subsequently treated like other samples.

X-ray-diffraction, differential thermal, and microscopic analyses were the principal analytical tools used for mineral determinations. Of the three methods, X-ray techniques were the most extensively employed. Differential thermal analyses were used for some special purposes such as confirming the presence of kaolinite in samples giving a 14 Å X-ray diffraction spacing, the second order of which at 7 Å might be confused with the first basal kaolinite reflection. However, in general, X-ray diffraction proved to be most satisfactory for sorting out the several components of mixtures of clay minerals.

Coarse grains that did not pass the 64-micron sieve from all samples of the Mississippian soils and zones, 2, 6, 8, and 10 were examined microscopically. Quartz, feldspar, muscovite, coal, pyrite, and calcite were the major coarse-grained constituents. Quartz constitutes more than 90 per cent of the coarse material. Feldspar rarely makes up as much as 5 per cent of the sample, and in most samples the feldspar grains range from clear and unweathered to highly altered. Tourmaline, garnet, zircon, rutile, and biotite were recognized in a few samples, and hornblende was found in only two samples. Common pigmenting agents are finely disseminated coal and the ferric hydroxides, lepidocrocite and goethite.

Samples for X-ray diffraction were prepared and studied by several techniques. Most extensively used were X-ray spectrometer traces of oriented clay aggregates. Spectrometer traces were also run of the crushed but unfractionated samples in order to get a rough idea of the mineralogy of the whole sample. Although the trace of the unfractionated sample was not nearly so good as that from an oriented slide, it did show whether there was any considerable difference between the clay of the fine fraction and the clay of the whole sample. Further information on particle-size

variation of minerals within the less-than-2-micron fraction was obtained by running spectrometer traces of the backs of some oriented aggregates as well as the fronts to see whether the coarser clay-sized particles which settled first next to the glass supporting slide differed from the finer particles on the front of the aggregate. Glycol-treated oriented aggregates of all samples were X-rayed to detect the presence of expandable montmorillonite. All slides giving any indication of the presence of chloritic material were heated to from 450° to 550° C. to establish its identity.

Varieties and Amounts of Clay Minerals

Interpretation of X-Ray Data

The principal clay minerals present in underclays are illite, a poorly crystallized type of kaolinite which varies somewhat in its degree of disorganization, and mixed-layer illite-montmorillonite or more rarely illite-montmorillonite-chlorite; about one-third of the samples also contain a 14 Å chloritic mineral. Montmorillonite never occurs as separate mineral grains but is always mixed-layered with other minerals. All spectrometer traces of glycol-treated samples show a broadening or shifting of the 001 illite peak, but a distinct 17 Å reflection never appears. Powder patterns were made of about 10 per cent of the samples, some of which contain 14 Å clay; all showed prism reflections for dioctahedral clay minerals only. This evidence and the relative intensities of the basal reflections on the spectrometer traces indicate that aluminous clay minerals are the dominant variety in underclays.

As previously mentioned, the coarser less-than-2-micron particles tend to settle first during preparation of oriented aggregate slides. The 14 Å chloritic material is almost always more abundant in the coarser fraction on the backs of these slides. The relative amounts of kaolinite and illite on the fronts and backs of slides are fairly constant, but when appreciable differences are noted, either is likely to be more abundant in a given particle size. Mixed-layer material commonly is most abundant on the fronts of the oriented slides.

The 14 Å chloritic mineral was classified into one of four groups depending upon the effect of heat treatment to 450° C. on the first three basal X-ray reflections.

CLASS 1: When heated to 450° C. and air-quenched, the 14 Å peak disappears and the 7 Å peak does not change, which indicates that the 7 Å reflection is due solely to kaolinite. This variety rarely gives a 4.7 Å (003) peak.

CLASS 2: The 14 Å and 4.7 Å peaks disappear, and the decrease in the 7 Å peak height is usually less than the height of the original 14 Å peak.

CLASS 3: The 14 Å reflection is little changed, but the 4.7 Å peak disappears, and the 7 Å peak height decrease approximates the height of the 14 Å reflection. Further heating to 550° C. for half an hour in most cases enhances the 14 Å peak.

CLASS 4: The 14 Å and all higher basal orders remain unaffected at 450° C. However, when heated to 550° C. the 14 Å peak is enhanced, and higher orders disappear. The shift in intensities of the basal peaks by heat treatment to 550° C. is attributed by Brindley and Ali (1950) to a partial dehydration of the brucite layer.

The most widely used criteria for distinguishing chlorite and vermiculite, the two common 14 Å minerals, is the collapse of vermiculite from 14 Å to about 10 Å when heated to 300° or 400° C. because of the breakdown of the brucite layer, whereas chlorites are stable up to 600° C. On this basis Class 1 14 Å minerals are vermiculites; the low intensity of the higher-order basal X-ray reflections of the class 1 minerals is also characteristic of vermiculite. Class 4 includes fairly good chlorites. Classes 2 and 3 represent intermediate stages between vermiculites and chlorites. All the classes are transitional into the next, and in a few cases slight expansion of class 1 vermiculites with glycol treatment indicates some transitional tendency toward montmorillonite.

The relative amount of each clay component in a sample was evaluated on the basis of the relative areas enclosed by the peaks of the first-order basal reflections. Clays giving 001 peaks of equal sizes are recorded as present in equal amounts. This system is substantiated by experimental evidence only in part. Artificial mixtures of several poorly crystallized kaolinites with several illites or illite-montmorillonite mixed-layer clays (Schultz, 1955) show that these are best compared on a 1:1 basis. The use of the 1:1 ratio to evaluate the relative amounts of illite, illite-montmorillonite, and chlorite is not experimentally substantiated. However, the writer believes that the values are of the correct order of magnitude. Since all samples are analyzed in the same manner, results are good for comparative purposes.

Construction of Pie Diagrams

The manner in which X-ray traces of underclay samples were interpreted is illustrated in Figure 1. Traces of the front and back of the slide prepared from a typical sample are shown with one of the front after glycol treatment and one of the back after heat treatment to 450° and 550° C. First the areas of the 7 Å and 10 Å peaks of the front were obtained; the area is considered to be the sum of peak heights at the peak position and at half-degree intervals on either side of the peak position. The 7 Å/10 Å area ratio gives 41 per cent kaolinite and 59 per cent illite and mixed-layer material. Next the 10 Å peak on the trace of the glycol-treated slide was divided into an illite peak and a low-angle bulge representing the mixed-layer illite-montmorillonite. The areas were added up, and the illite/mixed-layer ratio was calculated to be 62/38. The proportion of montmorillonite to illite in the mixed-layer material is calculated by assuming that the mean position of the 001 diffraction in the interval between the 10 Å position of illite and the 17 Å position of glycol-treated montmorillonite will be proportional to the relative amounts of illite and montmorillonite in the mixed-layer component. The mean position of the 001 diffraction for the mixed-layer area is at 7.2° 2θ, corresponding to 12.27 Å, which is 2.27/7 of the way between 10 Å and 17 Å. Therefore, in the mixed-layer material the proportion of montmorillonite/illite = 2.27/7 = 32/68. From these figures the percentage of each component was calculated.

The peak area ratio was also calculated for the trace of the back of the slide and gave 7 Å/10 Å = 42/58 per cent. The 14 Å chlorite peak with a height of 30 counts represents a class 3 chlorite, since the peak persists after the slide is heated to 450° C., and the 7 Å peak height decrease almost equals the 14 Å peak height. The 4.7 Å peak also disappears. Therefor, the original 7 Å peak is the result of reflection from both chlorite and kaolinite particles. The 7 Å area per cent of 42 is broken into kaolinite and chlorite by subtracting the 30 peak height count of chlorite from the 260 7 Å peak height count and assuming that the remaining 230 counts represent kaolinite. The kaolinite/chlorite height ratio is then 230/30 = 87/13 = 37/5; of the 42 per cent clay which gives a 7 Å reflection, 37 per cent is interpreted as kaolinite and 5 per cent as chlorite.

To facilitate rapid comparison of samples the mineral per cents calculated as above are represented as slices of a pie diagram. The 32 per cent montmorillonite content of the mixed-layer component is represented by a line from one corner of the slice to a point on the opposite leg 0.32 times the radius in from the outside of the circle (shown by bracket). This system does not give an area which is directly proportional to the amount of montmorillonite in a sample. However, it is used to facilitate approximate recovery of the data by inspection, since the distance along a line is more easily estimated than is the area of a segment of a wedge-shaped slice. The kaolinite and chlorite contents of the back of the slide are represented on the outer circle of the pie. The class 3 chlorite is indicated by putting three dots in the chlorite segment (two dots were used for class 2 chlorites, etc.). No dots are shown for 14 Å components of unknown type.

The most common expression of glycol-treated mixed-layer material on the spectrometer traces is an asymmetrical bulge on the high-angle side of the illite peak as shown in Figure 1. Less commonly the mixed-layer material gives a distinct 001 peak separate from that of the illite. In this case, the segments representing the amounts of illite and montmorillonite in the mixed-layer clay are separated by an arc, the radius of which is proportional to the amount of illite.

Another clay component not illustrated in Figure 1 is a chloritic component in the mixed-layer material which appears on the spectrometer trace as a high-angle bulge on the illite peak after heating to 450° C. The relative areas of the bulge and the symmetrical 10 Å peak are taken to be indicative of the amount of mixed-layer chlorite, just as the amount of mixed-layer montmorillonite is evaluated from the glycol-treated slide in Figure 1. In some samples the presence of mixed-layer chlorite was determined, but the amount could not be evaluated. For these samples the chlorite is shown as a corner of the pie slice representing mixed-layer illite-montmorillonite. If the amount of any clay component could not be determined, its segment boundaries on the pie diagram are approximated with wavy lines.

Arrangement of Pie Diagrams in Figures

Figures 2 to 12 show the clay-mineral analyses of the fine fraction of all samples investigated. Locations and sources of outcrop data are listed in the Appendix. Pie diagrams are arranged on the figures to show relative positions of the samples within and adjacent to the underclay outcrops. Columns of contiguous

SMOOTHED SPECTROMETER TRACES

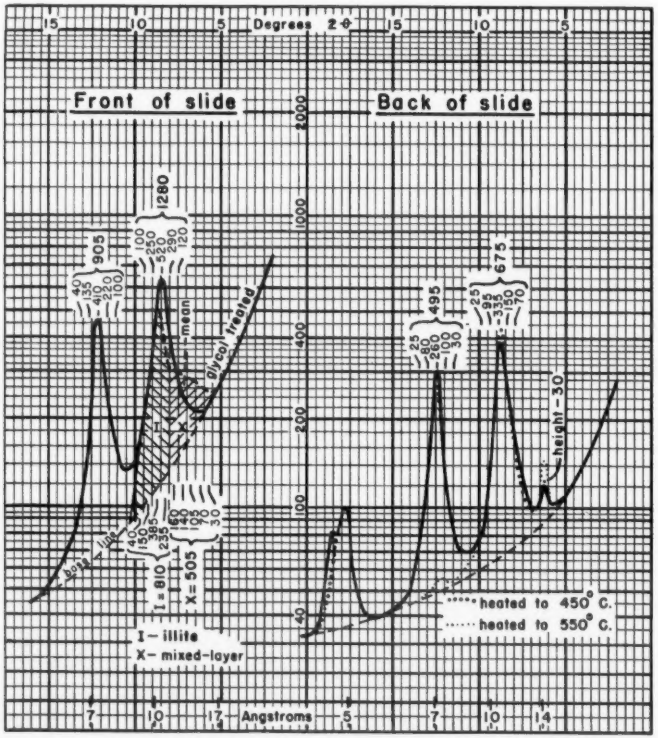

CALCULATIONS

Front of slide

K-Kaolinite
I-Illite
X-Mixed-Layer
M-Montmorillonite
Cl-Chlorite

$$\frac{K}{I+X}=\frac{905}{1280}=\frac{41\%}{59\%}$$

$$\frac{I}{X}=\frac{810}{505}=\frac{62\cdot 59}{38\cdot 59}=\frac{36\%}{23\%}<\quad M=\frac{2.27}{7.0}=32\%$$

Back of slide

$$\frac{K+Cl}{I+X}=\frac{495}{675}=\frac{42\%}{58\%}$$

$$\frac{K}{Cl}=\frac{260-30}{30}=\frac{87\cdot 42}{13\cdot 42}=\frac{37\%}{5\%}$$

PIE DIAGRAM

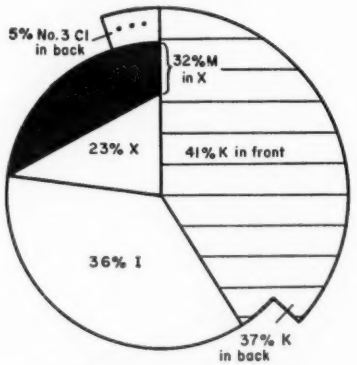

FIGURE 1.—CALCULATION OF MINERAL PERCENTAGES FROM SPECTROMETER TRACES

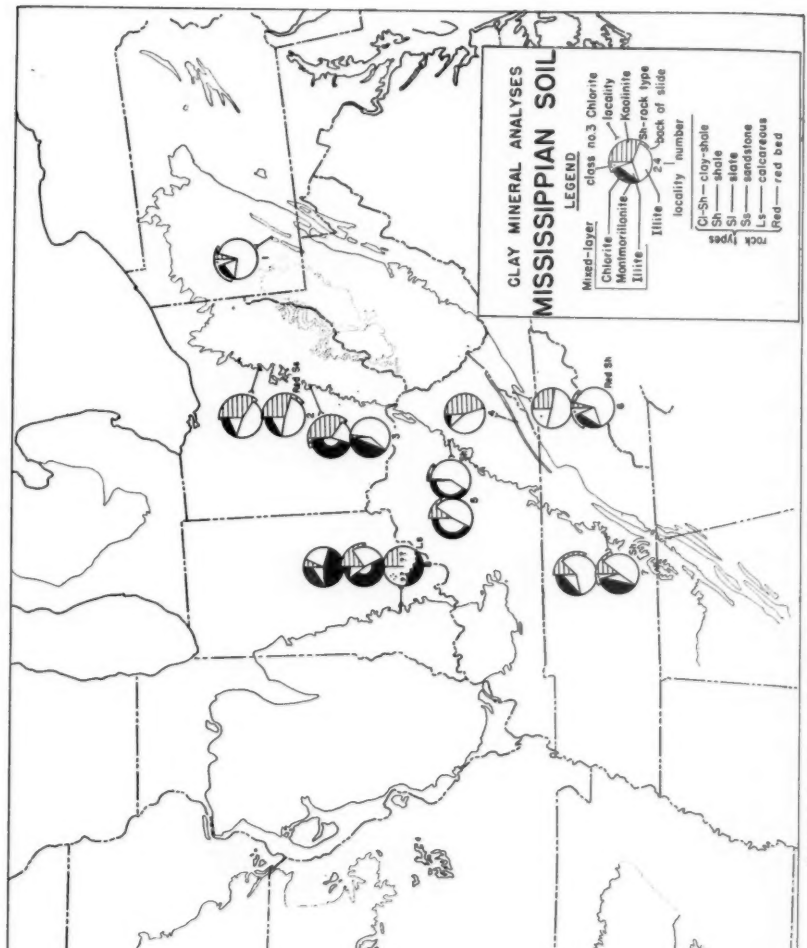

FIGURE 2.—CLAY-MINERAL ANALYSES: MISSISSIPPIAN SOILS

pie diagrams represent samples from successively lower stratigraphic positions within the outcrop. Abbreviations to the right of the pies indicate samples from rock types other than underclay (*e.g.*, "sh" = shale). The word "coal" to the right of the column (*e.g.*, Fig. 6, outcrop 1) indicates that a coal intervenes between the two beds sampled; in most cases the lower sample is an underclay, and the upper is a shale from above the coal. Two horizontally contiguous pies represent samples taken at the same horizon a short lateral distance apart.

Relationships Between Mineralogical Determinations and Field Observations

Underclay Profiles

One of the leading theories on the origin of underclays has been that they are residual soils. Were this the case, one would expect to find some indication of a soil profile in the distribution of the clay minerals. Pennsylvanian coals are thought to have formed in a humid climate. Although the climate is generally thought to have been warm and humid, Giles (1930) believes it may well have been a cool or temperate climate. As summarized by Grim (1953, p. 340–345), illite and, to a lesser extent, montmorillonite characterize the soils of cool, humid climates, whereas kaolinite is the characteristic mineral of soils in warmer, humid climates in areas of good drainage. Montmorillonite may precede kaolinite development during initial stages of soil formation (Sherman, 1952, p. 156), and soil development may not advance beyond the montmorillonite stage in poorly drained, black-soil areas (Grim, 1953, p. 342; Sherman, 1952, p. 157; Rolfe, 1954). A vermiculitic clay has been reported in soils from both warm (Rolfe, 1954; Pearson and Ensminger, 1948) and cool (Walker, 1947; Brown, 1953) climates. In very warm, humid, tropical climates, intense leaching in a well-drained soil would produce a laterite characterized by kaolinite and the hydrated oxides of aluminum and iron.

To determine whether the mineralogy of underclay profiles shows features indicative of lateritic weathering, numerous underclay exposures were sampled at intervals from top to bottom. As mentioned above, samples from various positions within an underclay profile are shown on the plates as vertical columns of contiguous pie diagrams. For example, four samples were taken at outcrop 10 of zone 6 (Fig. 8), three of which were from an underclay below the Lower Kittanning Coal, one at the top, one at the bottom, and one at an intermediate position. The fourth pie at the bottom represents a shale sample from just below the underclay. The shale sample is not considered in this section. Although not shown in the figures, large mica flakes and feldspar were also classified as absent, present, or abundant, and the amounts are compared on Table 2.

Table 2.—Mineral Composition Variations in Underclay Profiles

	Top	Same	Bottom
Kaolinite more abundant	31*	38	33
Montmorillonite more abundant	29	60	6
Feldspar more abundant	10	13	8
Mica more abundant	4	9	39
14A° mineral more abundant	6	12	31
14A° mineral more Vermiculitic	5	21	4

* in 31 profiles the top was more kaolinitic than the bottom

Mineralogical variations within underclay profiles (Table 2) were initially tabulated separately for the different stratigraphic zones, but since no significant variations were noted between the older and younger horizons, only the totals for all underclays are given. The first line shows the distribution of kaolinite. In 31 profiles the kaolinite was most abundant at the top of the underclay, in 33 cases the reverse was true, and in 38 profiles there was no significant variation—that is, the top and bottom were the same within 5 per cent. The kaolinite content does not vary significantly within the profiles. The quality or degree of crystallinity of the kaolinite also does not vary, because the kaolinite from the bottom of the profile is as poorly organized as that from the top of the same underclay.

The abundance of montmorillonite in mixed-layer material, of feldspar, and of mica is listed

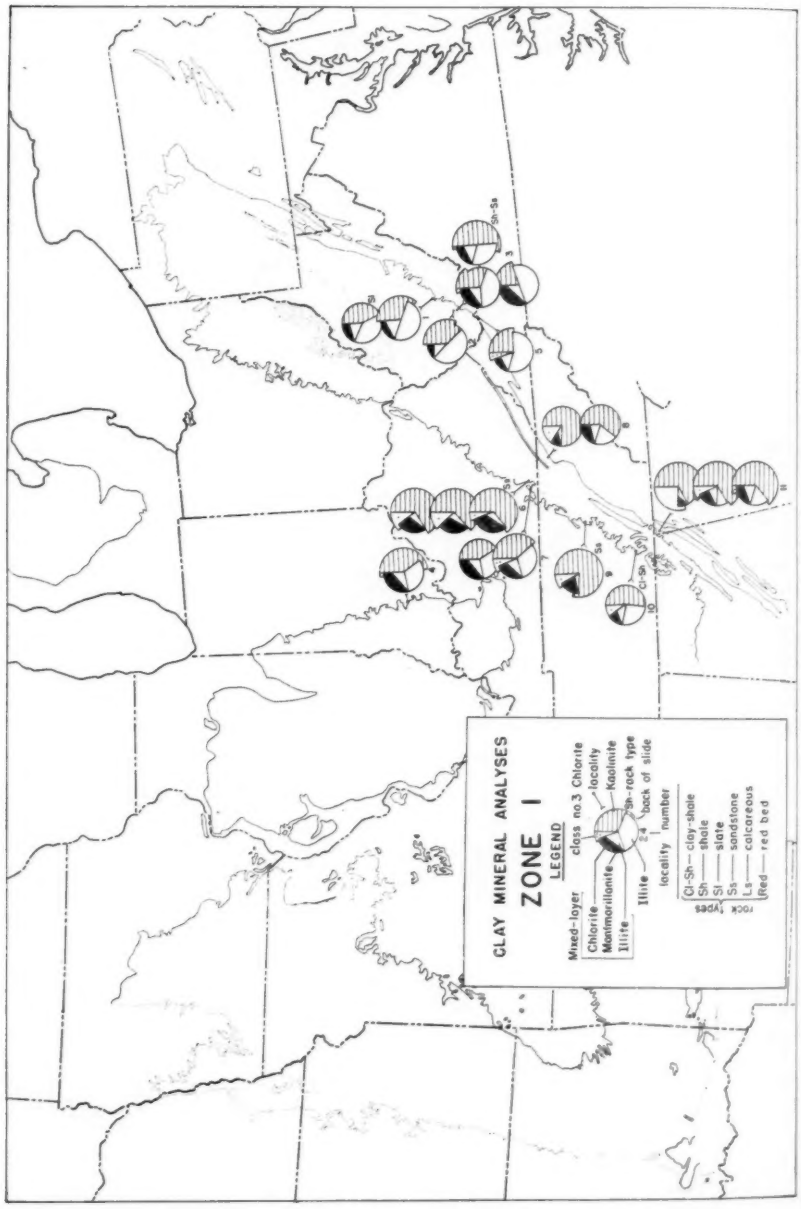

FIGURE 3.—CLAY-MINERAL ANALYSES: ZONE 1

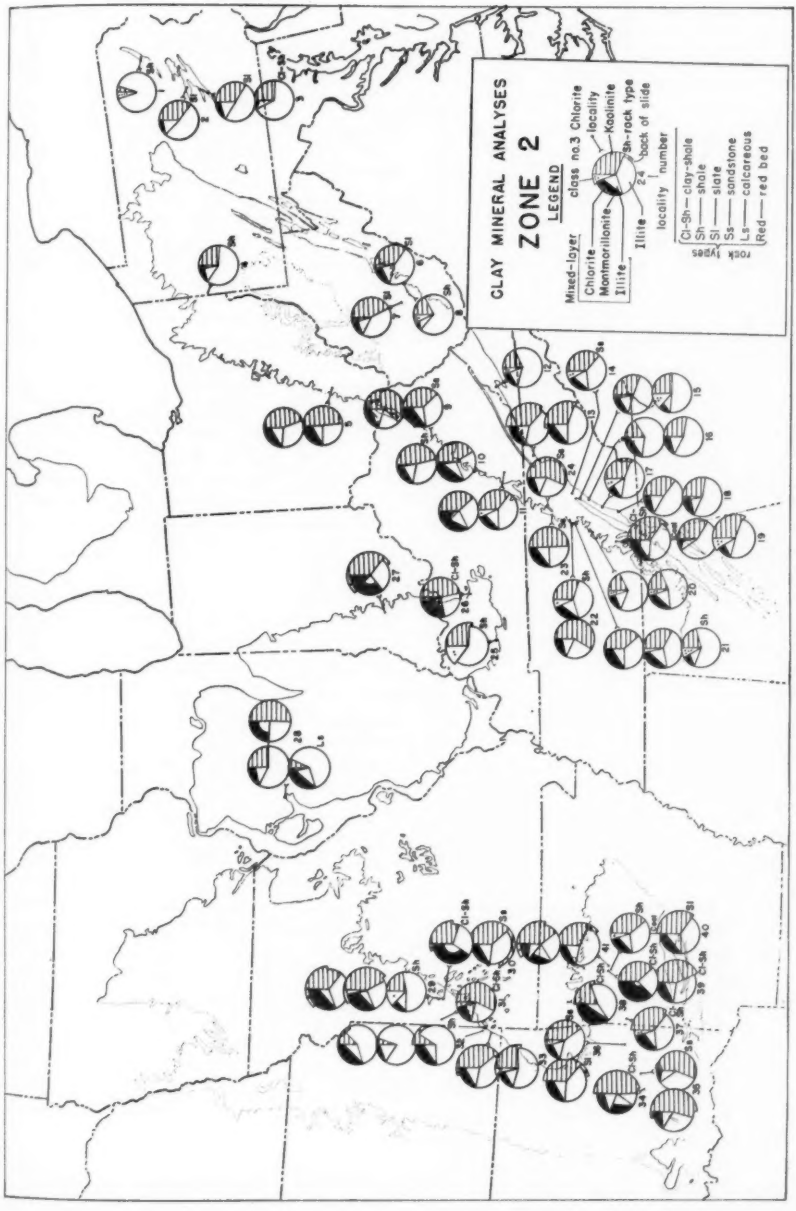

FIGURE 4.—CLAY-MINERAL ANALYSES: ZONE 2

FIGURE 3.—CLAY-MINERAL ANALYSES: ZONE 1

in Table 2 the same way as the kaolinite. The mixed-layer montmorillonite tends to be more abundant toward the top, and mica is much more abundant at the bottom of the underclay. In general, the abundance of feldspar shows no consistent variations throughout underclay profiles.

Chloritic minerals in underclays are classified in two ways in Table 2. First chlorites from tops and bottoms of underclays are compared on the basis of their abundance, regardless of the type of 14 Å material present. Next, they are classified on the basis of the type of chloritic mineral without regard to the amount present. The amount of chloritic mineral in an underclay is generally greatest in the bottom of the bed, but the type of chloritic mineral shows no consistent variation.

Other variations in abundance of minerals throughout underclay profiles were noted. Quartz is almost everywhere more abundant in the lower part of an underclay; in many cases underclays grade downward into sandstones. Mixed-layer clays having chlorite as a component in most places occur at the tops of underclays. In 15 occurrences where profile variations were studied, the mixed-layer illite-montmorillonite-chlorite occurred either at the top or throughout the profile but was never most abundant at the base of the underclay.

Absence of strong soil development at the site of deposition is indicated by a lack of consistent variations in kaolinite and feldspar content throughout underclay profiles. In general feldspar does not decrease nor does kaolinite increase in amount toward the top of the profile, as would be expected if intensive weathering had taken place since deposition. However, some of the profile features indicate a mild form of soil development. Abundance of mixed-layer clay at the top of the underclays, both of the illite-montmorillonite type and the type containing a 14 Å component, could be the result of weathering in a poorly drained environment. Such an environment is compatible with the common presence of coaly material and pyrite, both of which would be destroyed under well-drained conditions. This environment would also account for the lack of kaolinite profile variations, since kaolinite would not tend to develop where drainage is poor. Also, the greater abundance at the bottom of underclays of 14 Å material as distinct mineral grains rather than as a mixed-layer component can be explained by alteration of this material in the top of the underclay. Concentration of calcite and iron as concretions and fracture fillings in the bottoms of some underclays also indicates mild leaching by soil-forming processes.

Other profile variations, however, contradict the theory that underclays were subjected to even mild soil leaching. Chlorite, a mineral easily destroyed by weathering, occurs in the upper parts of underclays in as many places as does vermiculite, the more stable form of 14 Å material in soils. The underclay profile variations which have been noted do not coincide with those in modern soils involving a similar mineral assemblage which have been studied by Brown (1953), Rolfe (1954), and Pearson and Ensminger (1948). Although in many cases the proportions of the clays do not vary throughout the modern profiles, when they do vary, kaolinite is most prominent near the top of the soil, mixed-layer clay is most abundant near the base of the soil, and vermiculite, if present, is most abundant in the upper part of the soil. Also, in the modern soils, muscovite is persistent throughout the profile, whereas it is clearly concentrated at the base of underclays.

A consideration of particle-size variation of underclay minerals suggests an alternative explanation for their distribution in underclay profiles. The mica flakes used as a measure of the amount of muscovite are those not passing the 62-micron (350-mesh) sieve. Quartz also tends to be coarse-grained. As shown on the pie diagrams, 14 Å material is almost everywhere more abundant in the coarser backs of the settled slides than in the finer part on the fronts. On the other hand, mixed-layer clay tends to be most abundant in the fronts of the settled slides. Similarly, the coarser-grained minerals, quartz, muscovite, and chlorite, are most abundant in the bottoms of underclays, whereas fine-grained mixed-layer clay tends to be concentrated at the tops. Such a distribution of quartz, muscovite, mixed-layer, and 14 Å material can be explained as a simple sedimentary feature: that is, the carrying power of the transporting agent progressively decreased as the underclay was being deposited.

Relationships Between Underclays and Other Rock Types

General.—The mineralogy of underclays is compared with that of other closely related rock types, such as shales, sandstones, limestones, and red beds in Table 3. The mineralogical differences and similarities between

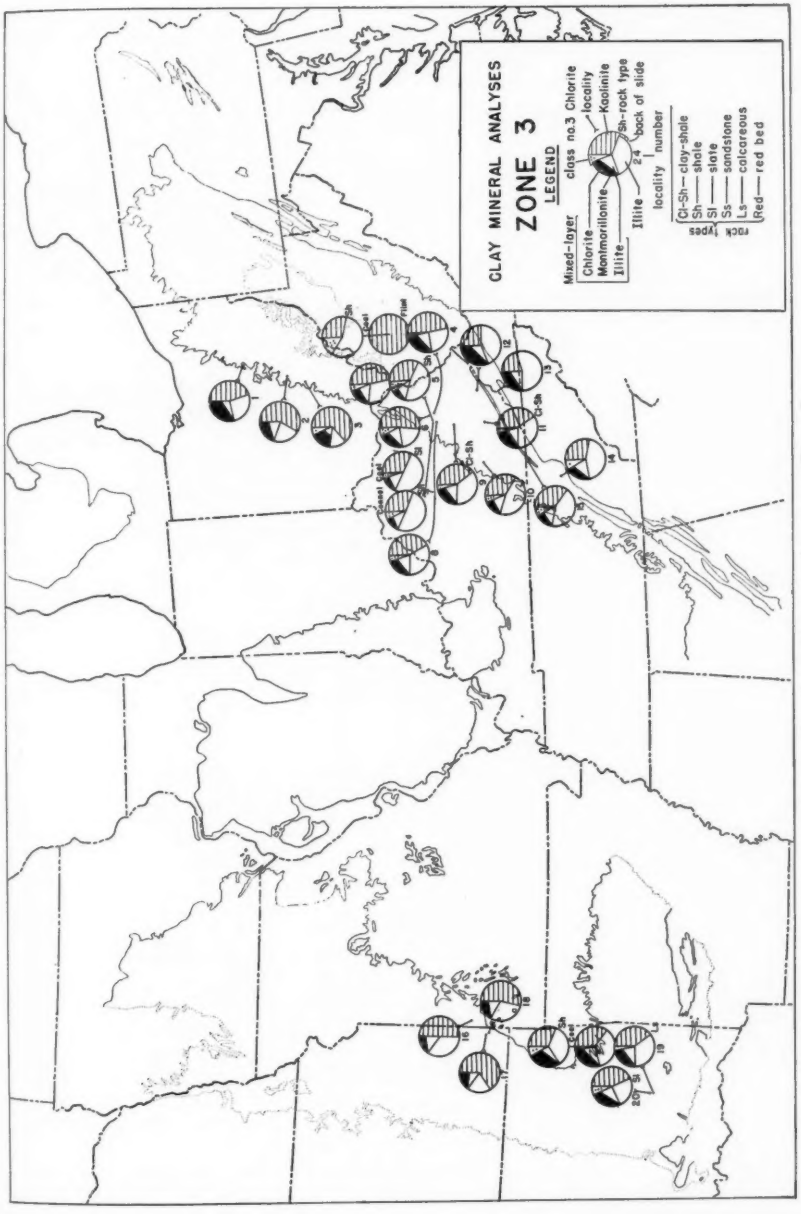

FIGURE 5.—CLAY-MINERAL ANALYSES: ZONE 3

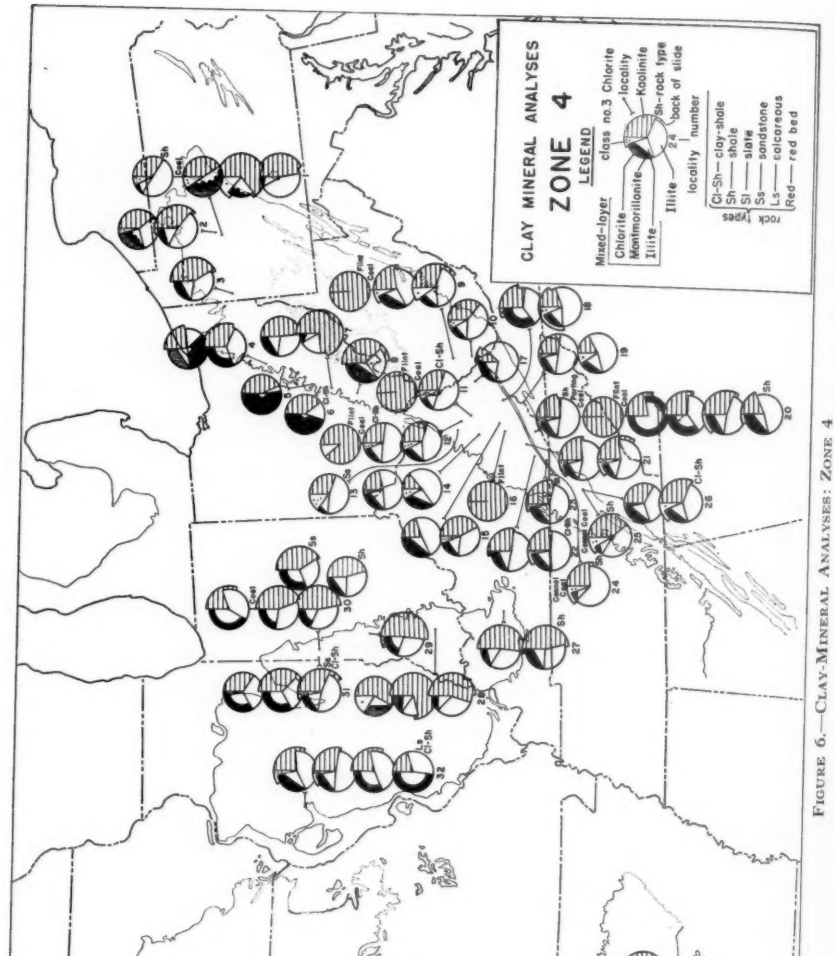

FIGURE 6.—CLAY-MINERAL ANALYSES: ZONE 4

the various rock types must be taken into account by any explanation of the origin and of the unique physical properties of underclays.

Shales.—For comparison with underclays, shales are divided into two categories: those above the coal, and those more closely related to the underclays below the coal. The latter occur at various positions with respect to the underclay. Most of them are below the underclay, but a few occur within the underclay, between the underclay and coal, or as a lateral equivalent of the underclay. Included with the shales below the coal are nine samples of a hard, black, fissile rock, with excellent plant impressions on the bedding surfaces, which is commonly called slate in the eastern coal fields.

As shown in Table 3, in 10 cases the shale above the coal was less kaolinitic than associated underclay, in three cases the kaolinite content was the same, and in only one case was the shale more kaolinitic. The kaolinite content of the shale would average perhaps two-thirds that of the associated underclay; the difference is greatest in areas of highly kaolinitic underclays. The kaolinite of the shale tends to be better crystallized than that in underclay. The shales also tend to contain less mixed-layer montmorillonite, and the 14 Å mineral is commonly more abundant and of a better crystallized, more chloritic variety.

The differences between underclays and the more closely related shales below the coals are much less pronounced. In 10 cases the shale was less kaolinitic, in 24 cases no significant difference was noted, and in 8 cases the shale was more kaolinitic. The kaolinite content of the underclays and shales below the coals appears to be about the same. However, the shales do tend to contain slightly less mixed-layer montmorillonite, although not so little as in the case of the shales above the coals.

Shale samples from zone 6 (Fig. 8) illustrate some of the generalizations made above. In Vermillion County, Indiana (outcrop 28), a maximum variation between a shale above the coal and the underclay is shown. The kaolinite content of the underclay averages 89 per cent; that of the shale is only 35 per cent. Of the remaining clay material, mixed-layer montmorillonite is proportionately more abundant in the underclay. In the Mid-Continent Basin, where the underclays are much less kaolinitic, the shale-underclay relationship still holds. For example, in Crawford County, Kansas (outcrop 36), the shale from above the coal contains about two-thirds as much kaolinite as the underclay and much less mixed-layer montmorillonite, whereas the shale from below the underclay is much more similar to it.

Sandstones.—Underclays commonly grade down into sandstones, and in places the coal rests directly on argillaceous sandstones which contain plant impressions similar to those of underclays. The relative abundance of kaolinite and mixed-layer material in the clay fractions of underclays and sandstones is summarized in Table 3. Generally speaking, the clay in sandstones is similar to that in near-by underclays. It contains about the same amount of kaolinite and the same or a slightly smaller amount of mixed-layer montmorillonite. For example, at Oak Hill, Ohio (zone 6, outcrop 15), the clay of the sandstone at the base of the underclay contains about the same proportion of kaolinite as the underclay and slightly less mixed-layer montmorillonite.

If the sandstones have not been appreciably altered subsequent to deposition, then the clays of the sandstones are indicative of the material brought in by the streams, and the similarity of the clays of the sandstones and underclays necessitates little or no post-depositional alteration of the underclay materials. However, the assumption that the sandstones have not been altered is equivocal. In any event, similarity of sandstone and underclay argillic components indicates that either each ex-

TABLE 3.—MINERALOGICAL RELATIONSHIPS BETWEEN UNDERCLAYS AND ASSOCIATED ROCKS

In one case (*) a shale from above the coal was more kaolinitic than the associated underclay below the coal.

	More	Same	Less
Shale above coal			
Kaolinite	1*	3	10
Montmorillonite	1	5	8
Shale below coal			
Kaolinite	8	24	10
Montmorillonite	5	17	20
Sandstone			
Kaolinite	5	10	4
Montmorillonite	2	11	6
Calcareous rocks			
Kaolinite	5	10	2
Montmorillonite	3	12	2
Redbeds			
Kaolinite	3	4	4
Montmorillonite	6	2	1

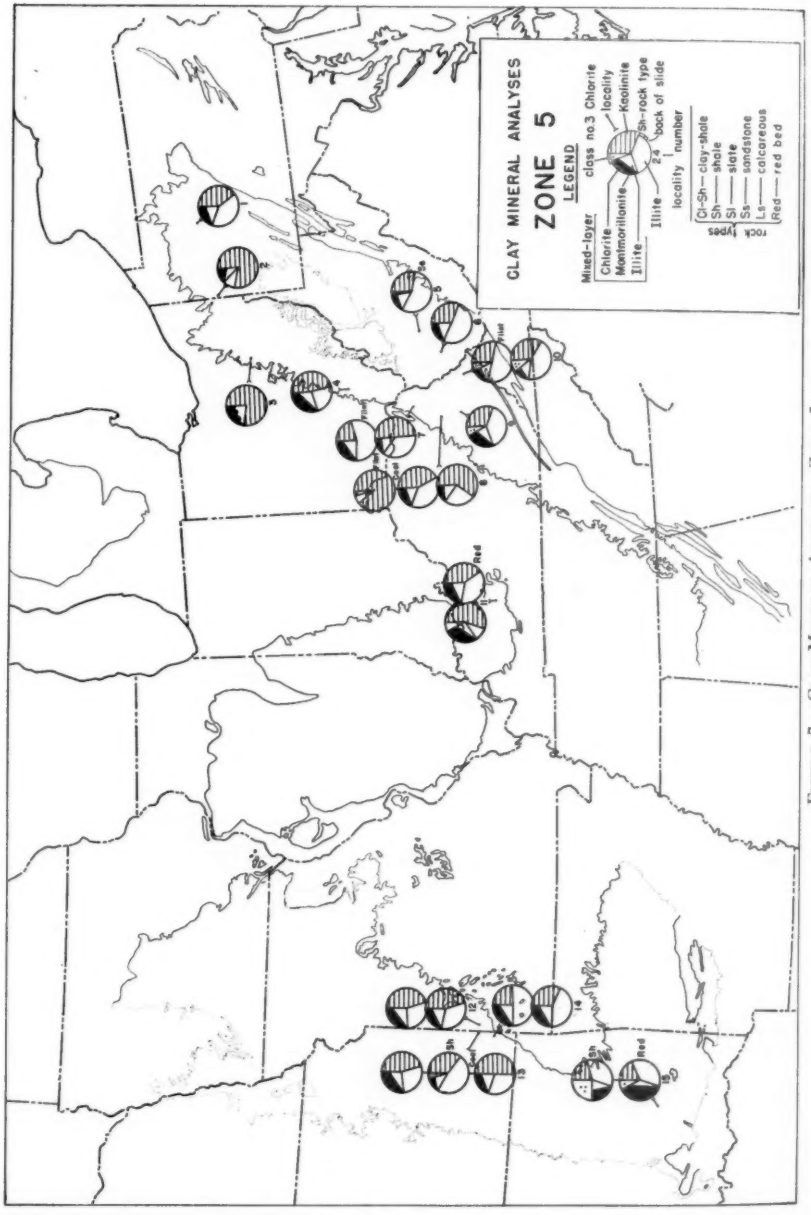

FIGURE 7.—CLAY-MINERAL ANALYSES: ZONE 5

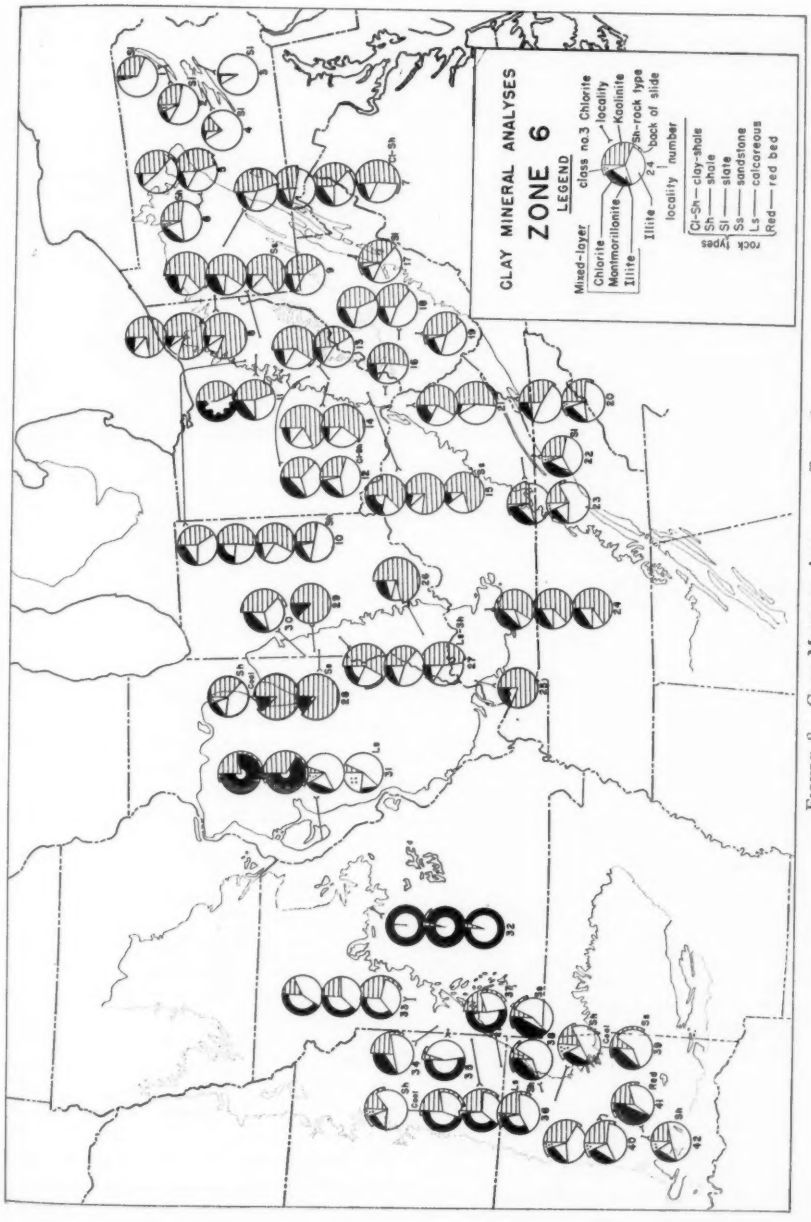

FIGURE 8.—CLAY-MINERAL ANALYSES: ZONE 6

FIGURE 7.—CLAY-MINERAL ANALYSES: ZONE 5

perienced nearly the same amount of weathering in place, or that no alteration of either occurred after deposition. If the clays of the sandstones differed considerably from the underclays, post-depositional alteration would have been indicated. The slightly less mixed-layer clay content of some sandstones may be related to particle size, because the transporting streams would tend to carry fine mixed-layer clay beyond sites of sandstone deposition.

Calcareous rocks.—Calcite is one of the first minerals removed by soil leaching. No kaolinite would form before all the calcite had been dissolved. Therefore, if the mineralogy of noncalcareous underclays is similar to that of calcareous underclay equivalents or to the argillaceous part of associated fresh-water limestones, no change in mineralogy after deposition would be indicated. As shown in Table 3, the kaolinite and mixed-layer montmorillonite content of calcareous rocks below coals is similar to that of noncalcareous underclays. The calcareous rocks also have similar amounts of chloritic components. For example, the calcareous lower part of the profile sampled at outcrop 32 of zone 4 (Fig. 6) is similar to the noncalcareous samples from the upper part of the underclay.

Red beds.—Red beds have been reported by several investigators (Waage, 1950, Fig. 10; McQueen and Greene, 1938, p. 23; Kansas Geological Society, 1937, p. 63, 70, 83; Cline, 1941, p. 26) as a lateral equivalent of underclays. Red-bed localities were probably relatively high, well-drained areas from which material could have been washed into the adjacent low-lying swampy areas where underclays and coals were deposited. The well-drained, oxidized, red-bed environment seems better for kaolinite development than does the poorly drained, reducing swamp environment.

Red-bed samples showing several types of areal relationships with coals and underclays were taken: (1) at a considerable lateral distance from the underclay and only approximately at the same stratigraphic horizon, (2) grading within a very short lateral distance into coals and underclays, and (3) directly underlying the coal bed. Examples of the long-range relationship are the red-bed samples taken from zones 5, 6, and 10 from central Oklahoma, which are compared with underclays farther north. Examples of the short-range comparison are most numerous from the shelf areas in zones 9 and 10.

The mineralogy of red beds is compared with that of underclays in Table 3. Red beds appear to be as kaolinitic as the underclays and to contain even more mixed-layer montmorillonite. On this basis red-bed areas seem a possible place for development of the high kaolinite and mixed-layer content of underclays. However, red beds are most abundant in the upper Pennsylvanian sediments, whereas the most kaolinitic underclays are those of lower Pennsylvanian age. On this basis, red beds could be at best only a minor source of materials for the highly kaolinitic, lower Pennsylvanian underclays.

Mississippian soils.—One source considered for the highly kaolinitic underclays of the lower Pennsylvanian strata is a regolith which may have developed between Mississippian and Pennsylvanian deposition. In the Appalachian shelf area of Ohio and Pennsylvania, for example, the highest Mississippian formation is the Maxville Limestone at the top of the middle Mississippian; the lowermost Pennsylvanian bed found in this area is the Sharon Conglomerate which is younger than 700 feet of lower Pennsylvanian (Pocahontas) beds in southern West Virginia. Thus the interval for possible regolith formation extends over the entire upper Mississippian (Chester) and at least part of the lower Pennsylvanian.

Samples were collected at the Mississippian-Pennsylvanian contact from what appeared to be Mississippian soils as well as from some of the normal rocks below the soils. The mineralogy of the clay-size fraction of these samples is shown in Figure 2. The samples are not notably kaolinitic, which indicates that they are not a major source of underclay materials.

Field Evidence of Coal-Underclay Time Relationships

Figure 13 illustrates types of field relationships pertinent to the time of underclay development. Figure 13*a* is of an outcrop of the Ravenscroft Coal in White County, Tennessee (zone 2, outcrop 21). The edge of a channel sandstone intervenes between the underclay and coal and must therefore intervene between their times of formation. Figure 13*b* shows faulting relationships observed in a Summit Coal outcrop near Ft. Scott, Kansas (zone 7, outcrop 11; analyses in Figure 9 are for the Mulky Coal underclay of zone 7, not for the overlying Summit Coal underclay which exhibits the illustrated faulting relationship). The underclay formed, was faulted, and the

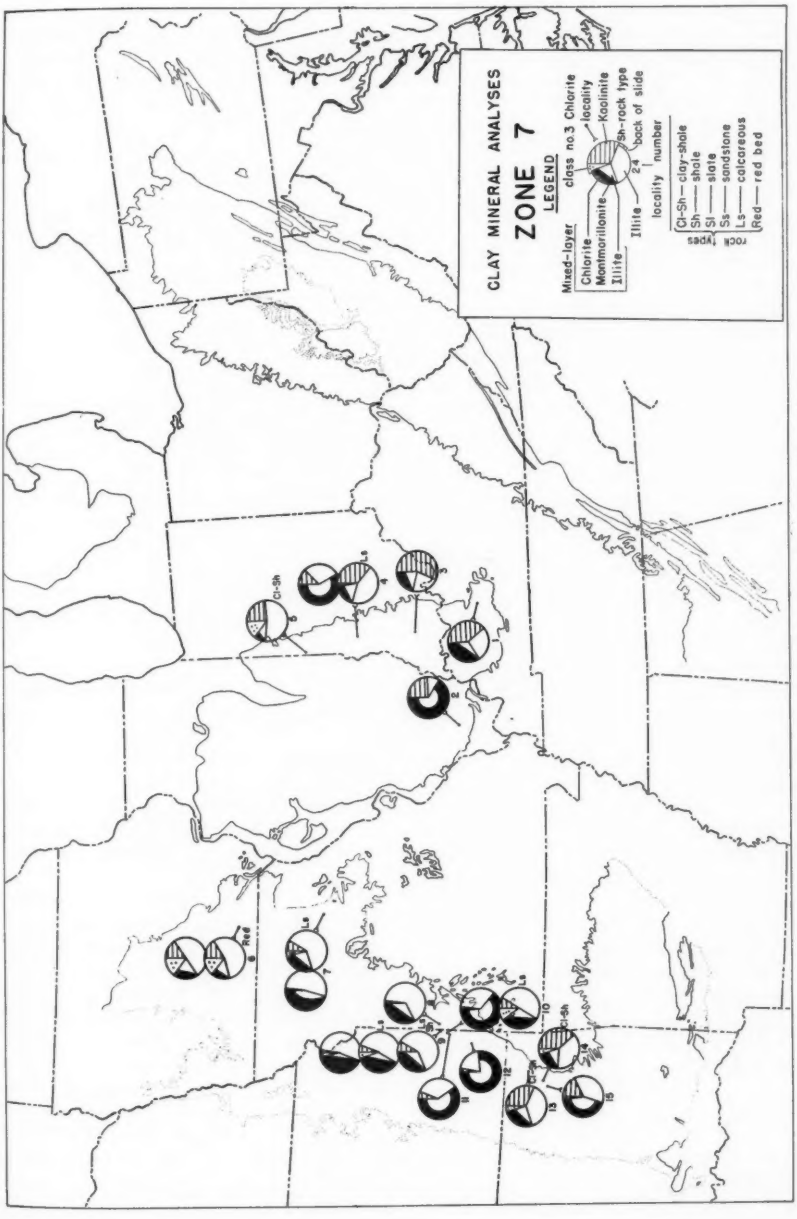

FIGURE 9.—CLAY-MINERAL ANALYSES: ZONE 7

scarp planed off; the coal was then deposited and later faulted.

If the underclays were a soil formed by leaching by organic acids derived from coal-forming plant material, one might expect some relationship between the thickness of the coal and of the underclay within a limited area. Previous observations (Ries, 1927, p. 29; Stout, 1923, p. 551; Weller, 1930, p. 123) indicate that there is no such relationship. Some underclays have no overlying coal, and some coals are not underlain by underclays. The underclays sampled for this study also showed no relationship between coal and underclay thickness or between these and the mineralogy of the underclays.

The fairly common occurrence of shales, limestones, and in one case (zone 8, outcrop 23) a marine brachiopod-bearing shale between underclays and their overlying coals also tends to separate their times of formation. The plants of the coal bed could hardly have been responsible for formation of the underclay without affecting the intervening layers.

The field observations described above divorce coal and underclay formation in time but do not necessarily indicate that organic acids from vegetation which may have decayed before coal formation did not form a soil. The outcrop illustrated by Figure 13*c* is in a clay pit in Holmes County, Ohio (zone 8, outcrop 5). Samples *a* and *b* are from the thin underclay on the edge of the channel; samples *c* and *d* came from the thick underclay in the center of the channel. In outcrop 1 of the same zone, sample *c* is a similar channel flank equivalent of samples *a* and *b*. Thickening of these Middle Kittanning underclays is much more readily explained as channel filling by transported argillaceous material than as a soil feature. The minerals of the samples suggest that the channel fillings were not washed in from the channel flanks but came from some more distant source. Another feature that indicates little or no soil formation on underclays is the common preservation of such delicate features as plant impressions and tiny coal bands that would be destroyed by burrowing roots.

Slickensides and Flint Clays

The soil theory of the origin of underclays explains slickensides as the result of slipping during compaction after the underclay was churned and loosened by burrowing roots. Since underclays apparently are not soils, some other explanation is needed.

The best explanation of slickensiding in underclays is the hypothesis of compaction of a sediment deposited in a loose, hydrous condition. The process is tentatively believed to be related to the content of organic and clay material. Montmorillonite more than any other clay bonds and holds water. Although there is no close relationship between slickensides and the minerals of underclays, mixed-layer montmorillonite-illite usually in amounts greater than 25 per cent is a characteristic component and is the only clay material common to all plastic underclays. Although nonslickensided, bedded shales above the coal may contain abundant organic material, they characteristically contain little mixed-layer montmorillonite.

TABLE 4.—ORGANIC CONTENT AND SLICKENSIDING IN UNDERCLAYS

	Nongray	Gray
Slickensided	4	96
Nonslickensided	54	91 (very sandy 72, 19)

The relationship between slickensides and the organic content of underclays as reflected in their gray color is summarized in Table 4. With only four exceptions, slickensides were found only in the gray, nonsandy underclays. Most of the gray underclays that were not slickensided were very sandy. It would be expected that abundant sand grains would minimize the tendency of the unconsolidated material to hold water and would also key potential slip planes together, thereby preventing slickensiding.

Organic material may, in some cases, cause flocculation of clays. The common association of organic material with slickensiding suggests that the organic material did cause flocculation of the underclay materials which, perhaps in conjunction with montmorillonite, caused entrapment of abundant water in the sediments. Slipping during compaction not only could develop the slickensides, but also could disrupt any bedding tendencies in the sediment.

In addition to being a factor in development of slickensides, the high mixed-layer montmorillonite content of underclays is also a probable explanation for their plasticity. As previously mentioned, typical plastic underclays contain more mixed-layer montmorillonite than do the associated shales of Pennsylvanian

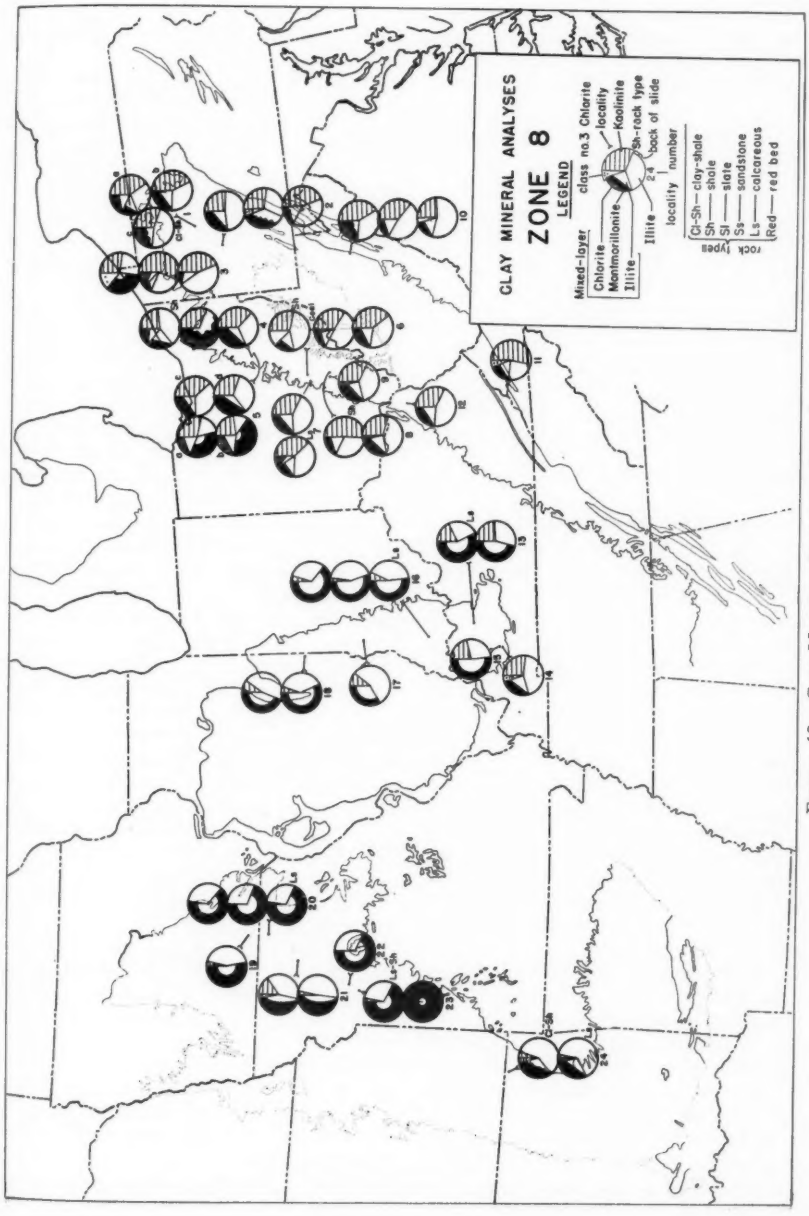

FIGURE 10.—CLAY-MINERAL ANALYSES: ZONE 8

age. Hard, nonplastic flint clays apparently contain no montmorillonite, mixed-layer or otherwise. This generalization is based on the literature, which gives no reference to montmorillonite in flint clays, and upon a few samples collected by the writer. The criteria

TABLE 5.—AVERAGE KAOLINITE CONTENT OF UNDERCLAYS
In per cent

ZONE	MID-CONTINENT BASIN			APPALACHIAN BASIN		
	Shelf	Int.	Deep Basin	Shelf	Int.	Deep Basin
10	19		20	29		
9	9			33	20	
8	3			34	33	53
7	5	29				
6	21	22		50	38	17
5	42			58	30	
4	48		30	42	27	29
3	57		40	52	38	25
2	38		40	49	48	26
1					57	42

used to differentiate flint clays from plastic varieties is that the flint clays do not slough in water. The two flint-clay samples taken below coal horizons (zone 9, outcrops 3 and 4) contained illite and a well-crystallized variety of kaolinite as the only clay components. Glycol treatment did not indicate the presence of expandable material. Several samples of the flint-clay parting of the Fire Clay Coal (zone 4) of West Virginia and Kentucky and two from similar partings in near-by coals of zones 3 and 5 in eastern Kentucky were analyzed. All were composed primarily of well-crystallized kaolinite. Two of these samples (zone 5, outcrops 7 and 10) which appeared to be flint clays proved to contain detectable amounts of expandable material. However, when soaked in water for several days both samples sloughed and therefore were not true flint clays.

Other factors suggest different modes of origin for flint and plastic underclays. Flint clays commonly exhibit clastic textures, which indicate reworking. Also, recrystallization phenomena in flint clays have been reported by several investigators (Bolger and Weitz, 1952; Foose, 1944; Waage, 1950; Teichmuller, 1952). In thin sections of flint-clay partings from coal beds, Teichmuller found large, well-crystallized kaolinite aggregates within plant cell walls. Since the kaolinite could not have penetrated the cell walls in its present form, it must have crystallized in place. Such evidence of reworking or recrystallization is absent or at best very rare in plastic underclays.

REGIONAL AND STRATIGRAPHIC VARIATIONS OF UNDERCLAYS

Shelf-Geosynclinal Relationships

The lower Pennsylvanian column thickens greatly from the northern shelf areas to the southern geosynclinal areas of the Appalachian and Mid-Continent basins. Several differences between the underclays in areas of thick and thin sediments can be seen in the field. In the deep basins, underclays are likely to be thin and sandy, and in many places slates occupy the stratigraphic position of the underclays below coals.

Average kaolinite content of the underclay zones in different parts of the Geosynclines is shown in Table 5. In the Appalachian Basin the thickness of Pottsville sediments increases only slightly southward across Ohio and northern Kentucky to the Paint Creek-Warfield fault zones; here there is a pronounced expansion in a short distance (Wanless, 1946, Fig. 1). A similar expansion of the interval occurs at the Pine Mountain fault. On this basis, the Appalachian samples are divided into three categories: (1) those from the shelf area to the north, (2) those from an intermediate area between the Paint Creek-Warfield fault zone and the Pine Mountain fault, and (3) those from the deepest part of the Appalachian Basin south of Pine Mountain. The location of these features is shown in Figure 14. The Mid-Continent area was divided similarly, although boundaries between the areas are not so well defined. The shelf area of Kansas and Missouri with sediments of fairly uniform thickness is separated from the area of thick geosynclinal sediments in southern Oklahoma and Arkansas by an "intermediate" area with a gradually expanding column lying between the Oklahoma-Kansas State line and the Arkansas River.

Some of the figures of Table 5 must be interpreted with caution. The average kaolinite content for zones 6 and 8 in the deep basins represents only a few samples. Values for zones 9 and 10 also represent a small number of samples, some of which are red beds. The 49 per cent kaolinite content of zone 2 of the Appalachian shelf area is an average of only two samples. Probably more significant than shelf-geosynclinal comparison of zone 2 in the Appalachian area is a comparison between the intermediate and the deep-basin areas, both of which are represented by numerous samples.

Zones 2, 3, 4, and 5 are best for comparison of the mineralogy of a fairly large number of samples from various parts of the Appalachian

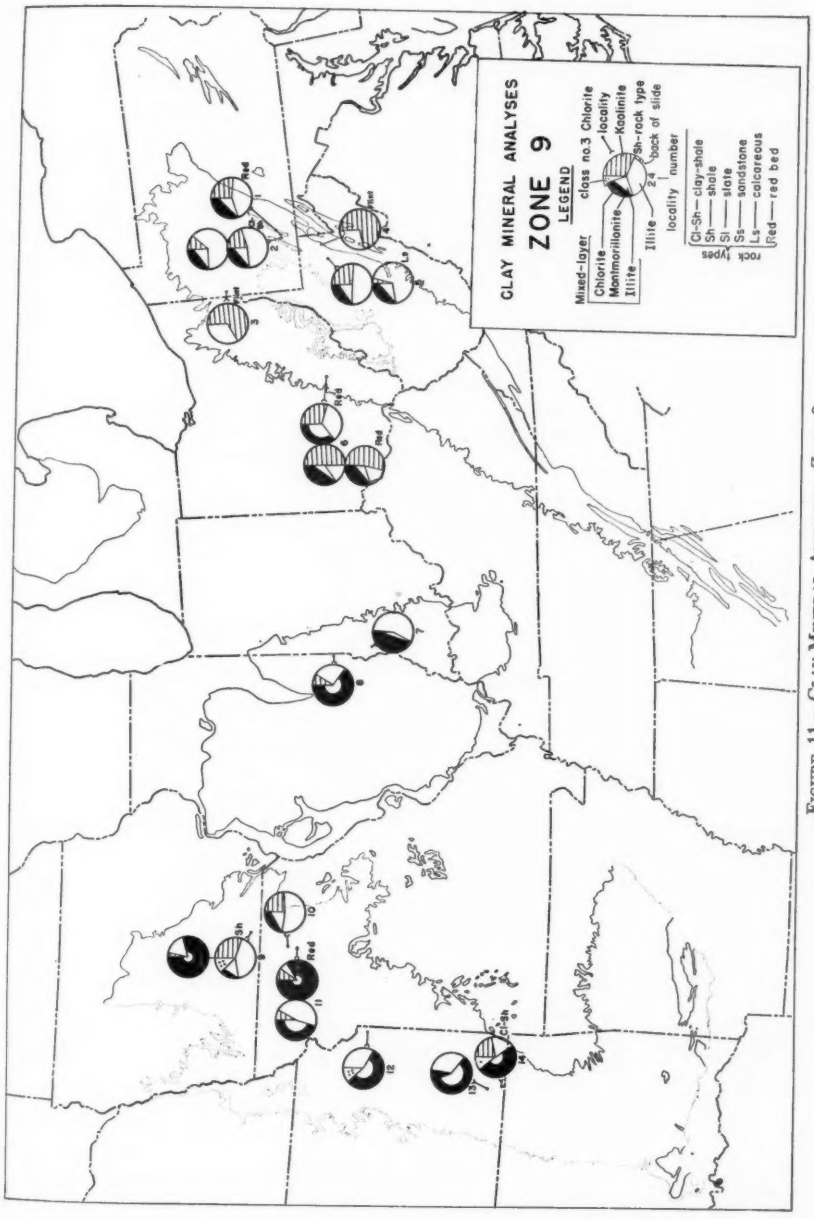

FIGURE 11.—CLAY-MINERAL ANALYSES: ZONE 9

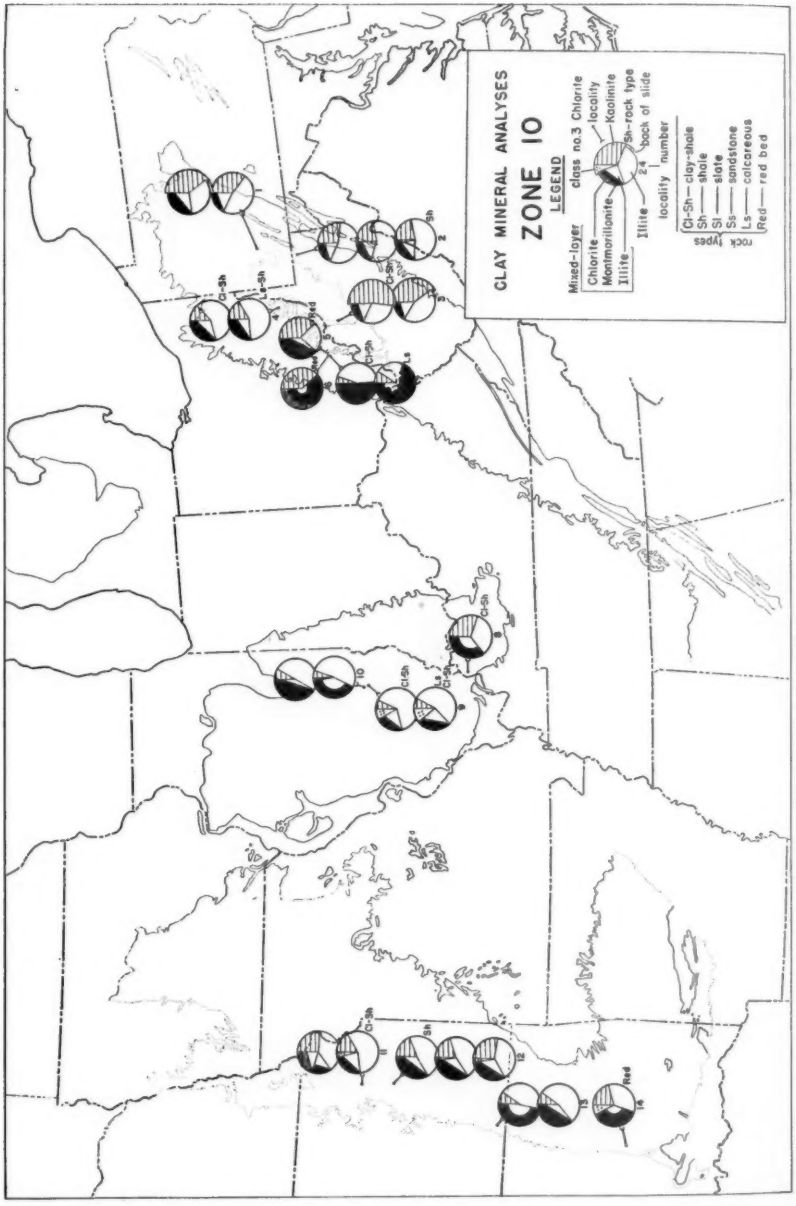

FIGURE 12.—CLAY-MINERAL ANALYSES: ZONE 10

Basin. As shown in Figures 2 to 12 and summarized in Table 5, underclays tend to become progressively less kaolinitic as the section becomes thicker. Flint clays from coal partings are not included in the averages. Unlike samples from all the lower zones, the single zone 8 sample contains more kaolinite than its shelf-area equivalents. This may be related to a lack of thickening in the Allegheny Series, including zone 8 in the southern part of the basin.

Data given in Table 5 for the Mid-Continent Basin are not so satisfactory as those for the Appalachian Basin because they represent fewer samples, and stratigraphic correlations are less certain. Zones 3 and 4 show the same decrease in kaolinite content with increased thickness of sediments as mentioned for the Appalachian Basin. The explanation for a lack of a similar decrease in the zone 2 kaolinites in the Mid-Continent Basin is not evident. The zone 7 variations are apparently related to factors other than sediment thickness and are discussed in the section on stratigraphic variations.

The sediments of the anthracite coal fields of Pennsylvania show a shelf-geosynclinal relationship with the thin Pottsville section in the northern field and the thick equivalent section to the south. Samples were taken from zones 2 and 6 in the anthracite area. Zone 6 samples show relationships similar to those in the Appalachian Basin; both of the samples from

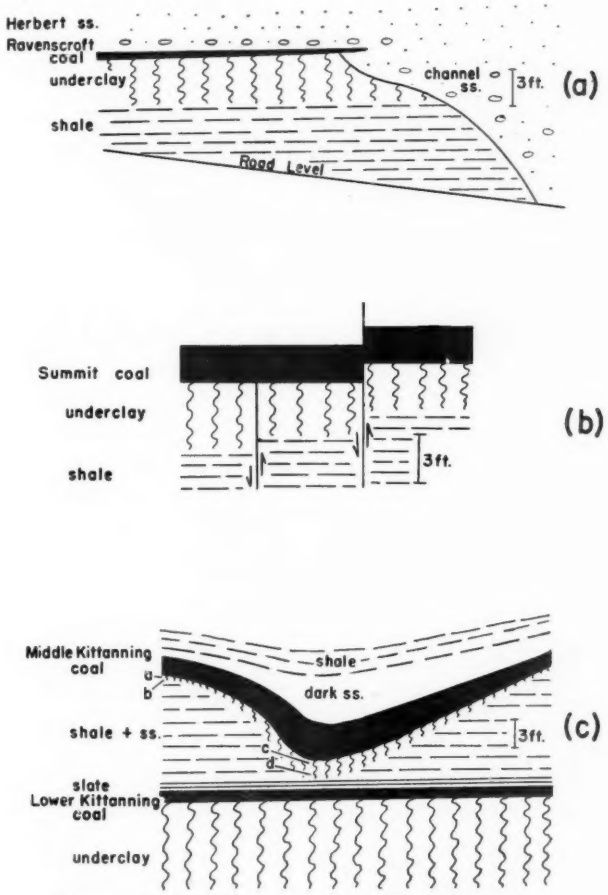

FIGURE 13.—COAL-UNDERCLAY FIELD RELATIONSHIPS

FIGURE 12.—CLAY-MINERAL ANALYSES: ZONE 10

the northern shelf area (Fig. 8, outcrops 1 and 2) are much more kaolinitic than those from the deep southern basin (Fig. 8, outcrops 3 and 4). All the zone 2 samples occurring below coals are from the southern field and have kaolinite contents similar to lower Pennsylvanian underclays from the geosynclinal area of the main Appalachian Basin. The shale sample from the northern field (Fig. 4, outcrop 1) is not associated with a coal but occurs at the approximate horizon of the zone 2 coal.

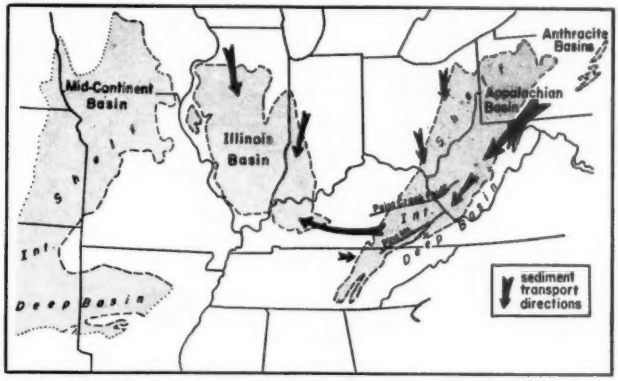

FIGURE 14.—SEDIMENT TRANSPORTATION DIRECTIONS IN PENNSYLVANIAN BASINS

Other mineralogical differences were noted between shelf and deep-basin underclays. The kaolinites from geosynclinal underclays tend to be slightly better crystallized than the typical, poorly crystallized kaolinites of the shelf. Most geosynclinal underclays contain less mixed-layer material and more and better crystallized varieties of chlorite.

Stratigraphic Variations

In Illinois, Grim and Allen (1938) found that underclays lower than the No. 2 Coal (zone 6 of this paper) are dominantly kaolinitic; those above the No. 2 Coal are dominantly illitic. One of the purposes of this study was to see if this generalization extended into the other major Pennsylvanian basins.

In the areas investigated in this study, almost all the lower Pennsylvanian underclays are more kaolinitic than those from the upper Pennsylvanian. However, if the National Research Council correlations are used the change begins at slightly different stratigraphic positions and varies in rapidity and intensity in different parts of the country. In the Appalachian Basin and eastern part of the Illinois Basin zone 6 underclays are among the most kaolinitic in the Pennsylvanian column, whereas, as shown in Table 5, in the Mid-Continent Basin the decrease in kaolinite is well advanced in this zone. According to Arthur White (Oral communication), the underclays of zone 6 in western Illinois are quite variable in their mineralogical composition; this area might be considered as transitional between the relatively low kaolinite contents of the Mid-Continent Basin and the high contents farther east. In the Appalachian Basin the kaolinite change is first noted in zone 8, and even this high in the column the decrease is much less pronounced than it is farther west. Although zone 7 and 8 underclays of the Mid-Continent Basin and most of the Illinois Basin contain little or no kaolinite, those of zone 8 in the east contain considerable amounts; their content is low only in comparison with that of the lower Pennsylvanian underclays. Figures 11 and 12 and Table 5 show this relationship between eastern and western areas to be true for zones 9 and 10 also; although more variable than in lower zones, the average kaolinite content is higher in the east than in the west.

Mineralogically the upper Pennsylvanian underclays of the southeast corner of the Illinois Basin seem to be intermediate between those of the rest of the Illinois Basin and those of the Appalachian Basin. In the Appalachian Basin the kaolinite content of these upper Pennsylvanian underclays averages about 30 per cent. In most of the Illinois Basin zone 7, 8, 9, and 10 underclays rarely contain more than 10 per cent kaolinite, whereas those in the southeast corner average about 25 per cent.

The regional and stratigraphic variation in the kaolinite content of underclays is paralleled by a change in the mixed-layer clay content and the abundance of marine beds. The upper Pennsylvanian underclays of the Mid-Continent Basin which are low in kaolinite contain abundant mixed-layer material, much more than the underclays of the Appalachian area or those of the lower Pennsylvanian of the Mid-Continent area. Limestone development reaches its peak in this same region of high mixed-layer, low-kaolinite rocks. The lowest marine limestones of considerable geographic extent in the Mid-Continent area are the thin, discontinuous Tiawah and Verdigris limestones just above zones 5 and 6 respectively. The decrease in kaolinite content is first noted in the zone 5 and 6 underclays, and the underclays of zones 7, 8 and 9 contain little or no kaolinite. The earliest widespread marine limestone is the Ft. Scott, just above the zone 7 underclay, and limestones maintain a maximum development in the Marathon Group and Missouri Series which include zones 8 and 9. These marine limestones tend to pinch out to the south, and the kaolinite content of zone 7 increases toward the south (Fig. 9). Marine limestones become less abundant in the upper Pennsylvanian strata of the Mid-Continent Basin (H. R Wanless, oral communication), and the underclays of zone 10 included therein tend to be slightly more kaolinitic than those of the underlying three zones.

Source Areas

The differences in mineralogy between shelf and geosynclinal underclays (those of the geosyncline contain less kaolinite and mixed-layer clay and more chlorite) are what would be expected if the underclays were residual soils. The great thickness of the geosynclinal sediments indicates a rapid rate of deposition, and rapid deposition would allow a relatively short period of time for residual weathering of the underclay. However, the differences noted may also result from weathering in separate source areas.

Erosion in the geosynclinal source area must have been rapid to supply the flood of sediments needed to fill the continually sinking basin. In contrast, deposition in the shelf area must have been relatively slow as indicated by the abbreviated section. Slow deposition implies slow erosion in the source area of the shelf sediments. Furthermore, the erosion-deposition cycle of shelf underclays must have been unusually slow, even for the shelf area. Weller (1930, p. 122) estimates that the time of underclay formation may well have equaled the interval when all the rest of the rocks of the sedimentary cycle were deposited. The slow erosion would allow a long period for exposure to weathering and a long period for development of kaolinite. Weathering in the geosynclinal source areas has caused the geosynclinal underclays to differ from the enclosing shales, but these differences are not so great as on the shelf. Therefore retardation of the rate of erosion, transportation, and deposition during underclay formation in the geosynclinal area must have been less pronounced.

Such a process would explain the several similarities between the mineralogy of underclays and modern soils as well as coal-underclay time relationships and the lack of a soil profile development. The occurrence of kaolinite with well-crystallized chlorite, a combination unlikely to develop in a soil, could result from mixing of sediments during transportation, and the entire mineralogy need not fit one set of soil equilibrium conditions. The rate of erosion and length of time of weathering need not be the same in all parts of the source areas. The transported soil hypothesis is also favored over the residual soil theory of underclay formation because it does not require development of kaolinite in the reducing, poorly drained swamp environment implied by the abundance of coaly material and pyrite in underclays. If weathering in the source area controls the mineralogy of underclays, different sources must account for the differences in composition of shelf and geosynclinal underclays.

The concept of different source areas is supported by what is known of transportation directions from studies of cross-bedding in sandstones. Transportation directions are shown by arrows on Figure 14. Fuller (1955) concluded that the lower Pottsville Sharon Sandstone of Ohio came from the shelf area to the northwest from the Cincinnati Arch or Canadian Shield, whereas Potter and Siever (1956; oral communication) found that the Lee sandstones, also of lower Pottsville age, in deep basin areas of eastern Kentucky and West Virginia, came from the northeast. If these findings can be extended from sandstones to underclays, which seems reasonable, then the concept of different source areas as an explanation of mineralogical variations between shelf and geosynclinal underclays is further substantiated.

Sedimentary structure studies (Potter and

Siever, 1956) also help explain the mineralogical similarity between upper Pennsylvanian underclays of the southeastern corner of the Illinois Basin and equivalent Appalachian underclays. Cross-bedding indicates that these sediments were derived from the east—somewhere in the direction of the Appalachian Basin. Although these cross-bedding studies apply to lower Pennsylvanian Caseyville sediments, facies studies by H. R. Wanless (Oral communication) in the form of a sandstone-shale-limestone transition from the southeast corner of the basin to the St. Louis area indicate that spilling over of sediments from one basin to the other continued into upper Pennsylvanian time. A southeasterly source for the zone 8 underclay in Illinois is also indicated in a study by C. W. Spencer (1955, M. S. thesis, Univ. Illinois) who found that the grain size of the nonclay minerals increased in this direction. Spencer also found the most kaolinite in samples from the southeast corner of the State.

Interbasin Correlations

Two alternative correlations of the No. 2 Coal of Illinois (zone 6 of this paper) with the Appalachian section are considered by Wanless (1939, p. 68). The tentative interpretation shown in the Research Council chart and reproduced in Table 1 of this paper equates the No. 2 and No. 6 coals of Illinois with the Lower and Middle Kittanning coals of Ohio respectively. The second interpretation would correlate the No. 2 Coal of Illinois with the Middle Kittanning Coal with suitable shifts in correlations of the other coals. From a purely mineralogical viewpoint, the evidence seems to favor the first interpretation. The Lower Kittanning Underclay of Ohio and No. 2 Coal Underclay on the eastern edge of the Illinois Basin are highly kaolinitic, whereas the Middle Kittanning and No. 6 Coal underclays contain considerably less kaolinite. However, if the second correlation of the No. 2 Illinois Coal with the Middle Kittanning Coal were used, a highly kaolinitic underclay west of the Cincinnati Arch would be correlated with a less kaolinitic underclay to the east, controverting the general tendency of the eastern underclays to be more kaolinitic.

Probably the largest kaolinite deposits in the Pennsylvanian system of the United States are in the underclay of the Lower Kittanning Coal of Ohio. The correlations of Table 1 suggest why this is true. No persistent equivalents of the No. 4 and No. 5 coals of Illinois exist between the Lower and Middle Kittanning coals (Table 1). Consequently this must have been a time of unusually slow deposition of the Appalachian shelf sediments, providing a maximum time interval for soil leaching in their source area.

Summary

Samples from Pennsylvanian underclay localities in the Appalachian, Mid-Continent, and parts of the Illinois basins were analyzed, mainly by X-ray diffraction, to see how the mineralogy varied regionally and stratigraphically, how it varied within underclay profiles, and how it differed from that of closely related shales, sandstones, and limestones, and from these data to see what conclusions could be drawn regarding the origin of underclays.

Mineralogically, underclays are composed primarily of fire-clay-type kaolinite that varies in its degree of disorganization, illite, mixed-layer illite-montmorillonite or more rarely illite-montmorillonite-chlorite, and quartz; a 14 Å component ranging from vermiculite to chlorite is present in about one-third of the samples; feldspar, pyrite, and muscovite are the common accessory minerals.

A satisfactory theory of the origin of underclays must explain the following:

DISTRIBUTION OF MINERALS WITHIN UNDERCLAYS: Mixed-layer clay minerals are most abundant at the tops of underclay profiles. If chlorite is a component of the mixed-layer clay mineral, it is everywhere most abundant at the top of the underclay. Kaolinite and feldspar are equally abundant in the tops and bottoms of underclays. Quartz, muscovite, and chloritic material are concentrated in the lower parts of underclays. However, there is no systematic distribution of the type of chloritic material; the well-crystallized chlorite is as likely to occur at the tops of underclays as is vermiculite.

DIFFERENCES IN MINERALOGY BETWEEN UNDERCLAYS AND ASSOCIATED ROCKS: Shales from above the coals contain more chlorite and less mixed-layer montmorillonite and kaolinite than underclays; most of the kaolinite and chlorite of the shales is better crystallized. The shales, sandstones, and calcareous rocks more intimately associated with the underclays below the coals are mineralogically similar to the underclays. They contain about the same amounts of kaolinite, but the shales and sandstones tend to contain slightly less mixed-layer montmorillonite.

RELATIONSHIP OF UNDERCLAY TO COAL: All

underclays occur below coals or coal horizons. However, their thickness is not related to that of the overlying coal. In some places shale and less commonly sandstone beds occur between the underclay and coal. In one outcrop a fault offsets the underclay but not the overlying coal.

FEATURES WITHIN THE UNDERCLAYS: Underclays, by definition, are not bedded. Many contain slickensides, the presence of which is closely related to absence of sand and the presence of organic material. Well-preserved leaf impressions and tiny coal veinlets are common. In some underclays calcite and siderite occur in the lower parts of underclays as nodules and crack fillings.

REGIONAL AND STRATIGRAPHIC VARIATIONS: Geosynclinal underclays contain less kaolinite and mixed-layer clay minerals and more chlorite than shelf underclays. Underclays of the upper Pennsylvanian strata tend to be less kaolinitic than those of the lower Pennsylvanian rocks; the decrease is more pronounced in the western areas where mixed-layer clay material is the dominant constituent. The upper Pennsylvanian underclays of the southeast corner of the Illinois Basin have kaolinite contents more similar to those of equivalent Appalachian underclays than to the low kaolinite contents of equivalent underclays from the rest of the Illinois Basin.

The relationships between underclays and coals indicate that the underclays formed before the coals were deposited. Furthermore, lack of a soil profile similar to modern soils and similarity of the mineralogy of all rock types below the coals indicate that underclay materials are essentially as they were transported into the basin. Although some post-depositional leaching may have occurred as indicated by carbonate concretions in the lower part of some underclays, and although plants may have grown on top of the underclays as indicated by root impressions and a few stumps of trees in place, such weathering was mild and did not affect the argillaceous components of the underclay appreciably. In some cases it could not have been strong enough to destroy chlorite.

Diagenetic alteration in a coal swamp does not account for all the mineralogical features of underclays. Although a poorly drained, reducing, swampy environment, which is indicated by the abundance of coaly material and pyrite in underclays, is one in which montmorillonite and chlorite might develop, it is not favorable for kaolinite formation (Milot, 1952, p. 112).

The close parallelism between the abundance of mixed-layer montmorillonite in underclays and the abundance of marine limestones in the upper Pennsylvanian rocks of the Mid-Continent area prompts speculation on the influence of the sedimentary environment on the mineralogy of underclays. Although a marine or brackish water environment would be consistent with the low kaolinite contents of these underclays, it would not promote the formation of montmorillonite but would favor development of illite or chlorite. Again, similarity of the mineralogy of these underclays with that of other closely associated rocks below the coals indicates that these underclays were deposited with essentially their present mineralogical composition.

Except for the rare presence of well-crystallized chlorite, and regardless of the distribution of the minerals in underclay profiles, the bulk mineralogy of underclays, with their abundance of poorly crystallized kaolinite, mixed-layer clay and dioctahedral vermiculite does suggest an affinity to soils. The writer believes that underclays are best interpreted not as the result of residual soil weathering but of weathering in the source areas during periods of slow erosion which preceded almost complete stagnation of the erosion-deposition cycle when peats were formed. Variations in the mineralogy of underclays would then be related to different types of weathering in the source areas. Such weathering, the product of temperature, rainfall, drainage, time, and parent rocks, would not be the same in all parts of even a limited source area, so that a stream would transport an assemblage of minerals, perhaps including both kaolinite and well-crystallized chlorite, which need not be consistent with any one set of weathering conditions.

The kaolinite of underclays indicates weathering in a fairly warm and humid climate, perhaps similar to that in the southeastern United States today. Conditions were not tropical in the source areas, since the aluminum hydroxides which characterize laterites are absent in the plastic underclays. The decrease in kaolinite content and increase in the amount of mixed-layer clay in the upper Pennsylvanian underclays suggest a shift to a cooler or less humid climate; this shift must have been most pronounced in the west and occurred slightly earlier there. According to A. T. Cross (Oral communication), the most extensive change in the Pennsylvanian flora occurs at about the same stratigraphic position where the underclay mineralogy changes, which may also indicate a change of climate at that time. The distribution of minerals within the underclays, with concentration of the coarser quartz, mica, and chlorite in the base and fine-grained mixed-

layer clay in the top, can be explained as the result of a gradual decrease in transporting capacity of the streams. The underclays were probably deposited in a loose, hydrous, flocculated state, and slickensides developed during compaction.

The theory of weathering in different source areas to explain the mineralogy of underclays is supported by mineralogical differences between shelf and geosynclinal underclays and by what is known of transportation directions from studies of cross-bedding. In the Appalachian Basin cross-bedding indicates that the highly kaolinitic underclays of the stable shelves were derived from the mildy positive Cincinnati Arch or Canadian Shield where erosion must have been very slow. The less kaolinitic underclays of the deep part of the Appalachian Basin came from the northeast from the unstable side of the geosyncline where the rate of erosion must have been much greater, allowing less time for exposure to weathering agents.

The closer mineralogical similarity of the upper Pennsylvanian underclays of the southeastern corner of the Illinois Basin with those of the Appalachian Basin than with equivalent underclays in the rest of the basin is also probably the result of different source areas. Cross-bedding indicates that sediments spilled in the southeastern corner of the Illinois Basin from the east, from the direction of the Appalachian Basin.

References Cited

Ashley, G. H., 1940, Topographic and geologic atlas of Pennsylvania no. 75, Curwensville quadrangle: Pa. Topog. and Geol. Survey, 140 p.

Bolger, R. C., and Weitz, J. H., 1952, Mineralogy and origin of the Mercer fireclay of north-central Pennsylvania, p. 81–93, *in* Problems of clay and laterite genesis: Am. Inst. Min. Metall. Engineers St. Louis mtg. (1951) Symposium, 244 p.

Brindley, G. W., and Ali, S. Z., 1950, X-ray study of thermal transformations in magnesian chlorites: Acta Cryst., v. 3, p. 25–30.

Brown, George, 1953, The dioctahedral analogue of vermiculite: Clay Minerals Bull., v. 2, no. 10, p. 64–70.

Cleaves, A. B., and Stephenson, R. C., 1949, Guidebook to the geology of the Pennsylvania Turnpike: Pa. Topog. and Geol. Survey Bull. G24, 72 p.

Cline, L. M., 1941, Traverse of upper Des Moines and lower Missouri series from Jackson Co., Missouri, to Appanoose Co., Iowa: Am. Assoc. Petroleum Geologists Bull., v. 25, p. 23–72

DeWolfe, F. W., 1929, Topographic and geologic atlas of Pennsylvania no. 5, New Castle quadrangle: Pa. Topog. and Geol. Survey, 238 p.

Flint, Norman, 1951, Geology of Perry County: Ohio Geol. Survey Bull. 47, 234 p.

Foose, R. M., 1944, High-alumina clays of Pennsylvania: Econ. Geology, v. 39, p. 557–573.

Fuller, J. O., 1955, New discoveries concerning the Sharon conglomerate in northeastern Ohio: Geol. Soc. America Bull., v. 66, p. 159–167.

Geologic Map of Indiana, 1932, Div. of Geol., Dept. of Conservation, State of Indiana

Giles, A. W., 1930, Pennsylvanian climates and paleontology: Am. Assoc. Petroleum Geologists Bull., v. 14, p. 1279–1299

Graeber, C. K., and Foose, R. M., 1942, Topographic and geologic atlas of Pennsylvania no. 54, Brookville quadrangle: Pa. Topog. and Geol. Survey, 136 p.

Greene, F. C., and Pond, W. F., 1926, The geology of Vernon County, Missouri: Mo. Bur. Geology and Mines, v. 19, 152 p.

Grim, R. E., 1935, Petrology of the Pennsylvanian shales and noncalcareous underclays associated with Illinois coals: Am. Ceramic Soc. Bull., v. 14, no. 3, p. 113–119; no. 4, p. 129–134; no. 5, p. 170–176

—— 1953, Clay Mineralogy: N. Y., McGraw-Hill Book Co., 384 p.

Grim, R. E., and Allen, V. T., 1938, Petrology of Pennsylvanian underclays of Illinois: Geol. Soc. America Bull., v. 49, p. 1485–1514

Hendricks, T. A., and Parks, B., 1950, Geology of Fort Smith district, Arkansas: U. S. Geol. Survey Prof. Paper 221-E, p. 67–94

Hennen, R. V., and Reger, D. B., 1914, Preston County: W. Va. Geol. Survey, 566 p.

Jewett, J. M., 1945, Stratigraphy of the Marathon group, Pennsylvanian, in Kansas: Kans. Geol. Survey Bull. 58, 148 p.

Kansas Geological Society, 1936, Guide Book—Tenth Annual Field Conference, 74 p.

—— 1937, Guide Book—Eleventh Annual Field Conference, 108 p.

—— 1949, Guide Book—Lower Kansas River Valley Field Conference, 32 p.

Kentucky Geological Society, 1953, Guide to some Pennsylvanian sections in Morgan, Magoffin, and Breathitt counties, Kentucky, 28 p.

Krebs, C. E., 1916, Raleigh County and the western portion of Mercer and Sumner counties: W. Va. Geol. Survey, 648 p.

McCue, J. B., 1948, Clays of West Virginia W. Va. Geol. Survey, v. XVII, 234 p.

McQueen, H. S., and Greene, F. C., 1938, Geology of northwestern Missouri: Mo. Geol. Survey and Water Resources, v. XXV, 217 p.

Milot, Georges, 1952, Prospecting for useful clays in relation with their conditions of genesis, p. 107–114, *in* Problems of clay and laterite genesis: Am. Inst. Min. Metall. Engineers St. Louis mtg. (1951) Symposium, 244 p.

Moore, R. C., *et al.*, 1944, Correlation of Pennsylvanian formations of North America: Geol. Soc. America Bull., v. 55, p. 657–706

Newton, W. A., and Weller, J. M., 1937, Stratigraphic studies of Pennsylvanian outcrops in part of southeastern Illinois: Illinois Geol. Survey Rept. of Inv. 45, 31 p.

Pearson, R. W., and Ensminger, I. E., 1948, Types of clay minerals in Alabama soils: Soil Sci. Soc. America, v. 13, p. 153–156

Pierce, W. G., 1937, Southeastern Kansas coal fields: Kans. Geol. Survey Bull. 24, 122 p.

Potter, P. E., and Siever, Raymond, 1956, Sources of basal Pennsylvanian sediments in the Eastern Interior Basin—Cross-bedding: Jour. Geology, v. 64, no. 3, p. 225–244

Ries, Henrich, 1927, Clays, their occurrence, properties, and uses: N. Y., John Wiley & Sons, 613 p.

Rolfe, B. N., 1954, Mineralogy of soil profiles: Iredell and Durham soils of the Piedmont of North Carolina: Second Nat. Clay Conf. Proc., Nat. Acad. Sci., Nat. Res. Council pub. 327, p. 183–189

Schoewe, W. H., 1944, Coal resources of the Kansas City Group, Thayer bed, in eastern Kansas: Kans. Geol. Survey Bull. 52, pt. 3, p. 81–136

Schultz, L. G., 1955, Quantitative evaluation of the kaolinite and illite in underclays: Third Nat. Clay Conf. Proc., Nat. Acad. Sci., Nat. Res. Council pub. 395, p. 421–429

Shawnee Geological Society, 1938, Field Conference—A study of surface rocks from McAlester Shale to Thurman Sandstone through townships 4, 5, and 6 north, ranges 12 through 17 east, Pittsburg Co., Oklahoma

—— [not dated], Field Conference—A study of the surface rocks from the Calvin Sandstone to Permian through townships 6 to 10 north, Hughes, Seminole, and Potawatomie counties, Oklahoma

Sherman, G. D., 1952, The genesis and morphology of alumina-rich laterite clays, p. 154–161, *in* Problems of clay and laterite genesis: Am. Inst. Min. Metall. Engineers St. Louis mtg. (1951) Symposium, 244 p.

Stout, Wilbur, 1923, Coal formation clays: Ohio Geol. Survey Bull. 26, 588 p.

—— 1927, Geology of Vinton County: Ohio Geol. Survey Bull. 31, 402 p.

Teichmuller, M., *et al.*, 1952, Der erste Tonsteinfund im Achener Revier und die Frage nach der Enstehung der Graufen und Kristalltonstein (The first clay rock found in the Achen region and the question of the development of granular and crystalline clay rock): Geol. Jahrb., v. 66, p. 723–736

Unklesbay, A. G., 1952, Geology of Boone County: Mo. Geol. Survey and Water Resources, v. XXXIII, 159 p.

Waage, K. M., 1950, Refractory clays of the Maryland coal measures: Maryland Dept. of Mines and Water Resources Bull. 9, 182 p.

Walker, G. F., 1947, The mineralogy of some Aberdeenshire soil clays: Clay Minerals Bull. no. 1, p. 5–8

Wanless, H. R., 1931, Pennsylvanian cycles in western Illinois: Ill. Geol. Survey Bull. 60. p. 179–193

Wanless, H. R., 1939, Pennsylvanian correlations in the Eastern Interior and Appalachian coal fields: Geol. Soc. America Special Paper 17. 130 p.

—— 1946, Pennsylvanian geology of a part of the southern Appalachian coal field: Geol. Soc. America Mem. 13, 162 p.

Weller, J. M., 1930, Cyclical sedimentation of the Pennsylvanian period and its significance: Jour. Geology, v. 38, no. 2, p. 97–135

White, G. W., 1945, Upper Pennsylvanian and Lower Permian rock section at Blaine Hill, Belmont County, Ohio: Ohio Jour. Sci., v. XLV, no. 5, p. 173–179

—— 1949, Geology of Holmes County: Ohio Geol. Survey Bull. 47, 373 p.

Worthen, A. H., 1866, Economical geology of Illinois: Ill. Geol. Survey, v. 1, 541 p.

Agricultural Research Center, Beltsville, Maryland

Manuscript Received by the Secretary of the Society, March 11, 1957

Appendix. Sample Localities

Mississippian Soils

1. Pennsylvania, Westmoreland County, road cut on the north side of the Pennsylvania Turnpike 3 miles west of the Donegal toll gate (Cleaves and Stephenson, 1949, Pl. 27)

2. Ohio, Holmes County, Killbuck Township, sec. 15, along an east-west road 1 miles southeast of Killbuck (White, 1949, sec. 147)

3. Ohio, Perry County, Reading Township, sec. 27, cut along a north-south road 2 miles south of Somerset (Flint, 1951, sec. F127)

4. Kentucky, Harlan County, at the top of Pine Mountain on U. S. Highway 421 (H. R. Wanless, oral communication)

5. Kentucky, Powell County, road cut about 2 miles east of the junction of State routes 77 and 15, near an abandoned quarry on State Route 15 (H. R. Wanless, oral communication)

6. Virginia, Wise County, road cut along State Route 610 at the top of Little Stone Gap (Wanless 1946, sec. AA-30)

7. Tennessee, Van Buren County, road cut along State Route 30 about a mile west of Spencer in the scarp of the Cumberland Plateau (Wanless, 1946, sec. DD-7)

8. Indiana, Martin County, road cut at the bottom of a hill 6.5 miles east of Shoals on U. S. Highway 50 (Geological Map of Indiana, 1932)

9. Kansas, Cherokee County, sink hole 7 miles east of Scammon in the NE¼ sec. 9, T. 32 S., R. 25E.; take first road leading east after turning south from northwest corner of section, drive past house for about a quarter of a mile, walk northeast to sink hole (Pierce, 1937, p. 25)

Zone 1

1. West Virginia, Raleigh County, road cut along State Route 16 on the west side of the divide between Sofia and Tams from below the Fire Creek or Babcock coal (H. R. Wanless, oral communication)

2. West Virginia, Raleigh County, from the Stotesbury No. 11 mine of the Koppers Coal Co. at Helen, from below the No. 4 Pocahontas coal (Mr. Benedict, mine manager, oral communication)

3. West Virginia, Raleigh County, samples of underclay from below the No. 3 Pocahontas Coal near the tipple of the Amigo Coal Co., and a sample of sandy shale from immediately below the same coal near where the railroad crosses State Highway 16 at Amigo, about half a mile from the tipple (Krebs, 1916, geologic map)

4. Indiana, Orange County, from the Pinnick Whetstone quarry west of Baden from below the lowermost Indiana coal (H. R. Wanless, oral communication)

5. Virginia, Tazewell County, road cut 1 mile west of Pocahontas on Virginia Highway 644

6. Kentucky, McCreary County, road cut along Kentucky Highway 92 just west of where it crosses the South Fork of the Cumberland River between Hilltop and Yamacaw (Wanless, 1946, sec. KK-2)

7. Kentucky, McCreary County, clay just below Sewanee Conglomerate in road cut along Kentucky Highway 92 on edge of Cumberland Plateau near Wayne-McCreary county line

8. Tennessee, Campbell County, old mine along U. S. Highway 25W, in the Cumberland Mountain gap just north of LaFollette (Waneless, 1946, sec. KK-7)

9. Tennessee, White County, abandoned mine just below a road along the old railroad grade 1 mile north of Bon Air (Wanless, 1946, sec. DD-10)

10. Tennessee, Franklin County, along Mud Creek road north of Sewanee (Wanless, 1946, sec. EE-2)

11. Georgia, Dade County, small coal opening along White Oak Gap road, west of Trenton (Wanless, 1946, sec. AA-1)

Zone 2

1. Pennsylvania, Luzerne County, about 2 miles north of Pittston on the east side of the Susquehanna River; a 5-inch shale between the Goose Egg Conglomerate and the Mississippian red beds is the equivalent to the entire Pottsville section (H. R. Wanless, oral communication)

2. Pennsylvania, Northumberland County, about a quarter of a mile east of State Route 54 and 2 miles north of Mt. Carmel in an abandoned strip pit (Harold Arndt and Gordon Wood, oral communication)

3. Pennsylvania, Schuylkill County, from a strip mine on top of Broad Mountain a quarter of a mile east of State Route 125 between Hegins and Good Springs (Gordon Wood and Harold Arndt, oral communication)

4. Pennsylvania, Lawrence County, a few hundred feet north of a bridge on U. S. Highway 224 a quarter of a mile east of the Ohio-Pennsylvania State line in a small stream; a shale at about zone 2 was sampled just below the Connoquenessing Sandstone (DeWolfe, 1929, p. 57)

5. Ohio, Vinton County, Richland Township, south-central part of sec. 29, in a small creek south of an old sawmill beside the main gravel road and

about 75 feet vertically below the road (Stout, 1927, p. 71)

6. West Virginia, Fayette County, strip mine of the Tolley & Tolley Coal Co., about half a mile west of the junction of U. S. highways 19 and 60 near Clifftop (Mine manager, oral communication)

7. West Virginia, Fayette County, abandoned mine along the road between Ansted and Hawks Nest (H. R. Wanless, oral communication)

8. West Virginia, Fayette County, shale above the Sewell Coal in a strip mine above U. S. Highway 19 near Babcock Park (Mine manager, oral communication)

9. Kentucky, Powell County, a short distance east of outcrop 5 of the Mississippian soils

10. Kentucky, Pulaski County, mine of the Avon Coal Co., about 3 miles south of State Route 80 and 4 miles west of the Rockcastle River (H. R. Wanless, oral communication)

11. Kentucky, McCreary County, along State Route 90 just west of Cumberland Falls (Wanless, 1946, sec. KK-4)

12. Virginia, Wise County, small abandoned mine just west of outcrop 6 of the Mississippian soils

13. Tennessee, Campbell County, same as outcrop 8, zone 1

14. Tennessee, Cumberland County, in the mine of M. V. Powell, 2 miles west of Ozone along U. S. Highway 70 (Wanless, 1946, sec. HH-8)

15. Tennessee, Cumberland County, strip mine three-quarters of a mile south of State Route 68 and 9 miles northwest of the Cumberland-Rhea county line (M. V. Powell, oral communication)

16. Tennessee, Rhea County, along U. S. Highway 68 on the escarpment of Walden Ridge between Spring City and Grand View (Wanless, 1946, sec. AA-21)

17. Tennessee, Rhea County, 1 mile up Roaring Creek from Graysville and 500 feet vertically above the stream in an old mine in the north wall of the valley (Wanless, 1946, sec. AA-16)

18. Tennessee, Hamilton County, old mine just south of a gravel road up Walden Ridge just north of Falling Water Creek and about 4 miles south of Daisy (Wanless, 1946, sec. AA-8)

19. Tennessee, Grundy County, small strip mine on the west side of State Route 56 about 2 miles south of Coalmont (H. R. Wanless, oral communication)

20. Tennessee, Van Buren County, same as outcrop 7 of the Mississippian soils

21. Tennessee, White County, outcrop of the Ravencroft Coal along U. S. Highway 70 west of Bon Air in the western scarp of the Cumberland Plateau (Wanless, 1946, sec. DD-9)

22. Tennessee, White County, underclay below the Sewanee Coal taken at same locality as outcrop 21 of zone 2; a shale at the horizon of zone 2 containing marine fossils was also sampled along an old abandoned railroad grade along the edge of the Cumberland Plateau just north of Bon Air (Wanless, 1946, sec. DD-10)

23. Tennessee, Overton County, along a rural highway west of Green Pond (Wanless, 1946, sec. DD-14)

24. Tennessee, Fentress County, coal mine just north of State Route 85, 1 to 2 miles east of Wilder (Wanless, 1946, sec. DD-15)

25. Kentucky, Christian County, railroad cut of the L. & N. Railroad, 1 mile north of Crofton, sample of shale taken 15 feet below the Upper Caseyville Sandstone; should be at about the horizon of the Battery Rock Coal (H. R. Wanless, oral communication)

26. Kentucky, Grayson County, along a gravel road 0.2 mile west of Salt Lick (H. R. Wanless, oral communication)

27. Indiana, Martin County, U. S. Highway 50 road cut 2.6 miles west of Shoals city limits and 8 feet below the Upper Mansfield Sandstone which caps the ridges of the area

28. Illinois, Schuyler County, 2–3 miles north of Frederick, about 100 feet up the first ravine to the left from the mouth of Mill Branch (Wanless, 1931, p. 189, sec. 6)

29. Missouri, Vernon County, along the railroad in the north-central part of sec. 26, T. 36 N., R. 29 W., a few miles northeast of Dederick (Greene and Pond, 1926, p. 40–41)

30. Missouri, Vernon County, about 4 miles south of Dederick on the south bank of Clear Creek where it crosses the line between secs. 15 and 22, T. 35 N., R. 29 W (Greene and Pond, 1926, p. 42)

31. Missouri, Vernon County, half a mile east of Deerfield on the west bank of Drywood Creek just north of U. S. Highway 54 bridge in the SW¼ sec. 5, T. 35 N., R. 32 W. (David Rheinertson, oral communication)

32. Kansas, Cherokee County, same locality as outcrop 9 of the Mississippian soils

33. Kansas, Cherokee County, in the NW¼-NW¼ sec. 14, T. 33 S., R. 25 E., upstream from a roadside park just south of State Highway 96 (Pierce, 1937, p. 22)

34. Oklahoma, Pittsburg County, Lower Hartshorne underclay in a road cut just south of Adamson (Shawnee Geol. Soc., 1938, stop 7)

35. Oklahoma, Latimer County, strip mine in the Upper Hartshorne Coal on the Choctaw Indian Reservation, 1–2 miles northwest of Wilburton (State mine inspector, oral communication)

36. Oklahoma, LeFlore County, strip mine of the Evans Coal Co., in SE¼ sec. 17, 1–2 miles north of

Bokoshep (State mine inspector, oral communication)

37. Arkansas, Sebastian County, old strip mine in the Lower Hartshorne Coal 5 miles east of Hackett in the east-central part of sec. 17, T. 6 N., R. 31 W. (Hendricks and Parks, 1950, geologic map)

38. Arkansas, Washington County, 2 miles south of Baldwin in an old mine in the Baldwin Coal in the property of Fred Levi (M. E. Hopkins, written communication)

39. Arkansas, Johnson County, underclay below the Upper Hartshorne Coal in the wall of a Lower Hartshorne strip mine in the south-central part of sec. 31, T. 9 N., R. 24 W., 3 miles north of Hartman (M. E. Hopkins, written communication)

40. Arkansas, Johnson County, slate from below the Lower Hartshorne Coal in a strip pit just south of U. S. Highway 64 and 3 miles east of Hartman in the SE¼ sec. 9, T. 8 N., R. 24 W., and shale in pit wall above the coal (M. E. Hopkins, written communication)

41. Arkansas, Johnson County, clay pit in the underclay of the Lower Hartshorne Coal of the Eureka Brick Co., northeast of Clarksville in sec. 29, T. 10 W., R. 22 W. (M. E. Hopkins, written communication)

Zone 3

1. Ohio, Holmes County, Killbuck Township, same as outcrop 2 of the Mississippian soils

2. Ohio, Perry County, Madison Township, in a gully west of the road in W½ SW¼, sec. 5 (Flint, 1951, sec. F203)

3. Ohio, Perry County, Monday Creek Township, at the head of a gully in the NW¼NE¼ sec. 17 (Flint, 1951, sec. F51)

4. Kentucky, Morgan County, along U. S. Highway 460 at the Morgan-Magoffin county line, sample from below and above the Ambugy (Cannel City) Coal (Kentucky Geol. Soc., 1953, stop 4).

5. Kentucky, Morgan County, along U. S. highway 460, 7 miles west of Index, samples from below the Ambugy coal (Kentucky Geol. Soc., 1953, stop 2)

6. Kentucky, Morgan County, sample from below the "Grassy" coal in the creek bottom near the bridge at Index, across from the garage (Kentucky Geol. Soc., 1953, stop 3, Index side)

7. Kentucky, Morgan County, small mines in a "Grassy" cannel coal about an eighth of a mile up a dirt road which turns north from U. S. 460 about 0.6 mile northeast of Mize junction (H. R. Wanless, oral communication)

8. Kentucky, Morgan County, in stream bed 2.4 miles north of Hazel Green along state route 203, sample from below the "Grassy" Coal (Kentucky Geol. Soc., 1953, stop 1)

9. Kentucky, Breathitt County, along State Highway 15, 2 miles north of Jackson on the east side of the divide, from below the Ambugy Coal (Kentucky Geol. Soc., 1953, stop 8)

10. Kentucky, Laurel County, mine in Lilly coal 4 miles west of the junction of highways 80 and 25 at London (H. R. Wanless, oral communication)

11. Kentucky, Leslie County, in the south part of Hyden just east of a bridge, from below the Ambugy Coal (H. R. Wanless, oral communication)

12. Kentucky, Letcher County, from a mine in the Elkhorn coal 3½ miles north of Whitesburg on State Route 15 (Wanless, 1946, sec. TT-1)

13. Virginia, Wise County, from below the Elkhorn Coal along State Highway 160 west of Appalachia (Wanless, 1946, sec. TT-5)

14. Tennessee, Morgan County, along State Highway 116 east from Petros to the gap at the county line (Wanless, 1946, sec. MM-2)

15. Tennessee, Campbell County, abandoned mine in the Jellico Coal east of the dirt road going north from Newcomb into Scott County (Wanless, 1946, sec. MM-9)

16. Missouri, Barton County, strip pit 1½ miles southwest of Liberal (David Rheinertson, oral communication)

17. Kansas, Cherokee County, 3 miles east of Weir in a coal strip pit near the center of the west line of sec. 32, T. 31 S., R. 25 E. (R. S. Holmes, oral communication)

18. Kansas, Cherokee County, 4 miles southeast of Weir in a strip pit in the SW¼ sec. 7, T. 32 S., R. 25 E. (R. S. Holmes, oral communication)

19. Oklahoma, Pittsburg County, old strip mine just north of U. S. Highway 270 about 0.8 mile east of Alderson (Shawnee Geol. Soc., 1938)

20. Oklahoma, Pittsburg County, underground mine of the Lone Star Steel Co., 4 miles east of Krebs (Shawnee Geol. Soc., 1938)

Zone 4

1. Pennsylvania, Armstrong County, clay mine just across the Redbank River from Mayport (Graeber and Foose, 1942, p. 60)

2. Pennsylvania, Jefferson County, road cut along State Highway 28 just north-east of the Corsica road junction and about a mile east of Summerville (Graeber and Foose, 1942, p. 60)

3. Pennsylvania, Lawrence County, 1 mile northeast of Mahoningtown behind the old Lawrence School (DeWolfe, 1929, p. 52)

4. Ohio, Holmes County, Berlin Township, along

the dirt road 1 mile south of Berlin (White, 1949, sec. 72)

5. Ohio, Perry County, Madison Township, same as outcrop 2 of zone 3.

6. Ohio, Perry County, Reading Township, same as outcrop 3 of the Mississippian soils

7. Ohio, Perry County, Monday Creek Township, same as outcrop 3 of zone 3.

8. Ohio, Vinton County, old shale pit of the MacArthur Brick Co., at MacArthur (Stout, 1927, p. 110)

9. West Virginia, Logan County, about 7 miles east of Logan on the hill going up the west side of Blair Mountain (H. R. Wanless, oral communication)

10. West Virginia, Mingo County, just east of the pass where U. S. highways 119 and 52 join (H. R. Wanless, oral communication)

11. Kentucky, Magoffin County, along a side road from State Route 30, 0.3 mile south of Hendrix (Kentucky Geol. Soc., 1953, stop 10)

12. Kentucky, Magoffin County, along U. S. Highway 460 at Elsie (Kentucky Geol. Soc., 1953, stop 5)

13. Kentucky, Morgan County, same as outcrop 5 of zone 3

14. Kentucky, Breathitt County, same as outcrop 9 of the zone 3

15. Kentucky, Perry County, along state route 15, 5 miles north of Hazard (H. R. Wanless, oral communication)

16. Kentucky, Leslie County, old mine by State Route 80, 1.4 miles west of Wooton (H. R. Wanless, oral communication)

17. Kentucky, Pike County, along U. S. Highway 119 near the east side of Bent Mountain and 3–5 miles west of Canada; outcrop, (Wanless, oral communication); sec. (Wanless, 1939, Pl. 4, no. 17, Pl. 5, no. 15, and Pl. 6, no. 20)

18. Kentucky, Letcher County, same as outcrop 12 of zone 3

19. Virginia, Wise County, same as outcrop 13 of zone 3

20. Kentucky, Harlan County, mine opening on side of mountain east of Alva (Wanless, 1946, sec. TT-15)

21. Kentucky, Bell County, along State Route 21 about 14 miles north of Pineville; zone 4 underclay crops out near Coleman Mines (Wanless, 1946, sec. SS-6)

22. Kentucky, Bell County, section on small side road going east on the ridge crossed by the road leading from State Route 92 to Kajay (Wanless, 1946, sec. QQ-3)

23. Kentucky, Bell County, on the north side of Log Mountain in an abandoned mine up a hollow west of State Route 74, about 7 miles west of Middlesboro (Wanless, 1946, sec. QQ-5)

24. Tennessee, Campbell County, same locality as outcrop 15 of zone 3, but in a small mine farther north near the top of the divide

25. Tennessee, Morgan County, about 4 miles farther along the dirt road of outcrop 26; a lingula-bearing shale below a cannel coal, probably a few hundred feet above zone 4

26. Tennessee, Morgan County, ½–1 mile up a side road leading west up the ridge from the divide crossed by State Route 116 in locality of outcrop 14 of zone 3

27. Kentucky, Butler County, in a small mine about half a mile south of outcrop 11 of zone 5

28. Indiana, DuBois County, underground clay mine half a mile west of Hunningburg (Hayden Murray, oral communication)

29. Indiana, Owen County, wall of an abandoned strip pit in SW¼SW¼ sec. 2, T. 9 N., R. 6 W., about a mile north of Coal City (H. R. Wanless, oral communication)

30. Indiana, Fountain County, go 8.2 miles east on State Route 234 from its junction with U. S. route 41, turn north for 0.7 mile and then west for 0.7 mile to a small bridge, then go upstream for about 100 yards to the sample locality (Hayden Murray, oral communication)

31. Indiana, Vermillion County, a few hundred yards downstream from the bridge 1.7 miles west of Eugene (Hayden Murray, oral communication)

32. Illinois, Schuyler County, same as outcrop 28 of zone 2, but a little farther up the ravine

33. Missouri, Vernon County, just north of Deerfield in old quarry south of bridge in SW¼ sec. 6, T. 35 N., R. 32 W. (David Rheinertson, oral communication)

34. Missouri, Barton County, about 100 yards upstream from a small bridge 1 mile west and half a mile south of Liberal (David Rheinertson, oral communication)

35. Oklahoma, Pittsburg County, Secor Coal by old mine about 80 feet stratigraphically above outcrop 36 of zone 4.

36. Oklahoma, Pittsburg County, about 5 miles northeast of Krebs just east of State Route 31 in NW¼ sec. 28, T. 6 N., R. 16 E (Shawnee Geol. Soc., 1938)

37. Arkansas, Johnson County, strip pit of the Utah Coal Co. in sec. 18, T. 10 N., R. 25 W., about 6 miles north of Coal City (M. E. Hopkins, written communication)

38. Arkansas, Johnson County, dam spillway of Horsehead Lake 1–2 miles northeast of Hunt and about 4 miles northeast of locality 37

39. Arkansas, Johnson County, old strip mine in

the Philpot Coal 2 miles west of Harmony near gravel road

Zone 5

1. Pennsylvania, Jefferson County, in the Old Humphrey Quarry 1 mile east of Brookville (Graeber and Foose, 1942, p. 51)

2. Pennsylvania, Lawrence County, in the Ambrosia Coal Co. pit about 1 mile east of Bessemer on State Route 317 (Mine manager, oral communication)

3. Ohio, Holmes County, Salt Lick Township, in quarry of the Holmes Limestone Co. 1½ miles east of Benton (C. B. Moke, oral communication)

4. Ohio, Vinton County, strip mine by U. S. Highway 50 about 3 miles west of MacArthur (Stout, 1927, geological map)

5. West Virginia, Kanahwa County, first mine opening of the Winifrede Collieries about 1½ miles up the canyon from Winifrede; the Winifrede Canyon road goes southwest from State Route 61, 19 miles southeast of Charleston (H. R. Wanless, oral communication)

6. West Virginia, Logan County, same as outcrop 9 of zone 4 but a little farther west down the hollow

7. Kentucky, Carter County, near the top of the hill 4 miles east of Grayson along U. S. Highway 60 (H. R. Wanless, oral communication)

8. Kentucky, Morgan County, same as outcrop 6 of zone 3

9. Kentucky, Magoffin County, section along State Route 30 at the Magoffin-Breathitt county line (Kentucky Geol. Soc., 1953, stop 9)

10. Kentucky, Pike County, same as outcrop 17 of zone 4

11. Kentucky, Butler County, on U. S. Highway 231 (State Route 71) about 3 miles west of Aberdeen in grade up from a valley to the east (H. R. Wanless, oral communication)

12. Missouri, Barton County, same as outcrop 34 of zone 4 but on the opposite side of the road up a small ditch

13. Kansas, Crawford County, in the strip pit of the Macky-Clemmens Coal Co., 2 miles north of Mulberry in NE¼ sec. 24, T. 28 S., R. 25 E.; samples were taken from below the Pittsburg Coal, the overlying Tebo Coal, and the intervening shale (Mine manager, oral communication; Pierce, 1937, geologic map)

14. Kansas, Cherokee County, clay pit of the United Brick and Tile Co., at the southeast edge of Weir (R. S. Holmes, oral communication)

15. Oklahoma, Pittsburg County, just north of U. S. Highway 270, 5 miles west of McAlester and half a mile east of the Coal Creek bridge; maroon shales of the Boggy Formation are about equivalent to the Weir-Pittsburg coal (Shawnee Geol. Soc., 1938, stop 9)

Zone 6

1. Pennsylvania, Luzerne County, strip mine south of State Route 115 in the long hill east of Wilkes Barre

2. Pennsylvania, Luzerne County, highest strip pit on the mountain northwest of Kingston (H. W. Wanless, oral communication)

3. Pennsylvania, Schuylkill County, highest strip pit on Pisgah Mountain, ½–1 mile southeast of Tamaqua (M.L. Kidda, 1953, M.S. thesis, Univ. Illinois)

4. Pennsylvania, Northumberland County, strip pit just east of State Route 54 about 2 miles north of Mt. Carmel (Gordon Wood and Harold Arndt, oral communication)

5. Pennsylvania, Clearfield County, on steep slope about 50 feet above State Route 969, 1 mile southwest of its junction with State Route 453 and about 2 miles south of Curwensville (Ashley, 1940, Pl. II, sec. 7; p. 31)

6. Pennsylvania, Clearfield County, strip mine on the hill north of Lumber City (Ashley, 1940, Pl. II, sec. 5)

7. Pennsylvania, Armstrong County, behind the court house at Kittanning (H. R. Wanless, oral communication)

8. Pennsylvania, Lawrence County, in the quarry of the Bessemer Limestone Co., at Bessemer; section given by company superintendent follows DeWolfe (1929, Pl. IV)

9. Ohio, Tuscarawas County, clay pit of the Robinson Clay Co., near U. S. Highway 250 north of Uhlrichsville (C. B. Moke, oral communication)

10. Ohio, Holmes County, same as outcrop 3 of zone 5

11. Ohio, Holmes County, Clark Township, just north of Baltic in SE¼ sec. 25, in the quarry of the General Clay Products Co. (White, 1949, p. 254)

12. Ohio, Perry County, Clayton Township, sec. 26 in strip pit of the Sunnyhill Coal Co., about 3 miles north of New Lexington (Flint, 1951, p. 82)

13. Ohio, Athens County, York Township, quarry west of road only a few hundred yards after turning north from the Hocking River bridge mentioned in outcrop 9 of zone 8

14. Ohio, Hocking County, pit of Diamond-Hocking Valley Brick Co., near U. S. Highway 33 south of Haydensville (Myron Sturgeon, oral communication)

15. Ohio, Lawrence County, from pit of Ohio

Brick Co. of Oak Hill at Blackfork (Mr. Davis, owner, oral communication)

16. Ohio, Lawrence County, Frampton quarry about 1 mile east of State Route 75 and 6¾ miles north of the junction of routes 75 and 141

17. West Virginia, Barbour County, floor of strip pit just west of U. S. Highway 250 about 1½ miles south of Junior (A. T. Cross, oral communication)

18. West Virginia, Kanahwa County, about 3 miles west of Charleston on the east slope above Davis Creek along the road leading to the golf course (H. R. Wanless, oral communication)

19. West Virginia, Kanahwa County, about 1 mile farther up Winifrede Canyon above outcrop 5 of zone 5 at the mouth of the coal mine (H. R. Wanless, oral communication)

20. Virginia, Wise County, same as outcrop 13 of zone 3 but near the top of the gap

21. Kentucky, Carter County, middle coal exposed at same outcrop as 12 of zone 8

22. Kentucky, Bell County, same as outcrop 23 of zone 4, about 50 feet below summit of State Route 74 on the north side of Log Mountain

23. Kentucky, Bell County, same as outcrop 21 of zone 4, just below the gap on the north side of the divide

24. Kentucky, Ohio County, in stream bank just west of State Route 269, about 1 mile north of Schultztown and 4–5 miles southwest of Cromwell (H. R. Wanless, oral communication)

25. Kentucky, Union County, in bank of Tradewater River at Grangertown which is just west of Sturgis (H. R. Wanless, oral communication)

26. Indiana, Pike County, road cut on the north side of State Route 64 near the base of a long hill about 1 mile east of Stendal (H. R. Wanless, oral communication)

27. Indiana, Clay County, coal strip of the Ayrshire Collieries about 2 miles south and 2 miles west of Staunton (H. R. Wanless, oral communication)

28. Indiana, Vermillion County, along U. S. Highway 36 in the west bluff of the Wabash River (H. R. Wanless, oral communication)

29. Indiana, Vermillion County, clay pit of the Artistic Ceramic Co., about 4 miles north of outcrop 28 in the west bluff of the Wabash River, about 2–3 miles east of the Wabash Ordinance Plant (Hayden Murray, oral communication)

30. Indiana, Vermillion County, at the lower part of the bluff on the north side of the Vermillion River just across the State line from Illinois (H. R. Wanless, oral communication)

31. Illinois, Pike County, go north from Hadley 2½ miles, east for 0.6 mile to a bridge, then south along the creek for a quarter of a mile (Arthur White, oral communication)

32. Missouri, Boone County, 4 miles east of Columbia, just east of the bridge in NW¼NW¼ sec. 23, T. 48 N., R. 12 W. (Unkelsbay, 1952, p. 78)

33. Missouri, Henry County, strip mine of the Power Coal Co., 2 miles north of Germantown (Noah) and just east of county route E (mine engineer, oral communication)

34. Missouri, Vernon County, old strip mine in the east bank of Wolf Creek in NE¼NW¼ sec. 14, T. 37 N., R. 33 W. near Stotesbury (David Rheinertson, oral communication)

35. Missouri, Vernon County, half a mile east of Eve in a small strip,pit just south of U. S. Highway 54 and near the railroad overpass (Greene and Pond, 1926, p. 83)

36. Kansas, Crawford County, 2 miles southeast of Franklin in the walls of a strip pit near the southwest corner of sec. 21, T. 29 S., R. 25 E. (Pierce, 193, map)

37. Kansas, Labette County, near the center of sec. 32, T. 34 S., R. 21 E., in stream bottom 2 miles west of Chetopa (Pierce, 1937, map)

38. Oklahoma, Rogers County, strip pit 3 miles west of the Rogers County Coal Co. tipple at Sequoyah (State mine inspector, oral communication)

39. Oklahoma, Rogers County, strip pit at McNabb Coal Co. just north of State Route 33 about 3 miles east of Catoosa (State mine inspector, oral communication)

40. Oklahoma, Okmulgee County, strip pit of the McInnis and Grafe Coal Co., about 1 mile east of Henryetta out Trudgeon Street (Manager, oral communication)

41. Oklahoma, Hughes County, road cut along U. S. Highway 270, 8 miles east of Calvin in the scarp of the Calvin Sandstone (Shawnee Geol. Soc., 1938)

42. Oklahoma, Hughes County, road cut by U. S. Highway 270 just west of the bridge across the Canadian River at Calvin (Shawnee Geol. Soc., 1938)

Zone 7

1. Kentucky, Ohio County, along an abandoned dirt road just east of Prentice which is 3 miles north of Schultztown and about 3 miles west of Cromwell on State Route 269 (H. R. Wanless, oral communication)

2. Illinois, Williamson County, railroad cut just southwest of Marion about 100 yards north of the railroad bridge over a dirt road (H. R. Wanless, oral communication)

3. Indiana, Pike County, bank of small stream just northeast of State Route 64 near the bridge half a mile west of Stendal (H. R. Wanless, oral communication).

4. Indiana, Greene County, 1½ miles south of Jasonville in a small stream just east of State Route 59 in SW¼ sec. 17, T. 8 N., R. 7 W. (H. R. Wanless, oral communication)

5. Indiana, Vermillion County, south bank of the Little Vermillion River at Whites Mill which is 5 miles west of Newport on the township line (H. R. Wanless, oral communication)

6. Iowa, Appanoose County, along a creek about 100 yards south of a bridge and 2½ miles east of Monrovia in NW¼ sec. 1, T. 70 N., R. 17 W. (Cline, 1941, sec. XI)

7. Missouri, Macon County, wall of strip mine by a mine road in E½ sec. 12, T. 56 N., R. 15 W. about 6 miles southwest of Macon (Cline, 1941, sec. VII)

8. Missouri, Vernon County, west bank of a north-south road 4 miles northeast of Stotesbury, 0.2 mile north of the center of sec. 12, T. 37 N., R. 33 W. (David Rheinertson, oral communication; Greene and Pond, 1926, geologic map)

9. Kansas, Bourbon County, go 1 mile south of Fulton on U. S. Highway 69 and 4 miles east on a dirt road to the outcrop where the road climbs out of a small valley (Norman Plummer, oral communication

10. Kansas, Bourbon County, in railroad cut just east of the station at Ft. Scott (Norman Plummer, oral communication)

11. Kansas, Bourbon County, 3 miles west of Ft. Scott in the spillway of an irrigation dam (Norman Plummer, oral communication)

12. Kansas, Crawford County, in stream bank 1½ miles southeast of Girard in center of the NW¼ sec. 29, T. 29 S., R. 24 E. (Pierce, 1937, p. 78)

13. Oklahoma, Craig County, ditch along U. S. Highway 60 in SE¼ sec. 35, T. 36 N., R. 18 E. about 4 miles west of Estelle (Jewett, 1945, p. 141)

14. Oklahoma, Rogers County, 2–3 miles southwest of Foyil along the gravel road 0.1 mile west of SE. corner sec. 36, T. 23 N., R. 16 E. (Jewett, 1945, p. 136)

15. Oklahoma, Rogers County, cut along State Route 20, 3 miles west of Claremore near the center of the south line of sec. 11, T. 21 N., R. 15 E. (Jewett, 1945, p. 135)

Zone 8

1. Pennsylvania, Jefferson County, 1½ miles northeast of Baxter in a road cut of State Route 28 (Graeber and Foose, 1942, p. 38)

2. Pennsylvania, Armstrong County, along the cement road going north from the west end of the bridge of U. S. Highway 422 across the Allegheny River at Kittanning (H. R. Wanless, oral communication)

3. Pennsylvania, Lawrence County, same as outcrop 8 of zone 6

4. Ohio, Holmes County, Clark Township, sec. 6, road cut in top of hill three-eighths of a mile west of Charm (White, 1949, p. 252)

5. Ohio, Holmes County, Clark Township, same as outcrop 11 of zone 6

6. Ohio, Perry County, Clayton Township, same as outcrop 12 of zone 6

7. Ohio, Perry County, Jackson Township, sec. 26, samples from two localities; a 6-inch dark-gray, calcareous clay at the Middle Kittanning horizon from an abandoned strip pit in the Lower Kittanning Coal behind a farm house in the E½NW¼ of the section, and an underclay in a strip pit of a 2½-foot coal in the SE¼ of the section (Flint, 1951, geologic map and section F 330)

8. Ohio, Athens County, York Township, 11.3 miles northwest of Athens in a road cut on the northeast side of U. S. Highway 33 (Myron Sturgeon, oral communication)

9. Ohio, Athens County, York Township, cross the Hocking River at Nelsonville and go north for 1 mile over a hill; in a road cut on the east side of the road just before crossing a small bridge, the Middle Kittanning Coal crops out (Myron Sturgeon, oral communication)

10. West Virginia, Barbour County, in the walls of the strip pit of outcrop 17 of zone 6

11. Virginia, Wise County, about 100 feet above the main highway on a dirt road along the ridge leading south from State Highway 160 where it crosses the divide of the Cumberland Mountains at the Kentucky-Virginia State line (Wanless, 1946, sec. TT-5)

12. Kentucky, Carter County, top coal exposed in the U. S. Highway 60 cut 6 miles east of Grayson (H. R. Wanless, oral communication)

13. Kentucky, Ohio County, exposure below a fossiliferous marine limestone along an abandoned dirt road half a mile southwest of Maxwell, just before the road turns south; section (Wanless, 1939, Pl. 1, sec. 11); location (Wanless, oral communication)

14. Kentucky, Hopkins County, diamond core from the property of the Williams Coal Co., 3 miles west of Mannington (Mr. Leslie Lindsay, mine manager, oral communication); section (Wanless, 1939, Pl. 2, sec. 9)

15. Kentucky, Hopkins County, strip mine in Kentucky No. 11 and No. 12 coals about 3 miles southwest of Nortonville; section (Wanless, 1939,

Pl. 2, sec. 9); location (H. R. Wanless and mine manager, oral communications)

16. Indiana, Warwick County, road cut, just east of State Route 61–66 junction at Yankeetown (H. R. Wanless, oral communication)

17. Indiana, Sullivan County, bottom of strip pit of Robin Hood Coal Co., 1½ miles west of Gilmore; section (Wanless, 1939, Pl. 1, sec. 16); location (H. R. Wanless, oral communication)

18. Illinois, Vermillion County, outcrop along Grape Creek about half a mile upstream from a concrete bridge across Hawbuck Creek in sec. 2, T. 18 N., R. 11 W.; section (Wanless, 1939, Pl. 1, sec. 16); outcrop (H. R. Wanless, oral communication)

19. Iowa, Appanoose County, mine of W. M. Zaputil in the south-central part of sec. 19, T. 69 N., R. 18 W., about 2 miles southwest of Mystic (Cline, 1941, sec. XI)

20. Missouri, Putnam County, along the gravel road just north of the stream in the SW¼ sec. 22, T. 65 N., R. 18 W., about 6 miles southeast of Unionville (Cline, 1941, sec. VIII). Note: the section north of the river is new better than that south of the river in sec. 27, described by Cline.

21. Missouri, Grundy County, limestone quarry just north of Alpha (Cline, 1941, sec. IV)

22. Missouri, Ray County, ravine just northwest of the road junction at the southwest corner of sec. 14, T. 52 N., R. 26 W. (Cline, 1941, sec. III)

23. Missouri, LaFayette County, ravine upstream from where it crosses U. S. Highway 24, a quarter of a mile west of Myrick Station which is 1 mile west of Lexington (Cline, 1941, sec. II)

24. Oklahoma, Craig County, 6 miles west of Banzet in the southwest corner of sec. 27, T. 29 N., R. 18 E., where the main county gravel road crosses the creek (Jewett, 1945, p. 142, sec. 203)

Zone 9

1. Pennsylvania, Somerset County, at mileage marker 121½ of the Pennsylvania Turnpike, half a mile west of the Allegheny tunnel on the north side of the road, red clay about 50 feet below the Brush Creek coal (Cleaves and Stephenson, 1949, Pl. 26)

2. Pennsylvania, Somerset County, at mileage marker 116, 6 miles west of the Allegheny tunnel on the north side of the Pennsylvania Turnpike (Cleaves and Stephenson, 1949, Pl. 26)

3. Pennsylvania, Beaver County, near the top of the hill 1 mile east-southeast of New Galilee and just east of the cemetery (DeWolfe, 1929, p. 31)

4. West Virginia, Preston County, cut along the B. & O. Railroad below the wooden footbridge just south of Anderson (Blaser) from a clastic flint clay below the Lower Freeport Coal horizon (Hennen and Reger, 1914, p. 97)

5. West Virginia, Taylor County, quarry of the Hammond Brick Co. at Thornton (A. T. Cross, oral communication)

6. Ohio, Athens County, at the top of the hill mentioned in locality 9 of zone 8

7. Indiana, Sullivan County, slumped stream bank near the railroad in the east-central part of sec. 5, T. 7 N., R. 9 W., half a mile southwest of Sullivan (H. R. Wanless, oral communication)

8. Illinois, Edgar County, about half a mile downstream from a small bridge at the west edge of sec. 29, T. 14 N., R. 10 W. where a dirt road crosses the stream near the center of the section, about 8 miles east of Paris (H. R. Wanless, oral communication)

9. Iowa, Appanoose County, near the top of the shale pit at the western edge of Centerville where State Route 2 curves north; samples from the underclay and the shale 10 feet below the underclay (Cline, 1941, sec. XI)

10. Missouri, Sullivan County, stream bank on the farm of Albert Cocran in the NW¼ sec. 5, T. 62 N., R. 20 W. about 3 miles west of Milan (Cline, 1941, sec. VI)

11. Missouri, Sullivan County, samples from near a bridge 2½ miles south of Reger in sec. 8, T. 61 N., R. 20 W.; underclay from below a coal in the ravines north of the road and east of the bridge and the red bed from west of the bridge and just south of the road (Cline, 1941, sec. VI)

12. Kansas, Wyandotte County, west of Kansas City and 2–3½ miles east of the junction of State routes 132 and 32 along Route 32; sample from below the horizon of the Thayer Coal (Kansas Geol. Soc., 1949, stop 2)

13. Kansas, Montgomery County, west of Cherryvale, 0.2 mile west of the southeast corner of sec. 24, T. 31 S., R. 16 E. (Schoewe, 1944)

14. Kansas, Montgomery County, in the NW¼ sec. 26, T. 34 S., R. 16 E., along the road going up the bluff on the northwest outskirts of Coffeyville east of the country club (Kansas Geol. Soc., 1937, stop 16)

Zone 10

1. Pennsylvania, Westmoreland County, cut south of the Pennsylvania Turnpike, 2½ miles east of Irwin near a strip in the Pittsburgh coal (Cleaves and Stephenson, 1949, Pl. 28)

2. West Virginia, Monongalia County, about 3 miles west of Morgantown on the north side of State Route 7, ½–1 mile west of its overpass over U. S. Highway 19 (A. T. Cross, oral communication)

3. West Virginia, Richie County, along a gravel road 1.2 miles northwest of Petroleum from below the Lower Pittsburg Coal (McCue, 1948, p. 70)

4. Ohio, Belmont County, at base of long hill on U. S. Highway 40 just west of the bridge at Blaine (White, 1945)

5. Ohio, Athens County, in a small strip pit in the lower bench of the Pittsburg Coal near Uttley in sec. 26 of Bern Township (Myron Sturgeon, oral communication)

6. Ohio, Athens County, just east of the junction of State Route 377 and U. S. Highway 50A in sec. 29 of Ames Township (Myron Sturgeon, oral communication)

7. Ohio, Athens County, Bern Township, sec. 32 along a gravel road a quarter of a mile south of junction with State Route 632 (Myron Sturgeon, oral communication)

8. Kentucky, Union County, in gulch near an old mine in the bluff south of State Route 85, about 1 mile northwest of Henshaw (H. R. Wanless, oral communication)

9. Illinois, Jasper County, 2½ miles south of Gila along Mint Creek in sec. 31, T. 8 N., R. 9 E. (Newton and Weller, 1937, Pl. 1, sec. 1)

10. Illinois, Cumberland County, about 2 miles southwest of Woodbury in the SE¼ sec. 32, T. 9 N., R. 8 E. in the banks of Webster Creek (Newton and Weller, 1937, Pl. 1, sec. 5)

11. Kansas, Shawnee County, quarry a quarter of a mile south of a washed-out bridge across the Kansas River on what was U. S. Highway 40, just west of Topeka in SE¼ sec. 27, T. 11 S., R. 15 E. (Kansas Geol. Soc., 1936, stop 22)

12. Kansas, Osage County, about 2 miles northeast of Osage in NE¼ sec. 17 (Norman Plummer, oral communication)

13. Kansas, Chautauqua County, road cut on U. S. Highway 166, 12.4 miles west of its junction with State Route 99 and 2–3 miles west of Wauneta (Kansas Geol. Soc., 1937, stop 40)

14. Oklahoma, Seminole County, road cut on State Route 99, half a mile south of Seminole city limits (Shawnee Geol. Soc., not dated, stops 4 to 5)

BULLETIN OF THE GEOLOGICAL SOCIETY OF AMERICA
VOL. 69, PP. 403-418, 5 FIGS., 1 PL. APRIL 1958

URANIUM DEPOSITS UNDER CONGLOMERATIC SANDSTONE OF THE MORRISON FORMATION, COLORADO AND UTAH

BY DAVID A. PHOENIX

ABSTRACT

In southwestern Colorado and southeastern Utah, strata of conglomeratic sandstone are localized at the base of the Brushy Basin Member of the Morrison Formation of Jurassic age. These discrete lithologic units contain sedimentary structures oriented in a prevailing easterly direction. They are believed to cover about one-third of the underlying Salt Wash Member in southwestern Colorado and southeastern Utah, and they locally rest on ore-bearing sandstone in the Salt Wash Member. Eastward-trending planar cross-stratification and trough cross-stratification and a general westward coarsening of sediments in the conglomeratic sandstone strata suggest that they are the products of stream aggradation from westerly source areas.

Uranium-vanadium deposits in the uppermost, almost continuous, layer of sandstone of the Salt Wash Member are classified according to their association with the conglomerate strata. Of the 363 deposits studied in the uppermost sandstone layer of the Salt Wash Member, 101 are known to be directly beneath conglomeratic sandstone strata, 211 are below the projected extension of conglomeratic sandstone strata, 33 are beyond the safe limits of such projection, and 18 are lateral to the margins of conglomeratic sandstone strata. At places, near clusters of deposits in the uppermost sandstone of the underlying Salt Wash Member, conglomeratic sandstone strata of the Brushy Basin Member are also mineralized.

It is postulated that ground-water movement during deposition of the Morrison Formation in Late Jurassic time, localized the uranium and vanadium. The direction of this ground-water movement is believed to have been related to streams that deposited the conglomeratic strata, so that in the ore-bearing sandstone metal ions contained in the ground water were localized in places of high transmissibility and in the vicinity of decaying organic debris. According to the age of the ores, precipitation of the metals was much later than their localization, probably during Late Cretaceous or early Tertiary time.

CONTENTS

TEXT

	Page
Introduction and acknowledgments	404
Methods of study	405
Units mapped	406
Ore-bearing sandstone	406
Conglomeratic sandstone strata	407
Lithology	407
Stratigraphic position	408
Sedimentary structures	408
Elongation	409
Frequency of occurrence	409
Relation to uranium-vanadium deposits	409
Summary and conclusions	413
References cited	416

ILLUSTRATIONS

Figure		Page
1.	Map of part of the Colorado Plateau showing areas of study, distribution, and trend of conglomeratic strata at the base of the Brushy Basin Member of the Morrison Formation	405
2.	Lithologic and permeability characteristics of uppermost sandstone layer	406
3.	Isometric drawing showing the relation of the uranium-vanadium mines in sandstone of the Salt Wash Member to the conglomerate in the Brushy Basin Member of the Morrison Formation	411
4.	Isometric drawing showing the relation of the uranium-vanadium mines in sandstone of the Salt Wash Member to the conglomerate in the Brushy Basin Member of the Morrison Formation	412
5.	Geologic map showing the relation of the uranium-vanadium mines in the sandstone of the Salt Wash Member to the con-	

Page
glomerate in the Brushy Basin Member of the Morrison Formation 414

Page Facing page
1. Cross-stratification in the Morrison Formation 408

TABLE

Table Page
1. The relation of uranium-vanadium deposits in the uppermost sandstone layer of the Salt Wash Member to overlying conglomeratic strata at the base of the Brushy Basin Member of the Morrison Formation 410

Introduction and Acknowledgments

Uranium-vanadium deposits are widespread on the Colorado Plateau and have been the principal domestic source of these metals. Although the geologic environment of these deposits differs from place to place, nearly all the deposits have many features in common. In general they are widely distributed, largely restricted to a few stratigraphic layers of sandstone, and show a closer relationship to sedimentary features than to local centers of igneous activity or to structures resulting from regional deformation (Fischer, 1942; Fischer and Hilpert, 1952, p. 3–6). These features suggest that the deposits were formed from solutions introduced into the ore-bearing sandstone, perhaps before regional deformation, rather than along vertical channels such as fractures. The deposits were probably formed at a depth of not more than 10,000 feet at temperatures normal for these depths—100°–140°C.—(Coleman, 1957) and probably not later than Late Cretaceous or Early Tertiary time (Stieff, Stern, and Milkey, 1953). Crustal disturbance in the Colorado Plateau was probably initiated during this time, and volcanic rocks in the Animas and McDermott formations of Late Cretaceous or early Tertiary age in the San Juan region attest to near-by igneous activity (Larsen and Cross, 1956, p. 57). Changes in the chemical environment associated with the onset of these events may have been sufficient to cause precipitation of the ions of uranium and vanadium.

Theories of origin for the metals are divided between (1) a deep-seated hydrothermal source at or near the time of ore deposition and (2) a source in the sediments from which the metals are introduced either into ground water at or near the time of deposition or at some time later when solutions in the ore-bearing sandstone were confined by overlying mudstone and lateral movement was slow and governed by regional hydraulic gradients and the transmissibility of the aquifer. In the latter case the opportunity for enrichment of the solutions with uranium would be enhanced by the long period between deposition of the sediments and the calculated age of the deposits. However, it is also possible that weakly mineralized groundwater solutions were enriched during deposition of the sediments by such natural processes as evaporation and transpiration by plants, and shortly after burial of the ore-bearing sandstone the metals were localized by underflow connected with the deposition of younger sediments. The general tectonic stability of the Colorado Plateau until late Cretaceous or Early Tertiary time might also favor near stagnation of these mineralized pore fluids in areas of high transmissibility until later formation of the ore deposits.

Reasoning along these lines led to a reconnaissance and a detailed stratigraphic study of sediments above the uranium deposits in the Morrison Formation of Jurassic age. The ore-bearing sandstone of the Morrison Formation was also mapped in detail at several of the larger mining districts, and many miles of outcrop of the Morrison Formation was examined in southwestern Colorado and southeastern Utah.

In southwestern Colorado and southeastern Utah the Morrison Formation is composed of a lower Salt Wash Sandstone Member and an upper Brushy Basin Shale Member. The Brushy Basin Member is composed predominantly of variegated claystone containing varying amounts of silt and sand. Impure bentonitic clay forms much of the Brushy Basin Member and is in part volcanic in origin. Lenses of conglomeratic sandstone are common particularly near the base of the member in western Colorado and eastern Utah (Craig *et al.*, 1955, p. 156). The Salt Wash Member is a broad fan-shaped lobe of sediments with its apex in south-central Utah and its outer periphery in western Colorado. The western or apical portion of the lobe is permeable conglomeratic sandstone, and this changes laterally to alternating strata of sandstone and mudstone; in west-central Colorado the member is indistinguishable from the overlying Brushy Basin Shale Member. Clusters of uranium-vanadium deposits in the Morrison Formation impregnate sandstone near the top of the

Salt Wash Member; they occur in a broad belt that is roughtly arcuate and parallel to the outer periphery of the Salt Wash lobe of sediments; most of the deposits occur in a facies of the Salt Wash Member that is composed of claystone and lenticular sandstone (Craig *et al.*, 1955, p. 135–138; Fischer, 1942; Fischer and Hilpert, 1952).

The results of the detailed studies indicate that the uranium-vanadium deposits in the Salt Wash Member of the Morrison Formation tend to be clustered below lenticular strata of conglomeratic sandstone found near the base of the Brushy Basin Member. This report describes the character and occurrence of the conglomeratic sandstone strata and the underlying ore-bearing sandstone and also postulates relations of these strata to genesis of the ores. The data presented herein were obtained from 11 mining areas in southwestern Colorado and southeastern Utah (Fig. 1).

This study has drawn upon the extensive knowledge of the Morrison Formation and the uranium-vanadium deposits gained by the writer's colleagues, including R. P. Fischer, L. C. Craig, and D. R. Shawe of the U. S. Geological Survey.

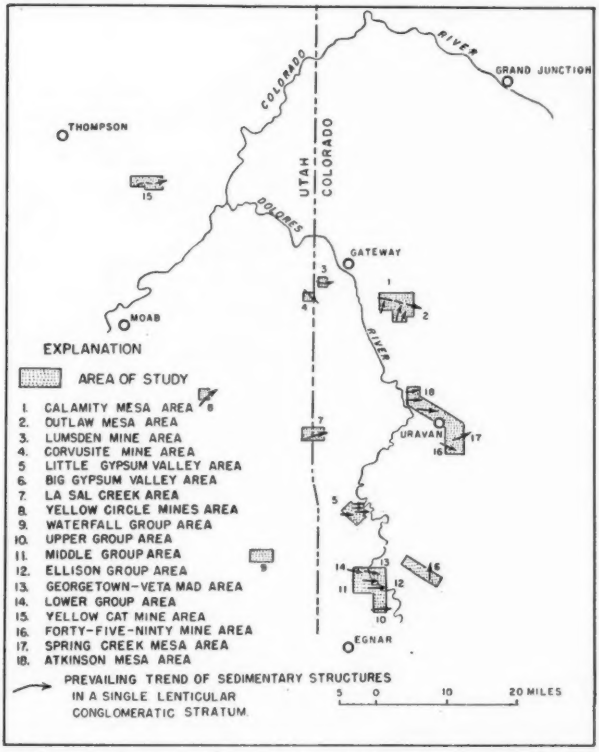

FIGURE 1.—MAP OF PART OF COLORADO PLATEAU SHOWING AREAS OF STUDY, DISTRIBUTION, AND TREND OF CONGLOMERATIC STRATA AT THE BASE OF THE BRUSHY BASIN MEMBER OF THE MORRISON FORMATION

METHODS OF STUDY

In southwestern Colorado, topographic maps on a scale of 1:24,000 were used as a base for mapping the distribution of conglomeratic sandstone at the base of the Brushy Basin Member. Contacts were drawn between these coarse-grained sediments and siltstone and mudstone above or below. The lithologic character of the almost continuous layer of sandstone near the top of the underlying Salt Wash Member also was mapped and studied because the sandstone contains most of the deposits of uranium-vanadium ore in the Mor-

rison Formation. In southeastern Utah, suitable base maps were not available.

The orientation of sedimentary structures was used to determine the directional trends of sediment transportation. In places where four or five closely spaced measured trends differ by less than 10° an average measurement was plotted. Where differences in directional trend were greater than 10° over several hundred feet of outcrop, each measurement was plotted. Where the mid-portion of vertical cliffs was inaccessible the trends of sedimentary structures were measured along the base and top of the cliff.

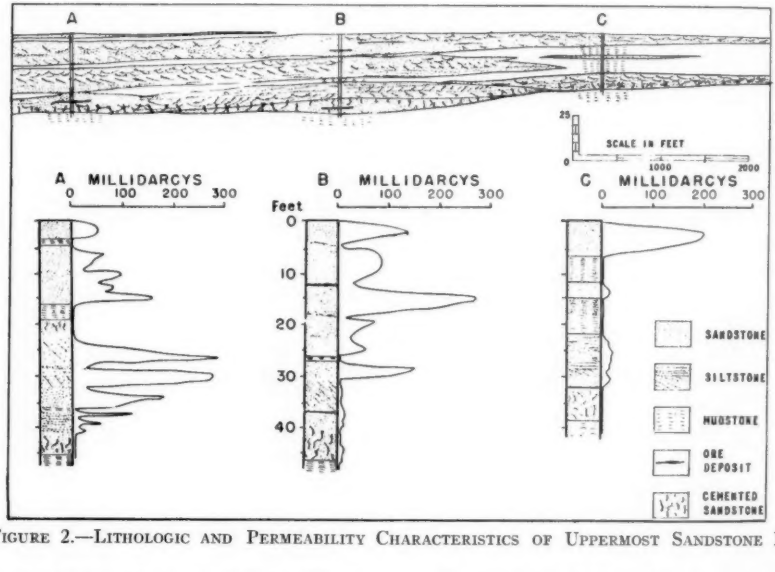

FIGURE 2.—LITHOLOGIC AND PERMEABILITY CHARACTERISTICS OF UPPERMOST SANDSTONE LAYER

The U. S. Geological Survey has carried on a program of diamond drilling in southwestern Colorado to explore the Morrison Formation in places where geologic conditions appeared favorable for the extension of known uranium-vanadium deposits or for the existence of hitherto unknown deposits. Systematic geologic logs of core of the Salt Wash Member are on record, but the overlying Brushy Basin Member has not been logged except in a few places. Where the Brushy Basin Member has been logged, the logs were utilized.

UNITS MAPPED

The units mapped and described in this report are the ore-bearing sandstone of the Salt Wash Member and strata of conglomeratic sandstone that distinguish the base of the Brushy Basin Member from the underlying Salt Wash Member. In most places the changes in lithology between these units are conspicuous and abrupt, usually from bedded sandstone or a coarse conglomeratic sandstone to a laminated siltstone or mudstone above and below. In places, however, mudstone between the coarse-grained strata gradually thins laterally to where the strata of sandstone are in disconformable contact. The strata of coarse-grained sediments in places end abruptly without change in thickness but more commonly thin to a pinch-out between layers of mudstone.

Data suggest that each stratum represents an accumulation of sediment left within the channel margins of an aggrading stream, whereas the mudstone and other fine-grained sediments are believed to represent flood-plain deposits that accumulated under relatively quiet and shallow-water conditions. Variations in the fine-grained sediments that usually separate the conglomerate strata have not been studied.

ORE-BEARING SANDSTONE

The ore-bearing sandstone is a collective term used to describe an almost continuous layer of sandstone at the top of the Salt Wash

Member of the Morrison Formation. It has been described by geologists working in widely separated parts of southwestern Colorado and southeastern Utah, for it contains most of the uranium deposits in the Morrison Formation (Fischer, 1942; Weir, 1952; Stokes, 1952; Phoenix, 1956; Boardman, 1956). In some mining districts other sandstone units in the Salt Wash Member of the Morrison Formation are ore-bearing locally, but they have not been sufficiently productive to attract attention. In the vicinity of uranium deposits lenticular strata of sandstone that compose the ore-bearing sandstone are superposed, and the sandstone is between 100 and 150 feet thick; away from the deposits at distances of between ½ to 3 miles the strata of sandstone gradually thin, and the stratigraphic interval consists predominantly of mudstone (Fig. 2). In plan, places where the ore-bearing sandstone is composed chiefly of permeable sandstone are oval, and the long dimension is usually parallel to the trend of sedimentary structures in the sandstone. In southwestern Colorado and southeastern Utah this trend is usually east or northeast. Some bodies of thick permeable sandstone cover 4 to 6 square miles, and they may be several miles long; the porosity of sediments within these areas ranges between 15 and 20 per cent. The permeability of the sandstone is greatest parallel to the trend of sedimentary structures, and in most places the ore deposits are elongate in the direction—*i. e.*, eastward or northeastward (Phoenix, 1956, p. 214, 217, 219).

The opportunity for mineral-bearing solutions to move laterally through the ore-bearing sandstone over distances of several miles was probably best in the same direction as the trend of the sedimentary structures, for this direction is also the direction of maximum permeability. However, the transmissibility of the ore-bearing sandstone ranges from greater than 150 meinzer feet where the sandstone is thickest to less than 50 meinzer feet where the sandstone is also thin and discontinuous. Because the strata of permeable sandstone that compose the ore-bearing sandstone are lenticular the opportunity for replenishment and solution movement in any lateral direction, after burial, was probably not great.

Conglomeratic Sandstone Strata

Lithology

The conglomeratic sandstone strata include sediments ranging from fine-grained sandstone to conglomerate containing pebbles an inch or more in diameter but in some places are composed almost entirely of either the fine- to medium-grained sandstone or of conglomerate; all these rocks are considered a part of the same phase of Morrison deposition. The coarse fraction—dominantly pebbles of chert and quartzite—is generally subangular to subrounded, and the sand grains are usually rounded to subrounded. In places the sediments are well sorted, particularly near the thinning margins of a stratum where fine- to medium-grained sandstone is the dominant rock type. In the central thicker portions of a stratum the sediments are poorly sorted, and pebbles of chert in medium- to coarse-grained sandstone is the dominant rock type. The sandstone at the top of the Salt Wash Member is not conglomeratic, is well sorted, and is medium- to fine-grained throughout. Graded bedding (Pl. 1, fig. 1) is locally present in conglomeratic strata more than 100 feet above the contact between the Salt Wash and Brushy Basin members, but it has not been observed in strata at the base of the Brushy Basin Member.

There appear to be significant regional differences in the lithology of the conglomeratic strata. In the Uravan area, Montrose County, Colorado (Fig. 1), pebbles in these strata rarely exceed half an inch in diameter, and medium-grained sandstone is the dominant rock type. In the Yellow Circle and La Sal Creek mine areas of southeastern Utah (Fig. 1), these strata contain pebbles 2 inches in diameter together with clay galls 2 or 3 inches in diameter embedded in coarse sand. A general westward coarsening of the conglomeratic sediments is believed to prevail between southwestern Colorado and southeastern Utah.

In most places the conglomeratic strata are dark brown or reddish owing to a large amount of iron oxide that either coats the sand grains or is intimately mixed with interstitial mudstone and with calcite cement. The pebbles in these sediments are red or green chert. Some of the conglomeratic strata, however, are light brown to yellow, and the chert pebbles are altered white or gray, so that on the basis of color alone they resemble strata of light fine- to medium-grained sandstone in the underlying Salt Wash Member. Silica overgrowths are abundant on sand grains in both the light and dark strata, but the sand, though partly cemented with silica, is friable. Carbonates commonly cement the sandstone, particularly near the base of a stratum.

Most of the sediments between and above the

conglomeratic rocks are mudstone with subordinate beds of siltstone and fine sandstone. In many places the mudstone is bentonitic, so that it swells when wet and is covered with talus. The conglomeratic beds are more resistant to erosion than are the fine-grained sediments, so that they form distinct but discontinuous ledges above the Salt Wash Member.

Stratigraphic Position

The stratigraphic position of the conglomeratic sandstone strata in the lower part of the Brushy Basin Member varies with respect to the underlying ore-bearing sandstone layer of the Salt Wash Member. In places the conglomeratic strata rest on the ore-bearing sandstone layer, but in most places laminated siltstone or mudstone lies between the conglomeratic strata and the ore-bearing sandstone. Above the Gray Daun mine, in the La Sal Creek mining district in southeastern Utah (Fig. 1), this mudstone is about 100 feet thick; at the Vanadium Queen mine, about 1 mile east in the same mining district, 10 feet of mudstone separate a conglomeratic stratum from underlying fine- to medium-grained Salt Wash Sandstone. In the Yellow Cat mine area, 36 miles north, a conglomeratic stratum rests upon sandstone of the Salt Wash Member. On Calamity Mesa and on the near-by Outlaw Mesa, Mesa County, Colorado, and in the Slick Rock area, San Miguel County, Colorado (Fig. 1, areas 1, 2, 10–14), mudstone between the conglomeratic strata and the ore-bearing sandstone layer is about 30 feet thick, although conglomeratic strata rest locally upon the ore-bearing sandstone layer of the Salt Wash. The writer believes that the conglomerate strata throughout southwestern Colorado and southeastern Utah probably represent the same sequence of deposition. These strata probably were deposted by aggrading streams that flowed northward and eastward.

Sedimentary Structures

Sedimentary structures of various kinds have been recognized in the strata of conglomeratic sandstone. In places a single stratum may contain tabular units of sandstone 2 or 3 feet thick within which the bedding is either horizontal, troughlike, or inclined. In addition, a stratum may contain a prevailing type of sedimentary structure even though it is composed of several distinct tabular unit of sand. Only those structures that indicate the direction of water movement were distinguished and measured in the field. All the strata contained the planar and trough cross-stratification types of McKee and Weir (1953, p. 387) and McKee and others (1953, p. 24), and in places current lineation (Stokes, 1947).

Trough cross-stratification is most conspicuous in strata that are conglomeratic; pebbles, commonly localized along the bedding planes, emphasize the troughlike form (Pl. 1, fig. 3).

According to Poole and Williams (1956, p. 230) the trough pattern is the result of two steps: erosion that produces plunging troughs and filling of the troughs by thin concave layers which conform in general to the shape of the trough floors. In the conglomeratic strata a set of cross-strata is as much as 20 feet wide from limb to limb, and the depth of the trough may be 7 or 8 feet; the size of the trough sets in any particular horizon seem to be, in general, of uniform scale. Generally, trough cross-stratification is more common in the central parts of lenticular conglomeratic strata; however in places units of sandstone of nearly uniform thickness are trough cross-stratified throughout. This type of structure has been developed in the laboratory by concentrated stream currents in multiple stages of flow and aggradation (McKee and others, 1953, p. 58).

Planar cross-stratification is not common, nor is it conspicuous in the conglomerate strata at the base of the Brushy Basin Member. Planar cross-stratified sandstone is commonly fine-grained, the dips of the individual beds are constant in one direction, and each inclined bedding plane terminates in the direction of its dip at a rather sharp angle. The surfaces against which the inclined bedding terminates above and below are planar and generally converge slightly; they are rarely more than 1 or 2 feet apart. Bedding may have a similar inclination in a section of rock broken parallel to the axis of

PLATE 1.—CROSS-STRATIFICATION IN THE MORRISON FORMATION

FIGURE 1.—Combined graded and inclined bedding in conglomeratic sandstone of the Brushy Basin Member of the Morrison Formation about 250 feet above the base of the member (7-inch ruler indicates scale).

FIGURE 2.—Current lineation on a bedding plane of sandstone in the Salt Wash Member of the Morrison Formation (13-inch ruler indicates scale).

FIGURE 3.—Trough cross-stratification in a conglomeratic stratum of the Brushy Basin Member of the Morrison Formation (13-inch ruler indicates scale).

FIGURE 1

FIGURE 2

FIGURE 3

CROSS-STRATIFICATION IN THE MORRISON FORMATION

trough cross-stratification, but the surface along which the inclined beds terminate is concave. In the laboratory, planar cross-stratification similar to that in conglomeratic strata of the Brushy Basin Member has been developed in subaqueous environments under conditions simulating delta construction (McKee and others, 1953, p. 48–53). The maximum dip direction of cross-stratification is the direction of delta growth, and in the field this direction is assumed to be the direction of stream movement and associated deposition.

The directions were the same in most places where the orientation of the long axis of trough cross-stratification was measured near a measurement of maximum dip direction of planar cross-stratification.

Current lineation (Pl. 1, fig. 2) is the term used to describe tiny parallel windrows of sand grains on bedding planes. It is common in sandstone that is medium- or fine-grained and horizontally bedded. Current lineation is believed to be oriented parallel to the direction of stream movement except where it splays outward from a common point. In such places the direction of splay is assumed to be the downstream direction. Current lineation is not common in sediments composing the conglomeratic sandstone strata of the Brushy Basin Member, although it is found in places where a stratum thins and becomes fine-grained, or near the top of a stratum where bedding is horizontal and the sandstone is fine-grained.

In the areas shown in Figure 1 the prevailing orientation is indicated by an arrow. In some places, as in the Slick Rock area, conglomeratic strata are superimposed, and the orientation shown represents a common trend of sedimentary structures in two or more strata. However, where sedimentary structures in superimposed strata diverge in orientation as they do near the Lower Group mines in the Slick Rock area and in the Forty-Five Ninty mine area near Uravan, the prevailing orientation of each stratum is shown on the map. Where they systematically change in orientation, the direction of change is shown by a curved arrow.

The prevailing easterly orientation of sedimentary structures represents the direction in which the streams flowed during deposition. In some places this direction is based on very few measurements; in others it is based on 20 or 30 measurements.

Elongation

Conglomeratic strata have been measured for almost a mile along their length, but they rarely exceed 2000 feet in width before they grade into or terminate abruptly against mudstone. As a general rule, strata that exceed 15 feet in thickness and 1000 feet in width are continuous for at least 3000 feet in the direction of the trend of their contained sedimentary structures.

On Calamity Mesa and near-by Outlaw Mesa, Mesa County, Colorado, the most continuous strata are elongated eastward parallel to the trend of their sedimentary structures, and, like beads on a string, they continue eastward for about 4 miles. They overlie and nearly parallel an eastward-trending belt of ore deposits in the uppermost sandstone layer of the Salt Wash. Outside the limits of the belt of the ore deposits on Calamity Mesa and Outlaw Mesa the conglomerate strata are less common; they trend generally northeastward. Thus, it would appear that during early Brushy Basin time the conglomerate strata above the ore deposits on Calamity Mesa and Outlaw Mesa were deposited along a master streamway that is now paralleled by a belt of mineral deposits extending through the Calamity Mesa and Outlaw Mesa areas.

Frequency of Occurrence

In many places conglomeratic strata at the base of the Brushy Basin Member are elongate parallel to valley walls; they are also discontinuous. These factors make it difficult to distinguish between conglomeratic strata and thus to make a count of their frequency of occurrence. In the Slick Rock area where the walls of the northward-trending Dolores River Canyon expose eastward-trending strata of conglomerate, individual strata are in places more than half a mile apart and are separated laterally by mudstone. In this area they appear to cover about one-third of the Salt Wash Member. In the Atkinson Mesa area they crop out at intervals of about 1200 feet, but sedimentary structural trends in at least two of the strata are parallel to the outcrop. Along the southwest side of the Big Gypsum Valley only one well-defined conglomeratic stratum about 1000 feet wide was found along a 4-mile outcrop of Brushy Basin rocks. Reconnaissance in southwestern Colorado and southeastern Utah suggests that not more than one-third of the Salt Wash Member is overlain by these strata of conglomerate.

Relation to Uranium-Vanadium Deposits

The writer believes that uranium-vanadium deposits in the Salt Wash Member of the

Morrison Formation are related to ground-water solutions that migrated laterally through the beds, probably soon after the accumulation of the sands. Because the conglomeratic strata at the base of the Brushy Basin Member are believed to have been deposited by streams, it would appear that a definite relation should exist between these strata and the ore deposits in the Salt Wash Member below, for as a general rule, the movement, the amount, and the chemical character of near-surface ground water is governed in large part by the environment prevailing at the land surface. The following data test the hypothesis that uranium-vanadium deposits and ground-water conditions in the Morrison Formation are related.

Table 1 groups 363 ore deposits in 18 widely scattered mining areas of southwestern Colorado and southeastern Utah into three main categories: (1) deposits below conglomerate strata, (2) deposits below projected extensions of conglomerate strata, and (3) deposits showing no obvious relation to conglomerate strata. The total number of discrete ore deposits in the areas that were studied may be somewhat less than the number present, for mine workings and drill holes commonly explore several closely connected deposits.

TABLE 1.—RELATION OF URANIUM-VANADIUM DEPOSITS IN THE UPPERMOST SANDSTONE LAYER OF THE SALT WASH MEMBER TO LENTICULAR CONGLOMERATIC STRATA AT THE BASE OF THE BRUSHY BASIN MEMBER OF THE MORRISON FORMATION

District and mine areas	Deposits below conglomerate strata		Deposits below projected trends of conglomerate strata	Deposits showing no obvious relation to conglomerate strata
	Explored by tunneling	Explored by drilling		
Gateway district				
Calamity Mesa area	11	17	46	4
Outlaw Mesa area	4	—	56	8
Lumsden mine area	2	—	—	—
Corvusite mine area	—	—	1	—
Gypsum Valley district				
Little Gypsum Valley area	9	—	32	10
Big Gypsum Valley area	1	—	—	—
Moab district				
La Sal mines area	3	1	—	—
Yellow Circle mines area	4	—	1	—
Monticello district				
Waterfall Group area	—	—	—	13
Slick Rock district				
Upper Group area	2	—	13	2
Middle Group area	3	—	12	—
Ellison Group area	1	3	—	—
Veta Mad area	2	—	—	1
Lower Group area	—	—	16	3
Miscellaneous	2	—	—	—
Thompson district				
Cactus Rat mine area	5	—	1	—
Uravan district				
Forty-five-Ninety mine area	8	2	—	—
Spring Creek Mesa area	3	7	—	—
Atkinson Mesa area	—	11	33	10
Totals	60	41	211	51

In the first category, deposits below conglomerate that are reached by tunnels are separated from deposits that have been discovered by drilling through the conglomerate. Deposits explored by tunneling are found in most of the mining districts in southwestern Colorado and southeastern Utah. The deposits in this category offer the strongest supporting evidence to

FIGURE 3.—ISOMETRIC DRAWING SHOWING THE RELATION OF URANIUM-VANADIUM MINES IN SANDSTONE OF THE SALT WASH MEMBER TO THE CONGLOMERATE IN THE BRUSHY BASIN MEMBER OF THE MORRISON FORMATION
Atkinson Mesa area, Montrose County, Colorado

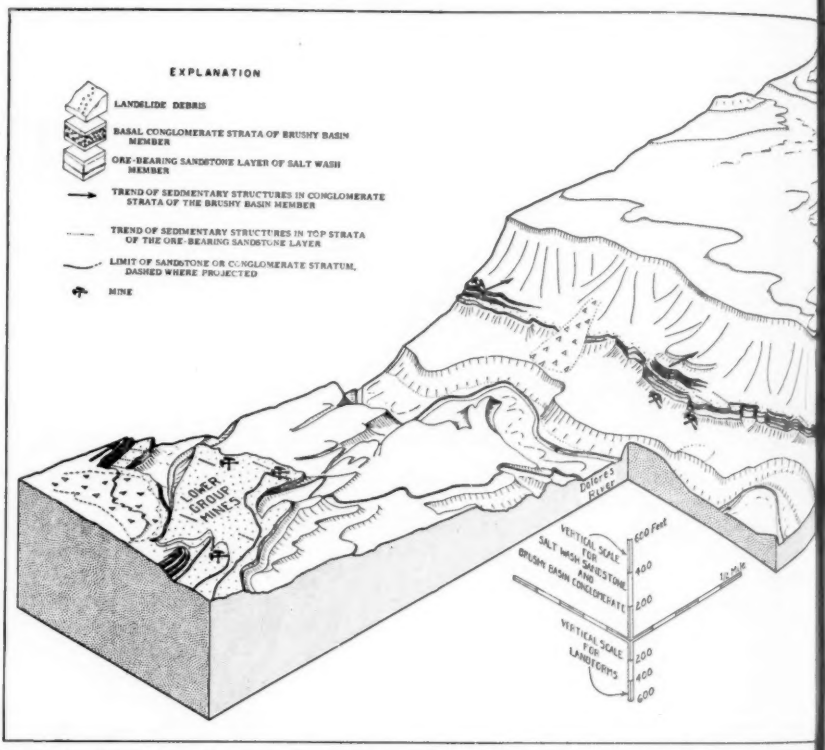
EXPLANATION
LANDSLIDE DEBRIS
BASAL CONGLOMERATE STRATA OF BRUSHY BASIN MEMBER
ORE-BEARING SANDSTONE LAYER OF SALT WASH MEMBER
TREND OF SEDIMENTARY STRUCTURES IN CONGLOMERATE STRATA OF THE BRUSHY BASIN MEMBER
TREND OF SEDIMENTARY STRUCTURES IN TOP STRATA OF THE ORE-BEARING SANDSTONE LAYER
LIMIT OF SANDSTONE OR CONGLOMERATE STRATUM, DASHED WHERE PROJECTED
MINE
LOWER GROUP MINES
Dolores River
VERTICAL SCALE FOR SANDSTONE AND GYPSUM BASIN CONGLOMERATE
600 Feet
400
200
1/2 mile
VERTICAL SCALE FOR LANDSLIDES
200
400
600

FIGURE 4.—ISOMETRIC DRAWING SHOWING THE RELATION OF THE URANIUM-VANADIUM MINES IN THE MORRISON FORMATION TO THE ORE-BEARING SANDSTONE AND CONGLOMERATE STRATA IN THE SLICK ROCK AREA, SAN MIGUEL COUNTY, COLORADO

bear out the observation that ore deposits underlie conglomerate strata at the base of the Brushy Basin Member. Twenty-eight per cent or 101 deposits are in this group.

Deposits in the second category—those below projected trends of the conglomerate strata—are in the top sandstone layer where it is stripped of its cover of Brushy Basin rocks, but where conglomerate is preserved in near-by hillsides. To analyze the relation between these deposits and the conglomerate strata, it was assumed that strata exceeding 1000 feet in width may reasonably be projected for 2500 feet along the trend of their sedimentary structures. In places where the lateral margin of a conglomerate stratum has been removed by erosion, the width of the part preserved was arbitrarily increased by half of the mapped width. These assumptions allow deposits in the top sandstone layer that were probably once overlain by the Brushy Basin Member to be included in the analysis. Fifty-eight per cent or 211 deposits are in this group.

In the third category are included deposits that are either (1) along the trend of conglomerate strata but beyond the limits of safe projection, or (2) lateral to the marginal pinchout of a conglomerate stratum. Deposits beyond the limit of safe projection of the conglomerate strata are found where the Brushy Basin has been removed from the top sandstone layer of the Salt Wash over broad areas, or where landslide debris obscures geologic relations in the Brushy Basin Member. Erosion has removed most of the Brushy Basin Member in parts of Little Gypsum Valley, whereas in the Waterfall group area and in a small part of the Outlaw Mesa area outcrops of conglomeratic sandstone are obscured by landslides. Thirty-four of the 51 deposits in the third category are thus classified as being out of the limits of geologic observation. The remaining 17 deposits are marginal to the pinchout of conglomerate strata. Four of the 17 were below the edge of a conglomeratic stratum, and the rest are laterally within 300 feet of a conglomeratic stratum. The 51 deposits in the third category constitute 14

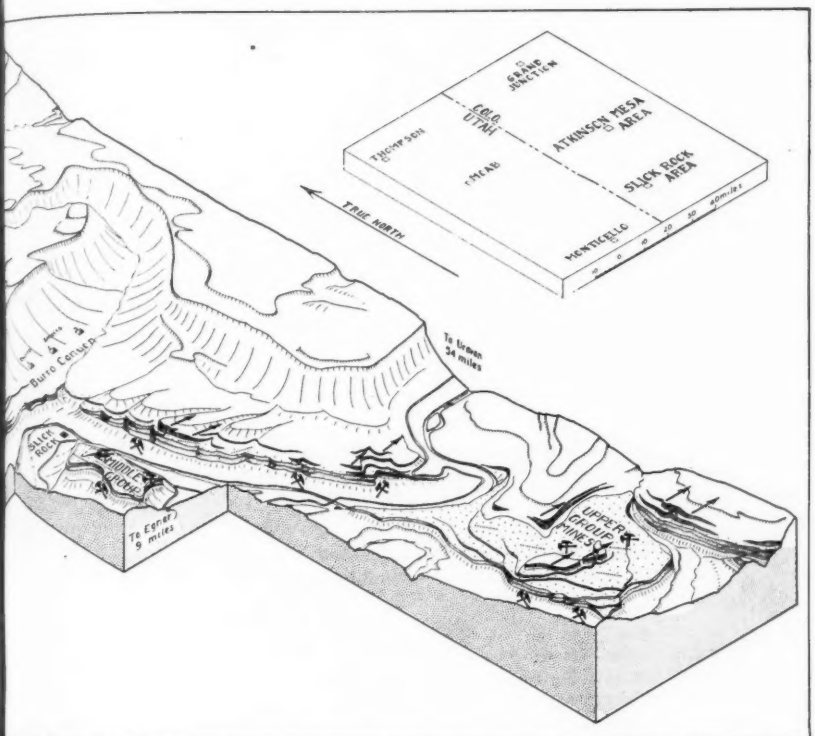

DSTONE OF THE SALT WASH MEMBER TO THE CONGLOMERATE IN THE BRUSHY BASIN MEMBER OF THE MATION

nel County, Colorado

per cent of all the deposits that were studied in the ore-bearing sandstone.

Exceptions to the suggested relation between ore deposits in the Salt Wash Member and conglomeratic strata in the Brushy Basin Member have been observed. In some places, notably in the Yellow Cat mine area, carnotite deposits are found in sandstone strata of the Salt Wash Member below their usual position near the top of the member. Moreover, one of the deposits in this area is localized in the conglomeratic strata at the base of the Brushy Basin Member. This latter occurrence is not unique to the Yellow Cat mine area, for the conglomeratic strata of the Brushy Basin Member are mineralized locally in other areas where notable producers of uranium-vanadium ore are found in the Salt Wash Member. The commonly observed relation between ore deposits in the sandstone of the Salt Wash and conglomeratic strata in the Brushy Basin Member is shown on Figures 3, 4, and 5.

Summary and Conclusions

The geology of the conglomeratic sandstone strata at the base of the Brushy Basin Member as it relates to the uranium-vanadium deposits is summarized as follows:

(1) Conglomeratic strata at the base of the Brushy Basin Member of the Morrison Formation and above an almost continuous layer of fluvial sandstone near the top of the underlying Salt Wash Member are sufficiently widespread to indicate that they constitute a distinct phase of Morrison deposition.

(2) Sedimentary structures in the conglomeratic strata including trough cross-stratification, planar cross-stratification, and current lineation indicate that the strata were deposited by streams. The accidents of stream erosion and deposition during Morrison time are believed to have destoryed parts of the strata, so that they are now discontinuous.

(3) In places sedimentary structures in the

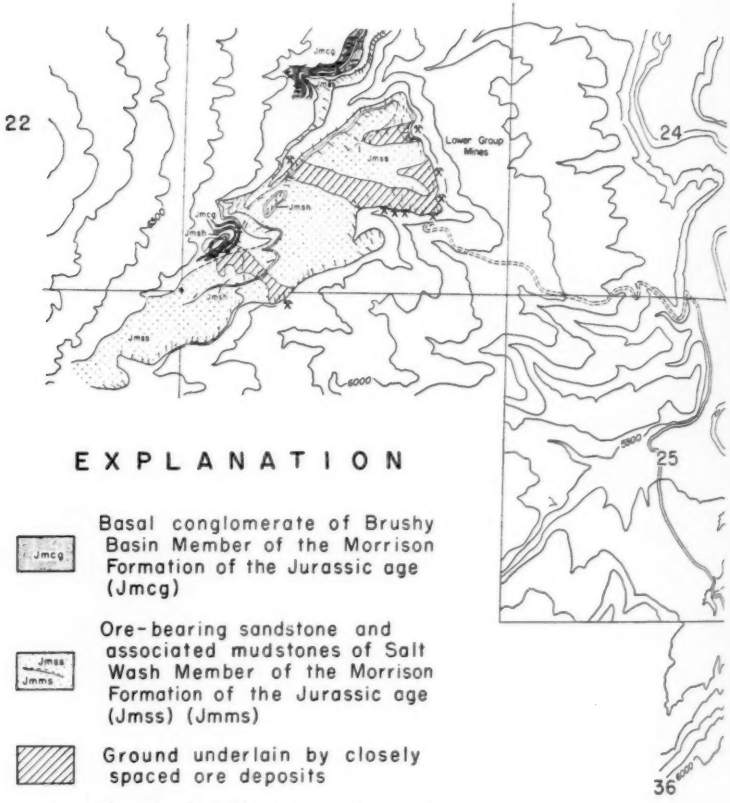

EXPLANATION

Jmcg — Basal conglomerate of Brushy Basin Member of the Morrison Formation of the Jurassic age (Jmcg)

Jmss Jmms — Ore-bearing sandstone and associated mudstones of Salt Wash Member of the Morrison Formation of the Jurassic age (Jmss) (Jmms)

Ground underlain by closely spaced ore deposits

Trend of sedimentary structure

Strike and dip of strata

Contact between strata

Mine; most symbols are offset from the true positions of the mine entries so as not to conflict with the geology

Land section corner found in field

1000 0 4000 FEET

Datum is mean sea level
Contour interval 100 feet
(Contours not shown where they overlap geologic lines)

FIGURE 5.—GEOLOGIC MAP SHOWING THE RELATION OF THE URANIUM-VANADIUM MINES IN THE SA... ONE OF ... MORE... ...RMATION ... Slick Rock area, ...guel Co...

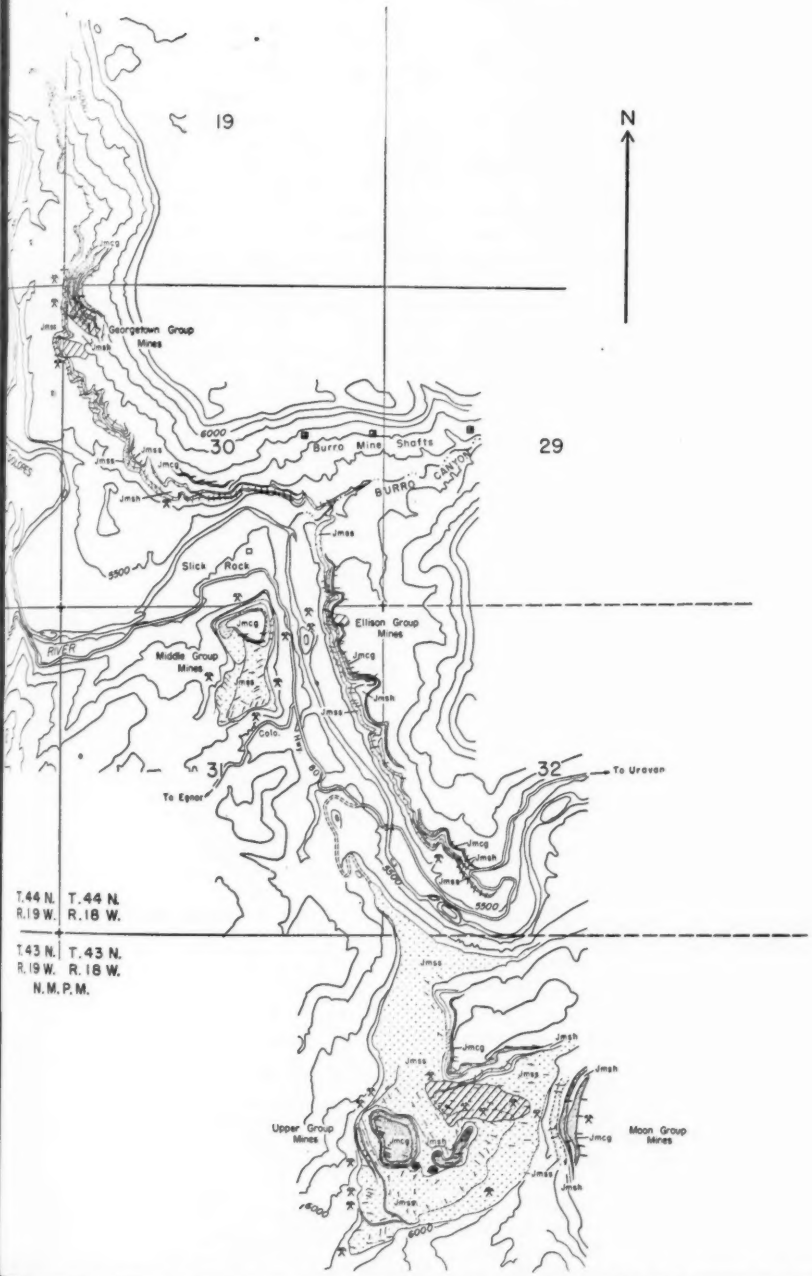

NE OF THE SALT WASH MEMBER TO THE CONGLOMERATE IN THE BRUSHY BASIN MEMBER OF THE MORRI FORMATION

area, Miguel County, Colorado

conglomerate strata change in orientation and suggest that they were formed by streams that were meandering. However, because the prevailing trend of the sedimentary structures is eastward and because sediments in the strata coarsen westward, a westerly source for at least the lower portion of the Brushy Basin Member is indicated.

(4) Sediments in the conglomeratic strata are prevailing coarser-grained than are those in strata of the Salt Wash Member, and they are less well sorted. The writer believes that these differences in character indicate a change from depositional conditions prevailing in Salt Wash time toward increased flow velocity. A source area capable of supplying large amounts of chert is also indicated by abundant chert pebbles in the strata.

(5) In most places the conglomeratic strata are separated from the underlying top sandstone layer of the Salt Wash by mudstone, but locally, as in the vicinity of some uranium deposits, they rest directly upon the top sandstone layer. Probably ground-water movement either from or into the underlying sandstone of the Salt Wash took place particularly through these "puncture points".

(6) Uranium-vanadium deposits in the underlying sandstone layer at the top of the Salt Wash Member are clustered below conglomeratic strata in areas where the physical characteristics of the ore-bearing sandstone are also favorable to ore deposits. Sandstone favorable to ore deposits is thick and permeable but thins laterally to a featheredge. The favorable places can be regarded as ground-water reservoirs.

If uranium and vanadium were present in the same amounts in the streams or the ground water accompanying deposition of the Morrison Formation as they are in present-day ground water from this formation (median amount of .10 ppm in 17 samples), then the ore deposits in the Morrison Formation could be related to processs initiated during deposition of these sediments. It can be postulated that streams depositing the Brushy Basin conglomerate were either contributing to or obtaining ground water from the Salt Wash sands and thus controlling ground-water underflow. Moreover, if the processes of evaporation and plant transpiration were active during Morrison time then the ground-water solution could have been enriched in uranium and vanadium. The enriched solutions could have been localized in the environment of decaying vegetation where the sands are thick and permeable. To maintain an environment of uranium-rich ground water in these places it is also necessary to postulate that lateral movement was negligible from late Morrison to late Cretaceous time. It is believed that near stagnation of these pore fluids during this period was favored by the general tectonic stability of the Colorado Plateau region, by the lenticular aspects of the ore-bearing sandstone and by the negligible vertical permeability of the Brushy Basin Shale Member. Precipitation of uranium and vanadium from the fluids in the pore spaces of the sandstone may have been initiated by the onset of igneous activity and regional deformation that characterized the beginning of the Tertiary in areas peripheral to the Colorado Plateau region and perhaps within the region as well.

References Cited

Boardman, R. L., Ekren, E. B., Bowers, H. E., 1956, Sedimentary features of upper sandstone lenses of the Salt Wash member and their relation to uranium-vanadium deposits in the Uravan district, Montrose County, Colorado, p. 221–226 *in* Page, L. R., *et al.*, Contributions to the geology of uranium and thorium by the United States Geological Survey and Atomic Energy Commission for the United Nations international conference on peaceful uses of atomic energy, Geneva, Switzerland, 1955: U. S. Geol. Survey Prof. Paper 300, 739 p.

Craig, L. C., Holmes, C. N., Cadigan, R. A., Freeman, V. L., Mullens, T. E., and Weir, G. W., 1955, Stratigraphy of the Morrison and related formations, Colorado Plateau region, a preliminary report: U. S. Geol. Survey Bull. 1009-E, p. 125–168, Figs. 19–31

Coleman, R. G., 1957, Mineralogic evidence on the temperature of formation of the Colorado Plateau uranium deposits: Econ. Geology, v. 52, p. 1–4

Fischer, R. P., 1942, Vanadium deposits of Colorado and Utah: U. S. Geol. Survey Bull. 936-P, p. 363–374, Pls. 53–57

Fischer, R. P., and Hilpert, L. S., 1952, Geology of the Uravan mineral belt: U. S. Geol. Survey Bull. 988-A, 13 p., Pls. 1–3, Figs. 1–5

Larsen, Esper S., Jr., and Cross, Whitman, 1956, Geology and Petrology of the San Juan region southwestern Colorado: U. S. Geol. Survey Prof. Paper 258, 303 p., 4 Pls., 58 Figs.

McKee, E. D., and Weir, G. W., 1953, Terminology for stratification and cross-stratification in sedimentary rocks: Geol. Soc. America Bull., v. 64, p. 381–390

McKee, E. D., Evensen, C. G., and Grundy, W. D., 1953, Studies in sedimentology of the Shinarump conglomerate of northeastern Arizona: U. S. Atomic Energy Comm., RME-3089, 48 p.

Phoenix, D. A., 1956, Relation of carnotite deposits to permeable rocks in the Morrison formation, Mesa County, Colorado, p. 213–219 *in* Page, L. R., *et al.*, Contributions to the geology of uranium and thorium by the United States

Geological Survey and Atomic Energy Commission for the United Nations international conference on peaceful uses of atomic energy, Geneva, Switzerland, 1955: U. S. Geol. Survey Prof. Paper 300, 739 p.

Poole, F. G., and Williams, G. A., 1956, Direction of sediment transport in the Triassic and associated formations of the Colorado Plateau, p. 227–231 *in* Page, L. R., *et al.*, Contributions to the geology of uranium and thorium by the United States Geological Survey and Atomic Energy Commission for the United Nations international conference on peaceful uses of atomic energy, Geneva, Switzerland, 1955: U. S. Geol. Survey Prof. Paper 300, 739 p.

Stieff, R. L., Stern, T. W., and Milkey, R. G., 1953, A preliminary determination of the age of some uranium ores of the Colorado Plateaus by the lead-uranium method: U. S. Geol. Survey Circ. 271, 19 p., Figs. 1–7

Stokes, W. L., 1947, Primary lineation in fluvial sandstones, a criterion of current direction: Jour. Geology, v. 55, p. 52–54

—— 1952, Uranium-vanadium deposits of the Thompsons area Grand County, Utah: Utah Geol. and Min. Survey Bull. 46, 51 p.

Weir, Doris Blackman, 1952, Geologic guides to the prospecting for carnotite deposits on Colorado Plateau: U. S. Geol. Survey Bull. 988-B, p. 15–27, Figs. 6–14

U. S. Geological Survey, Grand Junction, Colo.

Manuscript Received by the Secretary of the Society, December 11, 1956

Publication Authorized by the Director, U. S. Geological Survey

BULLETIN OF THE GEOLOGICAL SOCIETY OF AMERICA
VOL. 69, PP. 419-448, 15 FIGS., 4 PLS. APRIL 1958

GEOLOGY AND PETROLOGY OF THE MASINLOC CHROMITE DEPOSIT, ZAMBALES, LUZON, PHILIPPINE ISLANDS

BY W. C. STOLL

ABSTRACT

The Masinloc mine, the world's largest producer of refractory-grade chrome ore, is at Coto, Zambales, Luzon, Philippine Islands. Ore production from 1946 through 1952 was 1,605,867.6 long tons, containing 32.33 per cent Cr_2O_3. The ore occurs with other chromite deposits in a layered ultramafic complex, intruded by microdiorite and similar dikes and overlapped by Miocene sediments. Near the mine, the complex is composed of pseudostratified gneissose norite and olivine gabbro and massive saxonite serpentine and dunite serpentine. Dunite intrudes olivine gabbro; saxonite may also be intrusive.

The chrome deposits form a belt 8000 feet long, which lies in saxonite near its contact with olivine gabbro. The largest body is roughly oval and lies slightly inclined at the topographic surface; it is about 1800 feet long, 950 feet wide, and as much as 175 feet thick. It is composed of dense and disseminated ores with small quantities of associated dunite, melano-troctolite, and olivine gabbro.

Dense ore forms most of the deposit as well as fragments in dunite at the margins. It is a mosaic of chromite grains, interpreted as a compact mass of clusters, with about 10 per cent interstitial gangue, partly dunite serpentine and partly olivine gabbro. The chromite is fractured and in places anisotropic because of strain. It contains rare poikilitic enclosures of euhedral olivine and is corroded in contact with the silicates. Olivine gabbro gangue shows microscopic zonal distribution of minerals in the ore interstices.

Disseminated ore occurs as a selvage, dike, and marginal fragments, but mostly as large bodies with flowage banding, adjacent to dense ore. It is 60–80 per cent chromite, as corroded multigranular pieces, in a dunite serpentine matrix. Dunite is found mainly as a shell at the dense ore contacts. Dark troctolite forms segregations, pockets, and dikes, and olivine gabbro, similar to that in ore interstices, forms narrow dikes cutting ores and other rocks. The field relations show that dense chromite is the oldest and olivine gabbro the youngest component of the ore deposit. Disseminated ore, dunite, and melano-troctolite are probably almost contemporaneous.

Dense chromite has the formula $Cr_{41}Al_{54}$ (Mg_{74}), similar to Caribbean ores, and disseminated chromite has nearly the same composition.

Norite and olivine gabbro form the upper zones of the layered complex, and their pseudostratification and gneissosity originated through crystal sedimentation often interrupted.

The dense chromite bodies are regarded as xenoliths that have been borne upward in intrusive saxonite. Disseminated ore and associated dunite probably originated through corrosion and disruption of dense ore by peridotite and they accumulated next to the dense masses after movement had ceased.

The high Al and Mg contents of the chromite, as well as its reactions with olivine gabbro and peridotite, which tended everywhere to the generation of the pyroxene-free types troctolite and dunite, indicate that chromite crystallized from troctolitic magma. The ore composition and texture seem best explained by Bowen's hypothesis of the genesis of chromite: that spinel formed first through transformation of glomeroporphyritic clusters of olivine and basic plagioclase in reaction with magma saturated with forsterite, and that with falling temperature spinel was converted to chromite, olivine, and plagioclase. These, together with pyroxene, settled to form a compact deposit of clusters, beyond reach of liquid sufficient to resorb them.

Such deposits may have formed in the transitional zone of the complex. This and the subjacent ultramafic zones may have been subsequently heated and disrupted incidental to orogeny, and peridotite masses with solid inclusions of chrome ore irrupted

into higher levels of the complex. The temperatures then prevailing were high enough to fuse the olivine-gabbro ore matrix and commence anew the reaction between chromite and liquid.

CONTENTS

TEXT

	Page
Introduction and acknowledgments	420
Country rocks	422
Zambales ultramafic complex	422
General statement	422
Field relations	422
Norite	422
Olivine gabbro	425
Saxonite serpentine	426
Dunite serpentine	427
Microdiorite and andesite dikes	427
Microgabbro	428
Augite-hornblende andesite	428
Chromite deposits	429
Geology	429
Relations to gabbro-peridotite contact	429
Size and shape	429
Field relations of ores and associated rocks	429
Age relations	436
Joints and faults	436
Petrography	437
Dense ore	437
Disseminated ore	439
Dunite serpentine	439
Dark troctolite	439
Olivine gabbro dikes	440
Chemistry of the chromite	441
Genesis of the rocks and ores	443
References cited	447

ILLUSTRATIONS

Figure	Page
1. Geologic sketch map of part of South Lawis River valley, Zambales, Philippine Islands	423
2. Inclusions of light troctolite in dunite, Mabihinal River	425
3. Geologic plan of Masinloc chromite body, Zambales, Philippine Islands	430
4. Geologic sections of Masinloc chromite body, Zambales, Philippine Islands	431
5. Subangular blocks of chromite ore enclosed in dunite serpentine	432
6. Subrounded chromite ore blocks enclosed in dunite serpentine	432
7. Subrounded chrome ore inclusions	433
8. Inclusion of disseminated ore	433
9. Diagrammatic sketch of small body of dense ore with selvage of disrupted chromite	433
10. Narrow dike of disseminated ore cutting dense ore	433
11. Dike (?) of disseminated ore between walls of disseminated ore and serpentine	434
12. Sketch of outcrop: subparallel bands of dense chromite and a divergent band, in disseminated ore	434
13. Lens of dense chromite in disseminated ore	434
14. Branching bands or veinlets of chromite in dunite serpentine	435
15. Branching bands or veinlets of dense chromite in disseminated ore	435

Plate	Following page
1. Troctolite, olivine gabbro, accessory chromite in saxonite, brecciated ores	436
2. Disseminated ore, dunite, gabbroic dikes	
3. Textures of dense ore	
4. Textures of dense and disseminated ores	

TABLES

Table	Page
1. Ore production of the Masinloc mine, and average analyses (in per cent), 1946–1952	421
2. Subdivisions of the ultramafic complex in the vicinity of the Masinloc mine	424
3. Classification of ores and associated rocks in Masinloc deposit	432
4. Chemical analyses of Masinloc ores and concentrates	440
5. Calculation of composition of chromite in dense ore	442

Introduction and Acknowledgments

The Masinloc is one of a number of chromite mines in the province of Zambales, Luzon, on the western slopes of the Zambales Range, within about 30 miles of the South China Sea. Masinloc is the world's largest producer of refractory-grade chromite, and the Acoje mine is an important producer of metallurgical-grade ore. They are the only active mines in the area.

The chromite area is mountainous, thickly forested, and dissected by many streams that carry great quantities of water during the rainy season, July to September.

The Zambales coastal road, from which the mines are accessible, is reached from Manila by the highway through San Fernando, Pampanga, and Dinalupilian, Bataan. From Baguio or Manila, one may proceed also by way of Dagupan, Lingayan, and Dasol, in Pangasinan. Santa Cruz, Candelaria, and

Masinloc are the main towns on the coast road near the chromite district. The ore-loading pier is at Balagana, whence a road leads 16 miles up the valley of the South Lawis River to the barrio of Coto. Here, the Masinloc mine, camp, and heavy-medium plant are situated at altitudes of 500 to 1400 feet above sea level.

The main chromite occurrence is exposed on the sides and top of a hill 500 feet high and is mined in 12 benches, each 20–50 feet high. The ore is drilled, using wagon drills and jackhammers, and blasted. Coarse ore is loaded by hand into trucks and hauled to the storage bin at the loading pier. Finer ore is loaded by mechanical shovels and trucked to the plant, where much waste is eliminated by handsorting, screening, and heavy-medium separation. A narrow-gauge Diesel railroad has recently been built from Coto to Balagana in order to eliminate the more expensive ore transportation by trucks. At the port, ore is loaded directly into the holds of ships by conveyor belt.

The deposit, known variously as the Masinloc, the Coto, and the Consolidated, belongs to Consolidated Mines, Inc., of Manila and is worked by the Benguet Consolidated Mining Company. Mining commenced several years before the second World War, and prewar production is supposed to have been about 350,000 tons of ore. Production started again in 1946 and continued, expanding, until the present. The postwar production and average chemical analyses are given in Table 1. The average analyses and the analyses of individual shipments vary little from year to year. The variation is due mainly to the differing proportions of gangue in the ore, reflected in the silica content. No important variations have occurred in the composition of the chromite.

TABLE 1.—ORE PRODUCTION OF THE MASINLOC MINE, AND AVERAGE ANALYSES (IN PER CENT), 1946–1952

Year	Gross tons shipped	H_2O	Cr_2O_3	Al_2O_3	MgO	Fe	SiO_2	CaO	Total
1946	54,364.7	0.72	33.21	29.22	17.06	10.49	4.62	0.61	95.93
1947	177,637.9	0.84	32.54	28.93	18.55	10.91	5.05	0.57	97.39
1948	233,526.0	0.83	32.58	29.12	18.29	10.67	5.27	0.69	97.45
1949	165,956.4	0.79	32.88	29.17	17.51	10.73	4.59	0.57	95.84
1950	213,830.4	1.09	32.48	29.35	17.59	11.01	4.82	0.51	96.85
1951	298,087.0	0.94	32.37	29.28	17.79	11.21	5.07	0.70	97.36
1952	462,465.2	0.66	31.73	29.42	17.85	10.00	5.30	0.38	95.34
Total and averages	1,605,867.6	0.83	32.33	29.38	17.93	10.59	5.06	0.54	96.66

The field work, consisting of detailed mapping of the main deposit and a brief reconnaissance of the surroundings, was done during about 2 months in 1952 and 1953. Some preliminary microscopic work was also done at this time. The greater part of the study was done during 1954–1956, after the writer had left the Philippines. It was not possible to make quantitative petrographic analyses nor to provide chemical analyses of the rocks. The writer proposes to supply these deficiencies in a later publication.

Little geologic information is available on the Zambales Mountains, but this lack is being filled by field studies by the U. S. Geological Survey, whose future publications may be expected to throw light on the problems pointed out here, as well as on many others.

Flicano has been credited with the discovery of the Coto orebody, and he published the first information on the area (1926). Before the second World War, Dean F. Frasche made studies of the chromite deposits and rocks of Zambales for the Geological Division of the Philippine Bureau of Mines, but his findings were not published. Paul A. Schafer, consulting geologist of Manila, studied the Masinloc mine during many years as chief geologist of the Balatoc Mining Company and of the Benguet Consolidated Mining Company; the present writer has had the advantage of many discussions of Masinloc geology with him. The writer wishes especially to thank Virgil Everett Frank, general superintendent of Masinloc, and Mrs. Frank for their kind hospitality during his visits there. The chemical analyses quoted and some of the photographs are from the Benguet Consolidated Mining Company for which grateful acknowledgment is given.

Country Rocks

Zambales Ultramafic Complex

General statement.—In the valley of the South Lawis River east and west of the Masinloc mine (Fig. 1) the oldest rocks constitute an ultramafic plutonic complex forming part of the basement complex that composes the Zambales Mountains. According to Van Bemmelen (1949), these basic and ultrabasic rocks probably belong to the East Indian belt of young Mesozoic ophiolites, intruded in the geosynclinal foredeeps of mountain belts. They are transected by dikes of microdiorite, microgabbro, and andesites, all of which could possibly be correlated with lower Miocene volcanic rocks that appear on the east edge of the Zambales Range near Tarlac (Corby *et al.*, 1951, p. 106, Pl. 9). Along the upper edge of the coastal plain, the ultrabasic rocks are overlain with depositional contact by the Zambales limestone and the Santa Cruz formation, both Miocene (Corby *et al.*, 1951, p. 108–109).

Field relations.—Geologists have known for many years of the serpentines and gabbros in and around the chromite mines of Zambales, but the layered complex comprising these and other rocks has apparently not hitherto been recognized. Similar rocks, forming part of the complex, are known at the Acoje mine and also in about 12 other chromite workings, all embraced in a district about 10 by 20 miles. The size and shape of the area or areas occupied by the pluton, as well as the nature of the rock intruded, remain unknown.

The members composing the complex in the area studied are norite, olivine gabbro, saxonite serpentine, and dunite serpentine; all are easily distinguishable in the field. The feldspathic rocks are strongly pseudostratified, and the component layers differ greatly in composition. The saxonite serpentine and dunite serpentine are essentially massive and uniform. They are in all places greatly though variably serpentinized. A resumé of the rocks and of the mineral deposits and minor intrusives in each member is given in Table 2.

The layers in the pseudostratified rocks are parallel, and the contacts between them sharp. In places, a narrow stratum may gradually taper and terminate, and the layers above and below come together. The olivine gabbros, leucotroctolites, and olivine-bearing norites possess well-defined gneissoid texture, everywhere parallel to the pseudostratification.

The olivine gabbro is greatly folded with small open folds, a few feet in amplitude, and larger folds which are indicated by divergent attitudes of the strata from place to place. In the olivine gabbros exposed just east of the mine, in the Lawis and Mabihinal rivers, the general strike is northeast to east-southeast, and the dips are generally 20°–60° to the north or northeast. Folds were not noted in norite but may be present.

Small, coarse-grained gabbro pegmatites occur in some places where the stratification of the olivine gabbro is crumpled. The contacts of the pegmatite bodies follow the layering of the host rocks with only local transgressions. Narrow dikes of coarse, light gabbro and wider dikes of dark troctolite (Pl. 1, fig. 1) occupy fractures transecting the pseudostratification. Steep-dipping, ill-defined zones, resembling dikes but apparently alteration bands, cut across the layering at acute angles. They are a few inches to several feet wide and are composed of greenish plagioclase; the dark minerals apparently were obliterated.

The dunite serpentine belt that crosses the Mabihinal River, near the mine, is intrusive into the olivine gabbro member, as is shown by subangular inclusions of this light banded rock engulfed in dunite and in associated olivine-rich troctolite (Fig. 2).

Saxonite contains, in a few places, thin, sharply defined, parallel bands rich in pyroxene, which are continuous for at least several yards. The primary structure is otherwise massive. The plentiful slickensides that characterize serpentine rocks in many other localities are nearly lacking, but irregularly developed rhombic jointing, caused by tectonic forces, does occur. Slight faulting occurs especially in the mine area. The known chrome deposits lie in the saxonite serpentine.

The contacts of the saxonite are concealed. At the contact near the mine, no transitional zone exists between saxonite and olivine gabbro, such as might be present if the two rocks had a conformable relationship. The position of the saxonite seems to indicate that it must transect the pseudostratification of the olivine gabbro. Considering also, the intrusive relations shown by the petrographically similar dunite, it is probable that the saxonite also is intrusive into the pseudostratified feldspathic rocks.

Norite.—Norite is exposed along the road from Coto to the coast, between kms 11 and 20 (Fig. 1). A strongly pseudostratified part is at km 12, where the layers strike N. 50° W.

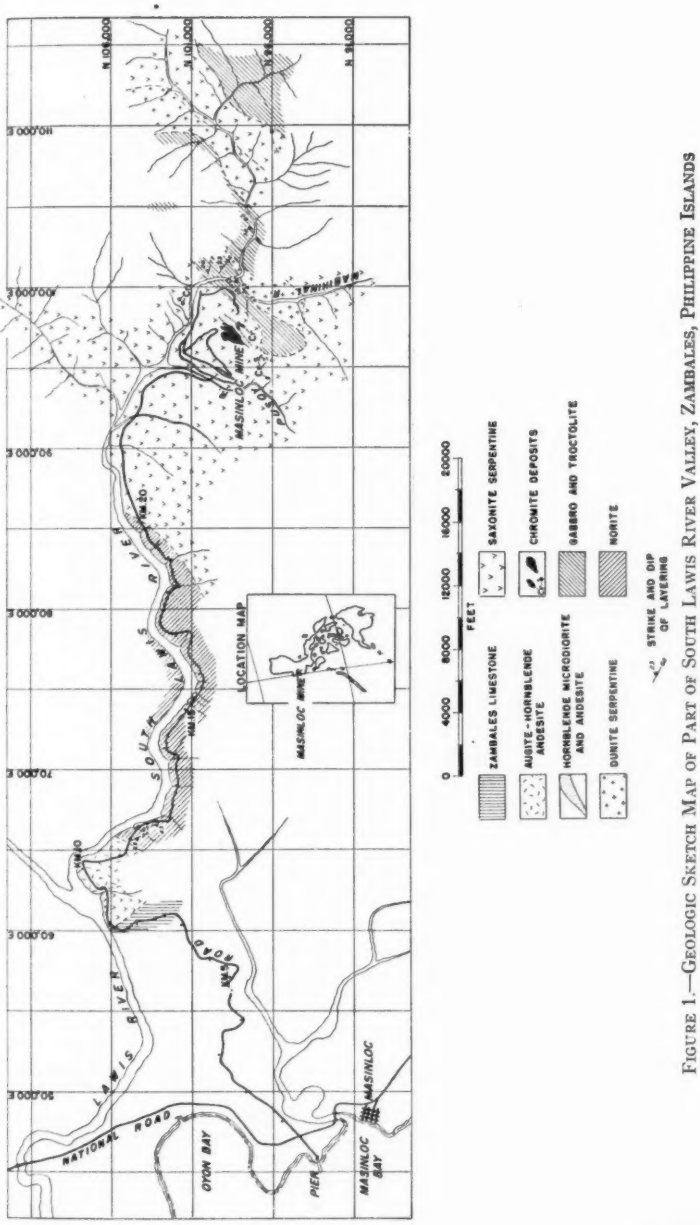

FIGURE 1.—GEOLOGIC SKETCH MAP OF PART OF SOUTH LAWIS RIVER VALLEY, ZAMBALES, PHILIPPINE ISLANDS

and dip 25° southwest. Here also it is cut by wide dikes of augite-hornblende andesite.

Most of the noritic member is massive norite, dark and phanerocrystalline in hand specimen

Table 2.—Subdivisions of the Ultramafic Complex in the Vicinity of the Masinloc Mine

Member	Component rocks	Associated intrusives and mineral deposits
Norite	Fine-grained norite with a few bands of coarser norite	
	Pseudostratified coarser-grained norite with layers of peridotite and pyroxenite	
Olivine gabbro	Coarse, pseudostratified, with layers consisting of: olivine gabbro	Concordant basic pegmatities
	leuco-troctolite	Melano-troctolite dikes
	diallage gabbro	Greenish alteration zones
	dunite	
	melano-troctolite	
	anorthosite	
Saxonite serpentine	Saxonite serpentine	Chromite deposits
		Gabbro and olivine gabbro dikes
		Melano-troctolite dikes
		Chrysotile deposit
Dunite serpentine	Dunite serpentine, with local phases of melano-troctolite	

and composed of plagioclase and pyroxene (roughly 3 to 2) with accessory iron ores, hornblende, and minor actinolite. Hornblende norites and olivine norites also occur. The texture is xenomorphic granular, and the grain is rather fine in most places, ranging from ½ to ¾ mm approximately. Layers of coarse norite are present, with grain size from 2 to 4 mm. The rock species range from norite and diallage norite, with a hypersthene/diopside ratio of 1 and greater, to hypersthene gabbros containing less hypersthene than diopside down to a proportion of about 1 to 4.

The plagioclase is labradorite, unzoned, and occurring ordinarily in anhedral, nearly equant, twinned grains but in a few places as rough, blunt laths. Some of it contains small enclosures of diopside.

Most of the hypersthene occurs in rounded grains; some grains show a suggestion of the prism form. It also occurs as large irregular grains, as much as 3 or 4 mm in maximum dimension, which contain small rounded enclosures of plagioclase and diopside, as well as exsolved lamellae of diopside. The pleochroism is weak or absent to strong; X = brownish pink, and Z = pale green. U-stage measurements of the optic angle of small, stout prismatic grains of hypersthene in hornblende norite gave an average of $2V/X$ of 58°, corresponding to a composition of 46 mol per cent of $FeSiO_3$. Measurement of hypersthene in a norite band interlayered with pyroxenite gave $2V/X$ greater than 78°, indicating a composition close to bronzite.

Diallage occurs in anhedral grains, pale green or brown, with strongly developed parting on 100. The extinction angle $Z \wedge c$ ranges from 39° to 43°. The measurement of $2V/Z$ in diallage in a hypersthene gabbro gave an average of 56°.

Brownish-green hornblende occurs as a minor constituent. In hornblende norite, the mineral is brown, with strong pleochroism: Z = brown, X = pale tan. It occurs plentifully in large formless grains enveloping the plagioclase and hypersthene.

A few small grains of olivine occur in some of the norites; they are partly altered to antigorite with abundant magnetite.

The proportion of opaque minerals (mainly magnetite) ranges from zero to 4 or 5 per cent. Some of the ore is molded on the edges of silicate crystals, indicating a late, interstitial crystallization. A heavy-mineral residue was concentrated from norite, then separated into magnetic and nonmagnetic fractions, and each was analyzed separately. The magnetic residue

contained 0.14% Cr, 0.04% Cu, and 0.04% Ni. The nonmagnetic residue contained 0.25% Cr, 0.02% Cu, and 0.01% Ni. Neither sample contained platinum.

to bastite, whereas the clinopyroxene remains fresh.

Olivine gabbro.—Olivine gabbro occurs in two or three belts, apparently trending north-

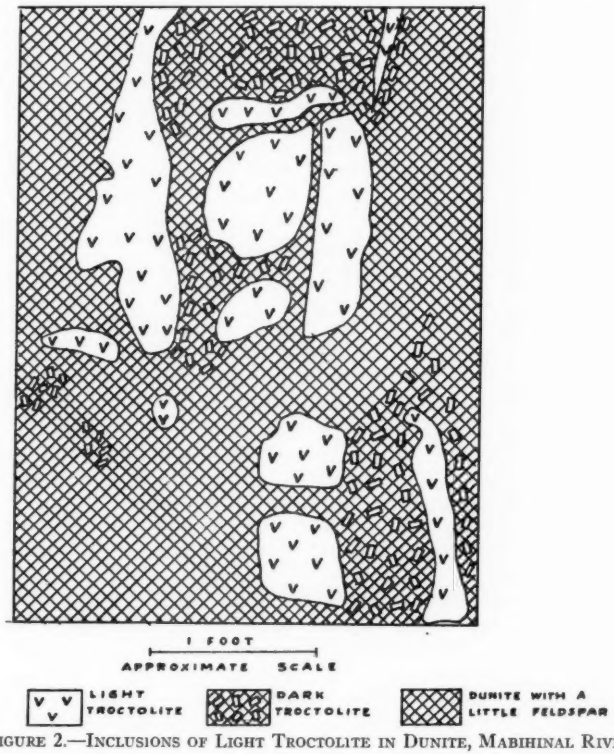

FIGURE 2.—INCLUSIONS OF LIGHT TROCTOLITE IN DUNITE, MABIHINAL RIVER

Layers composing pseudostratified norite are a fraction of an inch to many feet thick. Contacts are sharp. Several kinds of layers were observed: (1) coarse norite bands in fine norite, (2) thin olivine streaks in norite, (3) periodotite bands, and (4) pyroxenite bands, both interlayered with norite.

The periodotite layers are rich in olivine and poor in pyroxene, as well as vice versa. Some contain a little plagioclase, but most are altered to mesh antigorite with magnetite, and to bastite with chrysotile veinlets.

The pyroxenite layers are composed of diallage and hypersthene, in places with a little labradorite. The diallage has $2V/Z = 56°$ and $Z \wedge c = 43°$. The hypersthene has $2V/X = 80°$, corresponding to 22 mol per cent of $FeSiO_3$. The orthopyroxene in places is altered east, lying east of the mine (Fig. 1). It is composed of three dominant rock types: olivine gabbro, troctolite, and diallage gabbro; feldspar predominates over the dark minerals in all three. Dunite, olivine-rich troctolite, and anorthosite occur widely but scantily, as bands an inch to several inches thick, interlayered with the lighter rocks (Pl. 1, fig. 2).

OLIVINE GABBRO AND LIGHT TROCTOLITE: The olivine gabbro is composed essentially of plagioclase, olivine, and pyroxene, and the troctolite of plagioclase and olivine; the dividing line is taken as 5 per cent pyroxene. In hand specimen, both are light gray to medium gray; the tone depends on the proportion of feldspar. The gabbros contain roughly 15–30 per cent dark minerals; either olivine or pyroxene predominates. The troctolites

contain about 20–40 per cent olivine. The rocks are phanerocrystalline, with average grain size about 1–2 mm. The texture is gneissoid in most rocks, but in a few cases troctolite exhibits a spotted texture of dark round olivines evenly scattered in the light feldspar (forellenstein). Microscopically, the texture is xenomorphic to hypautomorphic, depending on the form of the plagioclases.

The plagioclase, calcic labradorite, occurs in most places as anhedra 1–2½ mm across, and in a few places as rough laths, some as long as 4½ mm, showing a marked tendency to a common orientation, with 010 parallel to olivine streaks. The feldspar shows twinning according to the albite and Carlsbad laws, as well as other twinning, including multiple twinning oblique to the albite twin lamellae. It is fractured with varying intensity. Many of the cracks converge upon clusters of olivine, making a roughly radial pattern that may indicate that the olivines were loci of stress relief. Rarely, the plagioclase shows mortar structure, as well as bent twin lamellae, wavy extinction, and shattering.

Most of the olivine occurs in clusters (synneusis texture) which almost everywhere show elongation and parallelism among themselves, giving rise to the characteristic gneissoid texture. Many individual crystals lie with their long axes in the plane of foliation. As seen in thin section, several such grains may lie end to end, forming a string. Separate grains as well as clusters are commonly situated at the grain boundaries of plagioclase. The grains are typically rounded and much smaller than the plagioclase individuals.

Pale-brown diopside, $Z \wedge c = 43°–45°$ commonly with diallage parting, occurs in troctolite as reaction rims on olivine, next to plagioclase. In olivine gabbro it occurs also as anhedral grains. The anhedra are isolated individuals at the grain boundaries of plagioclase.

A large crystal of orthopyroxene, pale brown and nonpleochroic, partly replaced by diopside, was observed.

Opaque minerals are scarce and occur as scattered crystals and formless grains. Accessory anhedral chromite is rare.

Plagioclase is partially replaced by a fine micaceous mineral (paragonite?), and the alteration is especially marked in the more fractured specimens. Olivine is everywhere partly altered to antigorite and magnetite and in a few places to talc, which is in turn replaced by antigorite. Small quantities of penninite and clinochlore, as well as of tremolite and actinolite, occur as patches and veinlets replacing the primary minerals and the serpentine. In a few places carbonate replaces serpentine pseudomorphs after olivine.

DIALLAGE GABBRO: In hand specimen, diallage gabbro is greenish gray and phanerocrystalline and shows no foliation. The essential minerals are plagioclase and diallage, the latter composing from 15 to 45 per cent of the rock. The grain size is 1–2 mm, and the texture is xenomorphic granular. Under the microscope diallage is pale brown and faintly pleochroic, with extinction angle $Z \wedge c$ about 44°. The feldspar is labradorite, in twinned, anhedral to subhedral grains. Some gabbro specimens contain spots of secondary amphibole which have replaced serpentine grains pseudomorphic after olivine. Actinolite occurs as fringes on pyroxene grains; it replaces some pyroxene completely, as well as feldspar partially. Opaque minerals are scarce or absent.

DUNITE: In dunite bands, only scarce relicts of olivine remain. No accessory chromite was observed. The grain size of the dunite appears to have been ½–1 mm. The principal secondary minerals, which replace antigorite, are penninite and clinochlore.

ANORTHOSITE: The bands of anorthosite are composed essentially of plagioclase in twinned grains, anhedral to subhedral, and generally 1–2 mm across. The feldspar is commonly slightly cracked and sheared. One slide shows pronounced granulation of the individuals at the grain boundaries; the fragments were recrystallized. A few grains of diallage and pseudomorphs after olivine occur.

Saxonite serpentine.—Saxonite consisted essentially of olivine and enstatite; the enstatite content ranges on the average from 15 to 25 per cent and is locally as high as 30 to 50 per cent. A little basic plagioclase is present locally. Near the chromite bodies the rock is converted to serpentine. Farther away, residual olivine and pyroxene are found. Saxonite serpentine, where unweathered, is black or dark green, and the olivine is dull, with mesh texture; pyroxene or bastite forms conspicuous, lustrous insets. On weathered surfaces saxonite serpentine is light; this discoloration extends downward from a fraction of an inch to many feet, then fades abruptly into the normal dark color of the unweathered rock. The light color is produced by a crypto-crystalline mineral, white in reflected light, which clouds the mesh serpentine but affects the bastite only slightly.

Olivine occurs as equidimensional grains more or less altered to antigorite. The fresh olivine

remnants are clear and colorless in thin section. The optic angle corresponds to chrysolite. Enstatite occurs as scattered single grains without crystal form and as grain clusters. It is very faintly colored, without pleochroism, and contains exsolved lamellae of what appears to be diopside. Most enstatite has been altered to bastite. Reaction rims of enstatite on olivine and of diopside on enstatite are exceptionally observed. The olivine and pyroxene grains range from 1 to 3 mm diameter, excepting a few large pyroxene individuals as much as 4½ mm long. The rock texture is xenomorphic granular.

Chromite is everywhere present as an accessory mineral; the grains are typically irregular and have curving projections which extend into the surrounding silicates. Some chromite occurs as clusters of wormlike forms, following in part the cleavages of pyroxene and bastite, or following grain boundaries and cracks in pyroxene and olivine (Pl. 1, figs. 3–6). Its late crystallization is therefore indicated. The close association with pyroxene is notable. In composition it is slightly different from the ore chromite, richer in Cr and Fe, and correspondingly poorer in Al and Mg.

Exceptionally, accessory chromite occurs as rounded, compact grains, which in some cases have resorption embayments, angular boundaries, and other characteristics of an early crystallized mineral.

The vermiform chromite, as well as the compact chromite, is translucent and yellowish to orange brown. An alteration shows as a blackening along grain boundaries and internal fractures, and in the thin projections of chromite extending from the main body of the grain. The opaque mineral is probably magnetite. In saxonite that has suffered little serpentinization, the blackening of the chromite is slight, and it seems therefore that the precipitation of magnetite was incidental to serpentinization of olivine. Some of the compact chromite grains have fringes of minutely crystalline magnetite.

Secondary hematite and limonite occur as ribbons and as rhombic, hexagonal, and lozenge-shaped crystals in bastite. Talc is present. Post-serpentine alteration is marked by small quantities of penninite, clinochlore, carbonate, fuchsite, and chrysotile. Chrysotile, in cross-fiber veinlets cutting antigorite and chlorite, was apparently the last mineral to form.

In a few cases strain is shown by bending of the exsolution lamellae in enstatite and by slicing of the accessory chromite particles. No other microscopic evidence of dynamic pressure was observed.

Dunite serpentine.—In hand specimen, dunite serpentine is dull black or gray where fresh and light on weathered surfaces. The texture is fine and compact. It is distinguished from saxonite by its smaller pyroxene and bastite content. Almost all the olivine, probably chrysolite, has been converted to antigorite and magnetite. Sporadic diopside and enstatite have been converted to bastite, and the scanty plagioclase has been replaced by fine chlorite and other secondary minerals.

Accessory chromite is widely and irregularly dispersed. All occurs as compact grains, some showing rectilinear boundaries and resorption effects. Alteration of the chromite is similar to that in the saxonite. Some grains appear almost completely replaced by magnetite. There is a notable difference between the compact accessory chromite of the dunite, evidently of an early crystallization, and the vermiform chromite of the saxonite. This difference can perhaps be explained as the result of the difference in Al content between the two rocks. The Al content of dunite, sufficient to permit the formation of a little plagioclase, allowed the early crystallization of chromite. Saxonite contained so little Al that the precipitation of chromite was retarded until Al and Cr had become sufficiently concentrated in the liquors remaining at the end of rock crystallization.

The microscopic texture of the dunite and the olivine relics shows that the olivine was serpentinized *in situ*, as was the saxonite.

Microdiorite and Andesite Dikes

The chrome deposit is crossed by a dike swarm numbering about 30 microdiorite dikes 2 feet thick or more and many smaller dikes. Most strike about northeast and dip 50°–80° southeast. The wider bodies are multiple, consisting of two or more parallel dikes side by side, and in places having intervening septa of chromite or serpentine. Few of the single dikes are more than 8 feet thick. The intrusive rocks appear to occupy simple dilation openings; there are no signs of slip movement. Their form is typically branching, with great variations of attitude. Locally the fissures were guided by joints in chromite and serpentine, but usually they cut across joints. The first fissuring and the intrusion and hypabyssal crystallization of dioritic magma were followed by renewed fissuring, which split the

dikes lengthwise down the middle or tore open one of the contacts. A second pulse of the same magma, crystallizing again as microdiorite or in places as andesite, ensued. Exceptionally, andesite cuts across the microdiorite bodies as separate dikes with divergent trends.

Dikes of this kind are found in many places distant from the mine, but it seems likely that the greater rigidity and brittleness of the chromite body had the effect of localizing the fissuring somewhat and therefore, also, the intrusives. The fissuring and intrusion split the ore body into a number of slices and spread it about 250 feet in a northwest direction. No chromite was lost thereby except the small blocks that were embodied in the dikes and cannot be mined. The dike fissures may have formed in response to local crustal tension (upward bending) caused by the thrust of magma beneath.

The well-developed platy cross-jointing is due to shrinkage of the magma upon crystallizing. The plates, separated by joints a fraction of an inch to several inches apart, lie nearly at right angles to the dike contacts and dip at steep angles. Where a dike makes a sharp bend, the joints form a radial pattern and stay more or less normal to the contacts. In places they penetrate the serpentine walls several inches, which indicates that the heat of the intrusion was great enough to make the walls somewhat plastic.

The dike rock is light gray to medium gray, with very fine granular texture grading to aphanitic at the margins. Fluidal texture parallel to the contacts is noticeable in the selvages. The texture is coarser in wide dikes than in narrow ones.

The constituent minerals are plagioclase, hornblende, quartz, accessory iron ores, apatite, biotite, and titanite, and secondary pyrite and hematite. The texture is hypautomorphic and microgranular. In the interior of the dikes, the average grain size ranges from about 0.1 to 0.2 mm, and in the selvages from 0.02 to 0.09 mm.

In the anterior parts, plagioclase and hornblende are present in about equal proportions, and quartz is highly variable, averaging roughly 10 per cent. In the selvages, hornblende is more abundant, and quartz very scanty, if not absent.

Plagioclase occurs as blunt ragged laths and as equant anhedral grains. It shows multiple twinning on 010, as well as other kinds of twinning. The lathlike crystals are zoned and have more basic cores and more acidic rims. The average composition is probably basic andesine. The hornblende, in ragged blades, is green and pleochroic: Z = green; X = pale yellowish green. The quartz is xenomorphic granular and interstitial to plagioclase. Brown biotite is present in traces.

The andesite differs mainly texturally from the microdiorite. Under the microscope slender laths of plagioclase and ragged grains of amphibole can be observed; they occur as phenocrysts in a mesostasis composed of microgranular feldspar and amphibole microlites. Accessory titanite is present.

Another dike specimen studied has a texture similar to the microgabbro but contains colorless amphibole instead of diopside. The plagioclase is labradorite. Titanite and apatite are present, and quartz is absent. This rock may be an intermediate member in a series extending between microgabbro and quartz-bearing microdiorite. The presence of titanite in all rocks and the microgranular texture that characterizes most of the rocks indicate that they are differentiates of a common magma. It is evident that they represent an igneous episode far younger than that which gave rise to the ultramafic complex and its chrome deposits.

The chromite deposit at Coto is traversed by a vein of white, coarse-grained quartz which contains small masses of chalcopyrite. The vein is probably related genetically to the dikes.

Microgabbro

A massive dike of diopside gabbro several feet thick cuts ore on one of the lower benches of the mine. It is light brown and has a fine sugary texture. Brecciated ore, cemented by the dike rock, occurs in a few places in this locality (Pl. 1, fig. 7).

The minerals are labradorite, colorless diopside, and abundant titanite. Diopside occurs as stout rounded prisms, and the plagioclase occurs as equant anhedral grains with a few larger lathlike phenocrysts. The average grain size is about 0.1 mm, and the texture is hypautomorphic microgranular.

Augite-Hornblende Andesite

Dikes of andesite intrude norite between km 10 and km 11 on the road between Coto and the port. In hand specimen the rock is dark and fine-grained. Under the microscope are revealed scattered stout phenocrysts of

twinned and zonal plagioclase and phenocrysts of augite as much as 1½ mm in maximum diameter. The augite, peripherally replaced by green hornblende, is light brown by transmitted light, and $Z \wedge c$ was measured as 49°. The mesostasis is composed of blunt laths of plagioclase in random orientation, with much green hornblende and accessory iron ore. The average grain size is around 0.15 mm.

Chromite Deposits

Geology

Relations to gabbro-peridotite contact.—Near the barrio of Coto are the big Masinloc deposit and 10 or 12 smaller ones. The smaller deposits tend to occur in clusters. All are strung out in a belt 8000 feet long, trending northeast. They are enclosed in serpentinized saxonite, and lie within 400–2300 feet of the contact between the saxonite and the olivine gabbro. The center of the main deposit is 1100 feet horizontally from the contact. There thus exists a rough parallelism between the contact and the string of chromite bodies (Fig. 1). The dip of the contact is unknown. The proximity of chromite deposits to a periodotite-gabbro contact was noted by the writer also at the Acoje mine, 10 miles north of Coto, and has been described from the Bay of Islands, Newfoundland (Smith, 1953, p. 411), and the Camagüey district in Cuba (Flint, de Albear, and Guild, 1948, p. 55–56).

On a ridge 1500 feet south of the mine, the contact was traced with test pits, and it makes here an abrupt 90-degree bend. Most of the small deposits, as well as the big one, lie close to this bend (Fig. 1).

Size and shape.—The main Masinloc deposit (Figs. 3, 4) has the form of a thick, irregularly curving plate, lying at a slight inclination, which has many large bulges, re-entrants, and other irregularities. It is exposed at the top and on the north and east slopes of a hill about 500 feet high; most of it lies almost parallel to the slopes of the hill. Except for irregularities, the ore body occupies a roughly oval area with a northeast-trending major axis 1800 feet long and a width of about 950 feet. In its thickest parts, the ore is 100–175 feet deep vertically. Originally the maximum thickness was probably about 250 feet. When mining began before the second World War there was a blanket of soft laterite with dense vegetation directly overlying the ore near the top of the hill, but this has since been stripped, and no vestige remains of the hanging wall in this part of the deposit.

The mine probably will have produced at least 4,500,000 long tons of shipping ore by the time it is exhausted, and this qualifies the deposit as one of the largest in the world—certainly the largest of the "sackform" deposits.

Field relations of ores and associated rocks.—The chromite ores are believed to be genetically related to dunite, gabbro, and troctolite with which they are closely associated in the mine. Hence the ores and rocks are all described together here as components of the ore deposit. Table 3 is a classification of them as well as a recapitulation of their modes of occurrence and contact relations.

DENSE ORE: The great mass of the deposits is dense chromite. The contacts with the adjoining ore and rocks are generally sharp, and the undisturbed ore is essentially massive. Planar and linear elements were searched for, but none found except an elongation and rough parallelism of the interstices in a few places. Brecciation is in places distinguishable in the field (Pl. 1, fig. 8).

Fragments both of dense and disseminated ore lie in dunite serpentine in the footwall of the ore deposit (Figs. 5–8). They range from pieces half an inch across to blocks 6 feet long and 3 feet wide, and even larger masses may be present. Some of the smaller fragments appear roughly ellipsoidal, but most are angular and have rounded corners. Most of the contacts are sharp and definite. The form, angularity, and sharp definition of the bodies identify them as having originated as solid enclosures. Near the borders of some large blocks, the dunite serpentine contains strings of chromite particles lying parallel to the contacts. These may signify that the contours of the solid blocks determined locally the flowage of the enclosing dunite.

The contacts of some blocks have been accentuated by slight rotational movement induced by external stress, and such surfaces are faintly striated and coated thinly with secondary minerals. The foliation observed in some of the serpentine next to such blocks may also have been produced by external stress.

A few ore fragments have irregular and gradational borders, signifying that they have suffered partial disruption.

DISSEMINATED ORE: Disseminated ore, consisting essentially of chromite more or less thickly scattered in dunite serpentine, has four distinct modes of occurrence (Table 3). A

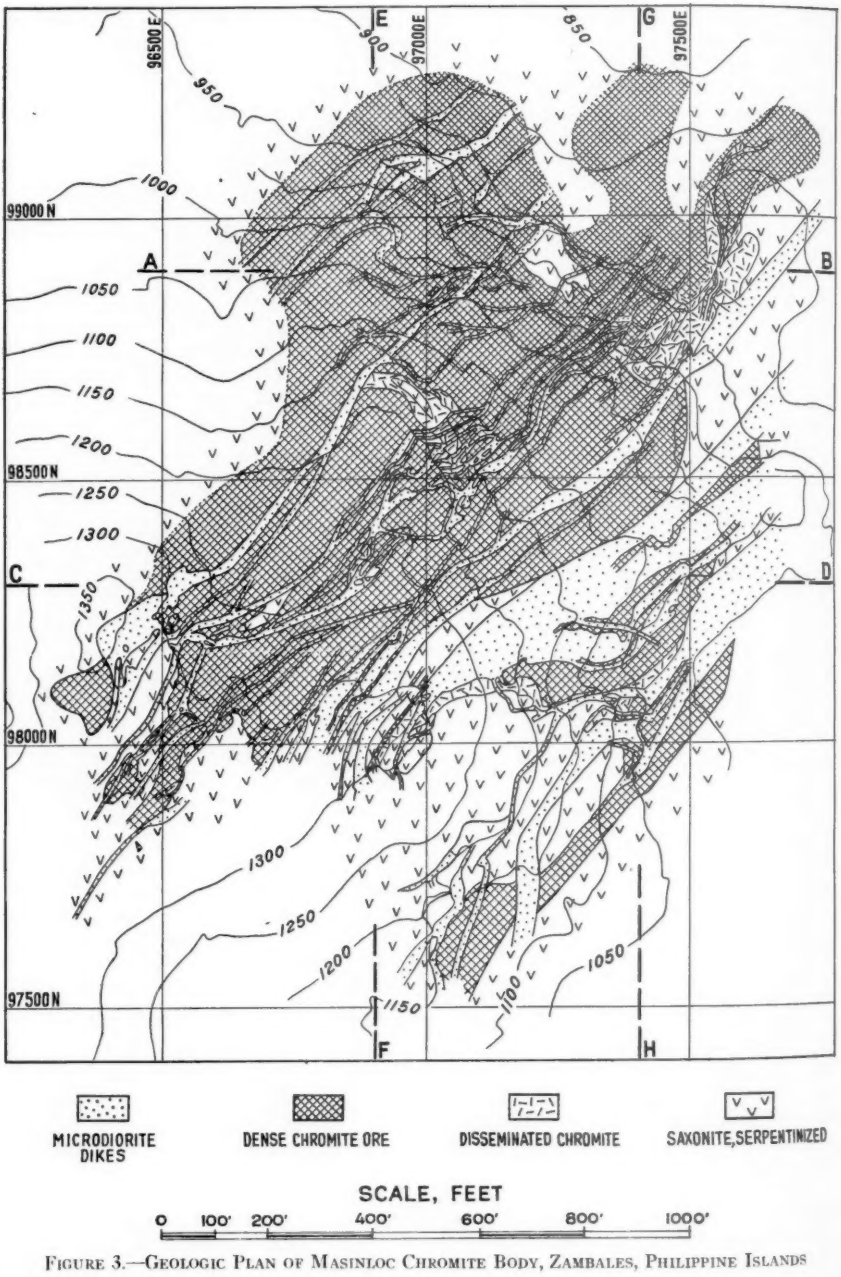

FIGURE 3.—GEOLOGIC PLAN OF MASINLOC CHROMITE BODY, ZAMBALES, PHILIPPINE ISLANDS

disseminated ore selvage was seen in only one place, where a small chrome body is exposed in an area of a few square yards surrounded by saxonite serpentine. It appears to be a slab a few feet thick, dipping almost vertically; only one contact is exposed. The interior of the mass is dense chromite. On its border is a selvage, 3–6 inches thick, of ore of a texture similar to that of other disseminated ore, and composed of 80 per cent chromite and 20 per cent green serpentine. Adjoining the selvage is a shell of dunite serpentine, apparently less than a foot thick, containing a few chromite grains. Beyond this is the saxonite serpentine country rock. Figure 9 is a sketch of the occurrence, and Figure 1 of Plate 2 is a photograph of a sawed section showing the dense ore, the selvage, and the shell.

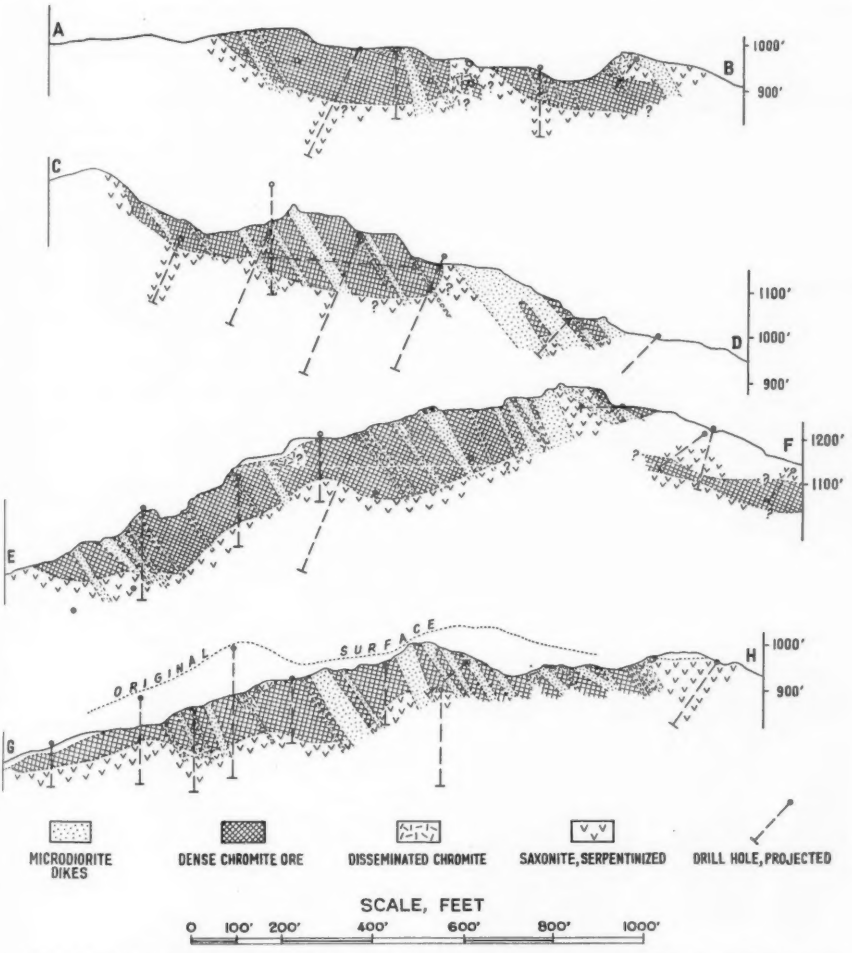

FIGURE 4.—GEOLOGIC SECTIONS OF MASINLOC CHROMITE BODY, ZAMBALES, PHILIPPINE ISLANDS

A narrow, sharp-walled dike of disseminated ore cutting dense ore is illustrated in Figure 10. The ore of the dike consists of roughly 40 per cent chromite in a matrix of yellow, weathered dunitic serpentine. Most of the chromite pieces, which in hand specimen can be seen to be deeply embayed, are several millimeters

TABLE 3.—CLASSIFICATION OF ORES AND ASSOCIATED ROCKS IN MASINLOC CHROMITE DEPOSIT

Type	Mode of occurrence	Contact relations
Dense ore	Main mass of the deposits	Generally sharp contacts against disseminated ore, dunite, and saxonite
	Small blocks enclosed in dunite serpentine at margins of main deposit	Sharp contacts
Disseminated ore	Selvage on edge of dense ore	Sharp to gradational contact with dense ore; sharp and irregular contact against dunite shell
	Dikes	Sharp contacts
	Large, nearly homogeneous bodies enclosed in dense ore or lying between dense ore and serpentine	Sharp contacts against dense ore
	Small blocks enclosed in dunite serpentine	
Dunite serpentine	Shell adjoining dense ore at many places, lying between it and saxonite serpentine country rock	Sharp contacts against dense ore; gradational into some of the disseminated ore
	Dikes (?) in ore and wall rocks	Sharp contacts
	Matrix of disseminated ore and of some dense ore	Interstitial to chromite particles
Dark troctolite	Segregations in dunite serpentine	Contacts ill defined
	Pockets in massive and disseminated ore	Sharp contacts
	Dikes cutting saxonite serpentine	Sharp contacts
Coarse diopside gabbro, olivine gabbro, and troctolite	Narrow dikes cutting ore and dunite and saxonite serpentines	Sharp contacts
	Matrix of dense ore	Interstitial to chromite particles

FIGURE 5.—SUBANGULAR BLOCKS OF CHROMITE ORE ENCLOSED IN DUNITE SERPENTINE IN FOOTWALL OF MAIN DEPOSIT

Contacts are sharp. Note streaks of chromite grains parallel to edges of blocks.

FIGURE 6.—SUBROUNDED CHROMITE ORE BLOCKS ENCLOSED IN DUNITE SERPENTINE

Footwall of deposit, Bench 1010. Contacts are sharp. The ore contains 70 to 80 per cent chromite.

across. Figure 11 shows an occurrence which is perhaps similar.

The third mode of occurrence is exemplified by six large bodies, some apparently entirely

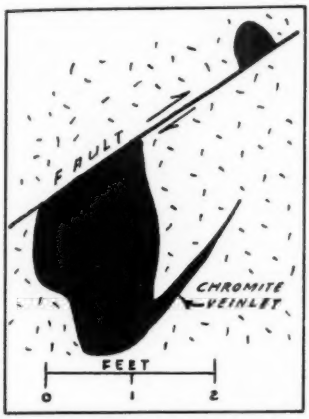

FIGURE 7.—SUBROUNDED CHROME ORE INCLUSIONS
With divergent veinlet or streak, in dunite serpentine, Bench 950.

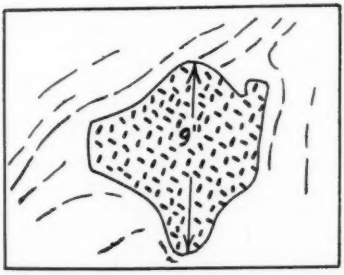

FIGURE 8.—INCLUSION OF DISSEMINATED ORE IN FOLIATED SERPENTINE, BENCH 980

enclosed in dense ore, and others lying between ore and a serpentine wall. The largest is at least 250 feet long and apparently 40–50 feet thick. Another may be 300 feet long and 10–15 feet thick. The smaller bodies have maximum dimensions greater than 100 feet.

The proportions of chromite in these large bodies range from about 60 to 80 per cent, and the chromite particles range from specks to pieces a centimeter across. Most are 1–5 mm in diameter. The ore texture as seen in the field depends mainly on the proportion of chromite and the size and shape of the particles. In the lower-grade disseminations, the serpentine gangue is plentiful enough to isolate individual particles, throwing them into visual relief, and

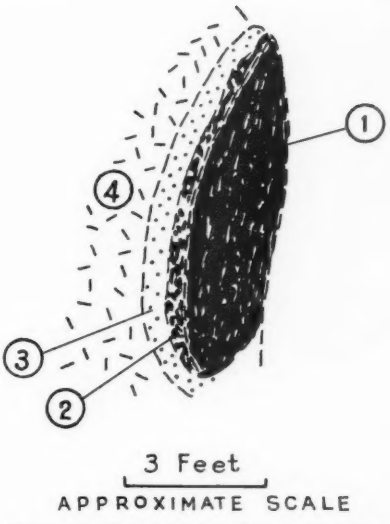

FIGURE 9.—DIAGRAMMATIC SKETCH OF A SMALL BODY OF DENSE ORE WITH SELVAGE OF DISRUPTED CHROMITE AND SHELL OF DUNITE SERPENTINE (FROM MEMORY).

(1)dense ore, (2) disrupted chromite with dunite serpentine gangue, (3) dunite serpentine shell, (4) saxonite serpentine country rock. In upper bench of mine.

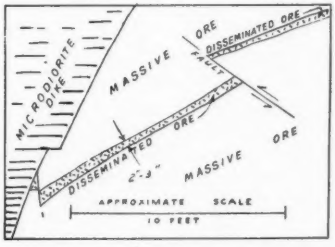

FIGURE 10.—NARROW DIKE OF DISSEMINATED ORE CUTTING DENSE ORE
Bench 950.

giving a conspicuous speckled texture. Where chromite is more plentiful, it forms a continuous meshwork, with interstitial serpentine (Pl. 2, fig. 2).

The larger pieces, where they are isolated in serpentine, are almost all highly irregular in outline. The edges may be ragged or smooth, angular or rounded, and internal spots of serpentine occur. A few pieces have nearly square outlines (Pl. 2, fig. 3). Some of these, as well as the more irregular pieces, seem to be multigranular. The granularity is suggested by unequal reflections from polished surfaces,

as well as by the distribution of strain anisotropism in thin section. The complex forms, even allowing for intense modification by corrosion, suggest also that they are aggregates rather than unit grains. The smaller pieces of chromite are also irregular.

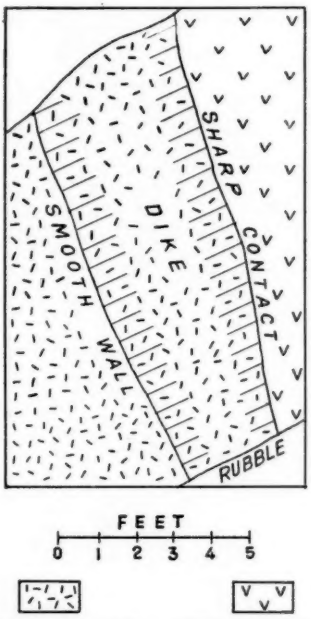

FIGURE 11.—DIKE (?) OF DISSEMINATED ORE BETWEEN WALLS OF DISSEMINATED ORE AND SERPENTINE
Joints occur normal to the contacts, as shown.

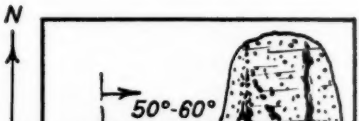

FIGURE 12.—SKETCH OF OUTCROP; SUBPARALLEL BANDS OF DENSE CHROMITE AND A DIVERGENT BAND, IN DISSEMINATED ORE
East-west joints about normal to banding.

In rich disseminations, individual chromite pieces can seldom be distinguished. The mineral occurs in grains partly interlocked with other chromite grains and partly in contact with interstitial serpentine.

In banded ore, the most conspicuous bands are nearly solid chromite (Pl. 2, fig. 4). In other bands chromite is only a little more abundant than in the adjacent ore, and there are all gradations between these extremes. Most of the bands are 1 or 2 inches thick; they extend 1 or 2 feet along the strike and then become indistinguishable from the ordinary disseminated ore. The bands also grade into ordinary ore across the strike (Fig. 12). Some bands are lenticular, as much as 6 inches thick but just as short as the thinner bands (Fig. 13). Bands occur singly and in groups of several parallel members, separated by layers several inches thick of poorer ore. Rarely a divergent streak unites two parallel bands.

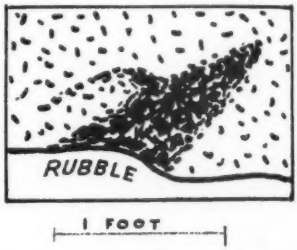

FIGURE 13.—LENS OF DENSE CHROMITE IN DISSEMINATED ORE
Bench 1320.

Closely packed aggregates of chromite occur also as small masses with gradational edges and irregular, indefinable shapes. They give a spotted structure to some of the ore. The texture of the dense bands and spots does not differ much from the texture of dense ore.

Another kind of banding or mottling arises from abrupt changes in particle size or in differences in the proportion of angular pieces (Pl. 2, fig. 5). The coarser-grained ore tends to have a higher proportion of angular pieces than the finer ore.

Although they are large, the disseminated ore masses form only a small part of the deposit. No structural feature was recognized that might have determined the position and shape of these masses except, perhaps, in some places, dense ore contacts. Where observed, the contacts of the disseminated ore bodies are sharp. The platy banding, interpreted as differential flowage banding, may be almost

parallel to the long axis of some of the bodies and, in places, is almost parallel to near-by dense ore contacts.

DUNITE: In hand specimen, dunite is distinguished from saxonite by the absence of

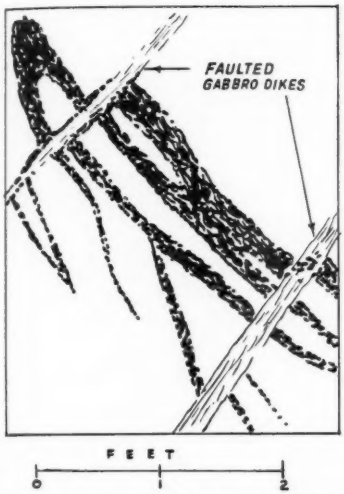

FIGURE 14.—BRANCHING BANDS OR VEINLETS OF CHROMITE IN DUNITE SERPENTINE
Bench 1290.

pyroxene and bastite, as well as by abundant scattered chromite and by the local presence of plagioclase. Serpentinization is intense.

Where the ore contacts have been explored by cuts or drill holes, the bordering rock is commonly found to be dunite serpentine (Pl. 2, fig. 6). Some contains sufficient plagioclase to be locally troctolite. Dunite shells around chromite deposits have been observed elsewhere (Thayer, 1942, p. 24). In the Masinloc deposit as well, an incomplete shell of this nature may exist. In many places it is only a few inches to a few feet thick. Saxonite is also observed in direct contact with dense ore.

Small dunite bodies, possibly dikes, are enclosed in dense ore and in saxonite beneath the ore deposit, as revealed in drill cores.

Chromite is dispersed in dunite in several ways: (1) as scattered pieces (Pl. 2, fig. 6), (2) as strings, wisps, and bands of thickly disseminated particles, with intervening layers of chromite-poor serpentine (Pl. 2, fig. 7), and (3) as small ramifying veinlike bodies (Fig. 14). Similar occurrences are seen in disseminated ore (Fig. 15).

At one place near the top of the mine, a body of unknown dimensions consists of dunite serpentine above and disseminated ore below. The contact is sharp, wavy, locally steeply dipping, and identifiable solely by the presence of abundant chromite on one side and its near absence on the other. Chromite streaks in the dunite have the same orientation as those in the

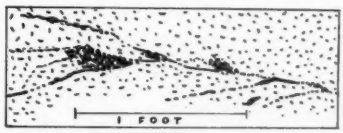

FIGURE 15.—BRANCHING BANDS OR VEINLETS OF DENSE CHROMITE IN DISSEMINATED ORE
Boulder.

ore, and the ore contains serpentine streaks with the same orientation. The contact is regarded as the surface of separation of settling clouds of chromite particles.

DARK TROCTOLITE: Dunite contains segregations of troctolite containing around 30 per cent plagioclase, interstitial to the predominant olivine or serpentine. Where the troctolite grades into dunite, the feldspar diminishes gradually to nothing in distances of a few inches or feet. The shapes of the segregations are indefinite.

Similar troctolite forms small pockets in ore and dikes cutting the country rock. The pockets are splotches, several inches across. Some are coarse-grained and rich in feldspar, and plagioclase penetrates between the ore grains, forming rims around them.

Two dikes of dark troctolite, one 7 feet and the other 6 inches thick, cut saxonite in the mine. The contacts are parallel and sharp. The rock is coarse-grained and black, with white specks of feldspar interstitial to the rounded olivine grains. Weathering produces brown cavernous surfaces.

OLIVINE GABBRO DIKES: Dikes of olivine gabbro, diopside gabbro, and light troctolite, fill fractures in the chromite ore and in the near-by dunite and saxonite. About 12 were seen in the mine; one was several feet thick, and all the others very narrow—from a quarter of an inch to 4 inches. A few similar diopside gabbro dikes cut serpentine and gabbro at places distant from known chromite deposits.

Although the dikes are narrow, the grain is coarse, about 1–10 mm. The diopside gabbro is composed of plagioclase and diopside. A narrow dike of this kind is shown in Figure 8 of Plate 2. The troctolite is essentially plagioclase (60–80

per cent) and olivine (20–40 per cent). (See Pl. 2, fig. 9.) All the dikes are altered, some nearly beyond recognition of their original character.

A few dikes cutting disseminated ore have conspicuous dark selvages of chromite or mixed chromite and serpentine. Figure 10 of Plate 2 illustrates such a dike, about 2 cm wide, with straight parallel walls. It strikes at about right angles to the banding in the enclosing disseminated ore. The chromite selvages are continuous and 3–15 mm wide. They are absent in dikes that cut plain serpentine. Their genesis is not known.

Age relations.—Field relations indicate that dense chromite is the oldest component of the ore deposit. The relations between dunite and disseminated ore indicate contemporaneity of crystallization in some places and different ages in others. The dikes of olivine gabbro are the youngest component.

Joints and faults.—Dense ore contacts have localized much of the movement caused by external stress. Many small faults also cross serpentine and ore, and indistinct zones of shearing are evident within the ore at several places. The most conspicuous result of tectonic pressure is the joint system that pervades ore and serpentine. There are three prominent sets of joints that strike, respectively, northeast, east, and northwest, with considerable variation of direction within each set. The directions and angles of dip are inconstant. The joints divide the ore and rock into massive rhombo-

PLATE 1.—TROCTOLITE, OLIVINE GABBRO, ACCESSORY CHROMITE IN SAXONITE, BRECCIATED ORES

FIGURE 1.—Dark troctolite. Black is serpentinized olivine; white and gray are plagioclase. Cobble. Scale in inches.

FIGURE 2.—Pseudostratified olivine gabbro member. Dunite and light troctolite bands. Scale in inches.

FIGURE 3.—Saxonite. Late accessory chromite in olivine and enstatite. br-enstatite, ol-olivine, s-serpentine, chromite-dark. M-111. Lower nicol only. 38×.

FIGURE 4.—Saxonite serpentine. Late accessory chromite in bastite, whose boundaries are marked in ink. b-bastite, s-mesh serpentine after olivine, dark, chromite. M-13, no nicols, 171×.

FIGURE 5.—Saxonite. Late accessory chromite in enstatite. Chromite-black, enstatite-en, olivine-ol, serpentine after olivine-s. The round spot is a bubble. M-31. Nicols 60°, 40×.

FIGURE 6.—Saxonite. Late accessory chromite in enstatite. Same slide as Figure 5 of Plate 1. Chromite-dark; enstatite-en. No nicols, 170×.

FIGURE 7.—Chromite ore breccia cemented by fine-grained diopside gabbro dike material. Scale in inches.

FIGURE 8. Brecciated ore cemented by olivine gabbro. Scale in inches.

FIGURE 9.—Brecciated ore. Rounded chromite grains in matrix of secondary minerals replacing plagioclase. M-325. Lower nicol only, 12×.

PLATE 2.—DISSEMINATED ORE, DUNITE, GABBROIC DIKES

FIGURE 1.—Disseminated ore (DCr) selvage gradational into dense ore (Cr). Dunite serpentine (D) forms shell next to selvage. From the occurrence illustrated in Figure 9. Scale in inches.

FIGURE 2.—Disseminated ore. Note complex form of individual chromite pieces. Scale in inches.

FIGURE 3.—Disseminated ore. Angular, multigranular chromite pieces in dunite serpentine matrix. Scale in inches.

FIGURE 4.—Disseminated ore with band of solid chromite. Scale in inches.

FIGURE 5.—Disseminated ore, showing mottling produced by differences of size, angularity and packing density of chromite pieces. Scale in inches.

FIGURE 6.—Weathered dunite serpentine with disseminated chromite. Scale in inches.

FIGURE 7.—Weathered dunite serpentine: a specimen rich in chromite occurring in bands. Scale in inches.

FIGURE 8.—Narrow diopside gabbro dike cutting saxonite serpentine in drill core. Scale in inches.

FIGURE 9. Light troctolite dike cutting disseminated ore. In the dike, the light areas are plagioclase and the dark areas olivine and antigorite. Scale in inches.

FIGURE 10. Olivine gabbro dike cutting disseminated ore. Note dark selvages of solid chromite along edges of dike. Scale in inches.

1

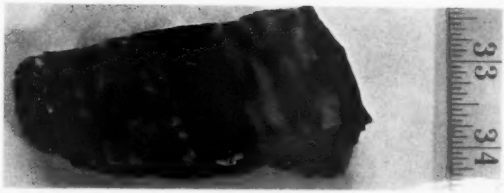

2

3

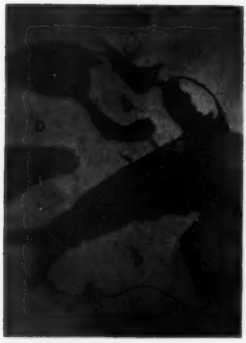

4

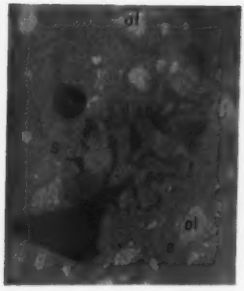

5

6

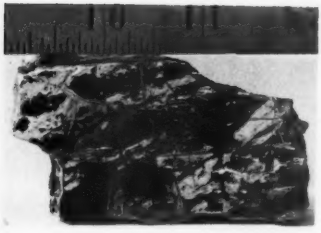

7

8

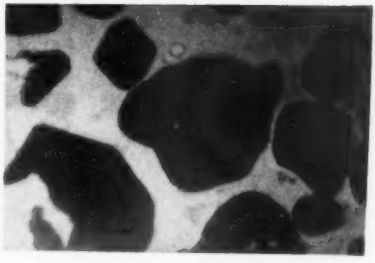

9

TROCTOLITE, OLIVINE GABBRO, ACCESSORY CHROMITE IN SAXONITE BRECCIATED ORES

1

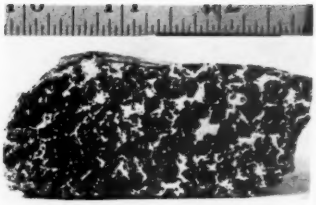

2

3

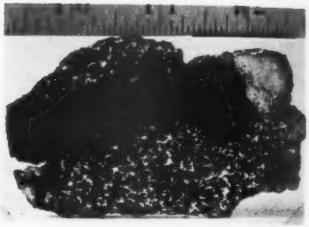

4

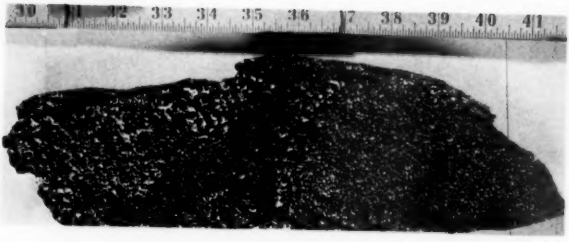

5

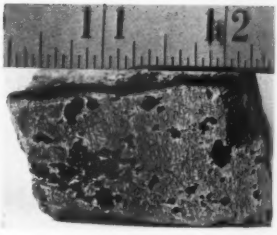

6

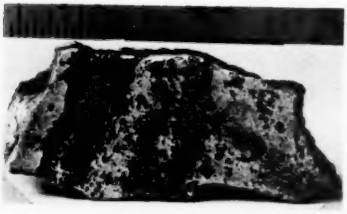

7

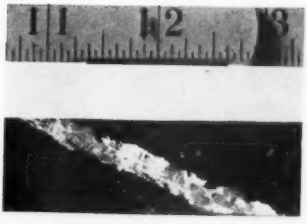

8

9

10

DISSEMINATED ORE, DUNITE, GABBROIC DIKES

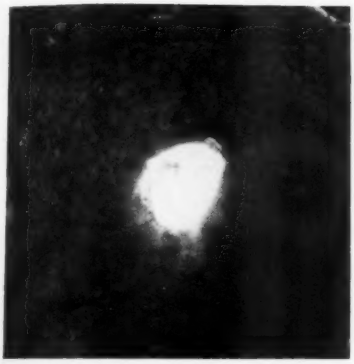

1

2

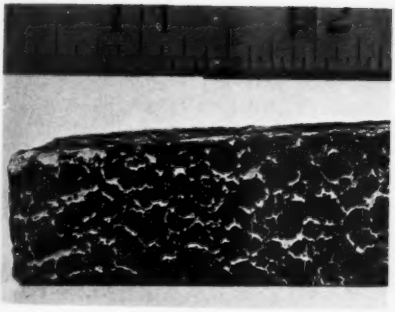

3

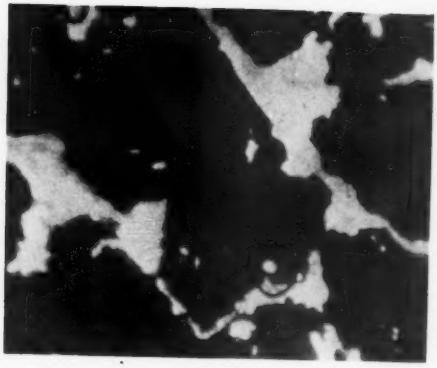

4

5

6

TEXTURES OF DENSE ORE

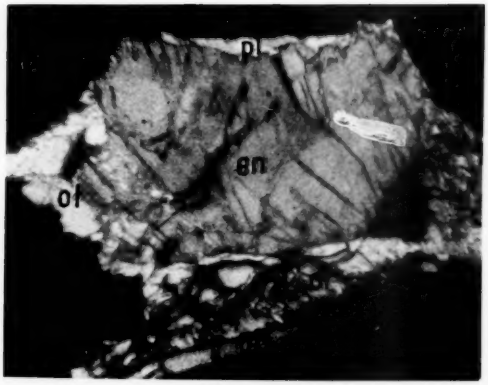

1

2

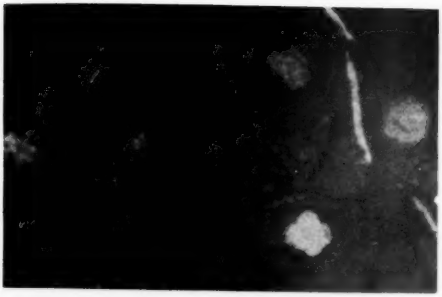

3

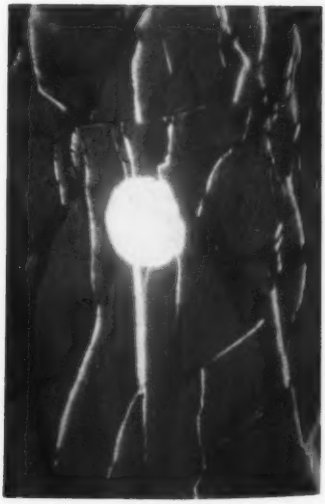

4

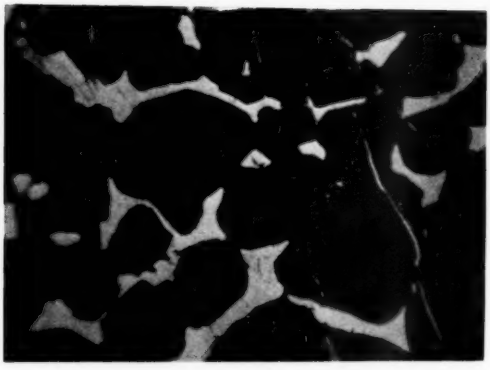

5

TEXTURES OF DENSE AND DISSEMINATED ORES

hedrons where faulting has not occurred. Other joints, closely spaced, are noticeable in some places.

Petrography

Dense ore.—Dense ore is a mixture of chromite with about 2–15 per cent (average 10.75 per cent) by weight of interstitial silicates. It may be classed as (1) massive and (2) brecciated. The gangue is of two kinds: (1) dunite and (2) olivine gabbro, both more or less altered.

The chromite occurs as interlocking grains. On roughly polished surfaces, individual grains are discernible in so far as they reflect light unequally. Seen in thin section, some of the chromite is birifringent because of strain, and the grains have different extinction positions. The alternate illumination and extinction show something of their size and the form of their boundaries. Locally, the chromite is crossed by threads of birefringent silicates outlining polygonal areas that are probably unit grains. They are 1–4 mm across, with an average diameter of 1½–2 mm, tending to be about equidimensional and anhedral or subhedral. In the hundreds of thin sections and hand specimens examined, not one contained a single clearly identifiable octahedron of chromite. The boundaries between grains may be described as "mutual"; most are sinuous, and a few are straight and angular, without marked interpenetration. The hypidiomorphic or allotriomorphic texture and the perfect fit among the individuals composing the mosaic of grains do not accord with the hypothesis of the crystallization and accumulation of the individuals. Mutual interference during growth from many closely spaced nuclei is indicated.

A few grains enclose rounded to euhedral crystals of olivine measuring about 0.2 mm parallel to c and 0.04 to 0.9 mm transversely (Pl. 3, fig 1).

In thin section the chromite is translucent and reddish brown. Invariably it is crossed by a network of fractures, curving and straight (Pl. 3, fig. 2), some of which are slightly open and filled with filaments of secondary silicates. The birefringent character of the chromite in a few places is further evidence of the stress to which it has been subjected. Scanty spots and streaks of secondary magnetite occur especially in the brecciated chromite.

In much ore, it is not evident whether the arrangement of the grains is original or has been slightly disturbed by later movements. In some specimens of massive ore, the distribution, size,

PLATE 3.—TEXTURES OF DENSE ORE

FIGURE 1.—Dense ore. Enclosure of olivine in chromite. No nicols, M-99, 258×.

FIGURE 2.—Dense ore with gangue of secondary minerals. Note cracks in chromite. M-105, no nicols, 18×.

FIGURE 3.—Dense ore from block engulfed in dunite serpentine at edge of main deposit. The chromite tends to occur in discrete grain clusters, but this texture has probably been here accentuated by mechanical disturbance. A rough preferential orientation of the interstices is evident. Scale in inches.

FIGURE 4.—Dense ore with olivine gabbro matrix. The edges of the chromite are ragged at this magnification. M-54, no nicols, 18×.

FIGURE 5.—Dense ore with interstitial plagioclase and enstatite arranged zonally with respect to the interstitial cavity. Note smooth curving edges of chromite. Dark-chromite, pl-plagioclase, en-enstatite. M-107, crossed nicols, 60×.

FIGURE 6.—Dense ore with interstitial plagioclase and enstatite. Rim of plagioclase (pl) lies between chromite (dark) and enstatite (en). Note smooth sinuous outline of chromite. M-54, nicols at 55°, 280×.

PLATE 4.—TEXTURES OF DENSE AND DISSEMINATED ORES

FIGURE 1.—Dense ore showing zoning of enstatite (en), altered olivine (ol), and plagioclase (pl) in interstice. Cr-chromite. M-107, crossed nicols, 59×.

FIGURE 2.—Disseminated ore. The matrix is serpentine and later chlorite. Note cracks, poikilitic texture of chromite, and corrosion effects at edges of chromite pieces. M-117, Lower nicol only, 18×.

FIGURE 3.—Disseminated ore. Poikilitic texture of chromite. The enclosures are olivine and serpentine. M-117, no nicols, 258×.

FIGURE 4.—Disseminated ore. Fractured chromite with black alteration bands and olivine enclosure altered to serpentine. M-98, no nicols, 58×.

FIGURE 5.—Part of a band of dense chromite in disseminated ore. The matrix is serpentine and chlorite. The packing of individual chromite pieces is unusually clearly shown. M-149-2, lower nicol only, 18×.

and shape of the larger interstices suggest that the grains tend to occur in clusters, closely packed, but not so tightly packed as are the individual grains composing a single cluster. The packing of the clusters is ordinarily tight enough to make it impossible to trace the outlines of any single cluster with certainty. The diameters of the clusters may range from several millimeters to about a centimeter, and their form seems to be compact. The boundaries as shown by the edges of the larger interstices are irregular and modified by corrosion. Figure 3 of Plate 3 shows dense ore in which the tendency to form groups is marked but has probably been accentuated by slight mechanical disturbance. A preferred orientation of the larger interstices is evident.

If such grain clusters exist in the undisturbed ore, the following classification of the interspaces can be made:

(A) Original interspaces
  (1) Larger interstices between clusters
  (2) Intragranular and intergranular cavities within clusters
  (3) Poikilitic enclosures within grains
(B) Secondary interspaces
  (4) Interfragmental spaces caused by brecciation and consequent dilation
  (5) Enlargements of pre-existing interspaces of the foregoing kinds through corrosion
  (6) Intergranular filaments occupying spaces formed during slight mechanical disaggregation of the ore
  (7) Transecting filaments caused by slicing
  (8) Veinlets filling cracks caused by local tension

In contact with the matrix, the chromite grains are either ragged (Pl. 3, fig. 4) or rounded. Corrosion embayments are present. In detail, at high magnification, most of the chromite boundaries are smooth. Exceptionally, grains show rectilinear boundaries against the gangue.

Olivine or serpentine is commonly the matrix of massive ore, and olivine gabbro that of the brecciated ore, but in a few places these relations are reversed. Olivine in the dunitic matrix occurs in grains from 0.2 to 0.5 mm in diameter; $2V/Z = 85°–89°$, corresponding to forsterite with 10 mol per cent of fayalite.

The gabbroic gangue consists of labradorite, forsterite, and enstatite in varying proportions, as well as a few grains of clinopyroxene (?). Labradorite (An60–65) forms anhedra 0.5–1.5 mm across, with polysynthetic twinning. Olivine forms clear, colorless rounded grains cut by meshworks of antigorite. A single grain measured has $2V/Z = 84°$, forsterite. Enstatite, much scantier, occurs as anhedral grains, 0.5 to 1.5 mm across, colorless where fresh and altering to talc and penninite. U-measurement gave values of $2V/Z = 76°–84°$, corresponding to 8 mol per cent $FeSiO_3$. $Z = c$, and exsolved lamellae of clinopyroxene occur parallel to the optic plane.

Where the three chief minerals of the olivine gabbro are present in the same thin section, they are in a few places disposed in concentric zones, in the way already described by Thayer (1946, p. 203–205) in ore from La Constancia, Oriente, Cuba. In the Constancia ore, a grain of diopside is replaced by a rim of enstatite, which is in turn replaced by a rim of olivine Next to the olivine and forming a rim against the chromite is anorthite. In two of the Masinloc slides (Pl. 3, figs. 5, 6) the plagioclase occurs as a thin rim next to the chromite, which has smooth, curving boundaries. Adjoining the plagioclase and occupying the central part of the interstitial cavity is enstatite. In another occurrence (Pl. 4, fig. 1) a zone of olivine is interposed between the plagioclase and the enstatite. Clinopyroxene was not observed in the sequence. Both the plagioclase and the olivine zones are discontinuous; the zonal boundaries are smooth and give no clue about the order of crystallization.

The conclusion of Thayer (1946, p. 205) that "these relations are believed to illustrate reaction of chromite rich in spinel with diopside gabbro under suitable conditions to form anorthite and forsterite" applies to the Masinloc occurrence. Similar evidence leading to the same conclusion is found in the mineralogy and texture of several of the narrow olivine gabbro dikes cutting chromite ore.

The zonal arrangement is exceptional. Both enstatite and olivine commonly occur next to chromite without the interposition of plagioclase, and xenomorphic plagioclase occurs commonly as the only gabbroic constituent throughout a single slide. The zoning, determined by special and local factors, appears to prove that reaction took place between chromite and interstitial magma, and that the magma consequently suffered a gradual compositional change while it crystallized.

Among the secondary minerals, the first to form was mesh antigorite replacing olivine. Many of the other secondary minerals, with the

exception of a little contemporaneous magnetite dust, replace serpentine, and none are replaced by it. These are chiefly tremolite, clinochlore, and penninite; tremolite is replaced by clinochlore and clinochlore by penninite. Talc replaces clinochlore and possibly penninite. The other alteration minerals identified are: noble serpentine, dolomite, sepiolite, brucite, chrysotile, fuchsite, kaemmererite (?), actinolite chrome-garnet, and limonite. Their age relations are uncertain.

Noble serpentine occurs as coatings on cracks in the ore. It is pale blue to pale green, soft, and translucent. Microscopically its structure is partly fibrous; the fibers are length slow with extinction angle about 18°. The quantity Ng was estimated as 1.548 and Np as 1.542. An anomalous blue interference color is observed.

Tremolite occurs as euhedral to subhedral grains from 0.04 to 1.1 mm long; $Z \wedge c = 18°$.

Clinochlore occurs in tablets and radial growths of blades. It is colorless. $Ng - Np = 0.007$, which gives it a distinctive white interference color in sections cut across the cleavage; all such sections are length fast. The optic angle is positive and very small. Z is sensibly normal to the cleavage, and $Y = b$. Nm is 1.583.

Most penninite occurs in colorless, fine-grained patches with a bluish-gray interference color and also as micro-veinlets. Coarse, silvery-gray micaceous flakes coating chromite ore are probably also penninite. They are positive with very small $2V$—the acute bisectrix is almost normal to the cleavage. $Nm = 1.584$; birefringence is very low.

Dolomite veinlets a millimeter to several centimeters wide cut the ore. The larger veinlets are coarsely crystalline; $N_0 = 1.684$.

Sepiolite occurs as greenish to white, talclike coatings on ore and as veinlets cutting noble serpentine. A powder examined microscopically showed a microcrystalline to cryptocrystalline felt, partly fibrous and partly granular, with very low birefringence. Some grains of the felt give N between 1.516 and 1.520, and others give N less than 1.516. This corresponds to sepiolite beta, which forms a matrix in which tiny fibrous crusts of sepiolite alpha are scattered. The fibers of sepiolite alpha are length slow, with wavy extinction; $Ng = 1.527$, and $Np = 1.525$.

Brucite, in exceedingly minute flakes, occurs as a minor constituent among the other alteration minerals. Chrysotile forms microscopic, cross-fiber veinlets cutting the ore. Fuchsite, the green chrome mica, is present in very small quantities, and kaemmererite is represented by a few flakes of olive-brown to tan, pleochroic chlorite. Green actinolite occurs as veinlets of coarse-bladed crystals cutting ore.

Emerald-green garnet forms coatings of tiny dodecahedral crystals on fractures in chromite. It is birefringent and shows twinning and growth zoning under the microscope. Quantity N is about 1.765, which indicates a rather low content of chromium.

Disseminated ore.—Seen microscopically, most of the chromite particles are extremely irregular, and their edges are rounded or angular, smooth or ragged, deeply embayed by corrosion. As in dense ore, the chromite is translucent and brownish orange in thin section, is everywhere fractured (Pl. 4, fig. 2), and has poikilitic texture (Pl. 4, fig. 3). Black alteration bands (Pl. 4, fig. 4) and mottlings, probably of magnetite, are more abundant than in dense ore but constitute only a small fraction of 1 per cent of the ore.

Microscopically, the serpentine matrix is nearly colorless where fresh. It was derived *in situ* from olivine; the outlines of the original olivine grains are distinguishable in many places. Olivine itself was not found. The quantity of included magnetite dust is very small. Bastite is absent. The chief hydrothermal minerals are clinochlore and penninite.

Parallel banded ore contains some bands of dense chromite that do not differ texturally from dense ore, either megascopically or microscopically. The existence of bands of differing densities of aggregation, ranging from dense to highly dispersed, shows that all the bands have the same nature: agglomerations of separate chromite pieces more or less closely packed. The densest bands, seen microscopically, are best explained as closely packed aggregates of exceptionally large pieces (Pl. 4, fig. 5).

Dunite serpentine.—Microscopically, the dunite associated with the chromite ore does not appear to differ from that of the dunite member of the ultramafic complex except that chromite is more abundant in the former, and that this chromite is perhaps entirely of the corroded kind that characterizes the disseminated ore. Chromite bands of different densities of aggregation are found in the dunite as well as in the disseminated ore. Where unaltered by chlorite, the dunite serpentine shows a microscopic texture derived from tightly packed, rounded olivine grains.

Dark troctolite.—Melano-troctolite, occurring as dikes cutting the serpentine walls of the deposit, is composed of about two-thirds olivine, most of which is altered to antigorite and mag-

TABLE 4.—CHEMICAL ANALYSES OF

Analyst: Booth, Garrett, and Blair, Philadelphia, Pennsylvania, unless noted otherwise

	(1)	(1a)	(1b)	(2)	(3)	(4)	(5)	(6)	(7)	(8)	(9)	(10)
Cr_2O_3	32.33	32.33	36.1	35.44	35.63	36.34	35.73	35.82	35.35	40.68	38.21	35.36
Al_2O_3	29.38	29.38	31.3	32.31	32.06	31.31	30.69	30.72	32.52	26.05	28.87	31.28
FeO*	13.60	9.70FeO 4.24Fe_2O_3	10.85FeO 4.75Fe_2O_3	13.37	13.36	14.00	13.64	13.64	13.09	16.08	15.27	15.35
MgO	17.93	17.93	17.00	17.42	17.73	16.85	17.85	17.83	18.01	16.22	16.04	16.33
CaO	0.54	0.54	.....	0.14	0.03	0.10	0.04	0.04	0.04	0.08	0.08	0.26
SiO_2	5.06	5.06	.....	1.18	1.02	1.01	1.26	1.33	0.79	0.98	1.32	0.90
	98.84	100.18†	100.0	99.86	99.83	99.61	99.21	99.38	99.80	100.09	99.79	99.48

* Total iron calculated as FeO, unless otherwise indicated

† Including 0.80 per cent combined H_2O and 0.20 per cent Na_2O, calculated

‡ Including TiO_2 0.14 per cent

(1) Average composition of 1,605,867.6 long tons ore, produced 1946–1952

(1a) Analysis (1) recalculated

(1b) Composition of pure chromite in ore, recalculated from analysis (1)

(2) Cleaned laboratory concentrate from sample of dense ore containing unusually little gangue; magnetic fractions removed

(3) Cleaned concentrate from sample of dense ore with unusually large amount of gangue, Bench 1350, magnetic fractions removed

(4) Cleaned concentrate from sample of dense ore with unusually large amount of gangue, second sample, Bench 1060, magnetic portions removed

(5) Cleaned concentrate from sample of dense ore with unusually large amount of gangue, third sample, Bench 1060, magnetic portions removed

(6) Cleaned concentrate from sample of dense ore with unusually large amount of gangue, fourth sample, Bench 1010, magnetic fractions removed

(7) Cleaned concentrate from sample of dense ore containing unusually little gangue, Bench 3

(8) Cleaned concentrate of dense ore from drill core 206, in extreme northeast part of main deposit

(9) Concentrate from dense ore, Hayden deposit

(10) Concentrate from dense ore, Marine Fraction, lower outcrop

netite dust; most of the rest is plagioclase, also altered, but apparently having about the composition of labradorite. Scattered greenish diopside occurs, and a pyroxene occurs scantily as narrow rims on olivine next to plagioclase. Accessory chromite grains occur embedded in olivine and feldspar. Rounded grains of an unidentified accessory opaque mineral, with poikilitic insets of altered olivine, occur in a few places.

Troctolite that forms segregations in dunite and irregular masses in ore has the same composition and texture as the dikes. The secondary minerals observed are chlorite, fuchsite, and hematite.

Olivine gabbro dikes.—The olivine gabbro dikes range from troctolite to diallage gabbro. Those dikes that cut serpentine rock appear to be composed essentially of coarse plagioclase and diallage, with little if any olivine. Reaction effects appear in the dikes cutting ore. Cusps and tiny hooked projections extending from the walls into the dike are effects of corrosion by the dike magma. Next to each wall is a thin rim of secondary minerals, apparently replacing feldspar. Directly inside the rim occurs a second zone, 3–4 mm thick, composed of olivine grains about three quarters of a mm in diameter, with interstitial plagioclase. There are commonly also microscopic shards of chromite, dislodged from the walls. The center part of the dike is coarser and composed chiefly of plagioclase with scattered anhedra of diallage and a few rounded grains of olivine. Enstatite occurs in a few places. The diopside is pale green, $Z \wedge c = 43°$, and $Nm = 1.678$. Some diallage grains possess reaction rims of another pyroxene, apparently enstatite. Pyroxene rims are also seen on some olivine grains.

The alteration is moderate to intense. Among

MASINLOC ORES AND CONCENTRATES

(11)	(12)	(13)	(13a)	(14)	(15)	(16)	(17)	(18)	(19)	(20)	(21)
38.34	36.15	34.81	35.8	33.55	35.76	36.09	35.06	35.77	35.59	36.14	38.89
28.96	33.25	32.35	33.3	33.44	31.67	32.24	31.18	25.85	26.42	29.93	23.04
14.63	19.95	13.52	11.7FeO 2.4Fe_2O_3	13.04	14.04	12.74	15.22	21.95	22.03	16.04	19.18
16.65	12.96	17.79	16.8	18.38	17.11	17.95	16.72	13.97	13.29	16.54	14.21
0.06	0.28	0.07	.....	0.06	0.12	0.04	0.12	0.08	0.04	0.08	0.05
0.85	1.12	1.59	.....	1.53	1.29	1.06	0.87	1.00	1.01	0.90	2.61
99.49	103.71	100.27‡	100.0	100.00	99.99	100.12	99.17	98.62	98.38	99.63	98.98

(11) Concentrate from dense ore, deposit north of Lawis River

(12) Cleaned concentrate of ore fragments in dunite serpentine, magnetic fractions removed, Bench 2. Analyst: Benguet Consolidated Mining Company

(13) Average composition of cleaned concentrates from four representative samples of disseminated ore

(13a) Composition of chromite in disseminated ore, recalculated from analysis (13)

(14) Cleaned concentrates from disseminated ore, magnetic fractions removed, Bench 950

(15) Cleaned concentrate from 3-inch selvage of disseminated ore next to dense ore, magnetic fractions removed, Bench 1320

(16) Cleaned concentrate from dense chromite band in disseminated ore, magnetic fractions removed

(17) Cleaned concentrate from branching chromite veinlets in dunite serpentine, magnetic fractions removed, Bench 1290

(18) Cleaned concentrate from dunite serpentine containing scattered chromite, magnetic fractions removed, Bench 950

(19) Cleaned concentrate from dunite serpentine containing scattered chromite, second sample, Bench 950, magnetic fractions removed

(20) Cleaned concentrate from chromite band or veinlet in dunite serpentine, magnetic fractions removed, Bench 1290

(21) Cleaned concentrate of accessory chromite in saxonite serpentine, Pusoy Bridge, magnetic fractions removed

the secondary minerals are antigorite, talc, penninite, clinochlore, tremolite, fuchsite, and kaemmererite (?).

Chemistry of the Chromite

Chemical analyses were made of Masinloc ores and of concentrates prepared from them in the laboratory, in order to establish the composition of the pure chromite and to investigate variations of composition that might be related to differences of geological occurrence. The analyses and descriptions are given in Table 4. The samples are chromite from dense ore and from disseminated ore in practically all their modes of occurrence and textural varieties, as well as chromite scattered in dunites occurring in the mine, and accessory chromite from the saxonite serpentine country rock. The two most important analyses have been recalculated to express the composition of the chromite. The gangue content of the other samples, shown by the percentages of SiO_2, is small enough to allow the analyses to be compared directly, without recalculation.

Analysis (1), representing the ore mined from 1946 to 1952, is recalculated as shown below. All the CaO and SiO_2 is deducted as labradorite and antigorite, and the remaining constituents, pertaining to chromite, are recalculated to find the percentages of FeO and Fe_2O_3, on the assumption that $RO = R_2O_3$ (Bateman, 1945). The mol fractions of the RO and R_2O_3 constituents are then computed, and the composition of the pure chromite is expressed according to the method devised by Johnston, as described by Thayer (1946, p. 205–206) (Table 5).

The Masinloc chromite, $Cr_{41}Al_{54}(Mg_{74})$, is compositionally about midway between chromian spinel and aluminian chromite and is of the

TABLE 5.—CALCULATION OF COMPOSITION OF CHROMITE IN DENSE ORE

Per Cent

	Cr_2O_3	Al_2O_3	FeO	MgO	SiO_2	CaO	Na_2O	H_2O comb.	Total
Average analysis ore, 1946–1952	32.33	29.38	13.60	17.93	5.06	0.54	(0.20)	(0.80)	99.84
4.36 per cent labradorite An_{60}	.....	1.31	.....	....	2.31	0.54	0.20	....	4.36
6.23 per cent antigorite	.....	.....	.....	2.68	2.75	....	....	0.80	6.23
Balance, in chromite	32.33	28.07	13.60	15.25	0.00	0.00	0.00	0.00	89.25
Chromite recalculated to 100 per cent	36.22	31.46	15.22	17.10	....	....	....	....	100.00
Mols	0.238	0.309	0.212	0.425	..	....	....	....	....

Trivalent: Cr_2O_3 0.238; Al_2O_3 0.309; 0.547

Bivalent: MgO 0.425; FeO 0.122; 0.547

Excess of FeO = 0.212 − 0.122, = 0.090

0.090/3 = 0.030, mols $FeO \cdot Fe_2O_3$

0.030 × 159.70 = per cent Fe_2O_3, = 4.8 per cent

4.8 × (2 × 71.85/159.70) = 4.31 per cent FeO

FeO in chromite is 15.22 − 4.31, = 10.91 per cent FeO

Fe_2O_3 in chromite is 4.8 per cent

	Cr_2O_3	Al_2O_3	Fe_2O_3	FeO	MgO	Total
Recast of chromite, calculated to 100 per cent	36.10	31.30	4.75	10.85	17.00	100.00
Mol fractions,	0.412	0.535	0.053	0.265	0.735	
		1.000		1.000		

Formula of chromite: $Cr_{41}Al_{54}Fe_5$ $(Mg_{74}Fe_{26})$

Norms (per cent): chromite, $(Mg, Fe)O \cdot Cr_2O_3$ 41.2

spinel, $(Mg, Fe)O \cdot Al_2O_3$ 53.5

magnetite, $FeO \cdot Fe_2O_3$ 5.3

100.0

End members (per cent): $MgO \cdot Cr_2O_3$ 20.0

FeO, Cr_2O_3 ..... 21.2

$MgO \cdot Al_2O_3$ 53.5

$FeO \cdot Fe_2O_3$ 5.3

100.0

same type as the chromites of the Caribbean province. It corresponds almost exactly to the average composition of chromites from the larger deposits of the Camagüey district, Cuba, which have the formula $Cr_{40}Al_{55}(Mg_{75})$ (Thayer, 1946, p. 209–214). The Camagüey deposits further resemble the Masinloc ones in that they occur in peridotite forming part of a stratiform complex that includes gabbro and troctolite, and in that they lie close to a serpentine-gabbro contact. They are further characterized, as at Masinloc, by dunite envelopes and by transecting dikes of gabbro and dunite (Flint, de Albear, and Guild, 1948, p. 47–56). A close genetic similarity is therefore surely indicated.

Analyses (2) through (7) and (10) show a close agreement with (1b). Analyses (9) and (11) are from outlying deposits and show a little more Cr_2O_3. Analysis (8) shows an even greater content of Cr_2O_3 and lower content of Al_2O_3. This sample comes from near the main deposit, but its divergent composition suggests that it comes from a separate ore body. The causes of the compositional differences are problematical but probably are related to slight

differences in physical-chemical environment during crystallization.

A recalculation of analysis (13) gives the result $Cr_{41}Al_{55}Fe_3(Mg_{72}Fe_{28})$. The disseminated chromite has, therefore, essentially the same composition, within the limits of sampling error, as the dense chromite. This is sustained by analyses (14) through (17), representing disseminated chromite in several different kinds of occurrence, which, moreover, do not display any significant chemical variation among themselves.

Analysis (18) through (20) represent chromite occurring as scattered grains in dunite associated with ore. Analyses (18) and (19) may indicate a slight substitution of Fe‴ for Al and of Fe″ for Mg; Cr remains constant. The chromite may have become more ferriferous during serpentinization of the rock.

Analysis (21), representing accessory chromite of late crystallization in saxonite country rock, shows differences both in the ratio Cr/Al and Mg/Fe″, compared to ore chromite, but these differences seem small considering the different modes of occurrence.

Genesis of the Rocks and Ores

The area studied is too small to allow drawing definitive conclusions about the genesis of the whole igneous complex. By analogy with similar rocks in other parts of the world, the distinctive pseudostratified norite and olivine gabbro represent two of the great upper zones of a stratiform complex, the basal zones of which are concealed. The exposed ultramafic rocks are partly intrusive into the feldspathic formations. These ultramafic rocks may have originated by the partial refusion and intrusion of the concealed basal zones. They may also have originated at even greater depth, that is, beneath the floor of the complex.

The norites and gabbros, which originally probably lay flat or slightly inclined, were formed by the building up, layer by layer, of crystals showered onto the floor of the magma chamber from the crystallizing magma above. The layers are too uniform and continuous to have been produced by flowage and too numerous and concordant to have arisen through multiple intrusion. There is no sign of metasomatism unless one considers to be such the resemblance of the igneous layering to sedimentary stratification. According to Hess (1938a), the layering is caused by fluctuating currents in the magma, for which there are a number of possible causes. Because of the specific gravity differences among the minerals crystallizing, the currents, from time to time, changed the proportions among the mineral species arriving at the floor. All kinds of bands and sequences could be produced in this way, even while the proportions of minerals crystallizing remained unchanged. The currents that produced the banding may have acted thousands of feet above the floor where crystal sedimentation was taking place.

Minerals that produce gneissosity in norite and olivine gabbro, *i.e.*, olivine and plagioclase, and perhaps also hypersthene, arrived fully crystallized at the floor of the magma chamber. Olivines tended to settle in clusters, and both clusters and individuals came to rest more or less flat. Contrarily clinopyroxene and most of the plagioclase occur in equidimensional grains mutually interlocked, which may indicate that they finished crystallizing *in situ*. The mortar structure in some anorthosites and gabbros may have been caused by the slippage of layers and the internal shifting of grains in the crystal mush, induced by seismic disturbances. Compaction of the crystal mush may also have caused shifting and breaking of grains. The larger folds in the pseudostratification most probably were caused by orogenic forces or by the forcefulness of the intrusion of ultramafic bodies.

Thayer (1942, p. 26–27) believes that some Cuban chrome deposits formed at greater depth and were carried upward to their present positions as solid enclosures in intrusive peridotite. He describes (Holguin district) large xenoliths of old basement rocks in a peridotite mass containing chrome deposits and notes that the deposits and the xenoliths are both distributed haphazardly. Planar and linear structures in the ore bodies are cut off by unfaulted igneous contacts. A similar mode of origin is postulated for the Camagüey deposits (Flint, de Albear, and Guild, 1948, p. 57–59).

At Masinloc, the evidence of the intrusive nature of the saxonitic serpentine in which the ore bodies lie is not conclusive. No enclosures of basement rocks were found, and the dense ore has no banded or linear structure whose relations to the ore contacts could be observed. Nevertheless, many features of the ore occurrence are most plausibly explained in accordance with the genetic ideas of Thayer.

Great buoyant powers of rising magma are inferred by Shand (1951) in his account of the manner of emplacement of a huge inclusion of crystalline limestone, 1 mile by three quarters of a mile, which lies enclosed in a stock, 6

miles square, of nepheline rocks intrusive into the red granite of the Bushveld complex in the district of Sekukuniland, eastern Transvaal. The source of the inclusion is the thick dolomite series of the Transvaal system, which lies beneath the floor of the Bushveld granite lopolith, about 3 miles below the present surface. Such a limestone block, if it were only 100 feet thick, would weigh about 170,000,000 tons. Considering the greater density of peridotite and the comparative smallness of the chromite masses, whose specific gravity is about 3.7, their buoyancy under the conditions postulated seems possible.

Chromite masses borne upward in such a way must have endured bending stresses tending to fracture them intimately and break them into smaller masses having shapes which were mechanically stronger. Pervasive microscopic fracturing is one of the notable features of the Masinloc chromite, while, in contradistinction, the enclosing peridotite shows no special evidence of stress other than jointing. The gross shapes of the bodies of dense ore are such that they would be resistant to bending and torsion. Tabularity might be inherited from an original layered form assumed during the original deposition.

The present distribution of the deposits in a belt lying subparallel to the contact of saxonite with olivine gabbro is regarded as a large-scale flowage phenomenon. The individual deposits are dispersed in a stream line whose direction of flow was partly determined by the wall of the intrusive.

The necessary mobility of the intrusive cannot be explained on the assumption that it was emplaced as a plastic mass of serpentine, because the rock is characterized by a granularity inherited from olivine and enstatite and by relicts of these minerals and must therefore have been serpentinized in place. The petrographic relations between rock minerals and accessory chromite seem to show that the accessory chromite crystallized after emplacement and after the primary fabric had assumed its present character but before serpentinization occurred. The extent to which olivine and pyroxene were already crystallized when intrusion took place cannot be inferred from the petrography. Whatever may have been the exact physical-chemical state of the mass, the geological and petrographical evidence appears to show that the peridotite possessed mass mobility, moderate or high temperature, tenuousness sufficient to penetrate microscopic openings, and a chemically reactive or corrosive effect on chromite. Where the term "magma" is used in connection with peridotite, only these characteristics are implied.

Disseminated ore began to form after the intrusive peridotite and included chromite masses had ceased to move. The different modes of occurrence of disseminated ore are believed to represent different stages of a single genetic process. The disseminated ore selvage and the dunite shell on the margin of a mass of dense ore mark the first stage. They seem to have resulted from the penetration of the surfaces of dense ore masses by enveloping peridotite, acting corrosively while in a heated and tenuous state, and guided in detail by microfractures and grain boundaries of the chromite. The dense ore masses were thus disrupted along their margins. The peridotitic magma became more ultrabasic, through added bases diffusing outward from the reaction surfaces where chromite was dissolving. Reaction took place and reached equilibrium, and crystallization occurred *in situ*, undisturbed by mass movement of the reaction products. The thickness of the reaction zone was determined principally by the range over which diffusion of substance was effective. The crystallized products of reaction are disseminated ore and dunite serpentine, disposed in natural zones parallel to and adjoining the dense ore contact.

Reaction between disseminated chromite and its matrix is manifested by the corrosion embayments that characterize the chromite. During reaction, the peridotitic material received such increments of MgO and FeO as ultimately to suppress the crystallization of pyroxene. In this connection, the absence of pyroxene and bastite in the gangue of disseminated ore will be recalled. The added Al_2O_3 permitted the eventual crystallization of plagioclase, limited in quantity by the low CaO and Na_2O in the system. Equilibrium was reached when the peridotitic material had received sufficient bases to become dunitic or troctolitic. The practical identity of chemical composition and petrographic character between dense and disseminated chromite shows that it did not change greatly. Its reaction may have been limited to simple dissolution.

Ordinarily the reaction products migrated and crystallized away from the reaction surface where they had formed. Fluidity and flowage are indicated by banding in disseminated ore and dunite and by dikes of disseminated ore, dunite (?), and melano-troctolite in and near the ore deposit. Fluidal movement may have been caused by slight shiftings and fracturings

of the dense ore masses as they settled more firmly in their bed of newly solidified peridotite. The migration of reaction products would have exposed the ore surfaces to renewed reaction. It would also have given rise to further mixing of dunitic material with chromite and to further size reduction of the chromite pieces through abrasion and impact. The large bodies of disseminated, partly banded ore are probably accumulations of migrated mixed material, localized by contacts, fractures, and other features now impossible to trace. Gravitative separation may have taken place in such migrated bodies after mass motion had almost ceased and before complete solidification supervened.

In all these larger bodies of disseminated ore, chromite crystals are absent, and there is no basis for supposing that chromite crystallized in them. The opposite is true: chromite dissolved and disintegrated.

The existence of disseminated ore and dunite in separate bodies may be explained by the natural zoning that occurred at reaction contacts, as well as by incompleteness of mixing during flowage and by local gravitational settling.

Some of the melano-troctolite near the ore deposits is a fraction of the dunite. The lower crystallization temperature of plagioclase allowed residual magma to accumulate. Minor movements or unequal compaction in the dunite may have caused the residuum to mobilize, forming troctolite segregations in dunite, and to migrate farther, forming pockets and dikes in the near-by ore and country rock.

The subangular blocks of ore enclosed in dunite serpentine near the edges, especially the lower edge, of the main deposit, seem to have broken off when the dunitic shell had not wholly crystallized and fluidal flow around the fragments was still possible. Reaction zones failed to form perhaps because the shell had already become saturated with bases, and therefore dunitic, through prior reactions. The rounding of the ore fragments shows, on the other hand, that the enveloping dunitic material effected some disaggregation of the ore along its contacts and dispersal of the ore particles.

The chrome ore bodies are thus envisaged as giant xenoliths, and the associated rocks and disseminated ores as reaction products generated and crystallized in an essentially closed system. Reactions would have gone on, however, during the entire time of contact between chromite and peridotitic magma and would have been limited by the magnitude of the surfaces of interaction and by the removal or nonremoval of the products. The removal and dispersal of the reaction products must have been favored by immersion in and motion through the intrusive mass during irruption into higher horizons. The accumulation of the products next to the dense ore masses could only have taken place after these masses had attained rest because of the advanced stage of crystallization of the peridotite. In such a state, a large, compact ore mass may have retained much of its heat and may have acted as a local heat source tending to maintain an envelope of peridotite as magma, after the rest of it had solidified. If this is true, the extent of the reactions would have been further limited by falling temperature and by saturation of the small available quantity of magma. The migrations of fluid reaction products would have been restricted to the proximity of their place of origin.

The apparent correlation in dense ore between brecciation and the presence of a gabbroic type of gangue, as well as the existence of similar dikes cutting the ore, may indicate that gabbroic magma was injected from external sources, but the association of gabbroic dikes and matrices with chromite bodies of the Cuban or Masinloc type is general and possibly can be better explained by the hypothesis that the gabbro is the original gangue that accompanied the ore at the time of its crystallization in greater depth.

As the chromite masses were enveloped and carried upward in the intrusive body this feldspathic matrix melted but was partly retained because of the dense texture of the ore. In so far as it escaped, it would have escaped from the superficial parts of each chromite mass, and its place would have been taken by inward-penetrating peridotitic magma, which, reacting with chromite, became dunitic. In this way it is possible to explain the presence in dense ore of both gabbroic and dunitic gangue materials.

The refusion of the matrix recommenced chemical reaction between it and the chromite. Fluidity and reactivity of the matrix persisted well after the chromite bodies had come to rest and after disseminated ore and dunite had been formed. At such a late stage, the ore and its walls were fractured slightly, and part of the interstitial liquid was squeezed into the fractures, where it crystallized as gabbro, olivine gabbro, and leuco-troctolite dikes, slowly and with continuing reaction, simultaneously with

the crystallization of the magma remaining in the ore interstices.

Inequilibrium and a tendency toward equilibrium between dense chromite and the dikes and ore matrix composed of gabbro are evidenced by corrosion of chromite and by zoning of the minerals in the matrix. The reaction tended to transform gabbroic into troctolitic magma. The dissolution of chromite continuously enriched the magma in Al, Cr, Mg, and Fe, with the result that the species of femic mineral crystallizing became successively more magnesian. The composition of the plagioclase, however, must have been determined by the original Ca and Na contents of the magma. Although much of the Al, Mg, and Fe supplied by chromite could probably be accounted for in plagioclase and olivine, the destiny of the Cr is not so evident. Thayer (1946, p. 204–205, 207) believes that reaction between chromite and gabbroic magma in Cuban ores resulted in the enrichment of the chromite in Cr, in accord with the hypothesis of Bowen (1928, p. 279–281). At Masinloc, this may also have occurred, but the gangue is so scanty compared to the chromite that it is doubtful that any but the smallest changes in chromite composition could have resulted. If chromite was notably enriched in Cr through reaction with magma, that enrichment must have occurred elsewhere than at the present site of the ore bodies. The presence of fuchsite, kaemmererite, and uvarovite among the secondary minerals indicates the final destination of some of the chromium.

The gabbroic magma in the ore interstices and dikes must have cooled and crystallized slowly, since the tendency to equilibrium is evident. The comparatively coarse grain, despite the smallness of these bodies, indicates the same thing. The great mass of chromite, compared to the scantiness of the gangue, and the wide dispersion of the gangue in the chromite are factors that must have favored rapid heat loss by the matrix if the chromite had been cool. During crystallization of the matrix, the temperature of the chromite masses may therefore have been near the temperature range of crystallization of gabbro.

The direction of the two reactions in which chromite participated, with gabbro and with peridotite, shows that the ore was in chemical harmony with dunitic and troctolitic magmas, but not with those containing modal pyroxene. It might therefore be supposed that the ore crystallized from a magma of a composition near forsterite-anorthite and that it subsequently underwent a change of environment. The high Al and Mg contents of the ore indicate that it crystallized from a magma rich in those elements. Thayer (1946, p. 206–217) points to the dependence of chromite composition on that of the mother magma, as well as to its sensitivity to later environmental change. He indicates (p. 206) that the Camagüey ores may have crystallized from a troctolitic magma, and this is also postulated in the present case.

The conditions attending crystallization of the dense chromite ores in depth may be inferred from the ore texture and composition. The compact xenomorphic-granular texture would signify that chromite crystallized from crowded nuclei whose growth was mutually interfering. Such a result might have been produced by the crystallization of a magma very rich in the constituents of chromite, in much the manner proposed by Bateman (1951), to explain the formation of some oxide ores. The form and distribution of the ore interstices suggest, however, that the dense ores are densely packed agglomerations of multigranular clusters. All the textural features as well as the composition of the chromite and of the gabbroic interstitial material seem best explained in accordance with Bowen's (1928, p. 277–281) theories about the formation of spinel in ultrabasic rocks and its subsequent conversion to chromite. Bowen refers especially to the equilibrium relations in the artificial system anorthite-forsterite-silica, in which spinel appears as a transient phase, but he asserts also the existence of such a spinel region in any liquid that can precipitate olivine and basic plagioclase. Osborn and Tait (1952) have since shown that a spinel field exists in the system diopside-forsterite-anorthite.

The magma composition would have been near the anorthite-forsterite binary limit (and hence troctolitic), since the spinel region lies near this limit. Tiny euhedral olivine enclosures in chromite might have been the first crystals to form and thus possibly indicate that the magma composition lay on the forsterite side of the spinel field. Spinel (containing the available Cr in ionic substitution for Al) would have formed by the transformation of glomeroporphyritic clusters of early olivine and basic plagioclase crystals through reaction with hotter, deeper magma saturated with forsterite. Upon cooling of the system below the lowest temperature of the spinel field, the reverse reaction would have commenced: the liquid would have reacted with spinel to form olivine and plagioclase, with the concomittant enrich-

ment of the remaining spinel in Cr, through abstraction of the other spinel constituents, to form chromite. By the settling and concentration of clusters of chromite, olivine, and plagioclase during the time when monoclinic pyroxene was beginning to precipitate, and by the consequent local exhaustion of the supply of liquid necessary to effect total dissolution of the chromite, a compact deposit of grain clusters, having much the same mineral composition as the present dense ore, may have formed and persisted, while the remaining mother magma finished crystallizing.

At a much later time, these primitive deposits were, by hypothesis, heated and disrupted and carried upward as inclusions in intrusive peridotite. The temperatures then prevailing were sufficiently high to fuse the olivine-gabbro constituents in part, thus commencing anew the same reactions between chromite and liquid that had been earlier interrupted.

The chromite deposits and enclosing peridotite may have originated deep within the same ultramafic complex in which they now occur, or at a still deeper horizon, beneath the base of the complex. If it is assumed that peridotite forms in the first instance always as an accumulative rock, the theoretical difficulties of forming a heated mass mobile enough to move as an intrusion would seem to be about as formidable in one place as in the other. Nonetheless, peridotite intrusives do occur. In the following, the first possibility is explored.

Hess (1938b) describes dunite crystallized from secondary magma formed by the refusion of peridotite near the base of the Stillwater Complex. The dunite occurs as small dikes and pipes intruding harzburgite formed by crystal setting. It consists of coarse olivine, some serpentine, accessory chromite, and secondary magnetite and chlorite. Hess ascribes the generation of the magma to a sinking of the base of the complex, with a consequent rise in temperature to the melting point of serpentine, the lowest melting fraction of the peridotite. Later experimental work by Bowen and Tuttle (1949) shows that no serpentine magma can exist below a temperature of 1000° C., and its existence in nature is thus in doubt.

Heating and disruption of the ultrabasic zones of the Zambales complex may have been caused by a sinking into regions of higher temperature or from a rise of the isogeotherms incident to orogeny. The disaggregation of the rocks may have been aided by their lack of interlocking texture—a consequence of origin through crystal accumulation. Mobility must be attributed to the presence of a fluid phase, partly H_2O, and this might have arisen through partial fusion or through additions of substance from below. Orogenic forces may have compelled the mobilization and irruption into higher levels of the complex of bodies composed partly of olivine and enstatite crystals, the powerful mass ascent carrying with it blocks of ore broken from such parts of the primitive deposits as happened to lie in the region affected by disruption, or which lay in the path of ascent of the intrusive.

It is surmised that chromite originally accumulated as stratiform or lenticular bodies in a zone of predominantly olivine and plagioclase rocks, transitional in position and in composition between the basal ultramafic zones and the upper feldspathic zones of the complex. Such a zone would represent, like the other great zones of a layered complex, a stage in the course of magmatic crystallization (Hess, 1938a). The localization of chromite in this zone would have resulted from a unique concurrence of certain physical and chemical conditions characteristic of the transitional stage. Perhaps it is at this middle stage that the magma attains the troctolitic composition necessary to the precipitation of transient spinel in quantity. The occurrence and genesis of the primitive deposits may well have been much the same as described by Smith (1953) for the chrome bodies of the Bay of Islands, Newfoundland.

The small compositional differences among the chromites from different bodies at Masinloc presumably indicate that the differing bodies originated at different horizons within the transitional zone. If this is true, then differences in chromite composition from place to place in the mine can be attributed to occurrence in physically separate masses, even though these may lie very close together.

Certain geological and petrographic facts do not fit into, or have not been fitted into, the genetic conception outlined in the foregoing: (1) the rare occurrence of pyroxene bands in the saxonite, (2) the occurrence of gabbroic, melano-troctolitic, and dunitic intrusive bodies at places remote from known chrome deposits, and (3) the apparent association of gabbroic gangue with brecciation of dense chromite.

References Cited

Bateman, A. M., 1951, The formation of late magmatic oxide ores: Econ. Geology, v. 46 p. 404–426

Bateman, J. D., 1945, Composition of the Bird River chromite, Am. Mineralogist, v. 30, p. 597–598

Bowen, N. L., 1928, The evolution of the igneous rocks: Princeton, N. J., Princeton Univ. Press, 334 p. (reprinted 1956 by Dover Pubs., Inc., N. Y.)

Bowen, N. L., and Tuttle, O. F., 1949, The system MgO-SiO_2-H_2O: Geol, Soc. America Bull., v. 60, p. 439–460

Corby, Grant W., *et al.*, 1951, Geology and oil possibilities of the Philippines: Philippines Dept. Agric. & Nat. Res. Tech. B. 21, 363 p.

Flicano, V., 1926, Chromite deposits in the Philippines: Tokyo, Third Pan Pacific Sci. Cong. Proc. v. 2, p. 1753–1754

Flint, D. E., de Albear, J. F., and Guild, P. W., 1948, Geology and chromite deposits of the Camagüey district, Camagüey province, Cuba: U. S. Geol. Survey Bull. 954-B, p. 39–63

Hess, H. H., 1938a, Primary banding in norite and gabbro: Am. Geophys. Union Trans., p. 264–268

—— 1938b, A primary peridotite magma: Am. Jour. Sci., v. 35, p. 321–344

Osborne, E. F., and Tait, D. B., 1952, The system diopside-forsterite-anorthite: Am. Jour. Sci., Bowen Volume, Pt. 2, p. 413–433

Shand, S. J., 1951, Eruptive rocks: N. Y., John Wiley & Sons, 488 p.

Smith, Charles H., 1953, Origin of the chromite deposits of the Bay of Islands, Newfoundland: Econ. Geology, v. 48, p. 408–415

Thayer, T. P., 1942, Chrome resources of Cuba: U. S. Geol. Survey Bull. 935-A, p. 1–74

—— 1946, Preliminary chemical correlation of chromite with the containing rocks, Econ. Geology, v. 41, p. 202–217

Van Bemmelen, R. W., 1949, The geology of Indonesia: vol. IA: The Hague, Govt. Printing Office, 732 p.

Viamonte 1133, Buenos Aires, Argentina

Manuscript Received by the Secretary of the Society, March 1, 1957

BULLETIN OF THE GEOLOGICAL SOCIETY OF AMERICA
VOL. 69, PP. 449-464 3 FIGS., 2 PLS. APRIL 1958

TEXTURAL AND SPECTROCHEMICAL STUDIES OF THE WHITE TANK QUARTZ MONZONITE, CALIFORNIA

BY JOHN J. W. ROGERS

ABSTRACT

Magmatic crystallization of the White Tank quartz monzonite, California, has produced two sequences of differentiation. One sequence is marked by an increase in the size of potassium feldspar crystals and an increase in the Ab/An ratio of the plagioclase from the older toward the younger rocks. The second sequence is marked by an increase in the Ab/An ratio of the plagioclase from the older toward the younger rocks and by the presence of primary muscovite and garnet in the younger rocks.

Textures vary with position in the intrusions. Quartz forms aggregates of several grains except near the margins of the intrusions, where it occurs as individual grains. Large potassium feldspar crystals that formed late in the first differentiation sequence are gray, grid-twinned, and commonly intergrown with sodic plagioclase; the earlier-crystallizing grains are pink, poorly twinned, and exhibit no such intergrowth. The more calcic plagioclase grains are zoned and imperfectly twinned, whereas the more sodic grains are twinned and poorly zoned. Biotite and most accessory minerals occur in aggregates, but sphene is scattered through the rock.

In the first differentiation sequence the amounts of lead and possibly strontium in the potassium feldspar decrease from older to younger rocks, and the amounts of barium and rubidium remain constant. In the second sequence, the amounts of barium, lead, and strontium in the potassium feldspar decrease during differentiation, and the amount of rubidium is constant.

CONTENTS

TEXT

	Page
Introduction and acknowledgments	449
Relationship of White Tank quartz monzonite to country rocks	451
Methods of study	452
Field study	452
Petrographic study	452
Spectrochemical study	452
Description of units	454
Unit 1	454
Unit 2	458
Unit 3	459
Unit 4	460
Differentiation and origin of White Tank quartz monzonite	461
Evidence for magmatic differentiation	461
Sequence 1; Units 1 and 4	461
Sequence 2; Units 2 and 3	461
Spectrochemical study of potassium feldspar in the White Tank quartz monzonite	463
References cited	464

ILLUSTRATIONS

Figure	Page
1. Index map	450
2. Quality of exposures and field evidence of differentiation in Unit 1	455
3. Diagrammatic sketch of typical intergrowth of microcline and plagioclase	456
Plate	**Facing page**
1. Textural varieties of quartz	456
2. Textures in the White Tank quartz monzonite	457

TABLES

Table	Page
1. Lines measured in spectrochemical analysis for the various elements	453
2. Modal analyses of samples from Unit 1	456
3. Modal analyses of samples from Units 2 and 3	460
4. Modal analyses of samples from Unit 4	460
5. Trace-element content of potassium feldspar	462
6. Locations of samples used in spectrochemical analysis	463

INTRODUCTION AND ACKNOWLEDGMENTS

The portion of Joshua Tree National Monument just south of Twentynine Palms, California, consists of a plutonic assemblage of igneous and metamorphic rocks. The area (Fig. 1) is approximately 125 miles east of Los Angeles, California. The geology of the area was described by Miller (1938).

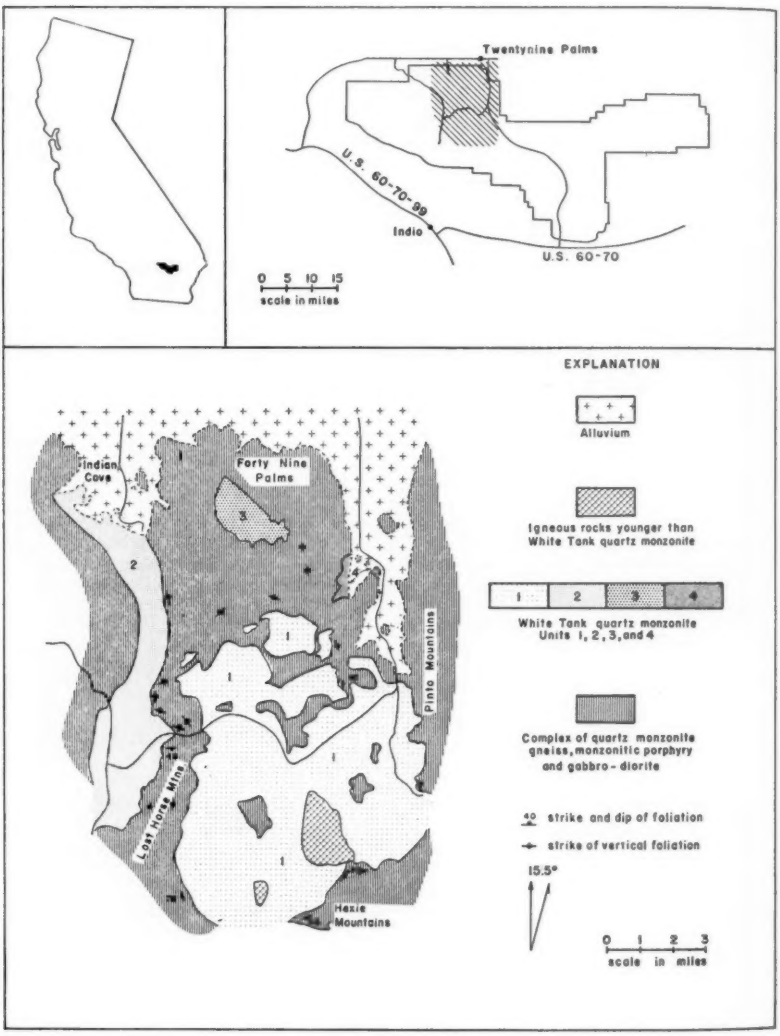

FIGURE 1.—INDEX MAP

The upper part shows the location of Joshua Tree National Monument and the area studied (shaded). The shaded area is shown in the lower map, in which the various units of the White Tank quartz monzonite have been delineated.

The White Tank quartz monzonite (White Tank monzonite) is the youngest major intrusion near Twentynine Palms. The formation (probably Jurassic) crops out in four bodies, each of which is characterized by a quartz monzonite slightly different from that in the other bodies. Variations within the two largest intrusive masses provide evidence of gravitative differentiation within individual intrusions. Field, petrographic, and spectrochemical studies of these variations have been made, with emphasis on the textures and on the trace-element content of the potassium feldspar.

The geology of the area near Twentynine Palms, California, is described by Miller (1938). The geology of western Joshua Tree National

Monument is described by Rogers (in press); the writer has also published a summary and geologic map of part of the area (Rogers, 1954). Vertical variation in individual bodies of silicic to intermediate rocks has been noted by Sargent (1925) and Van Biljon (1939). Spectrochemical studies of variations in trace-element content through igneous differentiation sequences are described by Nockolds and Allen (1953) and Nockolds and Mitchell (1948).

The present paper describes field evidence of variations in and among the quartz monzonite bodies, the textures associated with the different types of quartz monzonite, and the spectrochemical variations of the potassium feldspar.

The work summarized in this paper was done from June 1953 to August 1954 and constituted part of a Ph.D. thesis project at the California Institute of Technology. The writer expresses his thanks to Dr. Ian Campbell, who supervised the project, and to Drs. H. S. Brown, J. P. Buwalda, A. E. J. Engel, D. F. Hewett, R. H. Jahns, T. H. McCulloh, J. A. Noble, and L. C. Pray. Aid with the spectrochemical study was given by Mr. A. Chodos, Mr. B. Ewing, and Dr. L. T. Silver. Dr. C. Croneis helpfully criticized the manuscript. The writer is grateful to the staff of Joshua Tree National Monument for permission to work in the Monument and for assistance in the field.

Relationship of White Tank Quartz Monzonite to Country Rocks

The White Tank quartz monzonite intrudes an igneous and metamorphic complex of quartz monzonite, gneiss, monzonitic porphyry, and small, scattered patches of gabbro-diorite. The bulk of this complex is gneiss and quartz monzonite. The gneiss is well foliated and consists of quartz, plagioclase (albite to andesine), and biotite. The quartz monzonite ranges from fine-grained and equigranular to coarse-grained and inequigranular and consists of approximately equal amounts of quartz, potassium feldspar, and plagioclase (oligoclase), with biotite and other accessory minerals. A monzonitic porphyry with large potassium feldspar crystals occurs along some gneiss and quartz monzonite contacts. Small bodies of gabbro-diorite, consisting for the most part of plagioclase (andesine to labradorite) and hornblende, are scattered throughout the complex. Though the units which constitute the complex are generally distinguishable, in many places the contacts are gradational, and the rock units are not easily recognized.

Structures within the igneous and metamorphic complex exhibit a north to northwesterly trend throughout much of the western portion of Joshua Tree National Monument. The gneiss is well foliated, and some of the quartz monzonite exhibits a foliation parallel to that of the neighboring gneiss. Large areas of quartz monzonitic rocks, however, are apparently structureless.

The White Tank quartz monzonite differs markedly in structural properties and border relationships from the rocks in the older igneous and metamorphic complex. Contacts of the quartz monzonite with its wall rocks are abrupt, as opposed to the gradational contacts between rock units within the complex. In contrast to the foliated appearance of much of the older complex, the bodies of White Tank quartz monzonite are commonly massive.

The White Tank quartz monzonite occurs as four separate bodies, designated as Units 1 to 4 (Fig. 1). These bodies are apparently isolated from each other by the older rocks of the igneous and metamorphic complex; no two of the quartz monzonite bodies are in contact, and all four probably represent distinct intrusions. In most places contacts of the quartz monzonite with the older rocks are slightly curved in broad outline, and the outcrop of Unit 1 is nearly circular. The scattered remnants of roof rock which overlie a horizontal surface on the northern part of the outcrop of Unit 1 indicate that the upper surface of the unit is probably nearly flat; similarly, the nearly horizontal contact between Unit 2 and the igneous and metamorphic complex which overlies the western part of the unit indicates that Unit 2 also has a nearly flat upper surface. The eastern edge of Unit 2 is roughly vertical through approximately 1000 feet from the lowest exposed rock (at the north of the outcrop) to the flat upper surface. Contacts of quartz monzonite and its wall rocks are also vertical on the sides of the Lost Horse, Hexie, and Pinto mountains, but the relief along the contact in these areas is only 100–200 feet. Since none of the intrusions exhibits a floor, the three-dimensional shape of the quartz monzonite bodies has not been determined.

In detail the bodies of the White Tank quartz monzonite cut discordantly across structures in the wall rocks. Only in broad outlines is there any indication that foliation in the wall rocks (the igneous and metamorphic complex) is deformed in relation to the White Tank quartz

monzonite. Some foliation trends in the wall rocks near the intrusions are warped out of the normal northwesterly trend into positions more nearly parallel to the contact with the quartz monzonite (Fig. 1). Other than this slight indication of a relationship between broad structures in the wall rocks and position of the intrusive bodies, no evidence has been found that the quartz monzonite has had any appreciable effect upon the country rocks. Contact metamorphism is apparently absent, and the abrupt contacts between quartz monzonite and wall rocks afford no evidence of assimilation of country rock.

Compositionally the White Tank quartz monzonite consists of roughly equal parts of quartz, potassium feldspar, and plagioclase, with minor amounts of biotite and accessory minerals. Modal compositions of samples from the different units are shown in Tables 2–4.

The White Tank quartz monzonite is the youngest major intrusive rock in the area. Aplite and pegmatite dikes cut the quartz monzonite and presumably are a late-stage phase of the intrusive activity. Younger rocks in the area consist of a granodiorite sill or dike, some silicic and basic dikes, and minor extrusive basalt.

Methods of Study

Field Study

Mapping was done on aerial photographs (scale approximately 3000 feet to 1 inch) obtained from the U. S. Air Force, Photographic Records and Services Division. The photographs covered part of the Pine Knot area. Maps were compiled from these photographs and a horizontal control obtained from maps prepared by the U. S. Land Office.

Estimates of the grain size and percentage of potassium feldspar in Unit 1 were made in the field as well as petrographically. The average sizes of potassium feldspar grains were obtained by measuring the maximum dimension of 25 or 50 grains as exposed on the outcrop. Percentages were determined by a rapid point count made by laying a ruler along a series of parallel lines and counting the grains under the half-inch marks; these percentages are shown in Table 2 as "field measurements of the per cent of potassium feldspar". These measurements are only approximations because of the irregularity of the rock surface and the large amount of albitic plagioclase intergrown with the potassium feldspar in the upper part of Unit 1.

Petrographic Study

In some thin sections quantitative data on composition and texture were needed. Mineral percentages were determined by a point count of 1000–1500 points. The average grain size of each mineral was determined by measuring the maximum diameter of 25 grains of the mineral as shown in the section. The number used to represent the grain size of a mineral was the average of these 25 measurements (or fewer if insufficient numbers of grains were available).

The composition of the plagioclase in most rocks was determined by the Michel-Levy method. In specimens of particular importance, these compositions were checked by measurement of indices of refraction in immersion oils. The composition of untwinned plagioclase was determined by index of refraction measurements where possible.

Spectrochemical Study

Determinations of trace-element content were made on 24 potassium feldspar samples. The first five specimens analyzed (numbers 37, 83, 90, 127, and 133) constituted a preliminary study to determine the best procedure and to discover the degree of correspondence between different parts of a hand specimen. Each rock sample was broken into two parts, and the separate pieces were prepared and analyzed individually to determine the variation within one hand specimen. All these specimens had been sawed for thin sections before the writer anticipated using them for trace-element analysis, and it was feared that the sectioning process might have introduced some contamination. Comparison of results from sectioned and nonsectioned samples from the same part of the rock indicates that sectioning has little effect on the purity of the potassium feldspar. All sections showed less than 5 per cent alteration (kaolinization) (estimated) of the potassium feldspar.

These five rocks were first broken into centimeter-sized fragments by pounding with a hammer on a steel plate. The samples were crushed in a diamond mortar, and clean cleavage flakes of potassium feldspar were picked out under a binocular microscope. These grains were crushed again in a diamond mortar, sieved through a silk screen to remove all material finer than 200 mesh, and passed through a Frantz Electromagnetic Separator (Model 506). The separator was set for 1.6 amperes and a 10-degree forward and a 10-degree side tilt. Biotite and muscovite were removed by the separator.

An examination, in index oils, of the samples at this stage of preparation showed that samples 83, 90, and 127 had an estimated plagioclase contamination of not more than 10 per cent; sample 133, which originally contained the lowest proportion of potassium feldspar, had about 25 per cent plagioclase; sample 37 was entirely perthitic microcline. Biotite was absent or extremely rare.

The samples were mixed with an equal weight of iron quartz, which is otherwise pure quartz containing 2 per cent ferric oxide by weight. Twenty-five mgm duplicates of each sample were then placed in one-quarter inch pure graphite electrodes

and were analyzed with the following exposure conditions:

Spectrograph: Jarrell-Ash 21 foot diffraction grating instrument with a dispersion of 5.2 Å/mm in the first order

Excitation: 15 amperes DC arc; sample as the anode; 4 mm analytical gap magnified 5 times and focused on the slit. Central 2 mm used with a slit width of 25 microns

Wave-length range: 2300–4800 Å, first order

Plates: Eastman-Kodak III-C developed at 20°C. for 4 minutes in DK-50

Densitometer: Applied Research Laboratory (ARL) model No. 2250

Each plate of 10 (duplicate) unknown samples was calibrated by measuring iron lines of known intensities in four pegmatite standards, burned last visible alkali volatilization with the following exposure conditions:

Spectrograph: Same as for other elements

Excitation: Same as for other elements; red filter added

Wave-length range: 6100–8700 Å, first order

Plates: Eastman-Kodak I-L

Densitometer: Same as for other elements

In all burns the bead was lost by its popping out of the electrode after visible alkali volatilization had ceased. Standards from 0.000012 per cent to 1.0 per cent of each alkali were burned on each plate and provided the calibration for determining the concentration of alkalies in the unknown.

Table 1 shows the lines measured in analyzing for the various elements.

Although the spectrographic procedure was

TABLE 1.—LINES MEASURED IN SPECTROCHEMICAL ANALYSIS FOR THE VARIOUS ELEMENTS

Element	Wave length(s)
Barium	3072, 4554 Å
Calcium	3159, 3179
Copper	3274
Gallium	2943
Lead	2833
Lithium	6104, 6708
Manganese	2801
Rubidium	7800, 7948
Strontium	3464, 4607
Titanium	3349
Vanadium	3184
Ytterbium	3289
Yttrium	3242
Zirconium	3273, 3392

2 at the top of the plate and 2 at the bottom. Measured intensities of the various lines of other elements in the unknown samples were converted to concentrations of the elements from standard curves, already prepared by Mr. A. Chodos of the California Institute of Technology Geology Department for the spectrograph and densitometer used. Lines so dense that they showed less than 5 per cent transmission were measured by clocking the time for the densitometer to scan through the range below 5 per cent and comparing with the time to scan the standard Fe 4405 Å line in the pegmatite standards.

Analysis for the alkali elements was made on samples prepared by mixing 90 per cent feldspar and 10 per cent Specpure sodium carbonate. Duplicate 25 mgm samples were burned for 5 seconds past the identical for all samples, the methods used in preparing the last 19 samples were different from those used with the first 5. The change was made partly to compare the two procedures by analyzing samples from the same part of the rock by each method and partly in the hope that the second method would yield purer samples.

Specimens 14, 102, 169, 356, 358, 502, 503, 504, 505, 506, 507, 508, 509, 510, 512, and 513 were not prepared in duplicate samples from different parts of the hand specimen. Instead, the whole specimen was ground in a rotating mill set to pass 0.2 mm fragments, and the powder was then treated as one unit. The next step was a screening out (with a silk screen) of all powder less than 200-mesh size. The remaining powder was then placed in a tetrabromoethane-acetone mixture of specific gravity 2.60, which just floated the perthitic potassium feldspar

and allowed sodic plagioclase to sink. The first separation was made in a beaker, and material which floated in it was decanted into a separatory funnel where the final separation was made. Investigation of the light material in immersion oils showed that it was almost entirely (greater than 99 per cent) perthitic potassium feldspar for all samples. This separate was then passed through the Frantz Separator and, finally, was hand-cleaned under a binocular microscope to remove the last traces of dark impurity. After this procedure, most of the remaining contaminants were plagioclase and quartz.

The pegmatite samples 49, 388, and 501, were prepared by hand picking the feldspar cleavage fragments. The analyzed samples were entirely perthite.

The elements of major importance in the present study are barium, lead, rubidium, and strontium. Other elements such as ferro-alloy materials, vanadium, titanium, and copper were probably introduced during preparation and analysis of the samples. Zirconium is undoubtedly introduced by small grains of zircon. Calcium and part of the strontium are probably present in the plagioclase part of the perthite or in plagioclase contamination. Ytterbium, yttrium, and possibly manganese reported in the analyses may be accounted for by the presence of biotite.

Trace-element concentrations of all samples are listed in Table 5 and are reported only to one significant figure except in cases where the measured value is midway between two figures (e.g., 150). The correspondence between two parts of a hand specimen may be seen by comparing the *A* and *B* parts of specimens 37, 83, 90, 127, and 133 listed in Table 5. Analysis of samples from the same parts of the quartz monzonite prepared by two different methods (which yielded different degrees of purity) also gave very similar results, as may be seen by comparing samples 83 and 513, samples 90 and 502, and samples 127, 504, and 510 in Table 5. It is believed that a difference in composition of more than 1 in the first figure for most elements signifies a true difference in composition.

Description of Units

Unit 1

Unit 1 of the White Tank quartz monzonite is exposed on a level surface in the northern part of the outcrop area and along a broad slope extending from the middle of the outcrop down to the lowest exposed rock, at the southernmost contact. Assuming that the present level surface in the rock was level (at least in a north-south direction) during crystallization, this slope provides 1000 feet of relief within the unit and permits the detection of vertical lithologic variations. The ground surface also slopes down to the east from the central part of the outcrop area, and the rocks at the eastern and southern contacts are at approximately the same elevation. Scattered patches of roof rock overlying the northern part of the outcrop area indicate that the White Tank quartz monzonite exposed there is really the uppermost part of the intrusion.

A vertical variation in Unit 1 is marked by an increase in the size and a change of color of the potassium feldspar grains from the presumed lower part to the presumed upper part. The lower part of the intrusion, which consists for the most part of equigranular quartz monzonite, is exposed at the southern part of the unit. A presumed transitional rock, which appears to be texturally intermediate between the lower and upper parts of the intrusion, crops out on the eastern edge of Unit 1. The upper part of the intrusion, which consists of porphyritic quartz monzonite, is exposed in the northern part of the unit (Fig. 2).

The writer believes that the different rock types in the well-exposed areas of Unit 1 represent different parts of a lithologic sequence which is gradational from the lower part to the top of a single intrusion. The three textural varieties may possibly represent genetically related rocks from separate intrusions that were not identifiable in the field. However, the quartz monzonite on the eastern edge of Unit 1 is texturally intermediate between the rocks in the other two areas of outcrop within the unit. If Unit 1 has been tilted slightly (less than 5°) east-northeastward, this intermediate quartz monzonite would have been originally at a level between the base and top of the intrusion and thus could readily be a part of a vertical lithologic variation formed by differentiation in one intrusive body. Furthermore the potassium feldspar in the well-exposed quartz monzonite in the northern part of Unit 1 is predominantly gray. Within this area, however, the feldspar crystals become smaller and gradually change from gray to pink toward the south. Consequently, the quartz monzonite in the upper part of Unit 1 appears to grade downward into rock types characteristic of other parts of the unit.

The uniformity of the rocks anywhere along a given level in Unit 1 indicates that the principal variation is vertical. Lateral change in both composition and texture occurs only within a few hundred feet of the borders of the intrusion and can generally be distinguished from the vertical change by tracing the variation horizontally away from the contact.

A number of vertical changes may be detected in Unit 1 on the basis of the following:

(1) Hornblende occurs only in the lower part of the intrusion.

(2) Upward in the intrusion the average maximum diameter of potassium feldspar grains increases from 3 mm to 8 mm; the color changes from pink to gray; and the amount of grid twinning increases. Complex intergrowths with sodic plagioclase are absent in the lower part of the unit but common in the upper part.

(3) Upward in the unit the average composition of plagioclase changes from An_{30} to An_{18}, and the crystals change from zoned and poorly twinned to well twinned and either unzoned or faintly zoned.

(4) Upward in the unit the size of biotite grains decreases from 1 mm to 0.25 mm, and the grains become more irregular.

(5) Extensive staining by ferric oxide appears only in the uppermost part.

In addition, the percentage of potassium feldspar may be smaller lower in the intrusion than near the top. This possibility is indicated both by field and micrometric measurements, but neither set of data is conclusive. The percentage of biotite may be greater in the lower part of the intrusion than it is near the top. Because the altered, highly irregular biotite grains in rocks from near the top of the intrusion are more easily removed from thin sections during grinding than are the well-

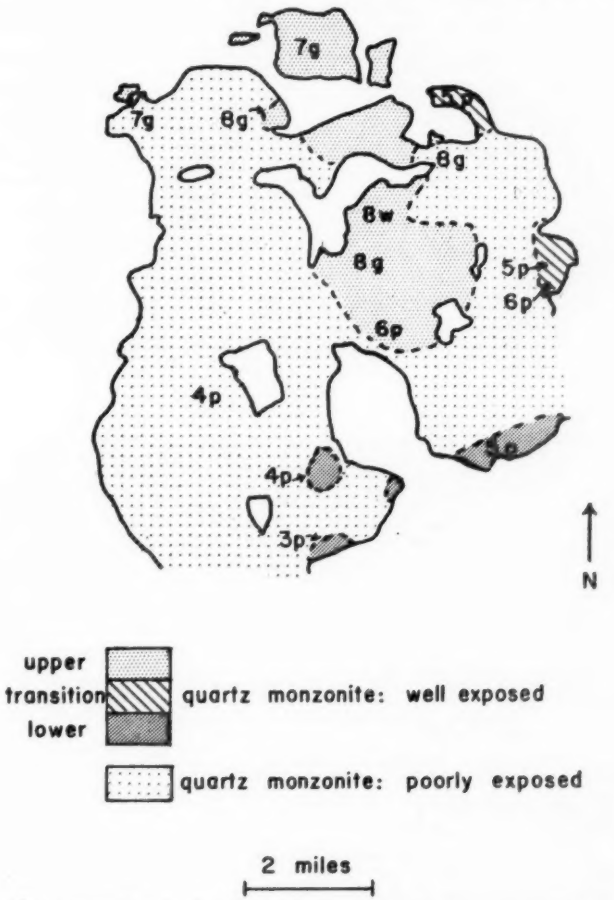

FIGURE 2.—QUALITY OF EXPOSURES AND FIELD EVIDENCE OF DIFFERENTIATION IN UNIT 1
Numbers refer to grain size of potassium feldspar (average maximum dimension in mm) as measured in the field. Letters denote color of the potassium feldspar: p = pink, w = white, g = gray.

formed crystals near the base, the apparent variation in biotite content cannot be considered unequivocal.

No vertical variations have been detected in the amount or texture of the quartz, and no variation in the amount of plagioclase or the nature of the accessory minerals has been definitely proven.

Horizontal variations in the quartz monzonite in Unit 1 occur only near some contacts. Toward the margin the quartz occurs in small, individual grains rather than in aggregates of coarse, undulatory, sutured grains. Also, the sizes of both plagioclase and potassium feldspar grains decrease toward some contacts with wall rocks.

TABLE 2.—MODAL ANALYSES (IN VOLUME PERCENTAGES) OF SAMPLES FROM UNIT 1

	Samples								
	Lower Part of Unit			Transitional Rock			Upper Part of Unit		
Minerals	43*	224*	506*	90*	704*	708*	85†	127†	205*
quartz	16.7	23.4	22.8	19.3	25.8	21.7	17.6	19.6	20.9
potassium feldspar	25.6	23.0	15.8	60.0	32.2	34.6	13.1	38.3	43.3
plagioclase	48.4	45.3	50.3	19.2	40.8	41.7	57.2	35.6	31.2
biotite	8.2	7.8	10.2	1.0	0.7	1.2	1.8	5.8	4.1
hornblende	0.2	trace							
accessory	0.8	0.4	0.9	0.4	0.4	0.9	3.8	0.7	0.5
epidote							6.5		
total points counted	938	1350	1091	1014	1138	1280	1169	1116	1000
field measurement of per cent of potassium feldspar				30	30	30	40	40	40

* Pink potassium feldspar
† Gray potassium feldspar

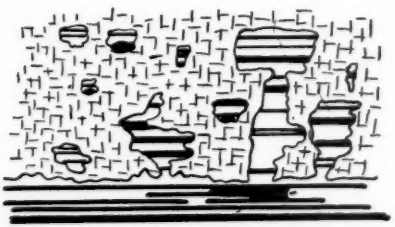

FIGURE 3.—DIAGRAMMATIC SKETCH OF TYPICAL INTERGROWTH OF MICROCLINE AND PLAGIOCLASE

In the lower part of Unit 1 (Table 2); the quartz monzonite is light brown to light gray, massive, medium-to coarse-grained, and equigranular.

Nearly all the quartz occurs in aggregates of 10 to 20 undulatory, fretted grains (similar to the grains shown in Figure 1 of Plate 1); each grain averages 1–1.5 mm across but some are as large as 6 mm. Contacts between two quartz grains are sutured, but contacts between quartz and feldspar are not. Some of the quartz (generally less than one-fourth) is in individual, interstitial grains anhedral against feldspar. These interstitial grains are not sutured and generally have a diameter of less than 1 mm.

Most of the potassium feldspar is untwinned, but some microcline twinning forms patches and narrow bands. All grains are anhedral, irregular, and have an average dimension of 3 mm with a maximum of

PLATE 1.—TEXTURAL VARIETIES OF QUARTZ

FIGURE 1.—Aggregate of undulatory quartz grains in Unit 2. Crossed nicols, ×25

FIGURE 2.—Fine-grained quartz monzonite showing interstitial quartz grains a few feet from contact with gneiss. Crossed nicols, ×25.

FIGURE 1

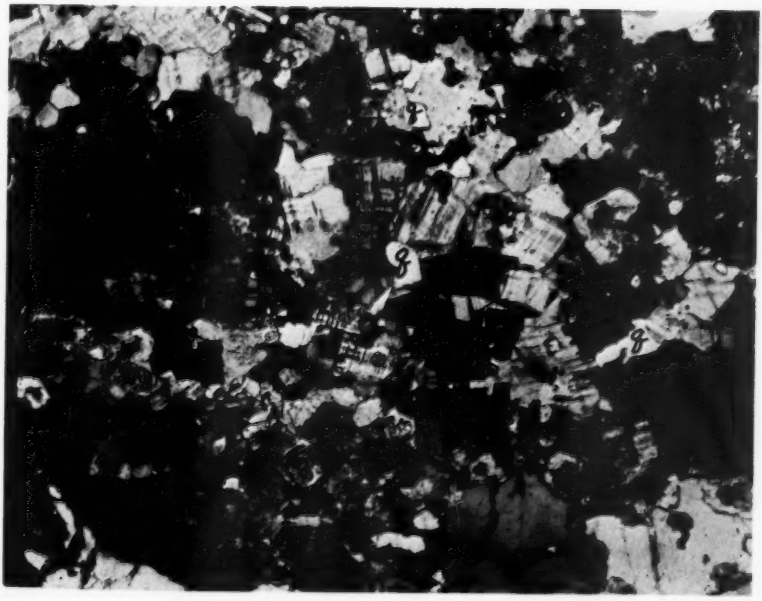

FIGURE 2

TEXTURAL VARIETIES OF QUARTZ

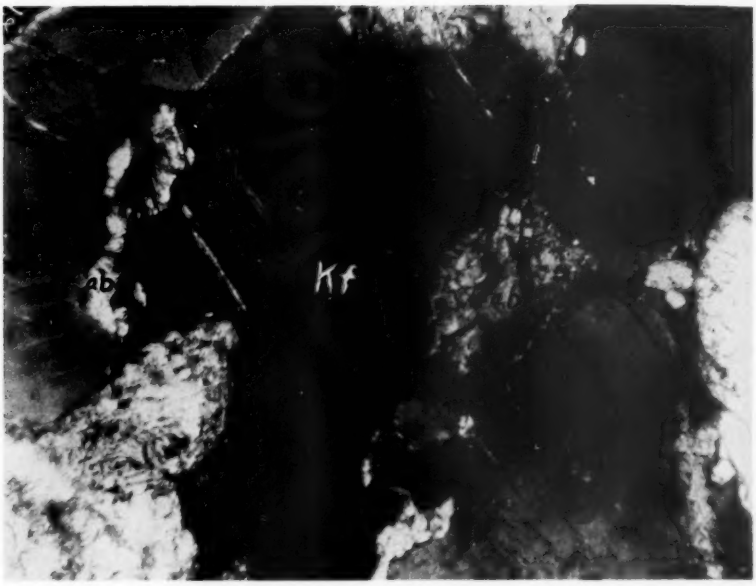

FIGURE 1

FIGURE 2

TEXTURES IN THE WHITE TANK QUARTZ MONZONITE

10 mm. Vein and rod perthite are uncommon. Some of the larger feldspar grains are poikilitic, and the common inclusions are plagioclase.

Subhedral laths of plagioclase have an average length of 2 mm and a maximum of 10 mm. Most grains are slightly zoned (An_{35} in the center to An_{20} at the rim) and show some oscillation. Grains which show the strongest zoning are generally untwinned; conversely, the twinned grains are unzoned. Twinning generally follows the albite law. A few grains are twinned according to the pericline law; these are more common in the lower part of Unit 1 than in other parts of the quartz monzonite.

A few plagioclase grains are rimmed by albite in optical continuity with the cores. These rims are sharply distinct from the rest of the grain and commonly occur only at the border between plagioclase and potassium feldspar (see Tuttle, 1952, for further discussion). Some rims are myrmekitic, and the quartz blebs are oriented across the rim and normal to the grain borders. Less commonly, myrmekite occurs in the large laths of plagioclase where they border potassium feldspar; in such cases the quartz blebs do not show any morphologic orientation, although some are optically oriented.

Biotite forms flakes approximately 1 mm long. It is pleochroic from yellow to brown, but chloritization and possibly other alterations make color determination difficult. The biotite commonly occurs in aggregates of several grains.

The principal accessory mineral is magnetite, but apatite, zircon, and sphene are also present. All the zircon is included in biotite, where it forms small pleochroic halos. Magnetite and apatite are also concentrated either as inclusions in the biotite or as separate grains associated with the biotitic aggregates. Sphene, however, is scattered through the rock. The accessory minerals are euhedral and much smaller than the essential minerals.

Some sections from the lowest part of Unit 1 contain a few small grains of common hornblende, pleochroic from yellow to blue green.

The plagioclase, especially in the centers of zoned grains, has been altered to sericite and epidote, and perhaps to some calcite. Some irregularly shaped epidote grains scattered through the rock may be primary. Kaolin is lightly scattered over both types of feldspar.

In the transitional part of Unit 1 (along the eastern edge of the unit) the quartz monzonite is inequigranular. The rock is light brown and massive, and the pink potassium feldspar grains are slightly larger than the other minerals.

The quartz occurs primarily in aggregates of undulatory, fretted, 1- to 2-mm grains. Small interstitial grains, present near the center of the intrusion, become increasingly abundant near the contact with the wall rocks. Within a few feet of the contact, all the quartz is interstitial, and the aggregates are absent (Pl. 1, fig. 2).

Potassium feldspar forms pink, anhedral grains with an average diameter of 5–6 mm. Almost all the grains exhibit grid twinning.

Most of the plagioclase occurs as either twinned or zoned subhedral grains. The average composition is An_{20}, which is intermediate between the compositions of the plagioclase in the upper and lower parts of Unit 1; the average size is 1.5 mm. A small amount of fine-grained, apparently pure albite forms textures similar to those in the lower part of the unit.

Biotite forms irregular grains pleochroic from yellow to brown. Most grains are highly altered.

Accessory minerals include zircon, apatite, magnetite, sphene, and allanite. The zircon, apatite, and magnetite generally form aggregates with the biotite flakes.

Plagioclase has been partly altered to sericite, and both plagioclase and potassium feldspar are slightly altered to kaolin.

Grain sizes of the major minerals increase inward from the contact through a zone up to 500 feet wide. Ten feet from the contact, quartz and both feldspars have average diameters of 1 mm.

In the upper part of Unit 1 (in the northern part of the unit) the quartz monzonite is porphyritic. The rock is gray, massive, and coarse-grained. About 30–40 per cent of the quartz monzonite consists of gray subhedral potassium feldspar crystals with an average maximum dimension of 8 mm. Some of the potassium feldspar grains show several zones, the outer one commonly being white. Toward the lower (southern) part of the outcrop, the gray color gradually changes through pinkish gray to bright pink.

Nearly all the quartz in the rock forms aggregates of undulatory, fretted, 2-mm grains.

The most characteristic textural feature of the large gray potassium feldspar crystals is the irregular, optically oriented intergrowths of microcline and sodic plagioclase (calcic albite or sodic oligoclase) (Fig. 3). Many of the gray "potassium feldspar" phenocrysts are approximately one-fourth albite. The border between the two feldspars is commonly irregular in detail, and many isolated patches of plagioclase with the same orientation as

PLATE 2.—TEXTURES IN THE WHITE TANK QUARTZ MONZONITE

FIGURE 1.—Albite around border of potassium feldspar in Unit 2. Crossed nicols, ×65

FIGURE 2.—Typical section of Unit 3. Major minerals are quartz (q), microcline (mi), plagioclase (p) muscovite (mu), and garnet (g). Crossed nicols, ×25.

the large grains occur throughout the microcline. The twin directions in these separate plagioclase grains are parallel to each other, but individual twin lamellae are not continuous from one patch to another. They are generally continuous over similar distances in the large, separate plagioclase laths. The lack of continuity of plagioclase twin lamellae, plus the fact that no plagioclase grains in the associated rock are as large as the gray microcline grains, suggest that the intergrowths did not form by replacement of plagioclase by microcline.

Some microcline grains also contain small inclusions of plagioclase which, though bearing common orientation, show no constant relationship to the orientation of the potassium feldspar.

In the top of the outcrop the outer parts of some potassium feldspar crystals exhibit graphic intergrowths with some small quartz grains. The transition between graphic and nongraphic parts of the feldspar grain is generally sharp and in some cases marks the border between two zones of slightly different optical orientation.

Plagioclase occurs in three textures. A little less than half the plagioclase is calcic albite-sodic oligoclase intergrown with potassium feldspar as described above. Another large fraction of the plagioclase consists of subhedral laths with a length of 1–2 mm and a composition of An_{15}. Almost all the laths are well twinned on the albite law, and most are unzoned or only slightly zoned. A very small amount of apparently pure albite forms either small rims optically continuous with adjoining, more calcic, plagioclase laths or occurs as tiny, irregular, interstitial grains (similar to the texture shown in Figure 1 of Plate 2). Textural features of the pure albite are similar to those in the lower part of Unit 1. Almost all the albite is in contact with potassium feldspar, and myrmekite is common in both types of albite.

Biotite in the upper part of the quartz monzonite forms small (0.25 mm-long), partly chloritized, ragged flakes, pleochroic from yellow to brown.

Accessory minerals consist of magnetite (altered to ferric oxide), apatite, sphene, zircon (which forms pleochroic halos in the biotite), and allanite. The biotite and accessory minerals, with the exception of sphene, commonly form aggregates.

The plagioclase has been altered to sericite, epidote, and perhaps some calcite. Some irregular epidote grains scattered through the rock bear no obvious relation to the plagioclase and may be primary. Kaolin is scattered in slight amounts over both plagioclase and potassium feldspar.

The uppermost rock in Unit 1 (a small cupola in the northern part of the outcrop) is extensively stained by ferruginous material which is not present in other parts of the rock.

Modal analyses of 9 samples from Unit 1 appear in Table 2.

Unit 2

The quartz monzonite in Unit 2 crops out on a relatively horizontal surface throughout most of its extent. At the northernmost edge of the unit, a moderately abrupt mountain front (vertical relief 1000 feet) exposes a section from the upper surface of the main body of quartz monzonite down to the lowest exposed rock of the unit.

Throughout most of the vertical range of Unit 2 no textural or compositional variation could be observed. The only variation occurs in the uppermost part of the unit, next to the wall rock along the northern part of the eastern edge of the outcrop. For approximately 2 miles along this part of the eastern contact, a marginal zone up to 200 feet wide is characterized by white potassium feldspar, highly albitic plagioclase, primary muscovite, and garnet. The rock in this eastern margin grades into the main part of Unit 2, and the variation may be either a lateral change away from the contact or a vertical differentiation.

The differences between the eastern margin of Unit 2 and the main part of the unit are: potassium feldspar is pink throughout Unit 2 except in the eastern margin, where it is white; plagioclase laths are zoned from about An_{30} at the center to An_{20} at the rim throughout most of Unit 2, but in the eastern margin the plagioclase is only slightly zoned and has an average composition of An_{15} to An_{10}; garnet and megascopic flakes of muscovite (apparently primary) are restricted to the eastern margin.

No difference between the modal compositions of the main part of Unit 2 and the eastern margin have been demonstrated, except for the presence of garnet and coarse muscovite in the margin.

The main body of quartz monzonite in Unit 2 is brown, medium-grained, equigranular, and massive.

Quartz occurs in aggregates of undulatory, fretted, 1- to 2-mm grains (Pl. 1, fig. 1). Some grains are interstitial to feldspars. In some potassium feldspar grains, thin quartz stringers follow cleavages or cut across the grains; some stringers are in optical continuity with adjoining quartz grains.

Most of the potassium feldspar is untwinned, but some borders and thin bands through the grains show grid twinning. Both vein and rod perthite are present but uncommon. The grains are anhedral to subhedral and have an average length of 5–6 mm. Inclusions of quartz in potassium feldspar have an

average diameter of 0.25 mm (which is smaller than the quartz grains in the rest of the rock), whereas inclusions of plagioclase average 1.5 mm long (the average size for plagioclase laths in the whole rock).

Most of the plagioclase forms subhedral laths 1.5 mm long. Many grains are zoned from An_{40} ni the center to An_{20} at the rim. Albite twinning is present except in the most strongly zoned grains. Some zoned grains are twinned at the edges but not in the center. Some of the plagioclase laths are rimmed by albite where they are in contact with potassium feldspar; small, irregular grains of albite (Pl. 2, fig. 1) are scattered throughout the rock, commonly near potassium feldspar. Inclusions of quartz in potassium feldspar are, in some places, rimmed by albite. Most myrmekite is restricted to albitic rims around plagioclase laths, but some of the laths are also myrmekitic.

Biotite forms flakes about 0.5–1 mm long. It is pleochroic from yellow to dark brown; some slightly greenish flakes probably result from slight alteration.

Magnetite, zircon, and sphene are accessory minerals. Zircon is generally included in the biotite as small pleochroic halos. Magnetite and biotite are commonly clustered together in aggregates of several grains.

Sericitization is intense in all plagioclase except albite and is especially concentrated in the more calcic parts of the zoned grains. Some of the white mica may be primary. Kaolin is scattered in small amounts over both feldspars. A little chlorite penetrates biotite in patches along the biotite cleavage.

The quartz monzonite in the eastern margin is tan to light gray, massive, medium-grained, and equigranular. It is distinguished from the main part of Unit 2 by its content of megascopic flakes of muscovite and scattered red garnets, the white color of the potassium feldspar, and the highly sodic composition of the plagioclase.

As in most of the quartz monzonite, quartz occurs primarily in aggregates of undulatory, fretted grains, each grain 1–2 mm in diameter. Some quartz forms individual, interstitial grains about 0.5 mm long.

Most of the potassium feldspar is untwinned, but small areas in some grains show microcline twinning. The feldspar contains rare vein perthite and no other type. Individual grains of potassium feldspar are anhedral, roughly equant, and have an average diameter of 5–6 mm.

Plagioclase forms subhedral laths having an average length of 1.5–2 mm. All grains are twinned on the albite law, and a few show a very faint, normal (?) zoning. The average composition is An_{10} to An_{15}. In addition to these large plagioclase laths, small rims of albite form textures similar to those in the rest of Unit 2.

Biotite forms ragged, thoroughly altered flakes 0.5–1 mm long.

Magnetite, sphene, zircon, and possibly some epidote are the accessory minerals. Garnet is so rare that it is unlikely to occur in thin section, but it can be identified in hand specimens. The garnet is presumed to be spessartite on the basis of its deep red to orange color and its alteration to a black powder (manganese oxide?).

Except for the pure albite, plagioclase is altered to sericite or muscovite, some of which forms flakes up to 0.5 mm long. Most books of white mica, however, bear no relation to other minerals and seem to be primary. Kaolin is lightly scattered through both feldspars.

Modal analyses of samples from Unit 2 appear in Table 3.

Unit 3

The White Tank quartz monzonite in Unit 3 is very similar to the micaceous eastern margin of Unit 2 but contains more muscovite and garnet and a more highly sodic plagioclase than the margin. Except for a fine-grained mixture of quartz and feldspar (about 10 per cent of the rock) in samples at the abrupt southern contact with the igneous and metamorphic complex, the quartz monzonite in Unit 3 apparently does not vary. The lack of relief in the area of exposure, however, prevents detection of any vertical variation. Modal analyses of three samples of Unit 3 are shown in Table 3, and a typical section is illustrated in Figure 2 of Plate 2.

All quartz forms individual, interstitial grains with an average diameter of 1.5 mm. The grains are slightly undulatory and are fretted in contacts with other quartz grains but not in contacts with feldspar.

All the potassium feldspar is twinned microcline. It occurs as white, anhedral, somewhat equant grains too small to be measured accurately in the field. In section, the average maximum dimension is 2 mm. Rod perthite is absent, but a little vein perthite occurs in most grains.

Plagioclase forms anhedral, lath-shaped grains with an average length of 1.5 mm. It is twinned on the albite law, unzoned, and has a composition of An_{03}. No rims or small grains of albite are present. Myrmekite is absent. Despite their highly sodic nature, the plagioclase grains are almost identical in shape, size, and other textural features to more calcic grains in other bodies of the quartz monzonite.

Muscovite forms flakes having an average length of 1 mm. A small amount seems to have formed by alteration of plagioclase, but most of it occurs as large flakes showing no relation to plagioclase and is almost certainly primary. A brown alteration product has formed along some cleavage planes.

Garnet forms euhedral, equant grains with an average diameter of 0.5 mm. Magnetite and apatite are rare; some small grains included in muscovite may be magnetite.

Both feldspars are slightly altered to kaolin.

Potassium feldspar grains are gray, have an average length of 10 mm, and are twinned in some parts. Vein perthite is abundant, but rod perthite is absent.

Plagioclase forms subhedral laths having an

TABLE 3.—MODAL ANALYSES (IN VOLUME PERCENTAGES) OF SAMPLES FROM UNITS 2 AND 3

	Samples								
	Main Part of Unit 2			Eastern Margin of Unit 2			Unit 3		
Minerals	6	13	25	170	171	193	356	357	359
quartz	39.4	26.3	32.0	29.9	25.7	44.3	39.8	33.8	30.8
potassium feldspar	20.2	32.1	23.2	24.2	22.5	26.3	21.5	19.8	22.7
plagioclase	38.0	40.7	40.5	45.1	51.0	24.7	31.4	38.2	40.6
biotite	2.3	0.7	4.1	0.4	0.4	2.2	0.2		
muscovite				0.4		2.2	6.7	7.2	5.7
accessory	0.3	0.2	0.3		0.3	0.4			
garnet							0.5	1.0	0.3
total points counted	1082	1215	1140	1272	1145	1299	1129	1134	1178

TABLE 4.—MODAL ANALYSES (IN VOLUME PERCENTAGES) OF SAMPLES FROM UNIT 4

	Samples	
Minerals	75	78
quartz	32.7	36.2
potassium feldspar	30.4	38.4
plagioclase	32.8	24.1
biotite	3.2	1.4
accessory	0.9	0.1
total points counted	1196	1139

Unit 4

Unit 4 includes a group of small, lithologically identical, bodies which crop out at approximately the same elevation. On the basis of its high content of coarse, gray, potassium feldspar crystals, Unit 4 appears to be closely related to the upper facies of Unit 1. Modal analyses of two samples of Unit 4 are shown in Table 4.

Throughout the unit, quartz forms aggregates of undulatory, fretted grains, each grain having a diameter of about 2 mm. Inclusions of quartz in potassium feldspar are much smaller than the quartz in these aggregates. Thin layers of fine-grained quartz follow the border between some feldspar crystals.

average length of 1.5 mm. All the laths are twinned on the albite law, are unzoned (or very faintly zoned), and have a composition of An_{25}. On the basis of relative relief, plagioclase in the perthite seems to have the same composition as the laths. One section contains an intergrowth between plagioclase (apparently An_{25}) and microline similar to the intergrowths in the upper facies of Unit 1.

Albitic rims around the plagioclase laths are most common near potassium feldspar and are best developed on inclusions in the microcline. Some rims are myrmekitic. Small irregular grains of albite are also mixed with the fine-grained quartz along some intergranular borders.

Biotite forms ragged flakes, which are pleochroic from yellow to brown and highly altered. Some chloritization has occurred. Magnetite, sphene, and zircon are rare accessory minerals.

White mica is an uncommon alteration of plagio-

clase and also forms veinlets in both feldspars; some of this mica may be primary. Kaolin forms a light dusting in both feldspars.

The fine-grained quartz and albite (and a small amount of the potassium feldspar) in Unit 4 constitute a groundmass which makes up approximately one-fifth of the rock. This groundmass is absent from all but the border zones of other units of the quartz monzonite.

Differentiation and Origin of White Tank Quartz Monzonite

Evidence for Magmatic Differentiation

On the basis of texture and mineralogy, the different parts of the White Tank quartz monzonite can be arranged into two sequences of differentiation. One sequence is exhibited by Units 1 and 4, the other by Units 2 and 3. The writer believes the variations have been caused by magmatic differentiation of an intruded melt of quartz monzonitic composition.

The vertical variation in Unit 1 (the upper part of which is similar to Unit 4) is readily explainable by gravitative settling of the early crystallizing constituents of a quartz monzonitic magma. This process is outlined in the description of Sequence 1. The correspondence between observed variations and variations expected from magmatic processes is an indication (though not proof) of magmatic origin.

The textural and compositional variations within and among the quartz monzonite bodies seem more indicative of magmatic processes than of granitization. If conditions in an area are such that physical-chemical equilibrium is maintained only by the conversion of large bodies of rock to quartz monzonite, it seems likely that conditions will not vary sufficiently over short distances to permit the formation of markedly different textures and compositions, either in the same unit or in different units. The crystallization of magmas, however, is almost certainly accompanied by changes in temperature, pressure, and composition from place to place in the intrusion. Consequently, the writer feels that magmatic differentiation accounts for the variations in the White Tank quartz monzonite more readily than does any process of granitization. The reasons for the differences between the sequences are not known.

Sequence 1; Units 1 and 4

Vertical differentiation in Unit 1 can be ascribed to early crystallization and gravitative settling of andesine, hornblende, and possibly biotite.

Except for the higher anorthite content of its plagioclase laths and the presence of a quartz-albite groundmass, Unit 4 is similar to the upper part of Unit 1. Both rocks are characterized by an abundance of coarse gray crystals of microcline. Possibly Unit 4 originated from an offshoot of differentiated magma from the upper part of Unit 1. The fine-grained groundmass in Unit 4 may indicate more rapid cooling of the small volume of Unit 4 as opposed to the relatively slow cooling of the larger volume of Unit 1.

Sequence 1 shows evidence of an increase in the water content of the residual magma during differentiation. The presence of separate crystals of both potassium feldspar and highly albitic plagioclase in the differentiated rock indicates crystallization from a probably highly fluid solution. (The relationships between potassium feldspar and albite in the presence or absence of water are discussed by Bowen and Tuttle, 1950.) Also the coarse grains of the potassium feldspar may be attributed to crystallization from a water-rich melt; for example, the coarse grain size of pegmatites (Jahns, 1953) may be the result of primary crystallization from a highly fluid magma. Possibly even such features as myrmekite and the various small grains and rims of pure albite formed by primary crystallization in a fluid melt. The White Tank quartz monzonite contains no texture which the writer feels can be explained only by some type of replacement reaction.

Reports of vertical differentiation in bodies of silicic plutonic rocks are uncommon. Sargent (1925) described an intrusion of diorite-granite (slightly more basic than the White Tank quartz monzonite) which exhibits both vertical and lateral differentiation. Van Biljon (1939) described numerous vertical variations within a granitic pluton.

Sequence 2; Units 2 and 3

Differentiation of the main part of Unit 2 has led to the formation of an albitic, micaceous margin along the upper part of the eastern edge of the unit. Because of its high content of primary muscovite, garnet, and highly sodic plagioclase, Unit 3 is considered to represent a continuation of this trend. During differentiation the Ab/An ratio in the plagioclase increases, and muscovite and garnet appear as primary minerals. Except for the appearance of

TABLE 5.—TRACE-ELEMENT CONTENT OF POTASSIUM FELDSPAR

All values are in parts per million. "?" indicates a defective burn or missing sample.

	Age	Sample	Ba	Pb	Rb	Sr	Ca	Cu	Ga	Li	Mn	Ti	V	Y	Yb	Zr
Sequence I (Unit 1)	Oldest; lower part	505	1000	60	2000	400	900	---	5	2	5	80	---	---	---	---
		506	2000	60	2000	400	7000	---	4	2	8	80	---	---	---	---
		133A	1000	40	?	700	10000	6	9	?	10	60	4	---	---	30
		133B	2000	60	2000	500	7000	4	7	2	5	70	2	---	---	15
	transitional part	90A	1000	20	2500	100	2000	5	6	2	4	60	8	---	---	---
		90B	1500	30	3000	200	2000	25	7	2	6	50	7	---	---	---
		502	800	20	2000	80	1000	---	5	2	20	50	---	---	---	---
	upper part	127A	1000	30	?	150	2000	10	9	?	4	60	10	---	---	---
		127B	1000	40	2000	150	2000	20	8	2	3	70	7	---	---	---
		504	1000	30	2000	100	1500	---	7	2	4	80	---	---	---	trace
		510	900	20	2000	150	2000	---	6	2	3	80	---	---	---	---
		508	900	20	1000	250	3000	---	6	2	2	100	---	---	---	trace
	Youngest	509	900	40	1000	250	2000	---	6	2	2	100	---	---	---	trace
Sequence II	Oldest; Unit 2	507	1000	90	3000	300	1000	---	6	25	20	40	---	---	---	---
		83A	2500	80	2500	500	6000	20	7	25	10	60	10	---	---	30
		83B	2500	100	3000	500	5000	5	8	40	10	40	3	---	---	20
		513	1500	90	2000	500	2000	---	6	10	30	60	---	---	---	trace
		169	400	90	4000	20	2000	---	7	5	30	60	---	---	---	trace
	Youngest; order uncertain: Unit 3	356	10	25	4000	4	800	---	8	4	30	50	---	---	---	15
		358	4	30	4000	3	500	---	8	20	40	40	---	---	---	10
		388	3	30	3000	3	700	---	10	3	70	40	---	---	---	25
	Aplite	14	700	100	4000	90	2000	---	7	2	30	60	---	---	---	15
		512	500	60	3000	200	2000	---	10	3	80	20	---	---	---	5
	Pegmatite	37A	6	60	3000	7	3000	9	20	3	20	20	6	---	---	---
		37B	3	40	4000	4	3000	20	20	2	20	20	6	---	---	---
	Unit 1; age uncertain	49	3000	50	3000	400	300	---	6	2	1	20	---	---	---	---
		102	800	40	2000	70	3000	---	5	2	20	80	---	---	trace	90
		501	100	30	3000	7	900	---	10	2	3	30	---	---	---	---
		503	600	15	900	60	6000	---	7	2	10	90	---	150	10	---

muscovite and garnet, differentiation seems to have produced no differences among the modal compositions of the various rocks formed.

samples of Units 1, 2, and 3. Results are listed in Table 5, and the locations of all samples are shown in Table 6.

TABLE 6.—LOCATIONS OF SAMPLES USED IN SPECTROCHEMICAL ANALYSIS

Sample	Unit 1
505, 506, 133A, 133B	lower part of the unit; near the southern edge of the outcrop
90A, 90B, 502	transitional part of the unit; near the eastern edge of the outcrop
127A, 127B, 204, 510	upper part of the unit; in the northern portion of the outcrop
508	cupola represented by a small hill in the northern portion of the outcrop
509	quartz monzonite dike cutting cupola (508)
49	pegmatite dike cutting lower part of unit
102, 503	fine-grained margin approximately 1" thick in contact with wall rock along the eastern and southern edges of the unit
501	pegmatitic segregation in the transitional part of the unit 2' from the eastern contact

Sample	Unit 2
507	lower part of the unit; near the northern edge of the outcrop
83A, 83B, 513	main part of the unit; in the central portion of the outcrop
169	albitic, micaceous, rim along the eastern margin of the unit
14, 512	aplite dikes cutting unit
37A, 37B	pegmatite dike cutting unit

Sample	Unit 3
356, 358	main part of unit
388	pegmatite dike cutting unit

The presence of water in the latest crystallizing magma (Unit 3) is indicated by the abundance of primary muscovite and the presence of separate crystals of both potassium feldspar and albite. The writer is unable to account for the occurrence of the differentiated part of Unit 2 along one border rather than throughout the upper part of the intrusion.

SPECTROCHEMICAL STUDY OF POTASSIUM FELDSPAR IN THE WHITE TANK QUARTZ MONZONITE

Spectrochemical analyses were made on potassium feldspar separated from various

Assuming that the sequence of formation of the potassium feldspar in various parts of the quartz monzonite might be correlative with the related differentiation sequence, the variation in trace elements in the feldspar may be followed through the differentiation process. Table 5 shows the two sequences of differentiation. The pegmatite (sample 49) near the base of Unit 1 is not included in Sequence 1 as its trace-element composition is very different from that of the other pegmatite samples (37 and 512) and it is apparently not a late differentiate of Unit 1. Age relationships of Unit 3 and the pegmatite and aplite dikes in Unit 2

are not certain, although the pegmatite is probably younger than the aplite.

The following general conclusions may be drawn concerning the distribution of trace elements in potassium feldspar:

(1) Lead is enriched in the earlier-crystallizing potassium feldspar in both sequences.

(2) Barium is enriched in the earlier-crystallizing potassium feldspar in Sequence 2 and shows little variation in Sequence 1.

(3) Strontium is least abundant in the later-crystallizing potassium feldspar in both sequences.

(4) The concentration of rubidium either does not change throughout either sequence or shows a very slight enrichment in the later phases.

References Cited

Bowen, N. L., and Tuttle, O. F. 1950, The system $NaAlSi_3O_8$-$KAlSi_3O_8$-H_2O: Jour. Geology, v. 58, p. 489–511

Jahns, R. H., 1953, The genesis of pegmatites; Pt. I, The occurrence and origin of giant crystals: Am. Mineralogist, v. 38, p. 563–598

Miller, W. J., 1938, Pre-Cambrian and associated rocks near Twenty-nine Palms, California: Geol. Soc. America Bull., v. 49, p. 417–446

Nockolds, S. R., and Allen, R., 1953, The geochemistry of some igneous rock series: Geochim. et Cosmochim. Acta, v. 4, p. 105–142

Nockolds, S. R., and Mitchell, R. L., 1948, The geochemistry of some Caledonian plutonic rocks; a study in the relationship between the major and trace elements of igneous rocks and their minerals: Royal Soc. Edinburgh Trans., v. 61, pt. II, p. 533–575

Rogers, John J. W., 1954, Geology of a portion of Joshua Tree National Monument, Riverside County, Map Sheet 24 *in* Jahns, R. H., *Editor*, Geology of southern California: Calif. Dept. Nat. Res., Div. Mines Bull. 170

—— in press, Geology of the western portion of Joshua Tree National Monument: Calif. Dept. Nat. Res., Div. Mines Bull.

Sargent, H. C, 1925, Notes on the petrology of the Penmaenmawr Mountain: pt. I; pt. II, The acid segregations and veins: Liverpool Geol. Soc. Proc., v. 14, p. 83–98, 123–142

Tuttle, O. F., 1952, Origin of the contrasting mineralogy of extrusive and plutonic salic rocks: Jour. Geology, v. 60, p. 107–124

Van Biljon, S., 1939, The Kuboos batholith, Namaqualand, South Africa: Geol. Soc. South Africa Trans., v. 42, p. 123–219

Department of Geology, The Rice Institute, Houston, Texas

Manuscript Received by the Secretary of the Society, February 5, 1957

Publications of the Division of the Geological Sciences, California Institute of Technology, Pasadena, California, Contribution No. 811

BULLETIN OF THE GEOLOGICAL SOCIETY OF AMERICA
VOL. 69, PP. 465-476, 8 FIGS., 2 PLS. APRIL 1958

EXPERIMENTAL DEFORMATION AND FAULTING IN WOMBEYAN MARBLE

BY M. S. PATERSON

ABSTRACT

In compressive stress-strain tests on a coarse-grained marble at various confining pressures up to 1000 kg cm^{-2}, special attention has been paid to the transition from brittle to ductile behavior. The application of low confining pressures suppresses the longitudinal fractures characteristic of failure at atmospheric pressure, and well-defined shear failures develop. The formation of the localized shear zones accompanies a gradual decrease in the stress needed for continued deformation but does not lead immediately to complete fracture. This behavior may be initiated by a type of plastic instability. Its relevance to geological faulting is discussed, since the shear zones developed in the marble specimens appear to be similar to geological faults.

At confining pressures above about 300 kg cm^{-2}, the stress-strain curves rise continuously without reaching a maximum, and the deformation is distributed throughout the specimen instead of being localized in shear zones or faults. This suggests that there is a depth in the earth's crust below which faulting cannot be expected in this rock.

The stress-strain curves have been analyzed to show the effect of confining pressure on the yield stress and on the stress at the maximum load. A few measurements on a fine-grained limestone are also included in an appendix.

Coloration of the marble by X radiation occurs after deformation at low confining pressures, but the effect becomes more marked at higher confining pressures.

CONTENTS

TEXT

	Page
Introduction	465
Acknowledgments	466
Experimental material and procedure	466
Results of tests	467
Analysis of test results	470
Microscope observations	472
X-ray coloration	472
Geological application	473
Some measurements on fine-grained limestone	474
References cited	474

ILLUSTRATIONS

Figure	Page
1. Fabric diagram of undeformed Wombeyan marble	466
2. Simplified sketch of testing apparatus	467
3. Typical stress-strain results for various confining pressures	468
4. Typical stress-strain results, extended to higher strains	469
5. Variation of angle of shear failure with confining pressure	470
6. Effect of confining pressure on the maximum stress	471
7. Effect of confining pressure on the yield stress	472
8. Stress-strain results for Wells Station limestone specimens and one Solenhofen limestone specimen	474

Plate	Facing page
1. Appearance of specimens after testing	468
2. Slickensides in shear zone	469

INTRODUCTION

There have been several experimental studies of the permanent or plastic deformation[1] of marble and limestone since the early work of Adams and Nicolson (1901) and von Kármán (1911); Robertson (1955) gives a bibliography. It is thus known that marble and limestone, while brittle at atmospheric pressure, show marked ductility (that is, ability to undergo plastic deformation) when subjected to a sufficiently high confining pressure. The purpose of the present work has been to study in more

[1] In this paper "plastic deformation" is used to describe any permanent deformation which does not depend greatly on time and can therefore be represented on a stress-strain curve; it does not include "creep", that is, strongly time-dependent deformation which can occur at constant stress.

detail than hitherto the transition from brittle to ductile behavior in marble. Stress-strain tests have been done at various confining pressures up to 1000 kg cm^{-2}, and the mode of deformation or failure has been correlated with the shape of the stress-strain curve. At low confining pressures the marble exhibits shear failures similar in appearance to geological faults. Therefore, the geological implications of these experiments are discussed in some detail.

Acknowledgments

The United States Bureau of Reclamation kindly supplied the drawings from which the triaxial testing apparatus was made. The writer wishes to thank Mr. H. Berry for the chemical analyses of the Wombeyan marble, Mr. K. R. Walker for pointing out that the appearance of the steps on experimentally produced slickenside surfaces does not conform to the description usually given in textbooks on structural geology, Dr. G. S. Watson for discussion on the statistical significance of the fabric pattern, Prof. D. T. Griggs and Dr. John Handin for criticisms of this paper, and Prof. J. C. Jaeger for many stimulating discussions during the course of the work.

Experimental Material and Procedure

The samples of marble were obtained from a quarry near Wombeyan in New South Wales. This rock is Silurian and has probably been affected by several orogenies. A chemical analysis of the marble showed that it contains 96.0 per cent $CaCO_3$, 2.5 per cent $MgCO_3$, and 0.2 per cent SiO_2. It is fairly coarse-grained (average grain size about $\frac{1}{4}$ mm), and most grains show notable twinning parallel to at least one, and usually two or three, sets of planes.

Fabric analysis (Fig. 1) shows that the marble has no pronounced anisotropy; after dividing the fabric diagram into equal areas in several ways, including by concentric circles about the center, chi-square tests showed that there was no significant departure from randomness in the measured orientations. This was borne out by the mechanical tests, in which specimens were cut from several unoriented blocks but gave similar results. About six specimens were cut parallel to each other from each block. Each block is distinguished by a symbol in Figures 6 and 7.

The test specimens were cylinders 2 inches in diameter and 5 inches long, the length-diameter ratio of 2.5 being chosen to minimize the "end effects" while avoiding buckling. During testing the specimens were jacketed with soft rubber of an eighth of an inch wall thickness

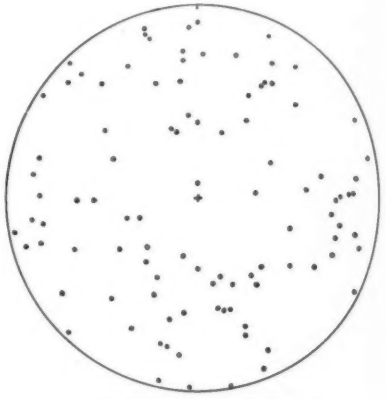

Figure 1.—Fabric Diagram of Undeformed Wombeyan Marble

Showing the surface true projection of the orientations of the C axes of 100 grains.

attached to steel end pieces with hoseclips. One of the steel end pieces engaged in a spherical seat which served to reduce bending constraints on the specimen.

The testing apparatus was constructed to the design of the Bureau of Reclamation (Balmer *et al.*, 1953) except for being modified to use a synthetic rubber 0-ring seal (Fig. 2). It was mounted between the platens of an Avery hydraulic compression testing machine which was used to apply and measure the load on the plunger (that is, the axial load on the specimen plus the load due to the confining pressure). The confining pressure was supplied from a Hart pressure bench, consisting of a hand pump, a screw press, and control valves, and was indicated by a Bourdon gauge. While the plunger was being pushed into the test chamber the pressure was kept constant by bleeding excess fluid through a needle valve and using the Hart screw press for fine control; this arrangement provided very sensitive control of the pressure. The maximum confining pressure used was 1000 kg cm^{-2}. The confining fluid was lubricating oil of S.A.E. 10 viscosity number.

The strains were obtained from readings of a dial gauge placed between the platens of the testing machine; dial gauges reading to $\frac{1}{10.000}$

inch or $\frac{1}{1000}$ inch were used, depending on whether small or large strains were being studied. The dial gauge readings included the elastic deflections in the apparatus. However, the load readings of the testing machine during straining of the specimen and during compression of the confining fluid only; both contain the parts due to friction, and therefore the stress

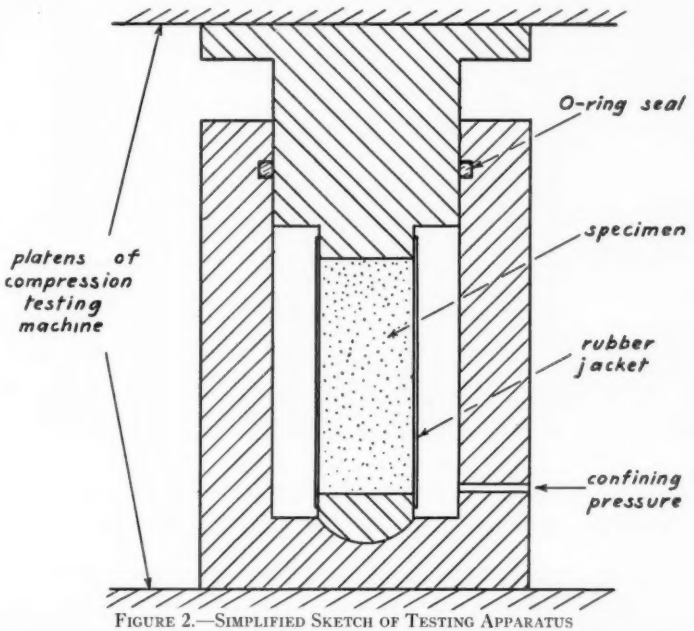

FIGURE 2.—SIMPLIFIED SKETCH OF TESTING APPARATUS

tests on a steel of known elastic properties showed that the deflection in the apparatus amounted to only about 10 per cent of the elastic strain in the marble. No correction has been made for it, since it has no significant effect on the analysis of the plastic properties of the marble. The tests were made at a constant rate of strain of about 0.003 per minute, except in the tests to larger strains where, in the later stages (indicated in Figure 4), the strain rate was approximately doubled. The load and strain readings were taken without interrupting the straining.

The chief source of error in deriving the load on the specimen arises from the friction of the plunger in the test vessel. An estimate of this friction was obtained from one half the difference between the elastic loading and unloading curves of a hardened steel specimen. The friction was approximately 3 per cent of the total load on the plunger. In practice, the results have been given in terms of the maximum differences of principal stresses in the specimen. These are obtained from the differences between differences themselves should not be in error due to friction by more than about 3 per cent. This error is probably not greater than the normal fluctuations in strength from specimen to specimen and, moreover, has less effect on comparisons between different specimens; therefore, no correction has been applied. Differences of up to 10 per cent, but usually less, are found in the load-deformation curves obtained from different specimens (generally of nonparallel orientation), tested under the same confining pressure, except at atmospheric pressure where there is much greater scatter.

RESULTS OF TESTS

Figure 3 shows a typical series of stress-strain curves at various confining pressures up to 1000 kg cm^{-2}. These specimens were cut in parallel orientation from the same block of marble except in the case of those for which the stress-strain curves are drawn as broken lines. In Figure 4 the results of the same tests are shown for larger strains, up to 20 per cent; the

discontinuities in the curves result from doubling the rate of strain in the subsequent parts of the tests.

Here, as elsewhere in this paper, the stress is quoted as the maximum difference of principal stresses, which is equal to twice the maximum shear stress. In every case the stress calculation is based on the initial cross-sectional area, and the stress plotted is therefore proportional to the load. This engineering convention is followed because the inhomogeneous nature of the deformation makes it impossible to specify the true stress. Similarly the strain is an average value, proportional to the shortening of the specimen and quoted without regard to inhomogeneities of strain.

The appearance of specimens after testing is seen in Plate 1; most of these specimens are ones to which the results of Figures 3 and 4 refer, but their appearance is typical of other specimens tested. At atmospheric pressure, brittle fracture occurs in an irregular manner, partly on surfaces approximately parallel to the axis of the specimen and partly on inclined surfaces, suggestive of shear failure. At a confining pressure even as low as 18 kg cm^{-2}, however, the longitudinal failures are suppressed, and a very distinct shear failure appears.

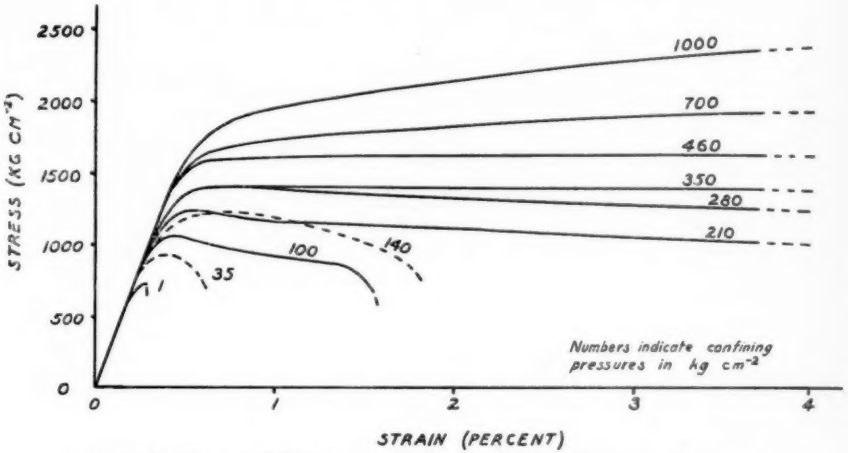

FIGURE 3.—TYPICAL STRESS-STRAIN RESULTS FOR VARIOUS CONFINING PRESSURES

The maximum principal stress differences, based on the original cross-sectional area, are plotted as ordinates.

Shear failures are produced at confining pressures up to about 300 kg cm^{-2} (Pl. 1, fig. 1). Below about 100–150 kg cm^{-2}, they follow only one shear plane, while at the higher pressures the shear failure usually occurs on two symmetrically inclined, intersecting planes. The reason for the change from failure on one shear plane to failure on a pair of conjugate planes as the confining pressure increases is not clear, but it could be influenced by increased restriction on rotation of the specimen during test. Thus it was found that, at 70 kg cm^{-2} confining pressure, conjugate shear zones formed if the spherical seat at the end of the specimen was removed, but only a single shear zone appeared when it was in use.

At confining pressures above 300 kg cm^{-2} (Pl. 1, fig. 2), the deformation is no longer

PLATE 1.—APPEARANCE OF SPECIMENS AFTER TESTING

FIGURE 1.—After deformation at lower confining pressures. From left to right: (a) atmospheric pressure: (b) 35 kg cm^{-2}, 1 per cent strain: (c) 100 kg cm^{-2}, 2 per cent strain; (d) 210 kg cm^{-2}, 12½ per cent strain. (The specimen on the right was initially somewhat shorter than the others.)

FIGURE 2.—After 20 per cent strain at higher confining pressures. From left to right: (a) undeformed; (b) 280 kg cm^{-2}; (c) 460 kg cm^{-2}; (d) 1000 kg cm^{-2} confining pressure. (All specimens were initially of the same length.)

FIGURE 1

FIGURE 2

APPEARANCE OF SPECIMENS AFTER TESTING

SLICKENSIDES IN SHEAR ZONE OF SPECIMEN AFTER COMPLETE FAILURE AT 210 kg cm^{-2} CONFINING PRESSURE

localized in one or two shear zones but is distributed through a larger volume of the specimen; at the highest pressures, the deformation is almost uniform throughout the specimen except for some restriction due to friction at the ends. In the case of specimens strained 20 per cent, those tested at a confining pressure of 1000 kg cm^{-2} remained approximately circular in cross section and so underwent approximately equal strains in all directions normal to the axis. At lower confining pressures, however, the specimens became more oval in cross section, and the deformation was not distributed so uniformly over their length. It may be concluded that, as the confining pressure is decreased, the shear strains are more concentrated parallel to one set of conjugate shear planes, an effect which culminates in the appearance of shear failure on one pair of these shear planes in specimens tested at a confining pressure of about 300 kg cm^{-2} or less. Many minor shear zones (similar to families of Lüders' bands) are often seen after large strains at confining pressures somewhat above this value.

If the load on the plunger of the test apparatus were rapidly decreased at the end of a test, specimens that had undergone large strains at the higher confining pressures usually broke up into small fragments, especially along planes normal to the specimen axis. This was avoided if the load was removed slowly.

When deformation at a low confining pressure is continued to the stage where the specimen separates along the shear zone when being removed from the test apparatus, the surface of separation shows well-defined "slickensiding" (Pl. 2) similar to that sometimes observed in geological faults. The slickenside grooves are parallel to the direction of shearing. Also, at right angles to the slickenside grooves there are small steps or ridges with their steep sides facing the direction opposite that in which the other part of the specimen moved, that is, the disposition of the steps is such as would be

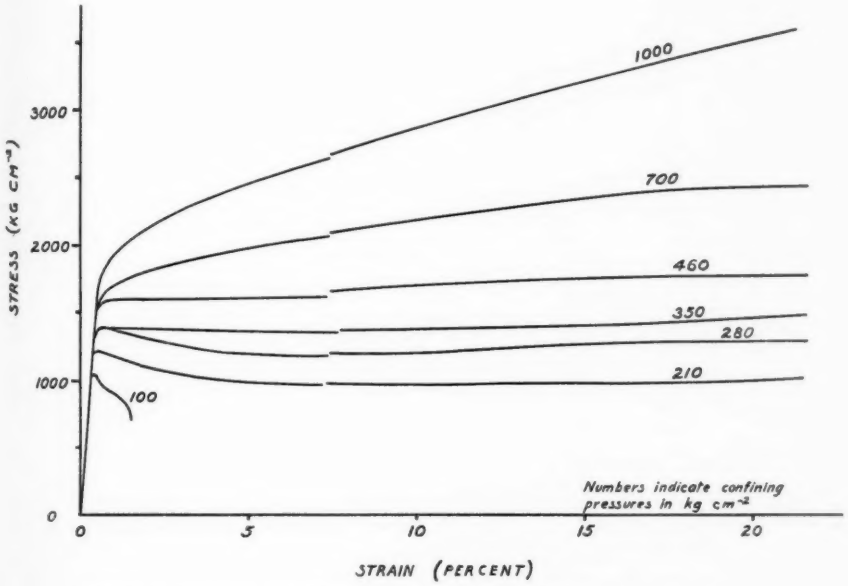

FIGURE 4.—TYPICAL STRESS-STRAIN RESULTS, EXTENDED TO HIGHER STRAINS

The discontinuities result from doubling the rate of strain in the subsequent parts of the test.

expected to hinder further slipping on the surface. The significance of this observation for structural geology is discussed later.

The angle between the shear failure and the specimen axis has been measured in the specimens which were tested under the lower confining pressures and which showed well-defined shear failures; the measured values are plotted against confining pressure in Figure 5. There is a slight increase in the failure angle—that is, the failure zone tends to be more steeply inclined to the specimen axis as the confining pressure increases.

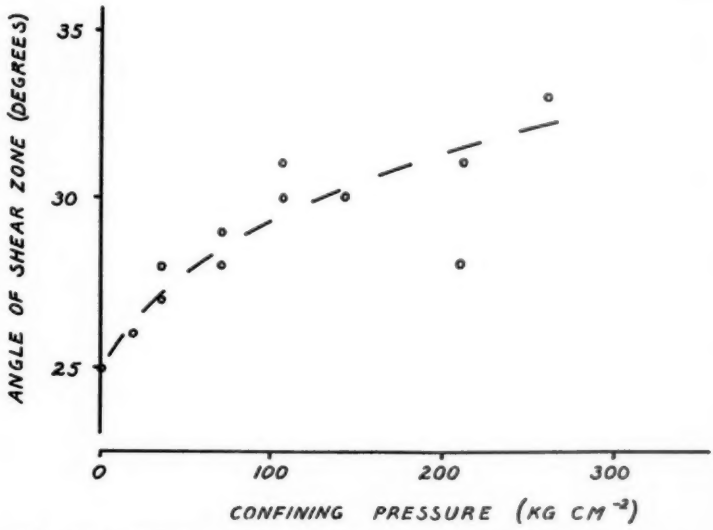

FIGURE 5.—VARIATION OF ANGLE OF SHEAR FAILURE WITH CONFINING PRESSURE

In summary, from the shape of the stress-strain curves and from the appearance of the specimens after testing, one may consider the experimental results in two groups for which the confining pressure is respectively below and above about 300 kg cm^{-2}:

(1) In tests made under the lower confining pressures the load passes through a maximum at a relatively small strain and thereafter falls steadily so that the larger the strain the less the load needed for further straining. The specimens deform mainly by a shearing confined to one or two narrow, oblique zones, and, if the straining is continued far enough, there may be complete shear failure with an accompanying, more rapid drop in load. As the confining pressure is increased, the load maximum occurs at higher strains and the specimen undergoes a greater uniform plastic strain before the shear zone appears.

(2) At the higher confining pressures the load continues to rise with increasing strain and does not show a maximum, that is, the greater the strain the greater the load needed for further straining. The deformation is distributed throughout the specimen (with some restriction at the ends due to friction). This behavior is typical of ductile, work-hardening materials such as copper.

ANALYSIS OF TEST RESULTS

The mechanical behavior of Wombeyan marble conforms in general to that of other marbles and limestones studied by previous workers. It becomes very ductile at relatively low confining pressures, probably because of its coarse grain size and high purity. The influence of confining pressure on its stress-strain properties is conveniently represented in graphs in which the maximum difference in principal stresses at a well-defined point on the stress-strain curve is plotted against confining pressure (Figs. 6, 7). In Figure 6 the stress at the maximum load is plotted, and here the lower confining pressures only are relevant since only for them does the load pass through a maximum. Figure 6

probably represents the stresses at which the localized shear zones begin to develop.

The effect of confining pressure on the stress at the maximum load can be alternatively represented in a Mohr diagram (Nadai, 1950, Chapter 10); the Mohr envelope is related to the plot of Figure 6 by a simple transformation (Goguel, 1948, p. 171). The Mohr envelope is thus approximately a straight line; from its slope Mohr's theory of failure would predict for all specimens the same angle of failure, approximately 30° (±2°). In view of the scatter in the experimental results, this is in fair agreement with the observations (Fig. 5), except perhaps at the lower confining pressures. A slightly curved Mohr envelope could be fitted more accurately to the observations, and this would be compatible with the small change in the angle of failure as the confining pressure is increased. However, it is doubtful whether the accuracy of the observations justifies such a refinement in the analysis.

Since the Mohr envelope for the stress at the maximum load can be approximated by a straight line, the Coulomb-Navier law (Nadai, 1950, p. 219) can be applied; the value of the "coefficient of internal friction" is found to be approximately 0.6. With this it can be shown that the value to which the load falls after passing through the maximum at confining pressures around 200–300 atmospheres cannot be accounted for wholly by the frictional term in the Coulomb-Navier equation; thus, either there is still considerable shear strength in the shear zone, or, if not, the coefficient of friction for the sliding of the two parts of the specimen over each other must be much higher (actually equal to 2.4 for the experiment at 210 kg cm^{-2} in Figure 4) than the coefficient of internal friction from the Coulomb-Navier equation.

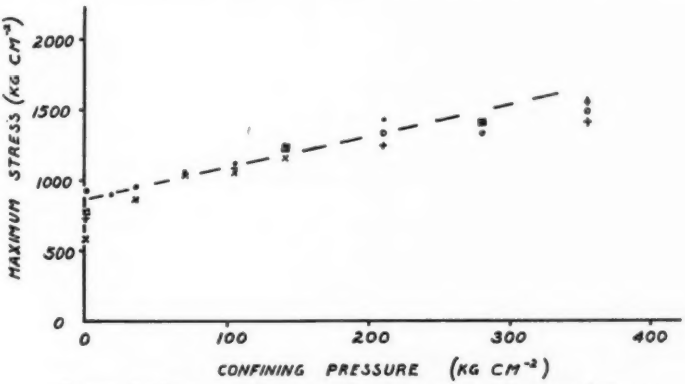

FIGURE 6.—EFFECT OF CONFINING PRESSURE ON THE MAXIMUM STRESS

(Plotted as maximum principal stress difference in the stress-strain curve.) Each symbol is used for specimens cut from the same block of marble.

The quantity plotted in Figure 7 is a "yield stress", arbitrarily defined as the stress at which 0.05 per cent permanent strain is reached (c.f. "proof stress" in engineering usage), there being no sharp yield point. This yield stress is slightly higher than the proportional limit, but for comparative purposes it can be specified with greater accuracy. It serves to define the threshold of appreciable plastic deformation. The variation of yield stress with confining pressure can be represented approximately by two straight lines (Fig. 7); the change from one slope to the other corresponds to the change from localized faulting to more uniform deformation. At first the yield stress increases with confining pressure, like the maximum load, but above about 350 kg cm^{-2} confining pressure, the rate of increase becomes small, and the yield stress is approximately constant.

The character of the deformation in the specimens can be predicted from the shape of the stress-strain curves (or, strictly speaking, of the load-deformation curves) by stability considerations similar to those which apply to the necking of metals in a tension test (Nadai, 1950, Chapter 8) or to the appearance of Lüders' bands in mild steel. While the load-deformation curve is rising, the deformation will tend to be distributed throughout the specimen, since excessive deformation in one

region would raise its resistance to further deformation above that in the rest of the specimen. Such deformation can be described as stable. On the other hand, an unstable situation arises when the load-deformation curve slopes downwards; excessive deformation in one region then lowers its resistance to further deformation below that of other parts of the specimen and deformation will therefore continue more easily in this region than elsewhere. Thus, in the marble specimens compressed at low confining pressure, deformation beyond the load maximum will continue more easily in a localized shear zone than throughout the specimen.

While one might expect this argument to apply to all materials, Prof. D. T. Griggs and Dr. J. Handin have pointed out that some experimental results throw doubt on its general validity. For example, dolomite has been observed to give a rising load-deformation curve and yet develop a localized shear zone.

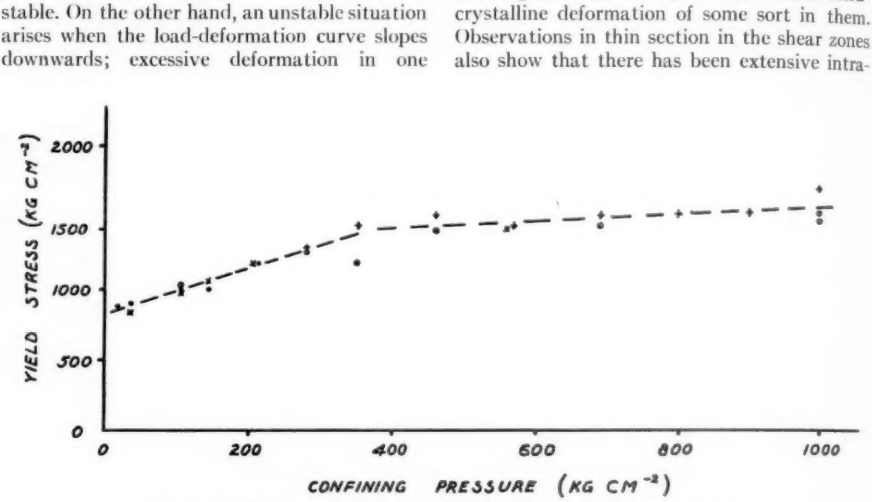

FIGURE 7.—EFFECT OF CONFINING PRESSURE ON THE YIELD STRESS

(Plotted as the maximum principal stress difference at 0.05 per cent permanent strain). Each symbol is used for specimens cut from the same block of marble.

MICROSCOPE OBSERVATIONS

Since there was already extensive twinning of the grains before deformation, it was not easy to observe the role of mechanical twinning in the deformation of the Wombeyan marble. A few observations on surfaces polished before deformation showed that many new, very thin, twin lamellae were formed in the course of deformation at high pressures, but it is not known how important twinning is in the formation of localized shear zones. Many bent twins are visible in thin section in the shear zones, showing that there has been considerable intracrystalline deformation of some sort in them. Observations in thin section in the shear zones also show that there has been extensive intracrystalline cracking, with the cracks sometimes extending through many crystals, as well as a considerable amount of intercrystalline cracking. Thus, in the terminology of Handin (personal communication), the mechanism of deformation in the shear zones appears to be partly "cataclastic" and partly "gliding" in nature.

The uniform deformation at higher confining pressures is probably mainly of gliding nature but observations on specimens after unloading also show some intragranular cracking.

X-RAY COLORATION

Calcite crystals, plastically deformed under conditions in which slip (translation gliding) would be expected, develop a strong and persistent bluish-purple color when irradiated with X rays or gamma rays (Przibram, 1927; Handin *et al.*, 1957; and observations by the author). Undeformed crystals, or crystals deformed by twinning only, do not develop this irradiation color. Therefore, it seems likely that ability to color under X radiation after deformation is an indication that slip has occurred. Wombeyan marble in its natural state does not color in this way when irradiated and so has

presumably been well annealed in its geological history.

Specimens of Wombeyan marble, deformed at various confining pressures, were irradiated for equal periods of time with X rays from a copper target in a crystallographic X-ray set operated at 40 kV. A specimen that had fractured at atmospheric pressure did not color, but all other specimens showed some coloration. The coloration was very slight for a specimen deformed at a confining pressure of 18 kg cm^{-2} but, for equal strains, it increased in intensity as the confining pressure increased. Coloration was strong in a specimen deformed at 1000 kg cm^{-2} confining pressure. These observations suggest that at very low confining pressures and under relatively small applied shear stresses some plastic deformation by slip occurs in addition to twinning.

Geological Applications

The localized shear zones in the specimens deformed at the lower confining pressures are similar in appearance to faults, and it is therefore interesting to consider the implications for faulting of these experiments. Many factors such as the pressure of interstitial fluids, the juxtaposition of rocks of contrasting mechanical properties, and the influence of creep processes over long periods of geological time will not be considered here, and therefore any conclusions can be of only limited application in the complex problems of structural geology. However, by first studying simple situations, it is always to be hoped that some principles may be elucidated which are applicable, with more or less modification, in more complicated situations.

The present experiments on marble show that at relatively low confining pressures a shear failure develops during deformation, whereas at higher confining pressures the strain is distributed fairly uniformly throughout the specimen, at least for strains up to about 30 per cent. This suggests that in calcite rocks, faulting will occur only at relatively shallow depths in the earth's crust, while general plastic deformation will occur at greater depths. Thus faulting cannot be expected in Wombeyan marble below a depth of about 1–5 km (or somewhat more if the pore pressure is high). The estimate of 1 km applies to reverse or strike-slip faulting where the stress system is similar to that in an experiment in which the specimen axis is horizontal and the shearing direction is in a vertical or a horizontal plane, respectively. The estimate of 5 km applies to normal faulting where the stress system is similar to that in a specimen with its axis vertical. The limiting depths for all other cases of faulting should fall between these limits. Since the temperature gradient in the earth's crust is roughly 30°C. per km at shallow depths (Turner and Verhoogen, 1951, p. 352), the rise of temperature with depth is not likely to affect these estimates appreciably.

For a fine-grained compact limestone, a larger confining pressure is needed to suppress the formation of localized shear zones, and accordingly faulting can be expected at 2 or 3 times the depths estimated for Wombeyan marble. However, the great ductility shown by all marbles and limestones at high confining pressures suggests that faulting will not occur in these rocks if they become buried in the deeper parts of the earth's crust, about 30 km or more.

Most other rocks exhibit localized shearing up to much higher confining pressures, and so faulting can be expected at considerable depths in the crust in most rocks if the conditions of stress are favorable. However, Goguel (1948, p. 330) has argued on other grounds that faulting will occur only comparatively near the earth's surface and he suggests that folding is more likely at greater depths.

The writer has suggested that the faulting observed in experiments on marble was, at least in its early stages, a feature of plastic deformation—that is, that the inception of faulting was due to the plastic instability of a material with a falling load-deformation curve. However, the fault zone probably soon develops into a region of fracture as more and more microscopic fracturing occurs, until the fault may be truly considered a fracture zone.

It is noteworthy that in the experimental deformation of marble and limestone, the localized shear zones never developed abruptly, except at atmospheric or very low confining pressure; the rate of strain was largely controllable throughout the experiment and was determined by the rate of movement of the platens of the testing machine. Therefore, even when faults do develop in calcite rocks, one would not expect earthquakes to be associated with them.

The observations on the "slickensided" surfaces produced when deformation of the marble is carried far enough at low confining pressures suggest that the sense of slipping on a fault cannot always be deduced correctly from

the orientation of the steps on the slickensided surface in the way it is described by many writers on structural geology (for example, Billings, 1942, p. 157; Hills, 1953, p. 131). It is was followed. The stress-strain curves are shown in Figure 8. The result of one test on the ultra fine-grained Solenhofen limestone is also included.

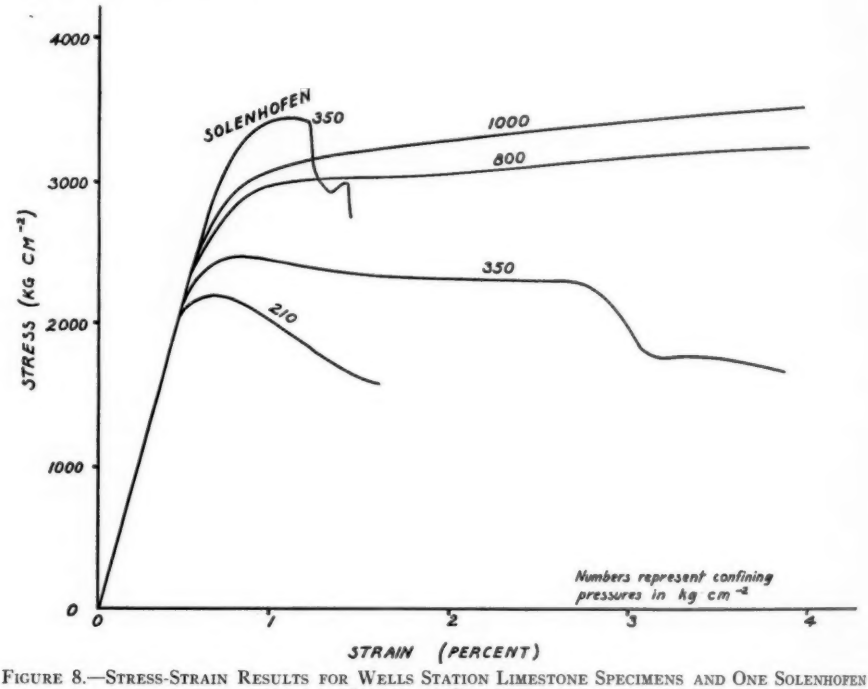

FIGURE 8.—STRESS-STRAIN RESULTS FOR WELLS STATION LIMESTONE SPECIMENS AND ONE SOLENHOFEN LIMESTONE SPECIMEN

The maximum principal stress differences, based on the original cross-sectional area, are plotted as ordinates.

said that "the steps on one wall face the direction towards which the other wall moved" (Hills). However, the sense of shearing is exactly opposite to this in the present experiments. This suggests that the sense of shearing should not be inferred from the appearance of a slickensided surface only, but should be confirmed by mapping.

SOME MEASUREMENTS ON A FINE-GRAINED LIMESTONE

An interesting comparison with the behavior of the Wombeyan marble is provided by a few tests on a fine-grained, fairly pure limestone (average grain size about 0.02 mm) from Wells Station, near Canberra, in the Australian Capital Territory. The same testing procedure

The fine-grained Wells limestone gives considerably higher stress-strain curves than the coarse-grained Wombeyan marble. Also, for similar shape of stress-strain curve and distribution of deformation, a higher confining pressure is needed for the Wells limestone; that is, for extensive deformation without faulting, a higher confining pressure is needed for the Wells limestone than for the Wombeyan marble. For Solenhofen limestone, a still higher confining pressure is needed to prevent faulting during deformation.

REFERENCES CITED

Adams, F. D., and Nicolson, J. T., 1901, An experimental investigation into the flow of marble: Royal Soc. London Philos. Trans., ser. A, v. 195, p. 363–401

Balmer, G. G., *et al.*, 1953, Physical properties of

some typical foundation rocks: U. S. Bur. Reclamation, Denver, Concrete Lab. Rept. no. SP-39, Fig. 2

Billings, M. P., 1942, Structural geology: New York, Prentice-Hall Inc., 473 p.

Goguel, J., 1948, Introduction à l'étude mécanique des déformations de l'écorce terrestre: 2d ed., Paris, Ministère de l'Industrie et du Commerce, 530 p.

Handin, J. W., Higgs, D. V., Lewis, R. R., and Weyl, P. K., 1957, Effects of gamma radiation on the experimental deformation of calcite: Geol. Soc. America Bull., v. 68, p. 1203–1224

Hills, E. S., 1953, Outlines of structural geology: London, Methuen and Co. Ltd., 182 p.

Kármán, Th. von, 1911, Festigkeitsversuche unter allseitigem Druck: Zeit. Ver. deut. Ing., v. 55, p. 1749–1757

Nadai, A., 1950, Theory of flow and fracture of solids, 2d ed., McGraw-Hill Book Co., New York, 572 p.

Przibram K., 1927, Weitere Versuche über die Verfärbung gepresster Salze: S. B. Akad. Wiss. Wien IIa, v. 136, p. 435–446

Robertson, E. C., 1955, Experimental study of the strength of rocks: Geol. Soc. America Bull., v. 66, p. 1275–1314

Turner, F. J., and Verhoogen, J., 1951, Igneous and metamorphic petrology: New York, McGraw-Hill Book Co., 602 p.

Department of Geophysics, The Australian National University, Canberra, Australia

Manuscript Received by the Secretary of the Society, March 11, 1957

Short Notes

BULLETIN OF THE GEOLOGICAL SOCIETY OF AMERICA
VOL. 69, PP. 477-482, 3 FIGS., 1 PL. APRIL 1958

FLOWTILL IN SOUTHEASTERN MASSACHUSETTS

BY JOSEPH H. HARTSHORN

Numerous bodies of till overlying stratified sand and gravel deposits near Taunton in southeastern Massachusetts (Fig. 1) were derived from superglacial debris, as is demonstrated by their stratigraphic positions in ice-contact stratified drift features. These till masses, which moved laterally from the glacier to lower adjacent outwash areas, are given the name "flowtill"[1] to distinguish them from till that is generally thought to be subglacial in origin or let down vertically from the glacier as superglacial or englacial till.

In some areas of southeastern Massachusetts, long low hills are composed of cores of sand and gravel mantled with till up to 20 feet thick; the origin of this till overlying sand and gravel is obscure, and it is mapped as ground moraine. At other places, however, till overlies fluvial sands and gravels or is interstratified with them in ice-channel fillings (crevasse fillings and eskers), kames, kame deltas, kame terraces, and kame plains that stand well above the surrounding terrain.

These ice-contact features are alike in one respect—the glaciofluvial and glaciolacustrine bodies stand above the surrounding lowlands, and the till masses themselves overlie the stratified drift and thus also stand above the lowlands. The ice-contact stratified drift in which flowtill is found was undoubtedly deposited in low spots in a stagnant glacier, on or near the subglacial terrain, or in channels between the glacier and adjacent hill slopes. Ice-contact slopes are characteristic of all these features, and the conditions of deposition were somewhat special, because at present fluvial and even lacustrine deposits end abruptly at scarps that fall away to lower ground. It seems highly improbable that local readvances of a heretofore stagnant glacier would move over these sharply defined features, deposit a thin layer of till, and withdraw, for, with the second episode of stagnation, fluvial or lacustrine sedimentation must resume in the same place and under the same special circumstances as before—in depressions surrounded by stagnant ice.

It seems obvious from the physiographic and stratigraphic relationships of these tills that they must be different in origin from the tills that are spread generally over southeastern Massachusetts. It must be emphasized, however, that the flowtills do not differ either in physical description or in grain-size distribution from tills of ground-moraine areas. The tills of southeastern Massachusetts have a dominantly sandy to silty matrix and are moderately easy to crush when dry. The range in grain-size frequency of the matrix is shown in Figure 2. Numerous pebbles, cobbles, and boulders are present. The tills are generally unoxidized and of some shade of gray to yellowish gray. The only noticeable difference between till in the ground moraine and till in the ice-contact outwash features is that there are fewer boulders in the latter. Both tills contain voids, although these are more common in the flowtill.

At least three ice-channel fillings near Taunton contain lenses of flowtill. Isolated patches of sandy gray till cap one of the features; the second ice-channel filling has till at the surface in a lens about 3 feet thick, 30 feet wide, and of unknown length; in a third the till is well down in the body of the ice-channel filling.

Kames, kame plains, and kame terraces near Taunton exhibit numerous examples of flowtill, but only two examples that show different stratigraphic situations are described here.

[1] Mr. C. A. Kaye of the U. S. Geological Survey has suggested that the word be *tillflow*, following such examples as *mudflow*, *earthflow*, *landslide*, *rockfall*, etc. The writer's emphasis is not on the process but on the material that has undergone lateral movement and is now at rest. *Flowtill* is a variety of till like superglacial till, englacial till, subglacial till, or lodgement till. Either term serves to emphasize the distinctive origin of the flowtill.

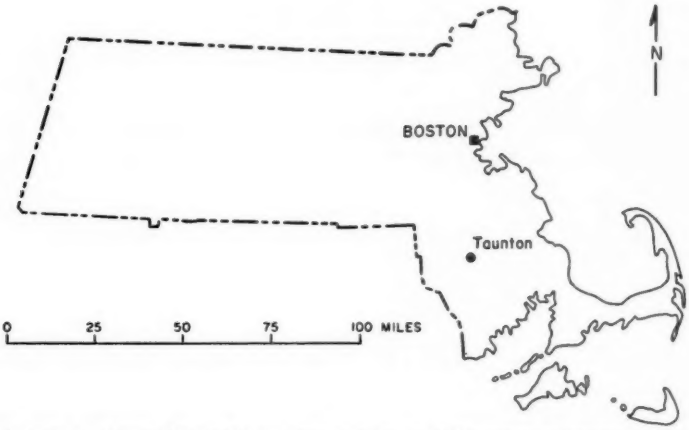

FIGURE 1.—INDEX MAP OF MASSACHUSETTS SHOWING LOCATION OF TAUNTON AREA

One example shows till at the top of a section; a second shows till interstratified with glaciofluvial deposits.

In a large abandoned gravel pit at Weir Village, just south of Taunton, a vertical face (Pl. 1, fig. 1) shows the following section:

	Feet	Inches
Artificial fill	3–4	
Soil		4
Eolian mantle and frost-heaved material (congeliturbate)	2–3	
Flowtill, yellowish gray to very light gray when dry, almost impossible to dig by hand; in 1956 had stood in a vertical face for at least eight years; sample 287C	4–6	
Sand, fine sand, silt and clay, general dip 8° to north	1–10	
Covered	20+	

The second example is in a pit on the shore of Lake Sabbatia, northwest of Taunton, in a large kame plain. A thin layer of flowtill of considerable areal extent is found near the top of the kame plain and extends as a bed of variable thickness down the sloping sides of the kame plain to a contact with adjacent formless masses of lower outwash. A section on the east face of the pit shows the following example of the stratigraphy, which differs from place to place within the pit:

	Feet	Inches
Soil		6
Eolian mantle and frost-heaved material with ventifacts (congeliturbate)		8
Fine to medium, loose, tan, horizontally bedded fluvial sand		24
Coarse pebble gravel, poorly sorted		18
Flowtill, yellowish gray to gray, clayey, cemented; sample 139-7		20
Horizontally bedded medium sand, coarse sand, and small pebble gravel, fine sand, and pebble gravel		30
Cross-bedded medium sand, dipping approximately south		8
Generally horizontally bedded fine sand		8
Covered	13	

A sample of flowtill (287C) was collected for grain-size analysis from a vertical face directly opposite the one illustrated in Figure 1 of Plate 1; the statistical measures are found in Table 1 and the cumulative curve describing the grain-size distribution of the matrix in Figure 2. The flowtill is very hard and compact when dry but has a smaller percentage of silt and clay than any other till sample in the area. In appearance, however, it resembles all other

PLATE 1.—FLOWTILL AND MUDFLOW

FIGURE 1.—Flowtill over stratified sand and gravel in a large kame near Weir Village, Taunton, Mass.
FIGURE 2.—Mudflow in ablation moraine on Malaspina Glacier, Yakutat Bay, Alaska.

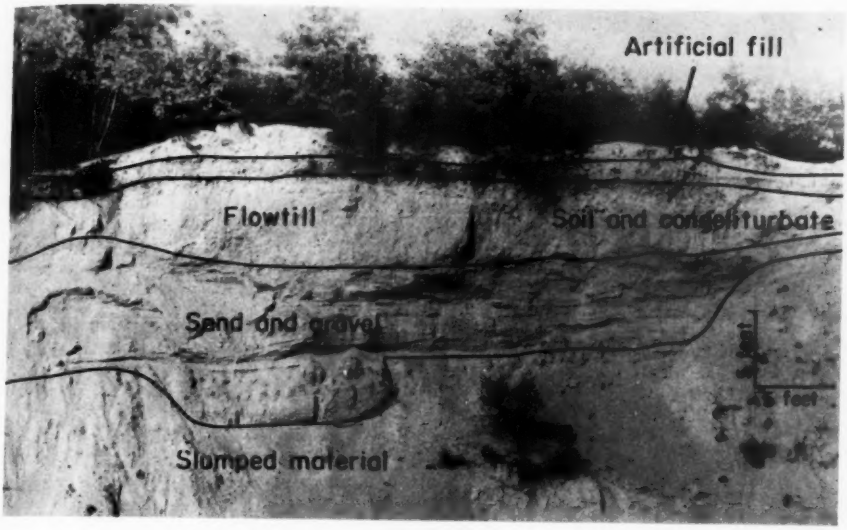

FIGURE 1

FIGURE 2

FLOWTILL AND MUDFLOW

tills of the area. No structure could be discerned in the till.

The flowtill in the second example is exposed in a lens ranging from about 6 inches to 3 feet and gravel; the fluvial material is generally undisturbed; the till masses are tabular to lens-shaped; in places the bodies of till occur at the top of the stratified drift, capped only by the

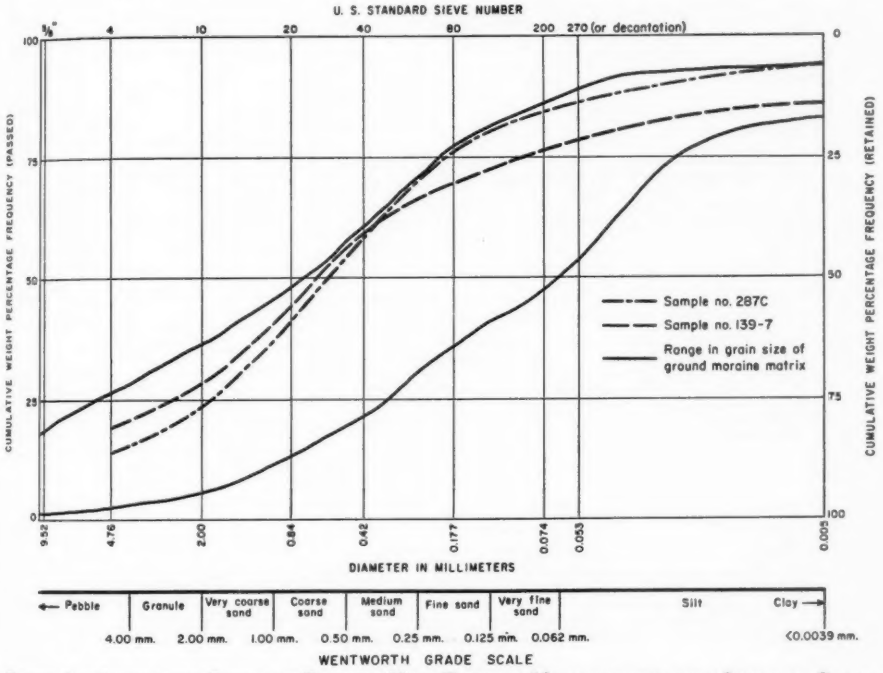

FIGURE 2.—CUMULATIVE CURVES OF FLOWTILL NEAR TAUNTON, MASSACHUSETTS, WITH LIMITS OF GRAIN SIZE OF GROUND-MORAINE TILL MATRIX
Analyses by C. Giacobbe, Department of Public Works, Commonwealth of Massachusetts

thick on the face of the pit. The flowtill is represented by sample 139-7, has more clay-size material than sample 287C, contains numerous sandy masses scattered through it, but is very similar in appearance to 287C.

The flowtill lenses described above have counterparts in at least two dozen places near Taunton, and in many other places in eastern Massachusetts, Connecticut, and Rhode Island (J. P. Schafer, personal communication; C. A. Kaye, personal communication). Till over sand and gravel described in the northeastern part of Massachusetts is attributed to readvance (Brown, 1933; Hansen, 1956, p. 62) but is interpreted by the present writer as flowtill. Everywhere near Taunton the flowtill bodies in or on stratified drift are grayish and occur as lenticular beds of varying thickness. The flowtill overlies beds or lenses of stream-laid sand

TABLE 1.—STATISTICAL MEASURES OF FLOWTILL

Sample	Median (mm.)	Q1 (mm.)	Q3 (mm.)	Sorting (So)	$\log_{10}$ So
287C	0.600	1.80	0.187	3.09	0.490
139-7	.662	2.65	.084	5.62	.750

ubiquitous congeliturbate, and elsewhere interbedded with the stratified drift. Boulders are common in the flowtill deposits.

The explanation most generally advanced for the phenomenon of till overlying outwash—that is, readvance of the ice—seem improbable here.

The origin of flowtill can be deduced from inspection of the margins of modern glaciers, as, for instance, the Malaspina Glacier of southeastern Alaska. Indeed, the writer has ob-

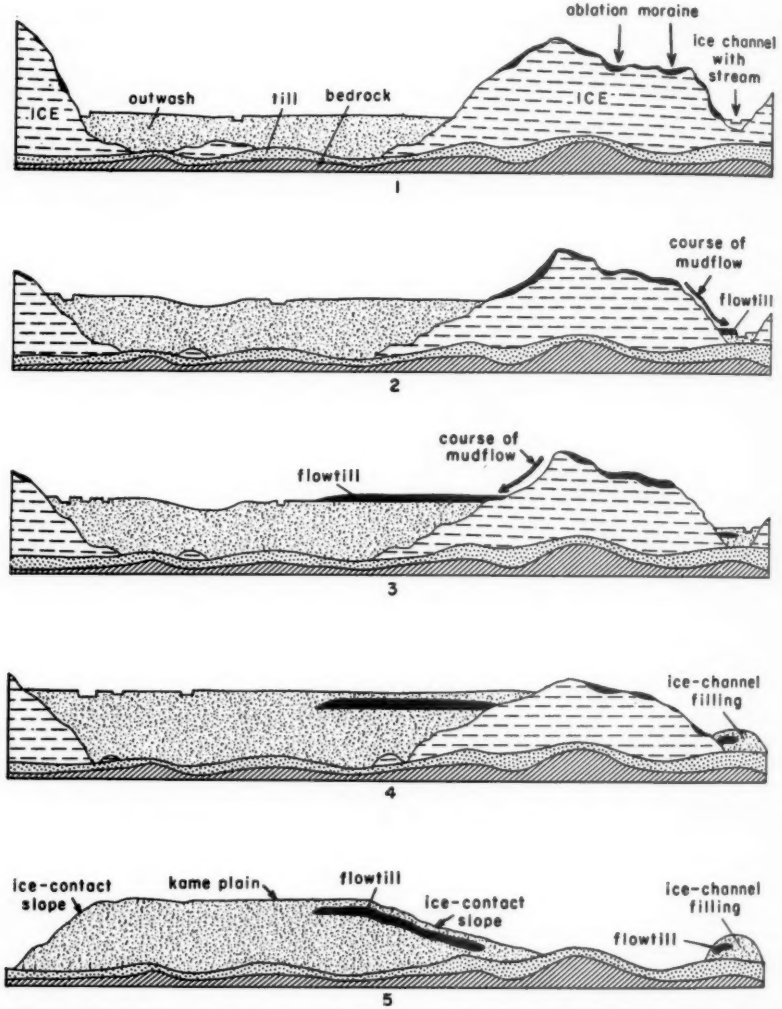

FIGURE 3.—SCHEMATIC DIAGRAM OF ORIGIN OF FLOWTILL IN A KAME PLAIN AND IN AN ICE-CHANNEL FILLING

(1) Glaciofluvial sedimentation between isolated blocks of stagnant ice with ablation moraine on the surface. (2) Ablation moraine moves off ice slope as mudflow and into narrow stream channel where it comes to rest as flowtill. (3) Ablation moraine moves off ice slope as mudflow onto large outwash area where it comes to rest as flowtill. (4) Continued sedimentation on large outwash area covers flowtill; stream flow is diverted, and ice blocks melt back from stream channel leaving ice-channel filling with buried lens of flowtill. (5) Complete melting of ice blocks; kame plain, surrounded by ice-contact slopes, remains with buried lens of flowtill parallel to surface; ice-channel filling completely isolated.

served nearly all phases of the process there. On the Malaspina, as on any glacier in temperate latitudes, the summer sun melts the ice wherever the warmth can penetrate the mantle of superglacial debris. As the ice melts, it releases all the particles, from clay to boulders, that were imbedded in the ice. These newly released pieces begin to gather in the hollows and valleys of the irregular ice surface. If there is very little washing or movement by rills and rivulets of water, the ablation moraine retains a fine-grained matrix instead of the coarse matrix

and bouldery composition so commonly attributed to deposits of superglacial till. Because the surface of the ice is a constantly changing environment, superglacial debris deposited in one place does not remain stationary long, but is caught up in a cycle of movement and change. Where there is very little washing of patches of albation moraine by superglacial streams, the superglacial debris eventually becomes saturated with meltwater and becomes a thick, muddy mixture of clay, silt, pebbles, cobbles, and boulders (Pl. 1, fig. 2). In the continuous process of inversion of ice topography, this mixture may come to lie at the top of a slope of ice where the debris eventually becomes unstable because of the large amounts of contained meltwater and moves down the ice slope as a mudflow, carrying boulders and all other other sizes of debris with it. At the base of the ice slope, or some distance out upon an adjoining flat, the mudflow stops. If the ice slope adjoins an outwash body, the mobile ablation moraine moves out over the outwash as a thin body of stony mud (Fig. 3). When the saturated stony mud dries out, it is a till as hard and compact as any till subjected to the weight of a glacier during lodgement as ground moraine.

If the flowtill has moved onto an area of active glaciofluvial sedimentation that will become an ice-channel filling, kame, kame terrace, kame delta, or kame plain when the supporting ice walls have melted away it may be buried under further increments of glaciofluvial sand or gravel or glaciolacustrine silt and clay. In this case, the flowtill will be found buried in the stratified ice-contact feature, as in the pit at Lake Sabbatia.

When the flowtill reaches its final position, it retains all the characteristics of the superglacial till from which it originated, and in parts of southeastern Massachusetts, at least, is indistinguishable from till considered to have been deposited subglacially. Doubtless some of the till in the ground moraine also has moved laterally from the last vestiges of wasting ice onto adjacent subglacial till mapped as ground moraine, but this cannot be distinguished from ground-moraine till let down vertically as superglacial till or from subglacial till.

Flowtill can be recognized easily when it occurs in anomalous stratigraphic positions in ice-contact features; if till with a similar origin can be delineated in ground moraine it can be mapped as flowtill. The essential feature of flowtill is its origin in ablation moraine that moves as a mudflow off glacier ice onto adjacent lower surfaces.

References Cited

Brown, T. C., 1933, The waning of the last ice sheet in central Massachusetts: Jour. Geology, v. 41, p. 144–158

Hansen, W. R., 1956, Geology and mineral resources of the Hudson and Maynard quadrangles, Massachusetts: U. S. Geol. Survey Bull. 1038, 104 p.

U. S. Geological Survey, 270 Dartmouth St., Boston, Mass.

Manuscript Received by the Secretary of the Society, June 28, 1957

Publication Authorized by the Director, U. S. Geological Survey

BULLETIN OF THE GEOLOGICAL SOCIETY OF AMERICA
VOL. 69, PP. 483–486 APRIL 1958

DIFFERENTIATION OF THE MANTLE

BY FRANCIS BIRCH

An earlier discussion of the elasticity of the mantle (Birch, 1952) led to the conclusion that the lower part of the mantle might be homogeneous, and two possibilities were suggested (p. 282): "The whole mantle was originally homogeneous and layer D has remained unchanged, differentiation having affected only the layers above and including layer C; or differentiation has affected the whole mantle, with settling out of a uniform aggregate of the highest-melting components as high-pressure phases and rejection of lower-melting components toward the surface". Recent studies of uranium and potassium in meteorites throw light upon the degree and kind of differentiation in the mantle, on the hypothesis that the chondrites give the chemical composition of the primitive mantle or primitive Earth, except for the light elements (Urey, 1952; Suess and Urey, 1956).

Until the last few years, uranium determinations of chondrites have been few and discordant. The latest measurements, especially those of Hamaguchi, Reed, and Turkevich (1957), begin to converge toward a value of about 10^{-8} gm U/gm. The concordant measurements are shown in Table 1. A mean value of $1.1 \cdot 10^{-8}$ gm U/gm as given by Hamaguchi, Reed, and Turkevich will be adopted in the following discussion. This is, of course, subject to modification as further sampling proceeds.

Potassium has been determined by Ahrens, Pinson, and Kearns (1952), Edwards and Urey (1955), and Edwards (1955) for a total of about 60 chondrites. The values are surprisingly uniform; as a mean value, we take 0.083 per cent potassium, or 0.1 per cent K_2O.

Applying the mean value for uranium to the mass of the Earth ($6 \cdot 10^{27}$ gm) we find a total of $66 \cdot 10^{18}$ gm U. Suppose first that all of this has been concentrated in the "lithosphere" of $24 \cdot 10^{24}$ gm (Poldervaart, 1955, p. 133); this includes the thin oceanic crust. The average concentration is then 2.8 ppm, a value characteristic of "intermediate" rocks (Faul, 1954, Chapters 2 and 5). Most of the uranium would, on this assumption, now reside in the continental crust, the portions of the Earth beneath the oceans having contributed to the enrichment of the continental plates. Horizontal as well as vertical segregation is thus implied, and difficulties arise in explaining the apparent uniformity of heat flow over oceans and continents (Bullard, Maxwell, and Revelle, 1956).

In order to escape these difficulties, Bullard (1952, p. 202) proposed that "the total amount of radioactivity beneath unit area of continent and ocean is the same when summed down to a depth of a few hundred kilometers (heat generated deeper down has not had time to escape)". Expressed as mass per unit of surface, the total uranium content is 13 gm/cm^2. Distributed through a continental depth of 35 km (mass, 10^7 gm/cm^2) this gives a mean concentration of 1.3 ppm. This is somewhat lower than most of the estimates based on assumed proportions of typical granite and basalt; it is higher than for typical basalt, lower than for intermediate rocks. On the hypothesis of vertical segregation virtually all the uranium originally beneath the continents must now be concentrated in the crust. (Note that, had only the mass of the mantle been used, these values would be two-thirds as great). If the uranium had been removed only from layers B and C, 3.5 gm/cm^2 would be available, and the mean concentration for the continental crust could not exceed 0.35 ppm, about half that of average basalt. The thin oceanic crust, with a mass of some $15 \cdot 10^5$ gm/cm^2, can evidently not account for 13 gm/cm^2 of uranium, and most of this must still be distributed below the oceanic crust.

The potassium content of the Earth, applying the figure of 0.1 per cent to the whole mass, is $6 \cdot 10^{24}$ gm K_2O, or $1.2 \cdot 10^6$ gm/cm^2. On complete vertical concentration, this would mean 12 per cent for the continental crust; the probable figure is 2.2 to 2.4 per cent (Poldervaart, 1955, p. 133) so that some four-fifths of the potassium remains below the continental crust, and nearly all of it below the oceanic crust (Birch, 1951, p. 116; Holyk and Ahrens, 1953, p. 246).

Potassium is thus not so highly concentrated upward as uranium. We may surmise, however, that it has been completely removed from the regions below a few hundred kilometers. The principal argument for this is based on considerations of heat flow, though the close

association of potassium with uranium in igneous rocks gives qualitative support (Faul, 1954, Chapter 2, especially Adams, p. 91–97). With the adopted values for uranium and

TABLE 1.—URANIUM IN CHONDRITES

Chondrite	Uranium in 10^{-8} gm/gm	Reference
Modoc	1.1	Tilton, 1952, Thesis, Univ. Chicago
	1.2, 2.6	C. C. Patterson, in Hamaguchi *et al.*
	1.08	Hamaguchi *et al.* (1957)
Forest City	2.4	Hurley (1957)
	1.03	Hamaguchi *et al.* (1957)
Cumberland Falls	1.0	Davis (1950)
Akaba	0.84	Reasbeck and Mayne (1955)
Richardton	1.22	Hamaguchi *et al.* (1957)
Holbrook	1.26	Hamaguchi *et al.* (1957)

potassium, the present rates of heat generation are $0.48 \cdot 10^{20}$ cal/year for uranium, $1.35 \cdot 10^{20}$ cal/year for potassium; allowing $0.48 \cdot 10^{20}$ cal/year for thorium, we find a total of $2.3 \cdot 10^{20}$ cal/year ($1.8 \cdot 10^{20}$ cal/year based on the mass of the mantle). This is not significantly different from the rate of loss of heat from the Earth's interior, $2 \cdot 10^{20}$ cal/year (Bullard, 1954, p. 107; Birch, 1954, p. 646; Hurley, 1957). Unless this is coincidence, it implies that nearly all the heat currently generated is reaching the surface; this in turn, unless we envisage complex schemes of compensation, implies that all the heat sources are close to the surface, probably not deeper than several hundred kilometers. This must be true for oceanic as well as continental sectors because of the equality of heat flow, though the details of the distributions differ markedly with regard to uranium (and presumably thorium), and to a lesser extent with regard to potassium. If the uranium were distributed through a depth of 200 km below the oceans, the average would be about 0.2 ppm, or about one-third that of typical basaltic rocks. If, returning to the first hypothesis, all the uranium and thorium were concentrated in the "lithosphere", the average continental heat production per unit area would be more than twice the oceanic.

The above conclusions are no stronger than the chemical evidence on which they are based; they must be, in fact, weaker because of the chain of hypotheses, notably the assumption that the chondrites are representative of the whole Earth or the whole mantle. It seems worth remarking, however, that the "chondrite hypothesis" momentarily leads to the conclusion that the whole mantle has been differentiated, in the sense that uranium and potassium have been virtually eliminated from the deep interior and concentrated close to the surface; as a corollary, a somewhat similar behavior may be expected for other elements geochemically associated with uranium and potassium.

References Cited

Ahrens, L. H., Pinson, W. H., and Kearns, M. M., 1952, Association of rubidium and potassium and their abundance in common igneous rocks and meteorites: Geochim. et Cosmochim., Acta, v. 2, p. 229–242

Birch, Francis, 1951, Recent work on the radioactivity of potassium and some related geophysical problems: Jour. Geophys. Res., v. 56, p. 107–126

——, 1952, Elasticity and constitution of the Earth's Interior: Jour. Geophys. Res., v. 57, p. 227–286

——, 1954, The present state of geothermal investigations: Geophysics, v. 19, p. 645–659

Bullard, E. C., 1952, Heat flow through the floor of the Eastern North Pacific Ocean: Nature, v. 170, p. 202–203

——, 1954, The Earth as a Planet (G. P. Kuiper, *Editor*): Univ. Chicago Press, 749 p.

Bullard, E. C., Maxwell, A. E., and Revelle, R., 1956, Heat flow through the deep sea floor: Advances in Geophysics III, Academic Press, N. Y., p. 153–181

Davis, G. L., 1950, Radium content of ultramafic igneous rocks; III. Meteorites: Am. Jour. Sci., v. 248, p. 107–111

Edwards, George, 1955, Sodium and potassium in meteorites: Geochim. et Cosmochim. Acta, v. 8, p. 285–294

Edwards, George, and Urey, Harold C., 1955, Determination of alkali metals in meteorites by a distillation process: Geochim. et. Cosmochim. Acta, v. 7, p. 154–168

Faul, H., 1954, Nuclear geology: N. Y., John Wiley and Sons, 414 p.

Hamaguchi, H., Reed, G. W., and Turkevich, A., 1957, Uranium and barium in stone meteorites: Geochim. et Cosmochim. Acta, v. 12, p. 337–347

Holyk, W., and Ahrens, L. H., 1953, Potassium in ultramafic rocks: Geochim. et Cosmochim. Acta, v. 4, p. 241–250

Hurley, P. M., 1957, Test on the possible chondritic composition of the Earth's mantle and its

abundance of uranium, thorium and potassium: Geol. Soc. America Bull., v. 68, p. 379–382
Poldervaart, Arie, *Editor*, 1955, Crust of the Earth, Geol. Soc. America Special Paper 62, 762 p.
Reasbeck, P., and Mayne, K. I., 1955, The ages an origin of meteorites: Nature, v. 176, p. 186–188
Suess, H. E., and Urey, H. C. 1956, Abundances of the elements: Rev. Mod. Physics, v. 28, p. 53–74
Urey, H. C., 1952, The abundances of the elements: Phys. Rev., v. 88, p. 248–252

HARVARD UNIVERSITY, CAMBRIDGE 38, MASS.
MANUSCRIPT RECEIVED BY THE SECRETARY OF THE SOCIETY, NOVEMBER 25, 1957